REQ.NO. 0-9106

CONTRACT REPORT NO. 1SQ80-00161

"AN ANALYTICAL APPROACH TO THE DESIGN OF PILLARS IN COAL

PART 1: THE ANALYTICAL METHOD"

Final Report, Phase I

BY

K. Barron

Work on this project was conducted under the auspices of the Canada Centre for Mineral and Energy Technology, Energy, Mines and Resources, Canada

D.S.S. File #: 16 SQ 23440 - 0 - 9106
D.S.S. Contract Serial #: 1SQ80 - 00161
CANMET Project #: 334 - 101
CANMET Scientific Authority: Dr. D.F.G. Hedley

MICROMEDIA
JUN 28 1983

296 pp

SUMMARY

This report presents the theory and rationale behind the development of a computer program developed to analyse the stability of pillars in underground coal mines. The following is a summary of the steps within this analysis:-

1. The mean stress acting on the pillar is determined using either tributary area theory or Coates' modified pillar hypothesis.

2. A method for approximating the initial elastic distribution across the pillar is developed and is shown to be in good agreement with known elastic solutions.

3. The pillar is split into slices and the stresses acting on each slice are calculated and compared with the stresses required for fracture, using the Coulomb-Navier fracture criterion. If a slice fails, the residual stress capacity of the slice is calculated and the difference between this stress and the initial elastic stress on the slice is shed onto the, as yet, unfailed slices. Successive analysis of each slice in turn allows the depth of the fracture zone in the pillar to be determined; the stress distribution in the fracture zone and in the unfailed pillar core are also derived. Likewise the build up of confining stress in the fractured coal in the periphery of the pillar is derived; this confining stress is shown to build up exponentially.

4. A number of example analysis are performed and it is shown that:-

(a) under specific circumstances, when fracture first initiates at the pillar edge this fracturing must propogate immediately to the centre of the pillar. This is called CATASTROPHIC FRACTURE and is the model equivalent of a "pillar burst". The critical pillar width required to avoid catastrophic fracture is derived.

(b) under more normal circumstances, the fracture zone extends gradually into the pillar as the mean applied pillar stress increases. If the fracture zone extends to the centre of the pillar it is called "ultimate fracture" and the pillar strength is defined as that mean applied pillar stress required to just fracture the pillar to its' centre. The residual stress capacity of this failed pillar is calculated and the critical pillar width required to avoid ultimate fracture is also derived.

(c) If the fracture zone does not extend to the centre of the pillar, the pillar is stable and the stress distribution across the fracture zone and the central solid core is derived. The safety factor is also determined.

5. The fact that the lateral (confining) stress in the fracture zone builds up exponentially means that with wide pillars the stresses acting on a slice reach levels where, for all practical purposes,

further fracturing cannot occur and the pillar strength approaches infinity. This is not believed to be the case for coal pillars; it seems more likely that the stresses reach levels where a ductile or pseudo-ductile mode of failure can result in yielding of the pillar core. Consequently the Coulomb-Navier fracture criterion was abandoned and replaced by Mohr theory as expressed by a parabolic Mohr envelope.

6. A pseudo-ductile mechanism of failure is developed and a transition point between brittle and pseudo-ductile failure is defined as a point on the parabolic Mohr envelope. It is shown that once the pseudo-ductile failure criterion is envoked the slices will yield and there will be no further build up of confining pressure in the yield zone.

7. The program has been re-written to include this revised failure criterion. The pillar is split into slices and the initial stresses acting on each slice determined as before. The stresses on the slice are then compared with those at the transition point to determine whether the potential mode of failure of the slice is brittle (below the transition point) or pseudo-ductile (above the transition point). The stresses are then compared with the appropriate fracture criterion to determine whether the slice is stable or whether it fails by brittle fracture or by pseudo-ductile yield. The residual stress capacity of a slice failed by either mode is determined and the difference between this and the initial elastic stress is shed onto the, as yet, unfailed slices. Successive analysis of each slice in turn allows the depth of the fracture zone, the depth of the yield zone (if any), and the stress distribution in the fracture zone, yield zone and unfailed pillar core to be determined.

8. A number of example analysis are performed and it is shown that:-

(a) under specific circumstances, when fracture initiates at the pillar edge:-

(i) fracture can propogate immediately to the pillar centre. This is identical to the CATASTROPHIC FRACTURE described above.

or (ii) fracture can initiate, develop into the pillar, and then be followed by yielding which propogates immediately to the pillar centre. This is called CATASTROPHIC YIELD.

Both these cases could be regarded as models of "pillar bursts". The critical pillar widths to avoid catastrophic fracture or catastrophic yield are evaluated.

(b) Under more normal circumstances, the fracture zone extends gradually into the pillar to be followed either by a yield zone or by a stable elastic core. Likewise there may be a fracture zone, a yield zone and a stable elastic core.

If the fracture zone extends to the centre of the pillar it is, as before, called ultimate fracture and the pillar strength is again defined as the mean applied stress required to just extend the fracture zone to the pillar centre. The residual stress capacity of this fractured pillar is calculated and the critical pillar width to avoid ultimate fracture is also derived.

If the fracture zone extends into the pillar and is followed by a yield zone which then extends to the centre of the pillar, this is called "ULTIMATE YIELD". Pillar strength in this case in defined as the mean applied pillar stress just required to extend the yield zone to the pillar centre. Again the residual stress capacity of the yielded pillar can be determined and the critical pillar width to avoid ultimate yield can be calculated.

(c) If neither the fracture zone nor the yield zone extend to the pillar centre, the pillar is stable and the complete stress distribution across the fracture zone, yield zone and central elastic core is derived. The safety factor is also determined.

9. The report gives full details of all the above analytical steps and gives the computer program flow charts and the program listings. Example analysis are given to illustrate the sensitivity of the results to various input parameters. Phase II of this study will compare the results of this analysis technique with the experimental data on pillar stability that have been reported in the literature.

TABLE OF CONTENTS

Page No.

1. Introduction

1.1 Rationale 1
1.2 Objectives 1
1.3 Proposed Approach 1

2. Determination of the mean pillar stress concentration 4

2.1 Tributary area theory for mean pillar stress concentration 4
2.2 Coates' modified pillar hypothesis 6
  2.2.1 For long, deep mining zones 7
  2.2.2 For long, shallow mining zones 7
2.3 Use of Coates' pillar stress formulae 8

3. Vertical Stress distribution along the horizontal axis, at the mid height of the side wall, for single openings of various shapes, under a range of stress conditions 9

3.1 Maximum stress concentration, $\frac{\sigma_{p\ max}}{S_v}$, at mid height of the side wall of single openings 9
  3.1.1 For elliptical holes (theoretically exact solution) 9
  3.1.2 For rectangular holes (with rounded corners) 9
  3.1.3 For ovaloidal openings 9
3.2 Approximate vertical stress distribution along the horizontal axis, at the mid height, of a single hole of various shapes, under any applied stress ratio k 9
  3.2.1 Approximate vertical stress distribution curve 9
  3.2.2 Comparison of the approximate stress distribution with theoretical and experimental data 13
  3.2.3 Conclusion 20

4. Approximate vertical stress distribution, along the horizontal axis at the mid height of the side wall, for pillar with equal size openings on either side 21

4.1 Maximum stress concentration, Y_{mm}, at the mid height of the side wall of multiple openings 21
  4.1.1 For a row of ovaloidal openings 21
  4.1.2 For a row of elliptical openings 21
  4.1.3 For a row of rectangular openings 21

Page No.

4.2 Approximate stress distribution across a pillar when $Y_{mm} = \overline{Y}$ 22

4.3 Approximate vertical stress distribution when $Y_{mm} > \overline{Y}$, for pillars with equal size openings on either side 22

4.4 Comparison of the approximate stress distribution with theoretical and experimental data 25

  4.4.1 Pillars in an infinite row of equally spaced circular holes 25
  4.4.2 A four by four rectangular layout 27
  4.4.3 Three dimensional finite element solution for stress distribution at the mid height of pillars 30

4.5 Conclusion 33

5. Fracture zone development in pillars - theoretical analysis 34

5.1 Stresses on the i th slice of solid coal 34

5.2 Fracture criterion for solid coal 36

5.3 Theory for the stress development in a fractured pillar edge 37

  5.3.1 Residual stress capacity of the fractured slice 37
  5.3.2 Build up of confining stress P_3, in the broken coal 42

5.4 Load shed by the failed slice onto the central solid core 43

5.5 Conclusion 45

5.6 Examples of fracture zone development 45

  5.6.1 Sensitivity of the fracture zone depth to uniaxial compressive strength of broken coal, P_B 46

  5.6.2 Fracture zones and stress distributions across the pillars in the cross section C-C previously analysed (Appendix B and E) 46

6. Pillar strength and safety factor 50

6.1 Mean pillar stress for initiation of fracture 50

6.2 Residual mean pillar stress capacity of the pillar that has just failed, $\bar{\sigma}_{PR}$ 50

6.3 Concept of catastrophic fracture 55

6.4 Sequence of events as $\bar{\sigma}_p$ increases 55

6.5 Critical pillar dimensions to avoid total fracture 58

  6.5.1 Critical dimension for category 1 catastrophic fracture 58

Page No.

6.5.2 Critical pillar dimensions for category 2 ultimate fracture 61

6.6 Pillar strength and safety factor 64

6.6.1 Pillar strength 64
6.6.2 Pillar safety factor 65

6.7 Conclusion 67

7. Transition from brittle to pseudo-ductile failure and revised failure criteria 68

7.1 Transition from brittle to pseudo-ductile failure 68

7.2 Revised failure criteria 74

7.2.1 Requirement for brittle failure 74
7.2.2 Requirements for pseudo-ductile yield 76

7.3 Examples of fracture and yield zone development 79

7.3.1 Re-analysis fo pillars C1 to C5 79

8. Pillar strengths and safety factors - revised to include pseudo-ductile yield 84

8.1 Depth of the transition point 84

8.2 Load taken by the fracture zone 84

8.3 Residual mean pillar stress capacity of a pillar that has failed by yield ($\bar{\sigma}_{PRY}$) 86

8.4 Mean pillar stress for initiation of fracture 87

8.5 Sequence of events as $\bar{\sigma}_p$ increases 88

8.6 Critical pillar dimensions to avoid catastrophic fracture, catastrophic yield, ultimate fracture and ultimate yield 92

8.6.1 Critical pillar dimension to avoid catastrophic fracture 92
8.6.2 Critical pillar dimension to avoid catastrophic yield 92
8.6.3 Critical pillar dimension to avoid ultimate fracture 93
8.6.4 Critical pillar dimension to avoid ultimate yield 93

8.7 Pillar strength and safety factors 94

8.8 Variation of pillar strengths with P_B, ϕ_B, μ_B, A, W, b and h 94

8.8.1 Influence of P_B 94

8.8.2 Influence of ϕ_B 98

8.8.3 Influence of μ_B 98

Page No.

8.8.4 Influence of A 100
8.8.5 Influence of w 100
8.8.6 Influence of h 100
8. 9 General form of the pillar strength versus semi-pillar width curve 102
8.10 Effect of the choice of the number of slices 104

9. Pillar Program (By Stephen Thornton and Gary Boehm) 107
9.1 Program Flow 107
9.1.1 Main Program 107
9.1.2 Subroutines 109
9.2 Flow Diagram 109
9.3 Program Listing 113
9.4 Variables and Constants 134
9.5 User's Manual 138
9.5.1 Required Input 138
9.5.2 Program Use 138
9.6 Examples 140

10. Short program for pillar strengths, safety factors and shed load, assuming tributary area theory with rectangular pillars and rooms 142
10.1 Purpose of the short program 142

11. References 146

12. Acknowledgements 148

APPENDICES

		Page No.
Appendix A:	Nomenclature for Coates' pillar stress hypothesis	A 1
Appendix B:	Example of the use of Coates' pillar formulae	A 3
Appendix C:	Approximate analytical expressions for the maximum stress concentration, at the mid height of the side wall on the horizontal axis, for a single opening of various shapes, under a range of stress conditions	A 8
Appendix D:	Maximum stress concentration at the mid height of side wall, on the horizontal axis, of multiple openings	A16
Appendix E:	Example elastic stress distributions across a series of pillars	A28
Appendix F:	Coulomb-Navier failure theory expressed in different forms	A31
Appendix G:	Example of the build up of the residual stress capacity and the confining pressure in the fractured coal at a pillar edge	A36
Appendix H:	Load re-distribution from the failed slice onto the remaining unfailed slices	A41
Appendix I:	Parabolic equation for a Mohr envelope	A52
Appendix J:	Mohr Program - "Best Fit" to a curved Mohr Envelope	A85
Appendix K:	Short version of the pillar program	A106

TABLES Page No.

3.1 Vertical stress concentrations along the horizontal axis of ellipses, under uniaxial stress (k=0) 14

3.2 Vertical stress distribution along the horizontal axis of a circular opening, under a range of stress ratios 16

3.3 Vertical stress distribution along the horizontal axis of a rectangular hole, w/h = 10/12, k=0.1 18

4.1 Stress concentrations across a pillar - infinite number of equally space circular holes 25

4.2 Comparison of approximation with Logie's results (11) for rectangular rooms 28

4.3 Comparison with results of Yu and Toews element solution for rectangular pillars (12) 32

5.1 Input parameters for pillar analyses used in example analyses 47

6.1 Residual mean pillar stress capacity example 53

6.2 Examples: Load shed and critical pillar dimensions 59

6.3 Pillar strength variation with P_B and ϕ_B 62

7.1 Input parameters for pillar analyses used for pillar C1 to C5 80

8.1 Input parameters for investigation of influence of those parameters on pillar strength 96

9.1 Input data sheet 139

9.2 Nine example sets of input data 141

9.3 Example output - 1st data set - full format 141

9.4 Example output - 1st data set - short format 141

10.1 Example outputs - short program 145

APPENDIX TABLES

Page No.

Table B 1: Parameters and results for example use of Coates' pillar formulae — A 6

Table C 1: Stress concentrations, Y_m at the mid height of the boundary of rectangular holes — A 9

Table C 2: Stress concentrations, Y_m at mid height of boundary of ovaloidal holes — A13

Table D 1: Maximum stress concentration for a row of five circular openings (k=0) — A17

Table D 2: Maximum stress concentration for a row of five ovaloidal openings, $w/h = 2.0$, $k = 0$ — A17

Table E 1: Stress distribution across pillars - example section CC from Appendix B — A29

Table G 1: Example of build up of residual stress capacity and confining pressure in fractured coal at the pillar edge — A37

Table H 1: Vertical stress distribution across pillar for $S_v = 650$ psi and $\alpha = 0.5$ — A46

Table H 2: Influence of S_v on fracture zone development for variation of α — A49

Table I 1: Triaxial fracture strength data for coals (from Hobbs (17)) — A57

Table I 2: Processing of the data for the determination of A — A63

Table I 3: Triaxial fracture strength data for coals (from Hobbs (17)) — A65

Table I 4: Comparison of A values by methods 1 and 2 — A66

Table J 1: Example inputs for the Mohr program (18 data sets) — A104

Table J 2: Example outputs for the Mohr program (18 data sets) — A105

Table K 1: Example inputs for the short program (13 data sets) — A128

Table K 2: Example outputs for the short program (2 data sets) — A129

FIGURES

Page No.

Figure 1: Analytical approach to the determination of the stability of coal pillars 3

Figure 2: Nomenclature in determination of mean pillar stress 5

Figure 3: Vertical stress distribution along the horizontal axis, at the mid height, for a single opening 10

Figure 4: Vertical stress distribution on the axis of ellipses (k=0) 15

Figure 5: Vertical stress distribution along the horizontal axis, for circular openings 17

Figure 6: Vertical stress distribution along the horizontal axis, for a rectangular hole (h/w = .833, k = 0.1) 19

Figure 7: Schematic of the stress distribution across a pillar 23

Figure 8: Comparison of Savin's results (6) with approximation 26

Figure 9: Comparison of Logies' results (11) with approximation 29

Figure 10: Stress distributions in pillars determined by Yu and Toews (12) 31

Figure 11: Pillar divided into n_1 slices, each of width $\delta e = \frac{B}{n_1}$ 35

Figure 12: Forces acting on an elemental strip within the pillar 38

Figure 13: Sensitivity of fracture zone development to P_B 48

Figure 14: Fracture zone and vertical stress distribution across pillars C1 to C5 49

Figure 15: Condition for fracture initiation in the pillar 51

Figure 16: Stress distribution when fracture just reaches the pillar centre. 51

Figure 17: Increase in residual pillar stress capacity with pillar width 54

Page No.

Figure 18: Possible modes of pillar stability and fracture 56

Figure 19: Critical pillar dimension b_{c1}, to avoid catastrophic failure (category 1) 60

Figure 20: Critical pillar dimension, b_{c2}, to avoid ultimate failure (category 2) 63

Figure 21: Pillar strength variation with P_B and ϕ_B. 66

Figure 22: Triaxial test 69

Figure 23: Typical differential stress versus strain curves from triaxial tests 69

Figure 24: Shear resistance versus normal stress; Coulomb-Navier failure and frictional sliding 71

Figure 25: Shear resistance versus normal stress; Mohr failure theory and frictional sliding 71

Figure 26: Flow diagram for revised failure criteria 78

Figure 27: Mohr envelope assumed in example analyses 81

Figure 28: Stress distribution across pillars C1 to C5 82

Figure 29: Example computer output sheet for pillar C1 83

Figure 30: Depth of the transition point 85

Figure 31: Pillar that has just failed by yield 85

Figure 32: Possible modes of pillar stability and failure 89

Figure 33: Program logic for calculating pillar strengths, safety factors, failure mode and critical pillar dimensions 95

Figure 34: Strength variation with pillar width for a range of uniaxial compressive strengths of broken coal 97

Figure 35: Strength variation with pillar width for a range of angles of internal friction of broken coal 97

Figure 36: Strength variations with pillar width for a range of sliding coefficients of friction 99

Page No.

Figure 37: Strength variation with pillar width for a range of "Mohr" constants 99

Figure 38: Strength variation with pillar width for a range of semi-pillar widths 101

Figure 39: Strength variation with pillar width for a range of semi-pillar heights 101

Figure 40: General form of the pillar strength versus semi-pillar width curve 103

Figure 41: Examples cases for n_1 = 36, 180 and 360 slices 105

Figure 42: Effect of the number of slices on the vertical stress distribution 106

Figure 43: Flow diagram - main program 110-112

Figure 44: Rectangular pillar types and dimensions 143

Figure 45: Pillar strengths, safety factors for uniform pillar layouts with rectangular rooms 144

APPENDIX FIGURES

Page No.

Figure B 1: Plan of a coal mine in Western Canada A 4

Figure B 2: Cross sections through test pillars A, B, and C A 5

Figure B 3: Comparison of tributary area theory with Coates' hypothesis for pillars on Section C-C A 7

Figure C 1: Stress concentration at the mid height of the boundary of rectangular openings A10

Figure C 2: Coefficients a' and b' for rectangular holes A11

Figure C 3: Stress concentration at the mid height of the boundary of ovaloidal openings A14

Figure C 4: Coefficients a' and b' for ovaloidal holes A15

Figure D 1: Multiple openings with pillars between them A18

Figure D 2: Maximum stress concentration for a row of 2, 3, and 5 circular opening for a range of w/b ratios, k = 0 A19

Figure D 3: Maximum stress concentration for a row of circular and ovaloidal holes A19

Figure D 4: Average and maximum stress concentration for different extraction ratios A22

Figure D 5: Comparison of the average and the maximum pillar stress concentration A22

Figure D 6: Maximum stress concentration at the boundary of multiple ovaloidal openings - comparison of approximation with experimental results A24

Figure E 1: Elastic stress distribution across pillars in section C-C, Figure B1, Appendix B A30

Figure F 1: Coulomb-Navier failure theory expressed as a Mohr's envelope A32

Figure F 2: Relationship between the principal stresses and the stresses on the failure plane A32

Figure F 3: Coulomb-Navier failure theory expressed as a straight line relationship between σ_1 and σ_3 A32

Page No.

Figure G 1: Build up of residual stress capacity in broken rock-variation with ϕ_B A38

Figure G 2: Build up of confining pressure in broken rock - variation with ϕ_B A39

Figure G 3: Build up of residual stress capacity in broken rock-variation with P_B A40

Figure H 1: Pillar divided into n_1 slices ($n_1 = 14$) A43

Figure H 2: Effect of variation of the load shedding function A48

Figure H 3: S_v versus depth of fracture zone for different load shedding functions A50

Figure I 1: Parabolic Mohr envelope A53

Figure I 2: Relationships between $\frac{\partial T}{\partial \sigma}$ and θ A53

Figure I 3: Parabolic Mohr envelope A59

Figure I 4: Mohr diagram and envelope for Pentremar coal (bedding planes parallel) A67

Figure I 5: Mohr diagram and envelope for Pentremar coal (bedding planes perpendicular) A68

Figure I 6: Mohr diagram and envelope for Deep Duffryn coal (bedding planes parallel) A69

Figure I 7: Mohr diagram and envelope for Deep Duffryn coal (bedding planes perpendicular) A70

Figure I 8: Mohr diagram and envelope for Oakdale coal (bedding planes parallel) A71

Figure I 9: Mohr diagram and envelope for Oakdale coal (bedding planes perpendicular) A72

Figure I 10: Mohr diagram and envelope for Cwmtillery coal (bedding planes parallel) A73

Figure I 11: Mohr diagram and envelope for Cwmtillery coal (bedding planes perpendicular) A74

Page No.

Figure I 12: Mohr diagram and envelope for Barnsley Hard coal (bedding planes parallel) A75

Figure I 13: Mohr diagram and envelope for Barnsley Hard coal (bedding planes perpendicular) A76

Figure I 14: Mohr diagram and envelope for Barnsley Bright coal (bedding planes parallel) A77

Figure I 15: Mohr diagram and envelope for Barnsley Bright coal (bedding planes perpendicular) A78

Figure I 16: Mohr diagram and envelope for Terversal coal (bedding planes parallel) A79

Figure I 17: Mohr diagram and envelope for Terversal coal (bedding planes perpendicular) A80

Figure I 18: Mohr diagram and envelope for Markham coal (bedding planes parallel) A81

Figure I 19: Mohr diagram and envelope for Markham coal (bedding planes perpendicular) A82

Figure I 20: Mohr diagram and envelope for Linby coal (bedding planes parallel) A83

Figure I 21: Mohr diagram and envelope for Linby coal (bedding planes perpendicular) A84

Figure K 1: Flow diagram - short program A107

1. Introduction

1.1 Rationale

The ability to design coal pillars for underground coal mining operations is of prime importance in room and pillar mining during both the development and pillar extraction phases. Pillar failure during mining represents a major potential safety hazard and is generally avoided in practice by overdesigning the pillar using large safety factors, however, this may result in reduced extraction ratios and loss in reserve recovery. Likewise, in panel mining it is essential to be able to design stable barrier pillars between panels, not only for structural stability but also to prevent ventilation leakage between mined out areas which could cause spontaneous combustion and mine fires.

Although much rock mechanics research in the past has been devoted to assessing pillar loads and pillar strengths, no one approach to pillar design has been completely satisfactory, and pillar design still owes much to trial and error procedures during mining operations. A satisfactory analytical design method for determining stable pillar dimensions will not eliminate the necessity for design adjustments to be made on the basis of on-site conditions but would add greatly to the degree of confidence in the overall design of a mine layout and should allow recovery to be increased without sacrifice to safety. Further, such an analytical design method would give a "yardstick" against which field measurements can be interpreted, this should allow experience in one area to be transposed to another area reducing the trial and error period experienced when moving into a new mine.

1.2 Objectives

The objective of this study may therefore be defined as follows:-

Phase 1: To develop an analytical approach that will define coal pillar stability and lead to the evaluation of optimum pillar dimensions.

Phase 2: To evaluate the applicability of this analytical approach to pillar design by testing it using experimental data extracted from the literature.

1.3 Proposed Approach

The concepts upon which this approach to pillar stability assessment is based stem from concepts expressed by Wilson (1). These ideas can be expressed in the form of a simple hypothesis as follows:-

Hypothesis: A coal pillar under load may be considered to comprise a central, solid, core of coal surrounded by a peripheral zone of fractured coal; a pillar may be deemed to be unstable if either

(a) the fracture zone extends to the centre of the pillar
or (b) if the central solid core yields.

To develop this simple hypothesis in realistic terms the analysis must take into account the following factors:-

- the applied virgin stress ratio
- the mean pillar stress and its variation with the position of the pillar within the mining span
- the stress distribution across the pillar
- the dimensions of the pillar, the adjacent rooms and the mined area
- the physical properties of the solid, fractured and yielding coal
- the physical properties of the surrounding strata
- the existence of a fracture zone around the periphery of the pillar
- the presence of a high stress abutment zone beyond this periphal fracture zone
- the possibility of complete pillar failure by fracturing
- the possibility of limited bearing capacity caused by yielding of the pillar

The methodology for developing this analysis is to split the pillar into a number of equal slices and to analyse the stresses on each successive slice and to compare these stresses with the appropriate fracture or yield criteria for coal. Figure 1 gives the basic outline of the program logic steps to carry out such an analysis. The numbered steps in this figure represent fundamental steps for which analytical expressions must be derived. Of necessity, a number of assumptions and analytical simplifications must be made in accomplishing these steps; the significance of these assumptions will be discussed when they are made and all analytical approximations will be checked against theoretical or experimental data whenever possible. The first phase of this study therefore comprises the development and verification of the appropriate expressions for each of the fundamental steps indicated and the integration of these steps into a computer program to carry out the logic illustrated in Figure 1.

Phase 2 of the program attempts to assess the applicability of the analytical model developed in Phase 1 by comparison with field data. Many field studies have been made of pillar strength characteristics and have been published in greater or lesser detail. This literature has been sifted with the object of extracting input data for analysis in the model to allow comparison with the results of these studies.

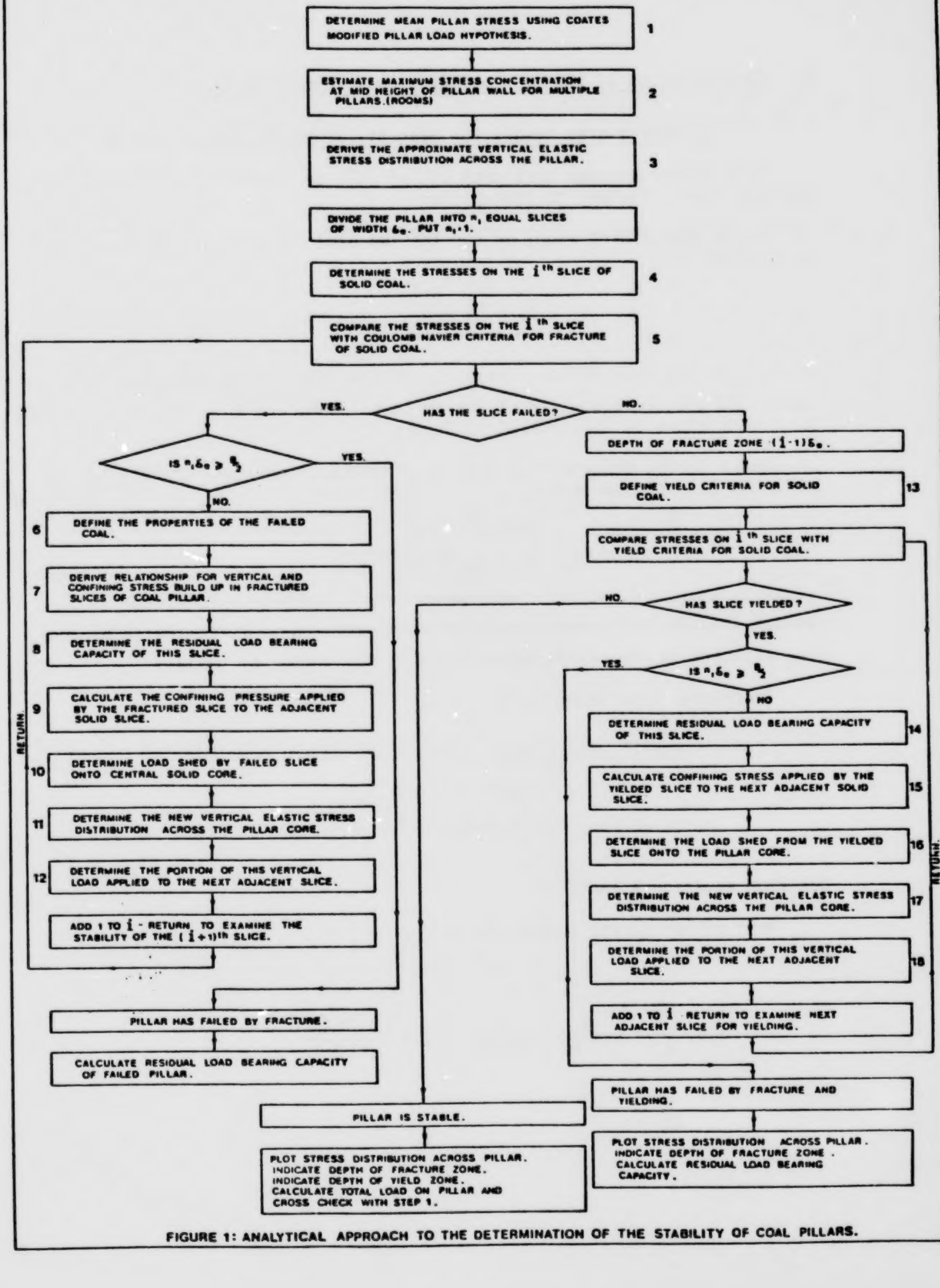
DETERMINE MEAN PILLAR STRESS USING COATES MODIFIED PILLAR LOAD HYPOTHESIS.
1
ESTIMATE MAXIMUM STRESS CONCENTRATION AT MID HEIGHT OF PILLAR WALL FOR MULTIPLE PILLARS.(ROOMS)
2
DERIVE THE APPROXIMATE VERTICAL ELASTIC STRESS DISTRIBUTION ACROSS THE PILLAR.
3
DIVIDE THE PILLAR INTO n1 EQUAL SLICES OF WIDTH δe. PUT n1=1.
DETERMINE THE STRESSES ON THE i th SLICE OF SOLID COAL.
4
COMPARE THE STRESSES ON THE i th SLICE WITH COULOMB NAVIER CRITERIA FOR FRACTURE OF SOLID COAL.
5
YES.
HAS THE SLICE FAILED?
NO.
IS n1δe ≥ B/2
YES.
NO.
6
DEFINE THE PROPERTIES OF THE FAILED COAL.
7
DERIVE RELATIONSHIP FOR VERTICAL AND CONFINING STRESS BUILD UP IN FRACTURED SLICES OF COAL PILLAR.
8
DETERMINE THE RESIDUAL LOAD BEARING CAPACITY OF THIS SLICE.
9
CALCULATE THE CONFINING PRESSURE APPLIED BY THE FRACTURED SLICE TO THE ADJACENT SOLID SLICE.
RETURN.
10
DETERMINE LOAD SHED BY FAILED SLICE ONTO CENTRAL SOLID CORE.
11
DETERMINE THE NEW VERTICAL ELASTIC STRESS DISTRIBUTION ACROSS THE PILLAR CORE.
12
DETERMINE THE PORTION OF THIS VERTICAL LOAD APPLIED TO THE NEXT ADJACENT SLICE.
ADD 1 TO i - RETURN, TO EXAMINE THE STABILITY OF THE (i+1)th SLICE.
PILLAR HAS FAILED BY FRACTURE.
CALCULATE RESIDUAL LOAD BEARING CAPACITY OF FAILED PILLAR.
DEPTH OF FRACTURE ZONE (i-1)δe.
DEFINE YIELD CRITERIA FOR SOLID COAL.
13
COMPARE STRESSES ON i th SLICE WITH YIELD CRITERIA FOR SOLID COAL.
NO.
HAS SLICE YIELDED?
YES.
YES.
IS n1δe ≥ B/2
NO
DETERMINE RESIDUAL LOAD BEARING CAPACITY OF THIS SLICE.
14
CALCULATE CONFINING STRESS APPLIED BY THE YIELDED SLICE TO THE NEXT ADJACENT SOLID SLICE.
15
DETERMINE THE LOAD SHED FROM THE YIELDED SLICE ONTO THE PILLAR CORE.
16
RETURN.
DETERMINE THE NEW VERTICAL ELASTIC STRESS DISTRIBUTION ACROSS THE PILLAR CORE.
17
DETERMINE THE PORTION OF THIS VERTICAL LOAD APPLIED TO THE NEXT ADJACENT SLICE.
18
ADD 1 TO i RETURN TO EXAMINE NEXT ADJACENT SLICE FOR YIELDING.
PILLAR HAS FAILED BY FRACTURE AND YIELDING.
PLOT STRESS DISTRIBUTION ACROSS PILLAR. INDICATE DEPTH OF FRACTURE ZONE. CALCULATE RESIDUAL LOAD BEARING CAPACITY.
PILLAR IS STABLE.
PLOT STRESS DISTRIBUTION ACROSS PILLAR. INDICATE DEPTH OF FRACTURE ZONE. INDICATE DEPTH OF YIELD ZONE. CALCULATE TOTAL LOAD ON PILLAR AND CROSS CHECK WITH STEP 1.

FIGURE 1: ANALYTICAL APPROACH TO THE DETERMINATION OF THE STABILITY OF COAL PILLARS.

2. Determination of the mean pillar stress concentration

2.1 Tributary area theory for mean pillar stress concentration

This theory assumes that each pillar will be loaded by the stress acting over the room tributary to that pillar.

For a long mining zone, or for the two dimensional case, this can be represented by:-

$$\overline{\sigma_p} = S_v \left\{\frac{W+B}{B}\right\} \tag{1}$$

where $\overline{\sigma_p}$ is the mean pillar stress, S_v is the virgin stress perpendicular to the seam, W is the average width of the adjacent rooms and B is the pillar width. The nomenclature is illustrated in Figure 2.

For a series of rooms and pillars of equal dimensions, the extraction ratio can be expressed as:-

$$R = \frac{A_o}{A_T} = \frac{(N+1)W}{(N+1)\ W+NB} \tag{2}$$

where A_o is the total roof area adjacent to the rooms, A_T is the total roof area adjacent to the mining zone, and N is the number of pillars.

Therefore, from equation 2:-

$$R = 1 - \left\{\frac{NB}{(N+1)\ W+NB}\right\} = 1 - \left\{\frac{1}{\left(\frac{N+1}{N}\right)\frac{W}{B}+1}\right\} \tag{3}$$

but from equation 1 and 3 :-

$$\text{Mean pillar stress concentration} = \frac{\overline{\sigma_p}}{S_v} = \frac{W}{B} + 1$$

$$\text{i.e. } \frac{\overline{\sigma_p}}{S_v} = \left\{\frac{R}{(1-R)} \cdot \frac{N}{(N+1)}\right\} + 1 = \frac{\left[1-\frac{R}{(1+N)}\right]}{(1-R)}$$

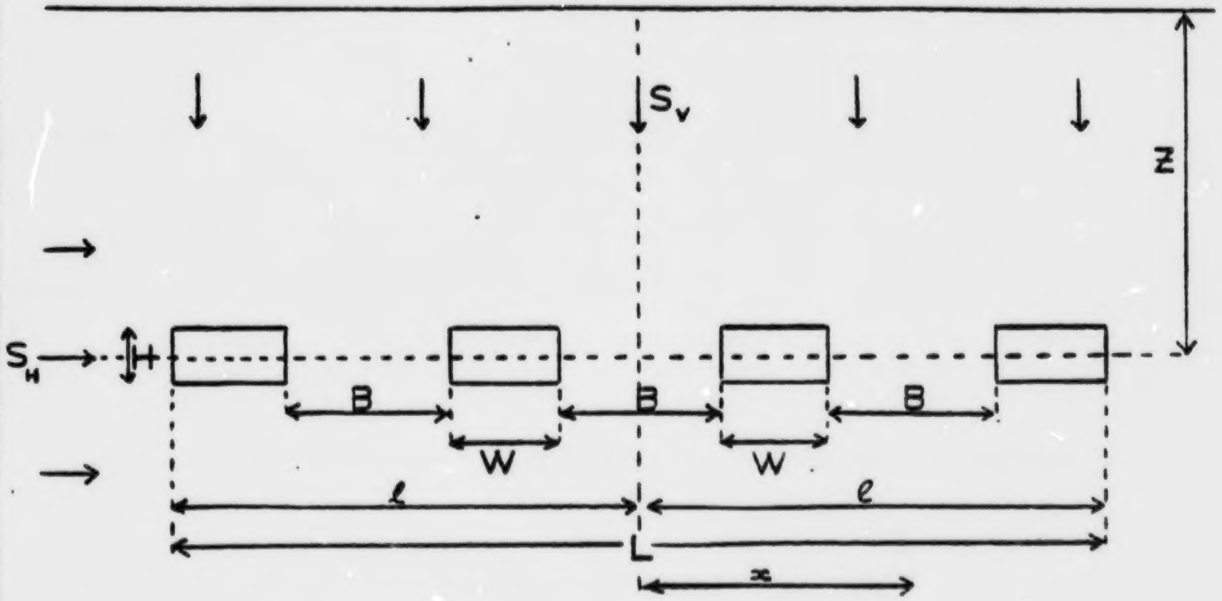
S_v
Z
S_H
H
B
B
B
W
W
ℓ
ℓ
L
x

FIGURE 2: Nomenclature in determination of mean pillar stress

Thus when N = ∞, $\frac{\overline{\sigma_p}}{S_v} = \frac{1}{(1-R)}$ (4)

This equation 4 is the one most often used in tributary area theory; however, when N is small it gives an answer that is seriously in error with respect to theory.

For example:- if N = 1

$\frac{\overline{\sigma_p}}{S_v} = \left\{\frac{R}{(1-R)} \cdot \frac{1}{2}\right\} + 1 = \frac{(2-R)}{2(1-R)}$ and not $\frac{1}{(1-R)}$ as given by equation 4.

Hence tributary area theory should always be expressed in the manner derived above as:-

$$\frac{\overline{\sigma_p}}{S_v} = \left\{\frac{\overline{\Delta\sigma_p}}{S_v} + 1\right\} = \left\{\frac{1-\left[\frac{R}{1+N}\right]}{(1-R)}\right\} \qquad (5)$$

alternatively this equation may be expressed as :-

$$\frac{\overline{\Delta\sigma_p}}{S_v} = \frac{R}{(1-R)} \cdot \frac{N}{(N+1)} = \frac{R}{(1-R)\ (1+1/N)} \qquad (6)$$

where $\overline{\Delta\sigma_p}$ is the increase in the mean pillar stress due to the mining of the rooms.

2.2 Coates' modified pillar hypothesis

Tributary area theory relates the mean pillar stresses to the extraction ratio; this has been useful in the past primarily due to the lack of any better theory. It is, however, unsatisfactory in so far as the geometrical properties, such as the span of the mining zone in relation to the depth below surface, pillar height, breadth and location within the mining zone etc. are all ignored. It has been shown (4) that tributary area theory cannot predict actual pillar loading with acceptable accuracy and cannot account for changes due to geometry or material properties.

Coates' (2, 3, 4) has developed an hypothesis for pillar loading which he then modified empirically to derive equation for the mean pillar stress concentrations. This hypothesis has the advantage that it does take into account the significant geometrical and material properties affecting pillar loading. It was shown (3) to produce quite good predictions for the loading of model pillars and to produce (4) more satisfactory comparisons with field measurements than did tributary area theory. The equations derived by Coates' for both deep and shallow mining zones are as follows:-

2.2.1 For long, deep mining zones ($Z' = \frac{Z}{l} > 0.8$)

$$\frac{\overline{\Delta\sigma_p}}{S_v} = \frac{2R(1-\frac{x'}{5} + h') - kh'(1-\nu+\nu_p n)}{\left(h'n + 1.8\,(1-R)(1+\frac{1}{N}) \left\{ 1 + \left[\frac{h}{1-\frac{x'}{5}} \right] \right\} + 2Rb'\,\frac{(1-\nu)}{\pi} \right)} \qquad (7)$$

where the nomenclature is given in Appendix A.

This equation is to be used when the general extraction ratio, R, is known and the local extraction ratio, r, is difficult to determine (e.g. when the room and pillar widths are irregular).

When r is easily determined, the following equation should be used:-

$$\frac{\overline{\Delta\sigma_p}}{S_v} = \frac{2R(1-\frac{x'}{5} + h') - kh'\,(1 - \nu + \nu_p n)}{\left[h'n + 1.8(1-r) \left\{ 1 + \frac{h'}{(1-\frac{x'}{5})} \right\} + 2Rb'\frac{(1-\nu)}{\pi} \right]} \qquad (8)$$

2.2.2 For long, shallow mining zones ($Z' = \frac{Z}{l} < 0.8$)

$$\frac{\overline{\Delta\sigma_p}}{S_v} = \frac{2R(1 - \frac{x'}{5} + 2h') + RK'_b - kh'(1-\nu+2\nu_p n)}{\left[2h'n + \left\{ 1.8 \left[1+ \frac{h'}{(1-\frac{x'}{5})} \right] + \frac{2K_{b'}}{3} \left[1 + \frac{h'}{(1-x'^2)} \right] \right\} \left\{ (1-R)(1+\frac{1}{N}) \right\} + 4Rb'(\frac{1-\nu}{\pi}) \right]} \qquad (9)$$

or, when r is easily determined:-

$$\frac{\Delta\sigma_p}{S_v} = \frac{2R(1-\frac{x'}{5}+2h') + RK_b' - kh'(1-\nu+2\nu_p n)}{\left[2h'n + \left\{1.8\left[1+\frac{h'}{(1-\frac{x'}{5})}\right] + \frac{2K_b'}{3}\left[1+\frac{h'}{(1-x'^2)}\right]\right\}(1-r) + 4Rb'\frac{(1-\nu)}{\pi}\right]} \qquad (10)$$

2.3 Use of Coates' pillar stress, formulae

The above formulae developed by Coates' will be used in this analysis to determine the mean pillar stress concentration as required by step 1 of the analytical approach illustrated in Figure 1.

An example of the use of these formulae to determine the mean pillar stress concentrations on pillars in a Western Canadian coal mine is given in Appendix B.

3. Vertical stress distribution along the horizontal axis, at the mid height of the side wall, for single openings of various shapes, under a range of stress conditions

3.1 Maximum stress concentration, $\frac{\sigma_{p\ max}}{S_v}$, at the mid height of the side wall of single openings

Let the maximum stress concentration at the mid height of the side wall for any single hole of height $H = 2h$ and width $W = 2w$ under an applied stress ratio $k = \frac{S_H}{S_v}$ be equal to $\frac{\sigma_{p\ max}}{S_v} = Y_m$. Then it is shown in Appendix C that this stress concentration may be closely approximated by the following formulae:-

3.1.1 For an elliptical hole (theoretically exact solution)

$$Y_m = (1-k) + 2(\frac{w}{h}) \qquad (11a)$$

3.1.2 For a rectangular hole (with rounded corners)

(approximation in range $0.25 < w/h < 4.0$)

$$Y_m = (2.048-0.919k) + 0.572 \log_e (\frac{w}{h}) \qquad (11b)$$

3.1.3 For an ovaloidal opening (approximation in range $0.25 < \frac{w}{h} < 4.0$)

$$Y_m = (2.97-1.044k) + 1.327 \log_e (\frac{w}{h}) \qquad (11c)$$

3.2 Approximate vertical stress distribution along the horizontal axis at the mid height, of a single hole of various shapes, under any applied stress ratio k

3.2.1 Approximate vertical stress distribution curve

Consider any single opening, of width-height ratio $\frac{w}{h}$, as illustrated in Figure 3. Let the centre of the hole be the origin of coordinate axis X and Y. Let Y be the vertical stress concentration, $\frac{\sigma_p}{S_v}$, and let $X = \frac{e}{w}$ where e is the distance along the horizontal axis from the centre of the hole and w is the semi-width of the hole (i.e. at the boundary of the hole on the horizontal axis $X = 1$).

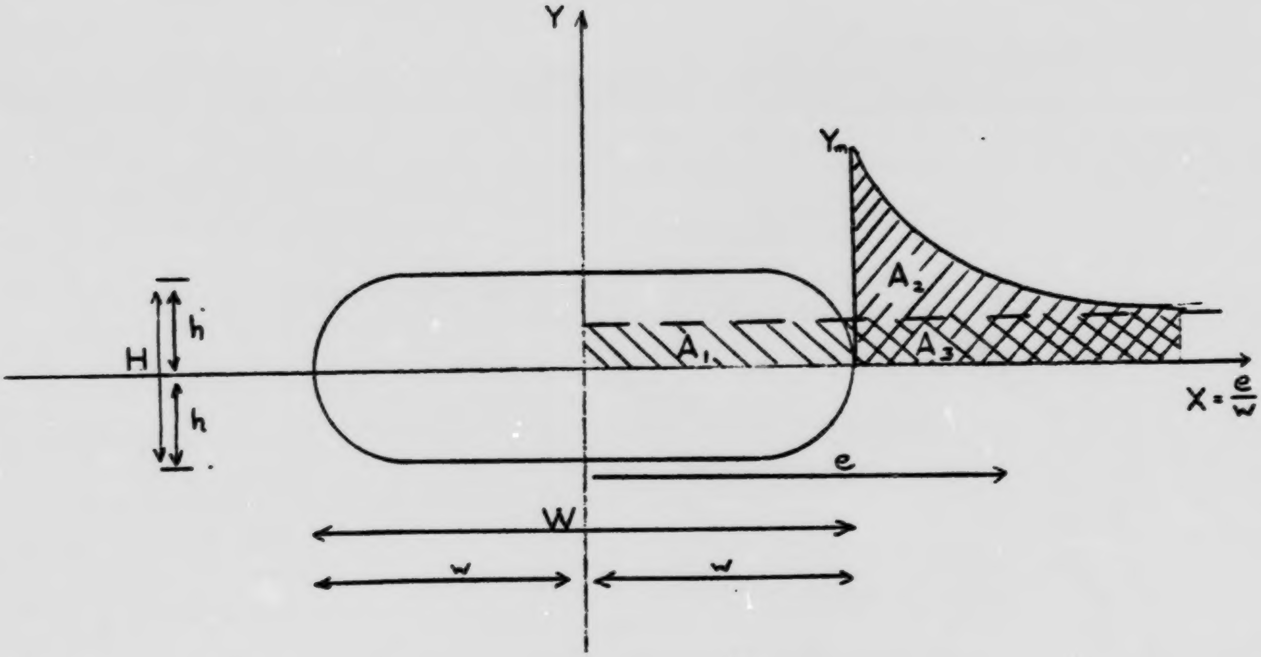
Y
Ym
A1
A2
A3
h
H
h
X = e/w
e
W
w
w

FIGURE 3: Vertical stress distribution along the horizontal axis, at the mid height, for a single opening

Now the vertical stress distributuion along the horizontal axis must satisfy three criteria:-

(i) When $X=1$ (i.e. at the boundary), the maximum stress concentration, Y_m, must be that given by equations 11a, 11b, or 11c, for the appropriate shape and stress ratio.

(ii) When X is large then the stress concentration, Y, must approach unity. (i.e. the virgin stress is approached at a large distance from the opening).

(iii) The total re-distributed load, as represented by the area A_2+A_3 under the stress distribution curve illustrated in Figure 3, must be equal to the total applied load before creation of the opening and represented by the area A_1+A_3.

Now the criteria (i) and (ii) suggest a curve whose maximum occurs at $X=1$ and which approaches an assymptotic value when X is large; this suggests that the curve might be approximated by a curve of hyperbolic form given by:-

$$Y = \frac{k_1}{(X+k_2)} + k_3 \qquad (12)$$

where k_1, k_2 and k_3 are constants.

A curve of this form will be assumed to approximate the stress distribution curve and the results of this approximation will be checked against real theoretical and experimental data. For any particular case it is therefore necessary to determine k_1, k_2 and k_3 from the criteria given above, as follows:-

To satisfy criterion (ii) it is assumed that when $X=10$ then $Y=1$, i.e. the virgin vertical stress is reached at a distance of 5 diameters (10w) from the opening. Now the area under this stress distribution curve is therefore given by:

$$A_2+A_3 = \int_1^{10} Y.dX = \int_1^{10} \left\{ \frac{k_1}{(x+k_2)} + k_3 \right\} dX$$

$$= \Big[k_1 \log_e(X+k_2) + k_3 X \Big]_1^{10}$$

$$= k_1 \log_e\left(\frac{10+k_2}{1+k_2}\right) + 9k_3$$

but to satisfy criterion (iii), this area must be equal to the mean load prior to creation of the opening, which equals $A_1+A_3 = 10 \times \frac{S_v}{S_v} = 10$.

Hence from criterion (ii) we have:

$$10 = k_1 \log_e \left\{\frac{10+k_2}{1+k_2}\right\} + 9k_3 \tag{13}$$

From criterion (i), when X=1 then $Y=Y_m$ the maximum stress concentration on the boundary as given by the appropriate equation 11 depending on the opening shape.

Thus substituting into equation 12 gives:-

$$\left\langle Y_m - k_3 \right\rangle = \frac{k_1}{(1+k_2)} \tag{14}$$

and to satisfy criterion (ii), as previously stated, when X=10 then Y=1. Hence substituting into equation 12 gives:-

$$(1-k_3) = \frac{k_1}{(10+k_2)} \tag{15}$$

Hence the three unknown constants k_1, k_2 and k_3 can be obtained from evaluation of these three equations:-

Eliminating k_3 from equations 14 and 15 gives:-

$$k_1 = \frac{(Y_m-1)(1+k_2)(10+k_2)}{9} \tag{16}$$

and eliminating k_1 gives:-

$$k_3 = \frac{(10-Y_m) - k_2(Y_m-1)}{9} \tag{17}$$

Hence, substituting into equation 13, from equations 16 and 17 for k_1 and k_3, and re-arranging gives:-

$$\frac{(Y_m-1)(1+k_2)(10+k_2)}{9} \log_e \left\{\frac{10+k_2}{1+k_2}\right\} - k_2(Y_m-1) - Y_m = 0 \tag{18}$$

Since Y_m is known then this equation may be solved for k_2. Having determined k_2 then equations 16 and 17 can be used to determine k_1 and k_3.

3.2.2 Comparison of approximate stress distribution with theoretical and experimental data

(A) For an ellipse under uniaxial load (k=0)

Table 3.1 gives the vertical stress distribution along the horizontal axis for four ellipses of width to height ratios ranging from 0.25 to 4.0, when under uniaxial compression (k=0). The theoretical values are taken from Obert and Duvall (8) and the approximate values are calculated using the procedure described above.

Figure 4 compares the theoretical data with the approximations; they are seen to be in excellent agreement.

(B) For a circular opening under a range of stress ratios

Table 3.2 lists the vertical stress distribution along the horizontal axis for a circular hole under a stress ratio k ranging from 0 to 2. The theoretical solution is given by the following equations:-

$$\sigma_\theta = \left\{\frac{S_H+S_V}{2}\right\}\left\{1+\frac{a^2}{r^2}\right\} - \left\{\frac{S_H-S_V}{2}\right\}\left\{1+\frac{3a^4}{r^4}\right\}\mathrm{Cos}\ 2\theta$$

and on the horizontal axis, $\theta=0$ and $r/a = X$, hence:-

$$Y = \frac{\sigma_\theta}{S_V} = \left\{\frac{1+k}{2}\right\}\left\{1 + \frac{1}{X^2}\right\} - \left\{\frac{k-1}{2}\right\}\left\{1 + \frac{3}{X^4}\right\}$$

The results of the approximate stress distribution obtained by using the method described above are also given in this table. Figure 5 gives a graphical comparison of these results for k = 0 and k = 1.0 .

In this case the approximation is in excellent agreement with theory for k ratios up to 1.5 . When K = 2 the error is large. Thus it is suggested that the approximation only be used in the range of k from 0 to 1.5 .

(C) For a rectangular opening, w/h = 10/12, k = 0.10

Table 3.3 compares the results obtained by the approximation method with a finite element solution (10) for a rectangular opening when w/h = 10/12 and k = 0. 10 . Figure 6 shows the graphical comparison of these results.

Again the approximation appears to be quite good and is acceptable.

TABLE 3.1: Vertical Stress Concentrations Along the Horizontal Axes of Ellipses, Under Uniaxial Stress (k = 0)

w/h = 0.25				w/h = 0.5				w/h = 2.0				w/h = 4.0			
Y max	1.5	1.5	-	Y max	2.0	2.0	-	Y max	5.0	5.0	-	Y max	9.0	9.0	-
k_1	-	.9875	-	k_1	-	.4820	-	k_1	-	.2509	-	k_1	-	.2054	-
k_2	-	.6665	-	k_2	-	-.5414	-	k_2	-	-.9377	-	k_2	-	-.9744	-
k_3	-	.9075	-	k_3	-	.949	-	k_3	-	.9723	-	k_3	-	.9772	-
X	Y*	Y**	% Dif.	X	Y*	Y**	% Dif.	X	Y*	Y**	% Dif.	X	Y*	Y**	% Dif.
1.0	1.5	1.5	0	1.0	2.0	2.0	0	1.0	5.0	5.0	0	1.0	9.0	9.0	0
1.75	1.336	1.3161	1.49	1.383	1.62	1.5217	6.07	1.108	2.675	2.4457	8.57	1.063	3.327	3.2953	0.95
2.429	1.229	1.2264	0.21	1.743	1.403	1.3501	3.77	1.228	1.928	1.8367	4.73	1.143	2.210	2.1954	0.66
3.062	1.160	1.1723	-1.06	2.088	1.273	1.2607	0.97	1.356	1.596	1.5722	1.49	1.234	1.773	1.7684	0.26
3.668	1.114	1.1352	-1.90	2.422	1.194	1.2503	-4.71	1.489	1.419	1.4275	-0.6	1.333	1.548	1.5500	-0.13
4.250	1.084	1.1083	-2.24	2.750	1.141	1.1673	-2.3	1.625	1.313	1.3374	-1.86	1.438	1.414	1.4203	-0.45
4.818	1.063	1.0875	-2.30	3.073	1.106	1.1394	-3.01	1.764	1.243	1.276	-2.65	1.546	1.325	1.3366	-0.87
5.375	1.047	1.0709	-2.28	3.392	1.083	1.1181	-3.24	1.904	1.196	1.2320	-3.01	1.656	1.263	1.2786	-1.23
5.923	1.038	1.0573	-1.86	3.708	1.061	1.1012	-3.8	2.046	1.161	1.1987	-3.25	1.769	1.219	1.2357	-1.37
6.464	1.030	1.0459	-1.54	4.022	1.053	1.0875	-3.3	2.189	1.135	1.1728	-3.33	1.884	1.184	1.2030	-1.60
7.0	1.024	1.0362	-1.19	4.334	1.044	1.0761	-3.1	2.333	1.126	1.1521	-2.32	2.0	1.158	1.1775	-1.68
8.321	1.015	1.0173	-0.23	5.107	1.029	1.0546	-2.5	2.696	1.081	1.1150	-3.14	2.295	1.113	1.1328	-1.78
9.625	1.010	1.0034	+.65	5.875	1.020	1.0394	-1.91	3.062	1.060	1.0904	-2.87	2.594	1.083	1.1041	-1.95

* from Obert and Duvall (8)

** Calculated from approximation $Y = \frac{k_1}{(X+k_2)} + k_3$

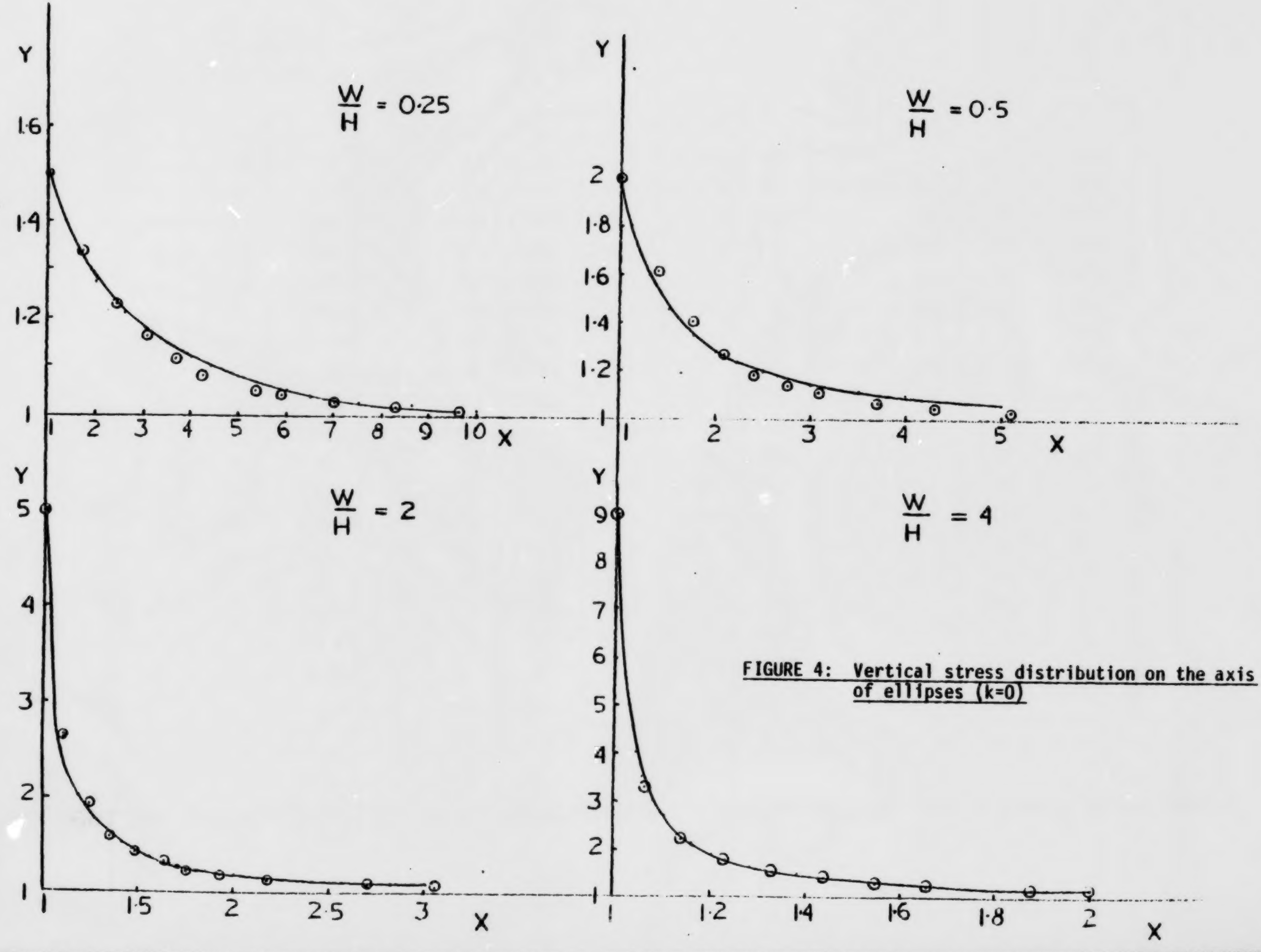

FIGURE 4: Vertical stress distribution on the axis of ellipses (k=0)

TABLE 3.2: Vertical Stress Distribution Along Horizontal Axis of a Circular Opening, Under a Range of Stress Ratios

	k = 0			k = 1/3			k = 1			k = 1.5		
Y_m	3.0	2.97		2.67	2.62		2.0	1.93		1.5	1.41	
k_1	-	.3288			.3610			.5084			1.424	
k_2	-	-.8361			-.7824			-.483			1.677	
k_3	-	.9641			.9608			.9466			.878	
X	Y*	Y**	%	Y*	Y**	%	Y*	Y**	%	Y*	Y**	%
1.0	3.0	2.97	1.0	2.67	2.62	1.9	2.0	1.93	3.6	1.5	1.41	6.4
1.25	1.93	1.758	9.8	1.84	1.733	6.2	1.64	1.61	1.9	1.49	1.365	9.1
1.5	1.52	1.459	4.2	1.49	1.464	1.8	1.44	1.446	-0.4	1.41	1.326	6.3
1.75	1.32	1.324	-0.3	1.32	1.334	-1.0	1.33	1.348	-1.3	1.33	1.294	2.8
2.0	1.22	1.247	-2.2	1.23	1.257	-2.1	1.25	1.282	-2.5	1.27	1.265	0.4
2.5	1.12	1.162	-3.6	1.13	1.171	-3.5	1.16	1.199	-3.2	1.18	1.219	-3.2
3.0	1.07	1.116	-4.1	1.09	1.124	-3.0	1.11	1.149	-3.3	1.129	1.182	-4.5
3.5	1.05	1.087	-3.4	1.06	1.094	-3.1	1.08	1.115	-3.1	1.097	1.153	-4.8
4.0	1.037	1.068	-2.9	1.045	1.073	-2.6	1.06	1.091	-2.8	1.075	1.129	-4.8
5.0	1.022	1.043	-2.0	1.028	1.046	-1.7	1.04	1.059	-1.8	1.049	1.091	-3.8
6.0	1.015	1.027	-1.1	1.019	1.030	-1.1	1.028	1.039	-1.1	1.034	1.064	-2.8
7.0	1.011	1.017	-0.6	1.014	1.019	-0.5	1.020	1.025	-0.5	1.025	1.042	-1.6
8.0	1.008	1.010	-0.2	1.011	1.011	0	1.016	1.014	0.2	1.019	1.025	-0.5
9.0	1.006	1.004	0.2	1.008	1.005	0.3	1.012	1.006	0.6	1.015	1.011	0.4
10.0	1.005	1.00	0.5	1.007	1.00	0.7	1.010	1.0	1.0	1.012	1.0	1.2

* from Obert and Duvall (8)

** by approximation

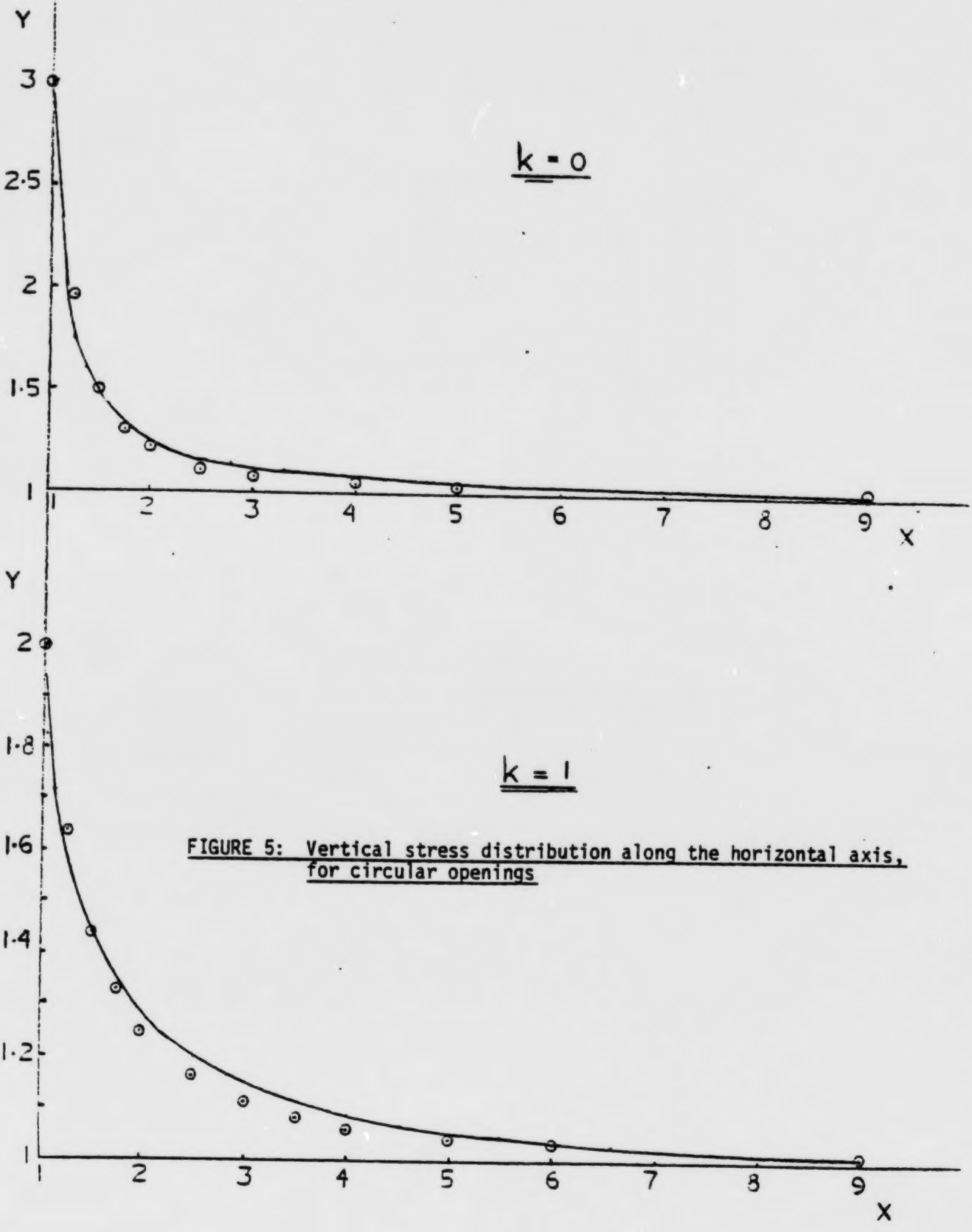

FIGURE 5: Vertical stress distribution along the horizontal axis, for circular openings

TABLE 3.3: Vertical Stress Distribution Along Horizontal Axis of a Rectangular Hole, $\frac{w}{h} = \frac{10}{12}$, $k = 0.1$

w/h = 0.833 k = 0.1			
Y_m	1.60	1.852	
k_1	-	.5446	
k_2	-	-.4007	
k_3	-	.9433	
X	Y*	Y**	% Dif.
1.0	1.60	1.852	-13.6
1.06	1.55	1.769	-12.4
1.26	1.50	1.577	- 4.9
1.67	1.40	1.372	2.0
2.04	1.30	1.276	1.9
2.50	1.20	1.203	- 0.2
2.74	1.15	1.176	- 2.2
3.50	1.10	1.119	- 1.7
4.68	1.05	1.071	- 1.9

* from finite element solution (10)

** from approximation

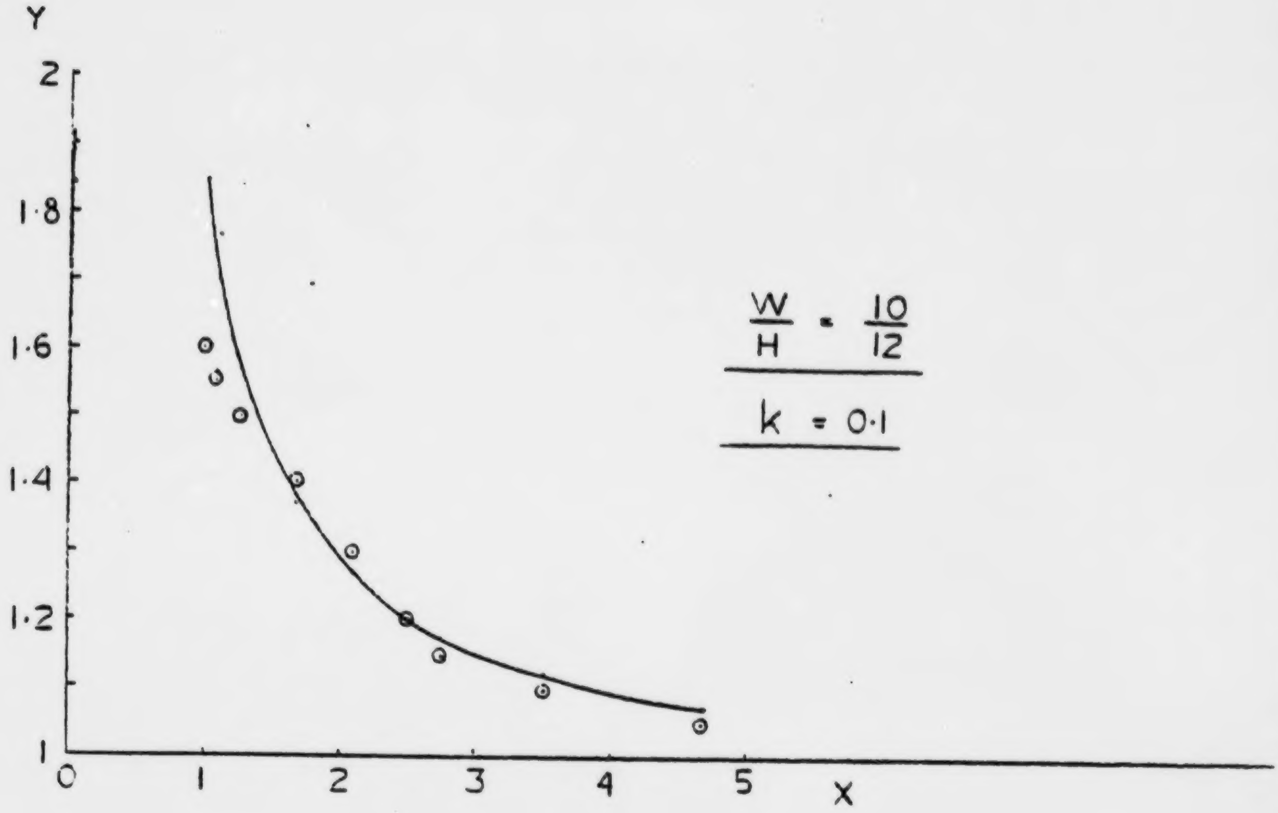

FIGURE 6: Vertical stress distribution along the horizontal axis, for a rectangular hole (h/w = .833, k = 0.1)

3.2.3 Conclusion

The stress distribution along the horizontal axis of single openings of various shapes at their mid height can be approximated using the approach given above. Comparison of the results using this approximation with theoretically and experimentally derived data gives close agreement provided that the stress ratio k is < 1.5 and $0.25 < w/h < 4.0$.

Although the section does not add directly to the determination of the stress distribution across a pillar (Step 2, Figure 1) it has been carried out to establish the validity of the approximation method. This method will now be applied to the pillar problem in the next section.

4. Approximate vertical stress distribution, along the horizontal axis of the side wall, for pillars with equal size openings on either side

4.1 Maximum stress concentration, Y_{mm}, at the mid height of the side wall of multiple openings

Let the maximum stress concentration at the mid height of the side wall on the horizontal axis for multiple holes of height H and width W under an applied stress ratio k be Y_{mm}. Let $\overline{Y} = \frac{\sigma_p}{S_v}$ the mean pillar stress concentration. Then it is shown in Appendix D that this stress concentration Y_{mm} may be closely approximated by the following formulae:-

4.1.1 For row of ovaloidal openings

Either $$\underline{Y_{mm} = (2.97 - 1.044k) + 1.327 \log_e \left(\frac{W}{H}\right) + 0.09 \left\{\left(\frac{W}{B} + 1\right)^2 - 1\right\}} \qquad (18)$$

or $$\underline{Y_{mm} = \overline{Y}} \qquad (19)$$

whichever be the larger value.

4.1.2 For a row of elliptical openings

Either $$\underline{Y_{mm} = (1 - k) + 2\left(\frac{W}{H}\right) + 0.09 \left\{\left(\frac{W}{B} + 1\right)^2 - 1\right\}} \qquad (20)$$

or $$Y_{mm} = \overline{Y}$$

whichever be the larger value.

4.1.3 For a row of rectangular openings

Either $$\underline{Y_{mm} = (2.048-0.919k) + 0.572 \log_e \left(\frac{W}{H}\right) + 0.09 \left\{\left(\frac{W}{B} + 1\right)^2 - 1\right\}} \qquad (21)$$

or $$\underline{Y_{mm} = \overline{Y}} \qquad (19)$$

whichever be the larger value.

The above formulae therefore gives the expressions necessary to accomplish Step 2 in Figure 1.

4.2 Approximate stress distribution across a pillar when $Y_{mm} = \overline{Y}$

As pointed out in Appendix D, for those cases above when the maximum stress concentration in the pillar along the horizontal axis at the mid height is approximately equal to the average pillar stress $\overline{Y}$, then it follows that the stress distribution across the pillar must be constant and equal to $\overline{Y}$.

4.3 Approximate vertical stress distribution when $Y_{mm} > \overline{Y}$, for pillars with equal size openings on either side

The vertical stress distribution curve across the pillar must, in this case, be symetrical about the centre of the pillar; hence only one half of this curve (i.e. one side) need be considered here since the other half will be its' mirror image, as illustrated in Figure 7.

It is assumed that the mean pillar stress concentration $\overline{Y}$ is known since it can be calculated from Coates' pillar formulae given in Section 2 for the appropriate position of the pillar in the mining span.

It is also assumed that the stress distribution curve can be approximated by an equation of hyperbolic form, as was established for the single opening case in Section 3.

$$\text{i.e.} \quad Y = \frac{k_1}{(X+k_2)} + k_3$$

where Y is the stress concentration factor $(\frac{\sigma_p}{S_v})$ at a distance e from the centre of the room, where $X = \frac{e}{w}$, where w is the semi-opening width.

It is also assumed that this stress concentration diminishes with distance from the opening such that, if it were to extend 5 diameters (10w) away from the room then the stress concentration would have reached the virgin stress concentration factor.

$$\text{i.e. when } X = \frac{e}{w} = 10 \text{ then } Y = 1$$

Further, at the boundary of the opening (X = 1) then $Y = Y_{mm}$ the maximum stress concentration factor given by equations 18, 20 or 21 for the appropriate shape of the room.

$$\text{i.e. when } X = 1 \quad Y = Y_{mm}$$

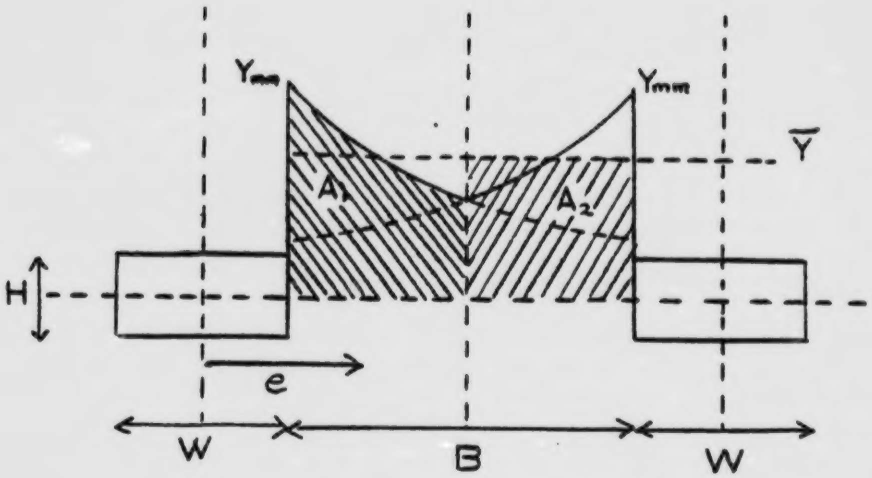

Y_{max}
Y_{max}
$\overline{Y}$
A_1
A_2
H
e
W
B
W

FIGURE 7: Schematic of the stress distribution across a pillar

Finally, for compatability of loads, the load represented by the area under the stress distribution curve across half the pillar, A_1, must be equal to the load represented by the mean pillar stress acting across that half a pillar, A_2.

$$\text{i.e.} \quad \overline{Y}\left(\frac{B}{W}\right) = \int_1^{(1+\frac{B}{W})} Y dX$$

Hence as with the single opening case, there are three criteria to be satisfied from which the three constants k, k_2, and k_3 can be determined:-

(i) when X=1, $Y=Y_{mm}$, hence

$$Y_{mm} = \frac{k_1}{(1+k_2)} + k_3 \tag{22}$$

(ii) when X=10 Y=1, hence

$$\underline{1 = \frac{k_1}{(10+k_2)} + k_3} \tag{23}$$

and (iii)

$$\overline{Y}\left(\frac{B}{W}\right) = \int_1^{(1+\frac{B}{W})} Y dX = \int_1^{1+\frac{B}{W}} \left\{\frac{k_1}{(X+k_2)} + k_3\right\} dX$$

$$= \Big[k_1 \log_e (X+k_2) + k_3 X\Big]_1^{(1+\frac{B}{W})}$$

i.e.

$$\underline{\overline{Y}\left(\frac{B}{W}\right) = k_1 \log_e\left\{\frac{1+\left(\frac{B}{W}\right) + k_2}{(1+k_2)}\right\} + k_3\left(\frac{B}{W}\right)} \tag{24}$$

Thus from equations 22 and 23 it can be shown that :-

$$\underline{k_1 = \frac{(Y_{mm}-1)(1+k_2)(10+k_2)}{9}} \tag{25}$$

and

$$k_3 = \left\{\frac{(10-Y_{mm}) - k_2(Y_{mm}-1)}{9}\right\} \tag{26}$$

and, substituting into equation (24) from equation 25 and 26, and re-arranging gives:-

$$\frac{(Y_{mm}-1)(1+k_2)(10+k_2)}{9}\log_e\left\{\frac{(1+\frac{B}{W}+k_2)}{(1+k_2)}\right\}+\left\{\frac{(10-Y_{mm})-k_2(Y_{mm}-1)}{9}\right\}\frac{B}{W}-\bar{Y}\cdot\frac{B}{W}=0 \qquad (27)$$

Since Y_{mm} is known then this equation may be solved for k_2. Having determined k_2 then equations 25 and 26 can be used to determine k_1 and k_3.

4.4 Comparison of the approximate stress distribution with theoretical and experimental data

4.4.1 Pillars in an infinite row of equally spaced circular holes

Savin (4, Page 150, Table 35) has derived a theoretical solution for the stress distribution across the pillars between an infinite number of equally spaced circular holes under uniaxial load,

$$(\text{ i.e. } \frac{W}{H} = 1, \quad \frac{W}{B} = 1 \quad \text{and } k = 0).$$

Table 4.1 lists Savin's results and also lists the results obtained by this approximation method. Figure 8 compares the two solutions. It is seen that the approximation gives an excellent representation of this theoretical data.

TABLE 4.1: Stress Concentrations Across a Pillar - Infinite Number of Equally Spaced Holes

ITEM	Results from Savin (4)	Approximation method, $\frac{W}{H} = 1$, $\frac{W}{B} = 1$, $k = 0$	
$\bar{Y}$	2.0	2.0	
W	1	1	
B	1	1	
Y_{mm}	3.24	3.24 from equation (18)	
k_1	-	0.7916	
k_2	-	-0.6595	
k_3	-	0.9513	
X=e/w	Y	Y	% Difference
1.0	3.24	3.24	0
1.2	2.36	2.38	-0.8
1.4	1.94	1.98	-2.0
1.6	1.74	1.76	-1.1
1.8	1.64	1.61	+1.9
2.0	1.61	1.51	+6.6

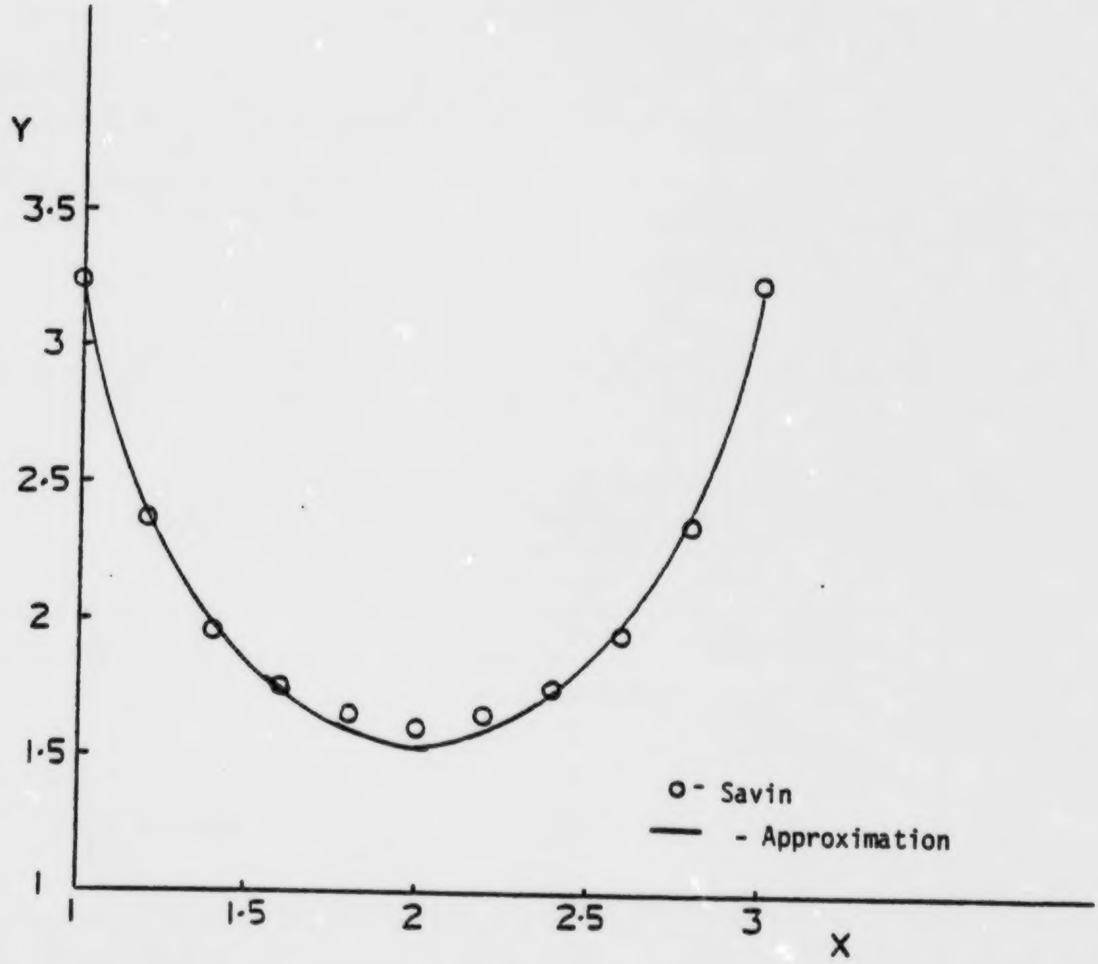

FIGURE 8: Comparison of Savin's results (6) with approximation

4.4.2 A four by four rectangular pillar layout

Logie (11) has conducted a three dimensional photoelastic study of the stress distributions in pillars in a four by four rectangular pillar layout. Table 4.2 gives the vertical stress concentrations at the mid height across one of the central pillars as determined by Logie for three different cases with different (W/B) and (W/H) ratios. Also tabulated are the results for the approximate stress distributions determined for these three cases using the preceeding approximation method; note that in this three dimensional case $\overline{Y}$ was determined from tributary area theory from $\overline{Y} = \frac{1}{(1-R)}$. Figure 9 compares Logie's solution with that using the approximation method.

Case 1, W/B = 0.415, W/H = 0.5 In this case the two solutions are in good agreement, although the maximum stress concentration on the pillar side wall determined by Logie is significantly less than that given by the approximation method.

Case 2, W/B = 0.414, W/H = 1.38 In this case the two solutions do not compare well. Logie's stress concentrations are all lower than that determined by the approximation method; once again the maximum stress concentration at the pillar wall is very much less than that given by the approximation method. Indeed this particular stress concentration factor of 1.75 is less than the mean pillar stress concentration determined by tributory area theory; it is difficult to see how this could possibly occur and must therefore raise some doubts as to the accuracy of Logie's experimental solution, particularly at the boundary.

Case 3, W/B = 1.24, W/H = 4.14 In this case the comparison of the two solutions is very poor. The approximation method involves the "small pillar" formula in which $Y_{mm} = \overline{Y}$ and this gives a uniform stress distribution across the pillar equal to a concentration of 5.0 . Logie's solution gives a quite rapidly changing stress distribution.

If, for Logie's results, the slope of the curve $\frac{\Delta Y}{\Delta X}$ is compared between Cases 2 and 3 over approximately the same range of X then the following results are obtained.

	X_1	X_2	ΔX	Y_1	Y_2	ΔY	$\Delta Y/\Delta X$
Case 2	1.31	2.02	-0.71	2.06	1.56	0.50	-0.704
Case 3	1.39	1.53	-0.14	3.80	3.34	0.46	-3.28

TABLE 4.2: Comparison of Approximation with Logie's Results (11) for Rectangular Rooms

PARAMETER	CASE 1			CASE 2			CASE 3		
k	0			0			0		
W/B	0.15			0.414			1.24		
W/H	0.5			1.38			4.14		
$R = \frac{(\frac{W}{B})^2 +1 -1}{(\frac{W}{B})^2 +1}$	0.244			0.50			0.80		
$\overline{Y} = \frac{1}{(1-R)}$ (Trib. Area)	1.32			2.0			5.0		
Y_{mm} (from Equation 21)			1.68			2.32			3.22
	X	Y (Logie)	Y Approx.	X	Y (Logie)	Y Approx.	X	Y (Logie)	Y Approx
k_1	-	-	8.403	-	-	17.26	-	-	
k_2	-	-	5.966	-	-	6.24	-	-	$\overline{Y}>Y_{mm}$
k_3	-	-	0.4737	-	-	-0.062	-	-	
	1.0	1.43	1.68	1.0	1.75	2.32	1.0	5.70	5.0
	2.0	1.47	1.529	1.31	2.06	2.22	1.1	5.95	5.0
	3.10	1.34	1.400	2.02	1.56	2.03	1.24	4.76	5.0
	4.5	1.25	1.277	3.42	Mid.	1.72	1.39	3.80	5.0
	7.7	Mid.	1.08				1.53	3.34	5.0
							1.81	Mid.	5.0

FIGURE 9: Comparison of Logie's results (11) with approximation

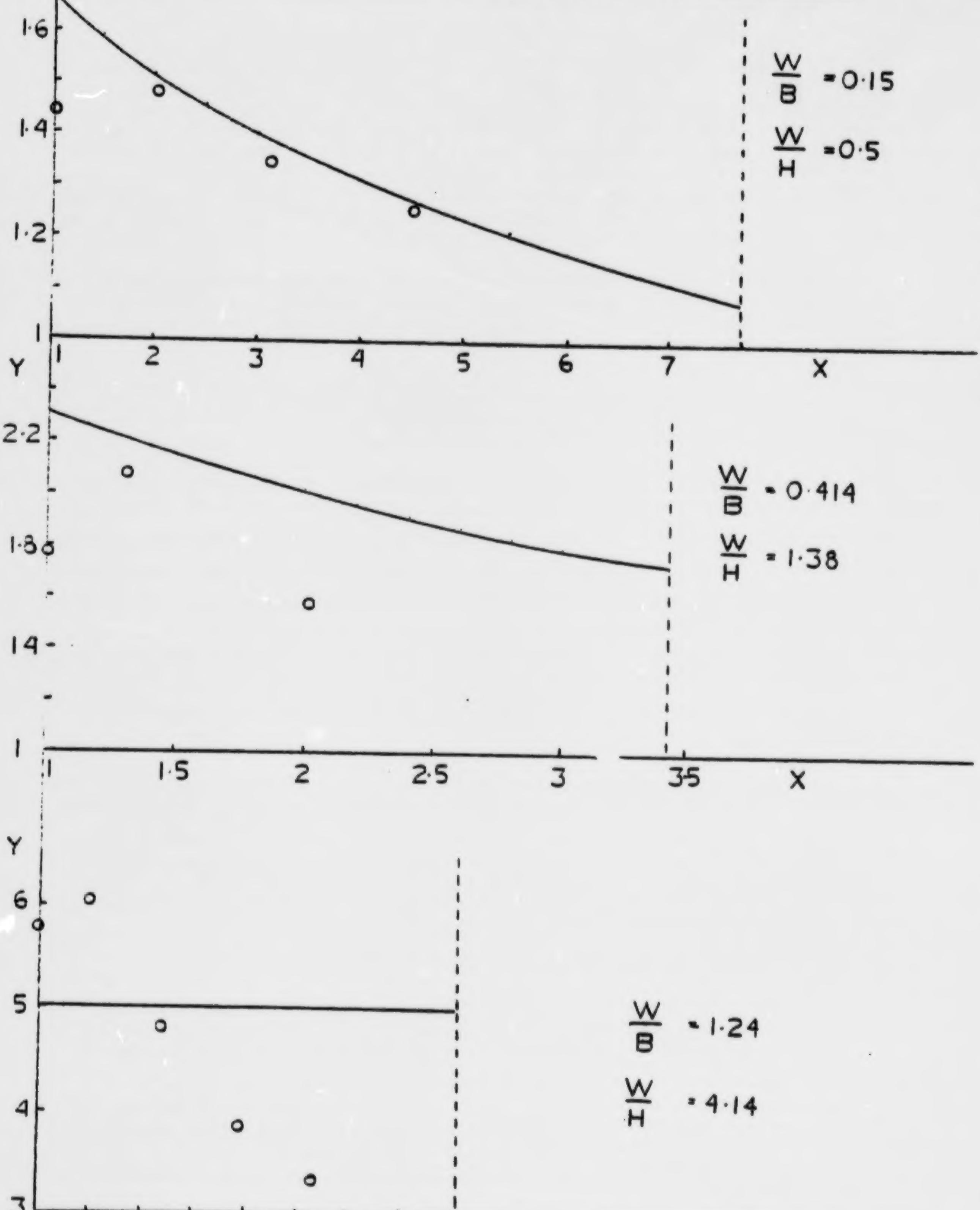

It is seen that the rate of change of Y with X is much greater in Case 3 than in Case 2; this is contrary to the observations of Obert and Duvall (see Appendix D) who noted that as the average stress concentration increases the stress distribution across the pillar becomes more uniform. Similarly the results of Yu and Toews (12), discussed in more detail in the next section 4.4.3, confirm the observations of a nearly uniform stress distribution across the mid height of the pillar for small pillars. Hence, once again, some doubts must be expressed with respect to the accuracy of Logie's results using the difficult experimental techniques of three dimensional photoelasticity.

Consequently it must be concluded that the approximation method does not agree very well with the experimental results obtained by Logie. There does however appear to be reasonable grounds to suspect the accuracy of Logie's results.

4.4.3 Three dimensional finite element solution for stress distribution at the mid height of pillars

Yu and Toews (12) developed a three dimensional finite element solution for the stresses in rectangular pillars and examined the effects of the stiffness ratio between the pillar and roof rock ($^{E}p/E_r$), of the extraction ratio R, and the pillar heights (H_p). Figure 10 shows the stress distributions in these pillars for 9 cases they considered. The nomenclature used by them and given in these figures is:- $^{\sigma_1}/p$ = major principal stress concentration (which on the axis of symmetry at the mid pillar height is the same as the vertical stress concentration); W_p = pillar width (c.f. B in this paper) B_p = pillar depth (not used in this paper), W_R = room width (W in this paper) and R equals the three dimensional extraction ratio.

Table 4.3 transposes the nomenclature to that used in this paper and gives the appropriate dimensionless ratios, the extraction ratio R, Y_{mm} as calculated from equation 21, $\overline{Y}$ as determined by tributary area theory, $\overline{Y}$ as determined from Coates' pillar hypothesis and Yu and Toews stress concentrations at the pillar centre, at the mid height of the edge and the mean of these two values, for each of the cases A to I. (Note that in each case, the $\overline{Y}$ determination by Coates' hypothesis assumed a span containing 100 pillars).

The following observations are made:-

(i) The vertical stress distribution across the pillar centre at the mid height obtained by Yu and Toews is in all cases quite uniform. The value of Y_{mm} determined from the approximation method using Equation 21 is in all cases less than $\overline{Y}$ given either by tributary area theory or by Coates' hypothesis. Hence the approximation method involves the uniform stress distribution solution equal to $\overline{Y}$, i.e. both the approximation method and the results of Yu and Toews indicate that the stress distribution is approximately uniform.

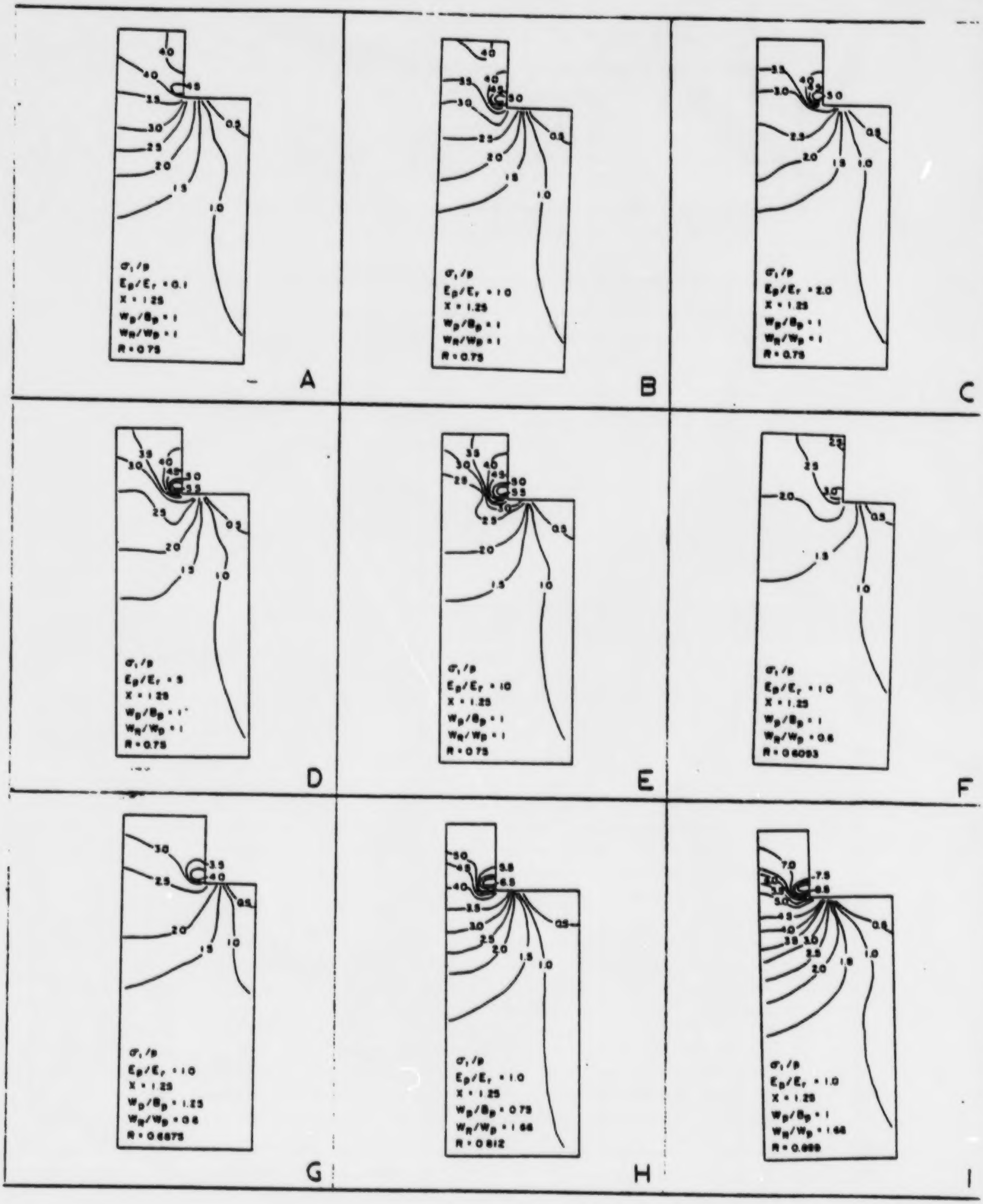

FIGURE 10: Stress distributions in pillars determined by Yu and Toews (12)

TABLE 4.3: Comparison with Results of Yu and Toews ' Finite Element Solution for Rectangular Pillars (12)

									Yu and Toews		
FIGURE	W/B	B/Bd	W/H	R	Ep/Er	Ymm from Eq. 21	$\overline{Y}$ (trib. area)	$\overline{Y}$ (Coates)	at Centre	at Edge	Mean
A	1	1	1	0.75	0.1	2.32	4	3.97	4.3	3.9	4.1
B	1	1	1	0.75	1.0	2.32	4	4.25	4.0	3.9	3.95
C	1	1	1	0.75	2	2.32	4	4.27	3.8	3.8	3.8
D	1	1	1	0.75	5	2.32	4	4.28	3.5	3.8	3.65
E	1	1	1	0.75	10	2.32	4	4.285	3.3	3.8	3.55
F	0.6	1	0.77	0.61	1	2.04	2.56	2.70	2.4	2.5	2.45
G	0.6	1.25	0.77	0.69	1	2.04	3.22	3.42	3.1	3.4	3.25
H	1.66	0.75	1.23	0.81	1	2.71	5.26	5.61	5.3	5.4	5.35
I	1.66	1	1.23	0.86	1	2.71	7.14	7.59	7.2	7.4	7.3

(ii) The values of $\overline{Y}$ given by tributary area theory and Coates' hypothesis are in reasonably good agreement with the mean value of this "uniform stress" distribution obtained by taking the mean of the concentration at the pillar centre and at the edge from Yu and Toews results. The maximum difference of 17% occurs in Case E when comparing with Coates' hypothesis when the stiffness ratio E_p/E_r is at the extreme value of 10.

(iii) The effects of varying the stiffness ratio E_p/E_r is interesting since, while it is neglected in tributary area theory, the results obtained by Yu and Toews show the directly opposite influence to that predicted by Coates' hypothesis, i.e. as E_p/E_r increased the stress concentration factors decrease in Yu and Toews results but increase using Coates' hypothesis. However it should be noted that Coates' (3,Page 90) cautioned that the range of the value of the parameter $n = \frac{E_r}{E_p} \{\frac{1- \mu_p^2}{1- \mu_r^2}\}$ covered by his experimental data was only from 1 to 1.7 and that for values of n outside this range, the hypothesis would have to be used with caution.

(iv) Despite the fact that Coates' hypothesis may be questionable in so far as the influence of the stiffness ratio, it is still believed to be better than tributary area theory since it deals far more satisfactorily with the influence of the other parameters such as position in the mining span etc.

It may therefore be concluded that the comparison between the results of the approximation method and those of Yu and Toews is quite acceptable. It is unfortunate that Yu and Toews did not derive any solutions for other than "small pillars"; consequently no results were available from them to compare against the approximation method for the "large pillar" cases.

4.5 Conclusion

The author has not been able to locate additional solutions in the literature against which to compare this approximation method; clearly additional comparisons should be made if or when they become available. Nonetheless for those comparisons which have been made the agreement is good, with the exception of some of Logie's data for which other factors raise doubts as to the accuracy of his experimental data. Consequently, while this approximation method cannot be said to be "proven", there seems to be sufficient evidence that it gives quite acceptable results and may therefore be used in this analysis procedure.

This therefore effectively completes Step 3 of Figure 1; the vertical elastic stress distribution can be approximated.

5. Fracture zone development in pillars - theoretical analysis

5.1 Stresses on the i th slice of solid coal

Divide the pillar into n_1 slices, each of width δe, as illustrated in Figure 11.

Then :-

$$\delta e = \frac{B}{n_1} \qquad (28)$$

Now the vertical stress concentration, Y, acting at the centre of any slice is given by :-

$$\underline{Y = \frac{k_1}{(k_2 + X)} + k_3}$$

where $X = \frac{e}{w}$, and e is the distance of the centre of that slice from the centre of the opening and w is the semi-width of the opening. Hence the vertical stress concentration on the first slice is given by :-

$$Y_1 = \frac{k_1}{(k_2 + X_1)} + k_3 \quad \text{where} \quad X_1 = \frac{w + \delta e/2}{w} = 1 + \frac{\delta e}{2w} = 1 + \frac{B}{n_1 W}$$

similarly the vertical stress concentration acting on the second slice is given by :-

$$Y_2 = \frac{k_1}{(k_2 + X_2)} + k_3 \quad \text{where} \quad X_2 = 1 + \frac{3}{2}\frac{\delta e}{w} = 1 + \frac{3B}{n_1 W}$$

Hence the vertical stress concentration acting on the i th slice is given by :-

$$Y_i = \frac{k_1}{(k_2 + X_i)} + k_3 \quad \text{where} \quad X_i = 1 + \frac{(2i-1)}{n_1}\left(\frac{B}{W}\right)$$

i.e.

$$\underline{\underline{Y_i = \frac{k_1}{\left[k_2 + 1 + \frac{(2i-1)}{n_1}\left(\frac{B}{W}\right)\right]} + k_3}} \qquad (29)$$

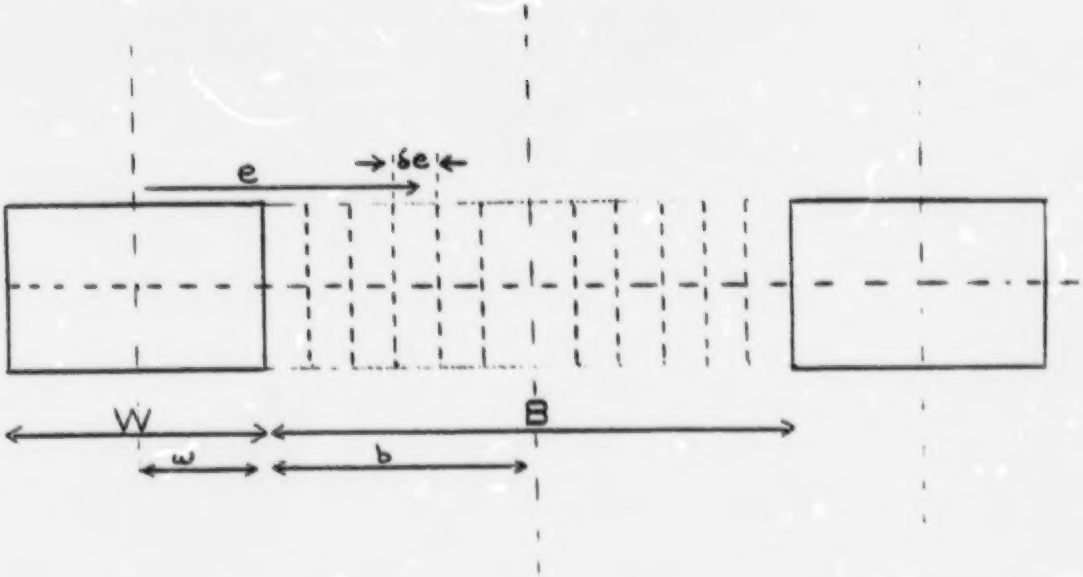

$$X = \frac{e}{\omega}$$

FIGURE 11: Pillar divided into n_1 slices, each of width $\delta e = \frac{B}{n_1}$

and the vertical stress, σ_{1i}, acting on this slice is given by:-

$$\sigma_{1i} = \gamma_i \, . \, S_v \qquad (30)$$

Thus, given k_1, k_2 and k_3, as determined previously, equations 29 and 30 can be used to determine the vertical stress concentration and the applied vertical stress respectively, acting on the centre of each slice prior to any failure occuring i.e. it approximates the elastic stress distribution across the pillar prior to failure. This is illustrated by example in Appendix E.

Two further points should be noted here. Firstly, with respect to the horizontal stress, σ_{3i}, acting on this slice; clearly for the first slice σ_{3i} is zero since it is a free boundary. However, for other slices σ_{3i} is unknown but must be the horizontal stress applied by the fractured rock of the adjacent failed slice. This value of σ_{3i} will be derived later from the consideration of the build up of horizontal stresses in fractured rock (See Section 5.3)

Secondly, the stress distribution on the unfailed slices will change from that given above as each successive slice fails, i.e. when the first slice fails it will retain some residual load bearing capacity and shed the remainder of the load originally applied on to the, as yet, unfailed slices. This re-distribution of stress must also be addressed each time a slice fails.

The next step is therefore to consider the physical properties of both the solid and fractured rock.

5.2 Fracture criterion for solid coal

In this analysis it will be assumed that the Coulomb-Navier fracture criterion will describe the stress conditions under which the solid coal will fail by fracture (other fracture criteria could be used if deemed appropriate). Appendix F gives the derivation of the Coulomb-Navier fracture criterion and expresses the equations in a number of different forms.

Lets ϕ_s be the "angle of internal friction" for the solid coal, let S_s be the shear strength of the solid coal and let σ_{cs} be the uniaxial compressive strength of the solid coal. Then, from Coulomb-Navier theory (Appendix F, equations F12 and F14) the following relationships apply at failure:-

$$\sigma_{1s} = \frac{2S_s \text{Cos}\phi_s}{(1-\text{Sin}\phi_s)} + \frac{\sigma_{3s}\,(1+\text{Sin}\,\phi_s)}{(1-\text{Sin}\phi_s)} \qquad (31)$$

and

$$\sigma_{cs} = \frac{2S_s \, \text{Cos}\phi_s}{(1-\text{Sin}\phi_s)} \qquad (32)$$

i.e.

$$\sigma_{1s} = \sigma_{cs} + \left\{ \frac{\sigma_{3s} \, (1+\text{Sin}\phi_s)}{(1-\text{Sin}\phi_s)} \right\} \qquad (33)$$

where the subscript s refers always to the properties of the solid coal.

Hence a solid slice of coal will fracture if:-

$$\sigma_{1i} > \sigma_{1s} \qquad (34)$$

i.e. fracture occurs if:-

$$Y_i S_v > \sigma_{cs} + \left\{ \frac{\sigma_{3s} \, (1+ \text{Sin}\phi_s)}{(1-\text{Sin}\phi_s)} \right\} \qquad (35)$$

Thus if the properties σ_{cs} and ϕ_s for solid coal are determined from tests in the solid coal, S_v is known, and Y_i is determined as given previously then it only remains to determine σ_{3s} to determine whether or not the slice fractures. As pointed out previously $\sigma_{3s} = 0$ for the first slice and, for the remaining slices must be the horizontal stress applied to this solid slice by the adjacent fractured slice.

5.3 Theory for the stress development in a fractured pillar edge

5.3.1 Residual stress capacity of the fractured slice.

Consider an elemental slice, of width δe, in the fractured portion of the pillar, as illustrated in Figure 12. Let H = 2h be the room height, let W = 2w be the room width and let e be the distance from the centre of the room to the elemental slice of width δe.

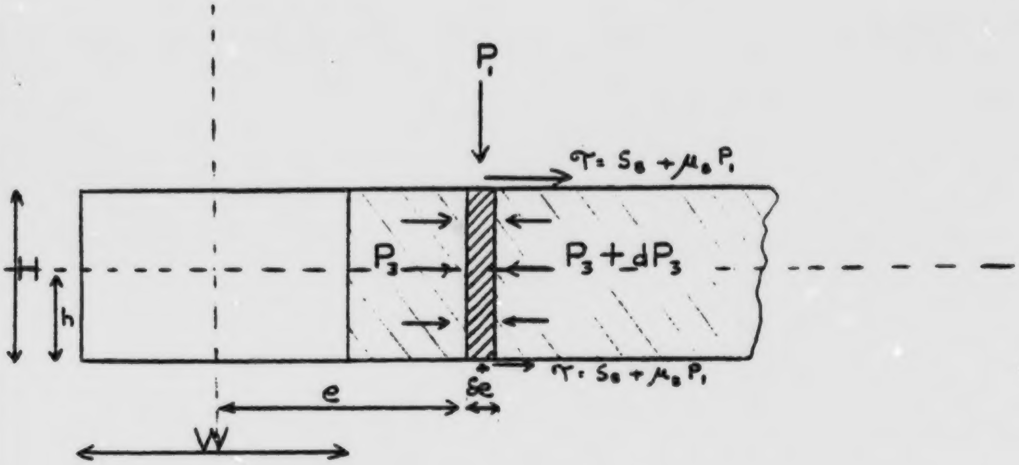
P1
τ = S0 + μ0 P1
P3
P3 ± dP3
H
h
e
δe
W
τ = S0 + μ0 P1

FIGURE 12: Forces acting on an elemental strip within the pillar

Let τ be the shear stress acting across the ends of the element.

S_B be the "cohesion" of the broken coal.

μ_B be the coefficient internal friction of the broken coal and tan $\phi_B = \mu_B$ where ϕ_B is the angle of internal friction of the broken coal.

P_1 is the vertical stress acting on the element of broken coal.

P_3 is the horizontal stress acting on one side of the element and $P_3 + dP_3$ is that acting on the other side.

Then, ignoring the weight of the slice, the following must be the equation for equilibrium of the forces acting on the slice (13):-

$$HdP_3 = 2(S_B + P_1 \tan \phi_B)\ \delta_e \qquad (36)$$

Now the fractured coal is regarded as a totally different material from solid coal, and it is assumed that this "new material" also obeys the Coulomb-Navier fracture" criterion, with its own specific material properties defined by the suffix B. Then the maximum vertical stress, P_1, which this element of broken coal can resist is given by the Coulomb-Navier criterion for this material (equation F12) as follows:-

$$P_1 = \frac{2\ S_B \operatorname{Cos}\phi_B}{(1 - \operatorname{Sin}\phi_B)} + P_3 \left\{ \frac{1 + \operatorname{Sin}\phi_B}{1 - \operatorname{Sin}\phi_B} \right\} \qquad (37)$$

Hence differentiating equation 37 gives:-

$$dP_1 = \left\{ \frac{1 + \operatorname{Sin}\phi_B}{1 - \operatorname{Sin}\phi_B} \right\} dP_3 \qquad (38)$$

Thus, from equations 36 and 38:-

$$dP_1 \left\{ \frac{1 - \operatorname{Sin}\phi_B}{1 + \operatorname{Sin}\phi_B} \right\} = \frac{2}{H} \left\{ S_B + P_1 \tan \phi_B \right\} \delta e$$

i.e.
$$\frac{dP_1}{(S_B + P_1 \tan \phi_B)} = \frac{2}{H} \left\{ \frac{1 + \operatorname{Sin}\phi_B}{1 - \operatorname{Sin}\phi_B} \right\} \delta e \qquad (39)$$

Integrating this equation, within the limits given by: when $P_1 = P_1$, $e = e$ and when $e = w$ then $P_1 = P_B$; and since $P_3 = 0$ when $e = w$ then P_B must be the uniaxial compressive strength of the broken coal, then:-

$$\int_{P_B}^{P_1} \frac{dP_1}{(S_B + P_1 \tan \phi_B)} = \frac{2}{H}\left\{\frac{1+ \mathrm{Sin}\phi_B}{1- \mathrm{Sin}\phi_B}\right\} \int_{w}^{e} de$$

i.e.

$$\left[\frac{1}{\tan \phi_B} \log_e (S_B + P_1 \tan \phi_B)\right]_{P_B}^{P_1} = \frac{2}{H}\left\{\frac{1+ \mathrm{Sin}\phi_B}{1- \mathrm{Sin}\phi_B}\right\}\Big[e\Big]_{w}^{e}$$

Hence:-

$$\left\{\frac{S_B + P_1 \tan \phi_B}{S_B + P_B \tan \phi_B}\right\} = e^{\frac{2}{H} \tan \phi_B \left\{\frac{1+ \mathrm{Sin}\phi_B}{1- \mathrm{Sin}\phi_B}\right\}[e - w]}$$

Thus,

$$P_1 = \frac{1}{\tan \phi_B}\left[\left\{S_B + P_B \tan\phi_B\right\} e^{\frac{2}{H} \tan \phi_B \left\{\frac{1+ \mathrm{Sin}\phi_B}{1- \mathrm{Sin}\phi_B}\right\}[e - w]} - S_B\right] \qquad (40)$$

but also, from Appendix F, equation F14:-

$$P_B = \frac{2S_B \mathrm{Cos}\ \phi_B}{(1- \mathrm{Sin}\ \phi_B)} \qquad (41)$$

Hence, substituting from equation 41 into equation 40, for S_B gives:-

$$P_1 = \frac{1}{\tan\phi_B}\left[P_B\left\{\left(\frac{1- \mathrm{Sin}\phi_B}{2\mathrm{Cos}\phi_B}\right) + \tan\phi_B\right\} e^{\frac{2}{H}\tan\phi_B\left\{\frac{1+ \mathrm{Sin}\phi_B}{1- \mathrm{Sin}\phi_B}\right\}\left[e-w\right]} - P_B\left(\frac{1- \mathrm{Sin}\phi_B}{2\mathrm{Cos}\phi_B}\right)\right]$$

which simplifies to become:-

$$P_1 = \frac{P_B}{2\,\mathrm{Sin}\phi_B}\left[(1+ \mathrm{Sin}\phi_B)\, e^{\frac{2}{H}\tan\phi_B\left\{\frac{1+ \mathrm{Sin}\phi_B}{1- \mathrm{Sin}\phi_B}\right\}(e-w)} - (1-\mathrm{Sin}\phi_B)\right] \qquad (42)$$

and, bearing in mind that $W = \frac{e}{w}$ and $2w = W$:-

$$P_1 = \frac{P_B}{2\,\mathrm{Sin}\phi_B}\left[(1 + \mathrm{Sin}\phi_B)\, e^{\tan\phi_B\left\{\frac{1+ \mathrm{Sin}\phi_B}{1- \mathrm{Sin}\phi_B}\right\}\frac{W}{H}(X-1)} - 1- \mathrm{Sin}\phi_B\right] \qquad (43)$$

i.e. this equation 43, gives the maximum vertical stress that the fractured slice can resist, and expresses it in terms of the physical properties P_B and ϕ_B of the fractured coal and the width/height ratio of the opening. Consequently P_1 can be determined and will be called the "residual stress capacity" of the slice.

5.3.2 Build up of confining stress P_3, in the broken coal.

From equation 37:-

$$P_3 = \frac{\left[P_1 (1 - \sin\phi_B) - 2S_B\cos\phi_B\right]}{(1 + \sin\phi_B)}$$

and from equation 41, substituting for S_B; this equation becomes:

$$P_3 = \left\{\frac{(1 - \sin\phi_B)}{(1 + \sin\phi_B)}\right\}\left\{P_1 - P_B\right\} \qquad (44)$$

Hence, having determined P_1 from equation 43, the horizontal stress P_3 within the broken coal can now be determined from equation 44. Now P_3 is the horizontal stress generated in the fractured coal and is thus the horizontal stress which is applied to the adjacent unfractured slice.

$$\text{i.e. } P_3 = \sigma_{3s} \qquad (45)$$

Appendix E makes use of some typical properties of fractured coal to illustrate how P_1 and P_3 build up in the fractured coal. It will be noted that P_1 and P_3 are dependent only on the properties of the fractured coal and on the width/height ratio of the room. Thus the rate of build up of the P_1 and P_3 in the fractured peripheries of pillar adjacent of rooms of equal size and shape in the same coal, will be identical. i.e. provided that fracture occurs, then the stress build up in the fractured coal is independent of the load applied to the pillar.

5.4 Load shed by the failed slice onto the central solid core

Before failure the vertical stress applied to the i th slice, σ_{1i}, is given by equations 29 and 30. After failure the stress remaining on this failed slice, the "residual stress capacity", P_1 is given by equation 43.

Hence the load shed from the failed slice, of unit depth, onto the central solid core of the pillar is given by:-

$$\Delta L = (\sigma_{1i} - P_1)\left(\frac{B}{n_1}\right) \quad \text{where} \quad \left({}^{B}/n_1\right) \text{ is the slice width.} \qquad (46)$$

The manner in which this load is re-distributed onto the remaining slices must now be determined; this is a key step in this analysis and, unfortunately, it involves an arbitrary assumption for which the author has been unable to find evidence, in support or to the contrary, within the literature. The rationale behind the assumptions used is discussed fully in Appendix H. The following equations summarize the findings given in Appendix H.

(a) when $Y_{mm} = \overline{Y}$ In this case the vertical stress distribution across the pillar prior to any failure is approximately uniform (section 4.2 and Appendix D). It is therefore reasonable to assume that the re-distribution of load due to fracture must also be uniform in order to ensure that the stress distribution on the central core remains uniform.

Hence the incremental stress to be added to the elastic stress already applied to each of the remaining unfailed slices is given by

$$\Delta\sigma_1 = \frac{\sigma_{1i} - P_1}{({}^{n_1}/_2 - i)} \; \frac{({}^{B}/n_1)}{({}^{B}/_{n_1})} = \frac{\sigma_{1i} - P_i}{({}^{n_1}/_2 - i)} \qquad (47)$$

Note: $(^{n}1/_{2})$ is used here and not n_1 since symmetry is assumed and only half the pillar will be analysed; this will lead to a slight discontinuity of stress at the pillar centre if the room widths or shape of the rooms on either side of the pillar are different and the pillar is treated as two separate half pillars. This discontinuity will however be quite small.

Hence the total new vertical stress applied to the slice adjacent to the failed slice is given by:-

$$\sigma_1 = \sigma_{1(i+1)} + \frac{\sigma_{1i} - P_1}{(n_{1/2}-i)} \tag{48}$$

and the lateral stress σ_3 applied to this next slice will be the confining pressure P_3 generated by the fractured coal of the adjacent failed slice and given by equation 44.

Consequently the stresses σ_1 and σ_3 applied to this next unfailed slice are known and can be compared with the failure criterion. If this slice fails then the residual stress capacity of this slice can again be determined and the incremental stress added to each of the remaining slices can again be determined as above. If failure does not occur then the final vertical stress distribution on the unfailed core can be determined (and will be uniform in this case). The above steps can be readily combined in a computer loop to consider each slice in turn.

(b) when $Y_{mm} > \bar{Y}$ In this case the initial stress distribution across the pillar is non-uniform and has been approximated by a hyperbola (section 4.3). In this case it is assumed in Appendix 4 that when a slice fails the excess stress shed onto the remaining slices is described by a general functional relationship given by:-

$$\Delta\sigma = f(\frac{1}{X^{\alpha}}) \tag{49}$$

It is then shown in this appendix that the stress shed by the first slice into the j th slice is given by:-

$$\Delta\sigma_j = \frac{\frac{1}{(j-1)^{\alpha}} \left[\sigma_{1i} - P_1 \right]}{\displaystyle\sum_{j=(i+1)}^{j=(^{n}1/_{2})} \frac{1}{(j-i)^{\alpha}}} \tag{50}$$

The new vertical stress distribution can therefore be determined by adding the incremental stress $\Delta\sigma_i$ to the original applied stress, for each slice in turn. The failure of the second slice under the new applied vertical stress can therefore be examined and, if this slice fails then the total stress shed by this slice can again be determined and the additional stress increments for the remaining slices can again be determined following the above procedure. This procedure is repeated successively for each slice in turn until a slice no longer fails, in which case the final stress distribution on the central core is given by the initial stress acting on each unfailed slice plus the accumulated increments from each failed slice.

The possible value of the assumed constant α was then considered in appendix H. A number of example cases were run with α ranging from 0 to 1. It was concluded on the basis of these example runs that α most probably was somewhere between these two values and it was arbitrarily assumed that the value of $\alpha = 0.5$ would be used in subsequent analysis in this paper.

It should be emphasized that this choice of α is arbitrary; unfortunately there is no evidence in the literature which will assist in the determination of α . Indeed α may not be a constant but may well vary with the pillar width. Further study of this load shedding relationship is recommended as or when evidence becomes available. The computer program has been written to allow α to be defined as an input parameter at the choice of the user. However, unless otherwise stated $\alpha = 0.5$ in all subsequent analysis in this paper.

5.5 Conclusion

The analysis carried out in this section gives the formulae necessary to achieve steps 4 to 12 in Figure 1. Consequently, this portion of the analysis, dealing with the fracture zone development, is now completed (pending any changes that may result from consideration of yield criteria for coal). The computer program has been written and the next section gives some example results and also considers the subject of pillar strength. The computer program will not be described and discussed at this stage but will be dealt with as a whole in Section 9 .

5.6 Examples of fracture zone development

The computer program at this stage of its development has been run to examine a number of example cases to illustrate a number of points and the type of results that can be obtained.

5.6.1 Sensitivity of the fracture zone depth to uniaxial compressive strength of broken coal, P_B

The fracture zone and stress distribution in pillar C4 (Appendix B) has been analysed for four cases in which P_B the uniaxial compressive strength of the broken coal has been given the values 0.1, 1.0, 10.0, and 100 psi respectively. Table 5.1 lists the other input parameters for this analysis. The results are shown in the graphs given on Figure 13.

It is seen from these figures that if $P_B = 0.1$ psi the pillar has fractured all the way through and has thus failed, whereas for high values of P_B there is a significant area of unfractured central core and the pillar will be stable. It is quite evident from these figures that the development of the fracture zone is very sensitive to the value of P_B. This is unfortunate because in practice P_B is a difficult parameter to determine accurately.

It also follows, from the analyses in Appendix E, that the fracture zone development will also be very sensitive to the value of ϕ_B the angle of internal friction of the broken coal. ϕ_B is however considerably easier to determine relatively accurately from laboratory tests than is P_B.

5.6.2 Fracture zones and stess distributions across the pillars in the cross section C-C previously analysed (Appendix B and E)

In Appendix B the mean pillar stress acting on five pillars in one mine cross section C-C were determined as an illustration of Coates' pillar stress formulae. In Appendix E, the same five pillars were analysed to illustrate the determination of the initial elastic stress distribution across each of these pillars in this mining span. These same five pillars in this mining span have now been analysed to illustrate the fracture zone development and the stress distribution after failure using the computer program. The input parameters used in this analysis are given in Table 5.1 . Figure 14 shows the results of this analysis.

It will be noted that, with the assumed parameters, pillar C2 will have fractured completely and would be deemed to have failed although it is still capable of resisting some load represented by the area under the stress distribution curve. In contrast the very wide pillar C3 clearly will resist significantly more load before it might fail.

TABLE 5.1 : Input parameters for pillar analyses used in the example analyses.

INPUT PARAMETER	PILLAR								
	C1	C2		C3		C4		C5	
		LHS	RHS	LHS	RHS	LHS	RHS	LHS	RHS
Sv - virgin vertical stress - psi	1540	1540	1540	1540	1540	1540	1540	1540	1540
R - general extration ratio	0.254	0.254	0.254	0.254	0.254	0.254	0.254	0.254	0.254
ℓ - semi length of mining span - ft.	315	315	315	315	315	315	315	315	315
x - coordinate of specific pillar - ft.	255	165	165	5	5	145	145	260	260
ω - semi room width - ft.	10	10	20	20	10	10	20	20	10
z - overburden depth - ft.	1400	1400	1400	1400	1400	1400	1400	1400	1400
b - semi pillar width - ft.	40	30	30	90	90	40	40	35	35
h - semi pillar height - ft.	5	5	5	5	5	5	5	5	5
μ_r - Poisson's ratio of surrounding rock	0.3	0.3	0.3	0.3	0.3	0.3	0.3	0.3	0.3
μ_p - Poisson's ratio of coal	0.3	0.3	0.3	0.3	0.3	0.3	0.3	0.3	0.3
E_r - modules of surrounding rock x 10 psi	5	5	5	5	5	5	5	5	5
E_p - modules of coal x 10^6 psi	1	1	1	1	1	1	1	1	1
OPENING SHAPE	Rect	Rect	Rect	Rect	Rect	Rect	Rect	Rect	Rect
$k = {}^{Sv}/_{Sv}$	0.33	0.33	0.33	0.33	0.33	0.33	0.33	0.33	0.33
N = number of pillars in span	5	5	5	5	5	5	5	5	5
OUTPUTS									
$\overline{\gamma}$ mean pillar concentration	1.242	1.260	1260	1.287	1.287	1.263	1.263	1.241	1.241
γ_{mm} - maximum pillar stress concentration	2.192	2.192	2.698	2.582	2.156	2.254	2.650	2.670	2.274
Stress distribution K_1	0.4867	0.3756	0.1384	0.6206	3.0530	0.5623	0.1973	0.1488	0.4046
K_2	-0.6086	-0.6999	-0.9192	-0.6239	1.1249	-0.5506	-0.8820	0.9118	0.6746
K_3	0.9482	0.9596	0.9848	0.9338	0.7256	0.9405	0.9784	0.9836	0.9566
INPUTS									
n_1 - number of slices in pillar	16	12	12	18	18	140 vertical	32	14	14
P_B - uniaxial strength broken coal - psi	1	1	1	1	1	see text	1	1	1
σ_c - uniaxial strength solid coal - psi	1000	1000	1000	1000	1000	1000	1000	1000	1000
ϕ_c - angle internal friction, solid coal	30°	30°	30°	30°	30°	30°	30°	30°	30°
ϕ_B - angle internal friction, broken coal	27°	27°	27°	27°	27°	27°	27°	27°	27°
α - load shedding function	0.5	0.5	0.5	0.5	0.5	0.5	0.5	0.5	0.5

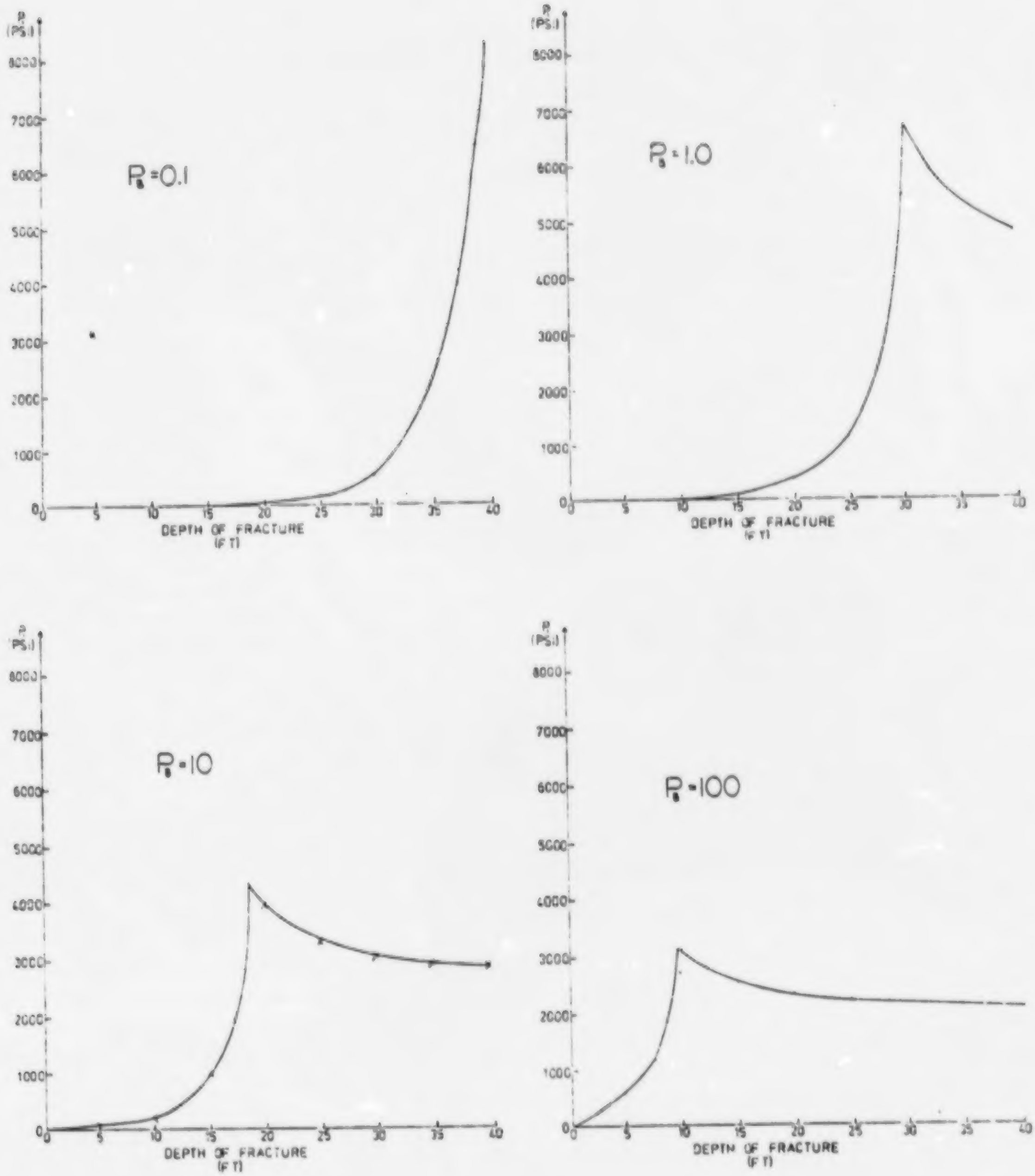

FIGURE 13: Sensitivity of fracture zone development to P_B

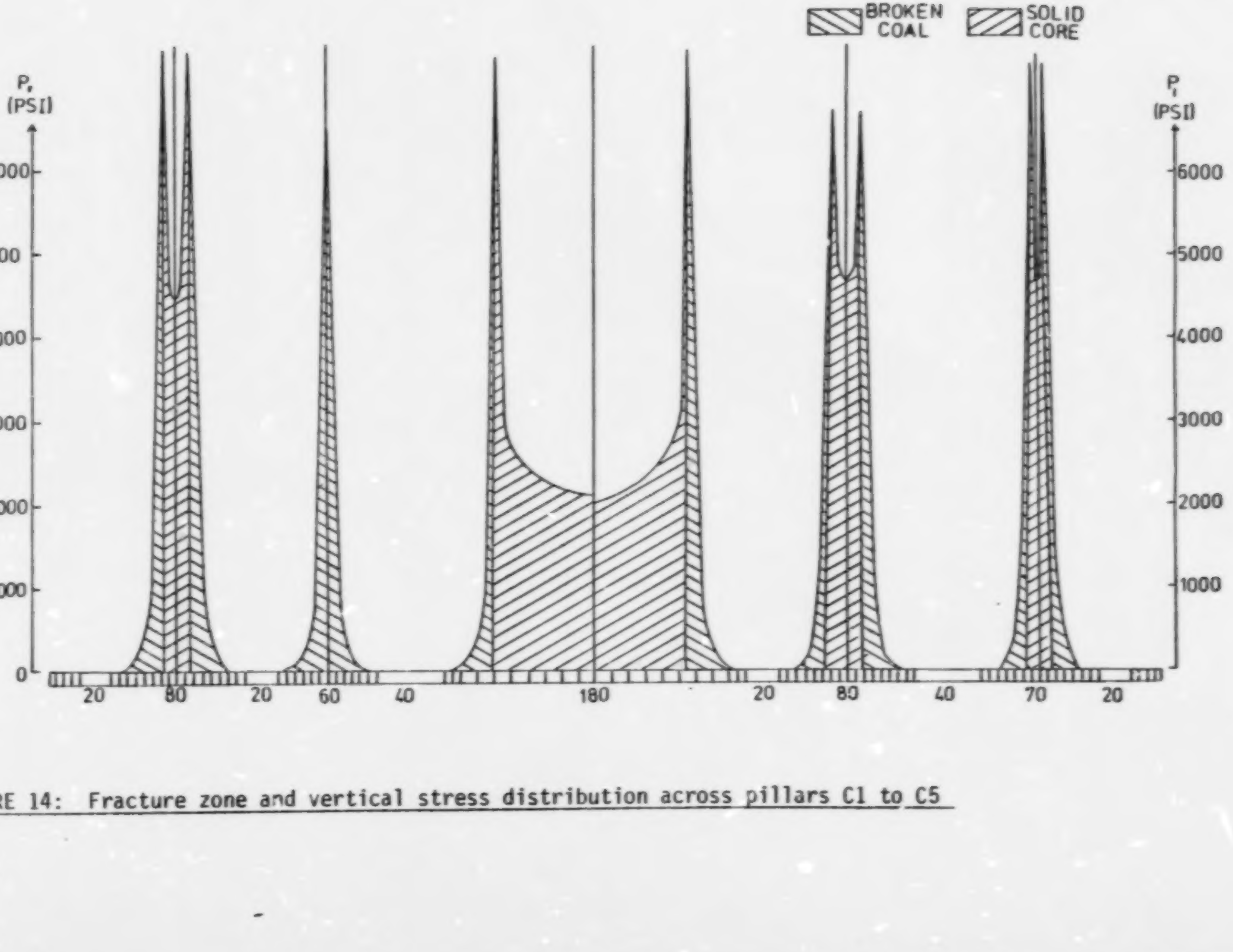

FIGURE 14: Fracture zone and vertical stress distribution across pillars C1 to C5

6. Pillar strength and safety factor.

6.1 Mean pillar stress for initiation of fracture.

There must be some minimum value of the mean pillar stress below which fracture cannot initiate in the pillar. Let S_{vc} be the critical value of the vertical virgin stress at which fracture can just initiate in the first slice. Then the stress acting at the mid height of this slice on the edge of the pillar is initially the maximum stress on any pillar element and is equal to $Y_{mm}\,S_{vc}$ and, for fracture to be able to initiate at this point, this stress must be equal to the unixial compressive strength of the solid coal, σ_c. (see Figure 15) i.e. fracture will initiate when:-

$$Y_{mm}\,S_{vc} = \sigma_c \tag{51}$$

and the mean pillar stress acting on the pillar when this occurs is given by:-

$$\bar{\sigma}_p\ (\text{min}) = \bar{Y}\,.S_{vc} \tag{52}$$

Thus, eliminating S_{vc} from 51 and 52 gives

$$\bar{\sigma}_p\ \text{min} = \frac{\bar{Y}}{Y_{mm}}\,.\,\sigma_c \tag{53}$$

It will be shown later that $\bar{\sigma}_p$ (min) also represents the minimum pillar strength.

e.g. for pillar C4: $\bar{Y} = 1.263$, $Y_{mm} = 2.254$, $\sigma_c = 1000$ psi then $\bar{\sigma}_{pmin} = 560$ psi

for pillar C5: $\bar{Y} = 1.241$, $Y_{mm} = 2.70$, $\sigma_c = 1000$ psi then $\bar{\sigma}_{pmin} = 460$ psi

6.2 Residual mean pillar stress capacity of the pillar that has just failed, σ_{PR}

The residual mean pillar stress capacity can be defined as the mean pillar stress required to just fail the pillar to its centre. The stress distribution when this occurs is illustrated in Figure 16; it is important to note that the stress distribution is solely dependent on the properties of the broken coal.

Now equation 43 defines the build-up of the vertical stress in the fractured coal as follows:-

$$P_1 = \frac{P_B}{2\,\text{Sin}\phi_B}\left\{(1+\text{Sin}\phi_B)\,e^{\tan\phi_B\left(\frac{1+\text{Sin}\phi_B}{1-\text{Sin}\phi_B}\right)\frac{W}{H}\,(X-1)} - (1-\text{Sin}\phi_B)\right\} \tag{43}$$

where $X = {}^{e}/w$ and $(X-1) = \frac{e-w}{w}$

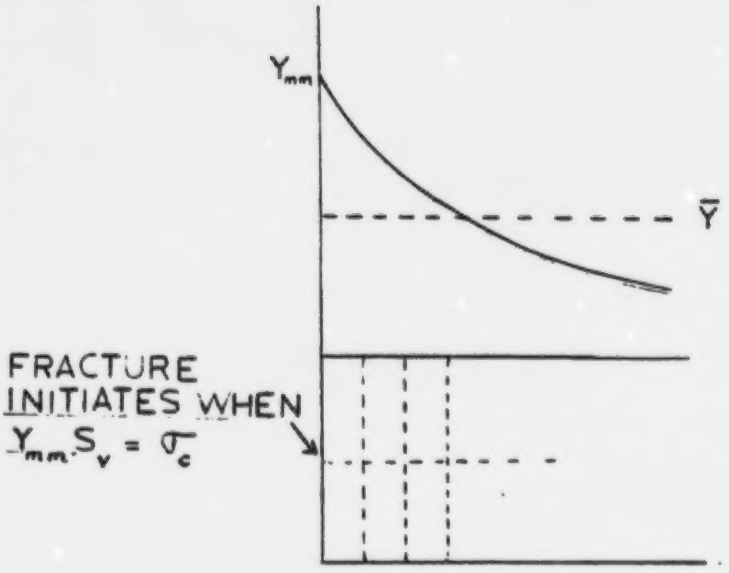
Y_{mm}
$\bar{Y}$
FRACTURE INITIATES WHEN $Y_{mm} S_v = \sigma_c$

FIGURE 15: Condition for fracture initiation in the pillar

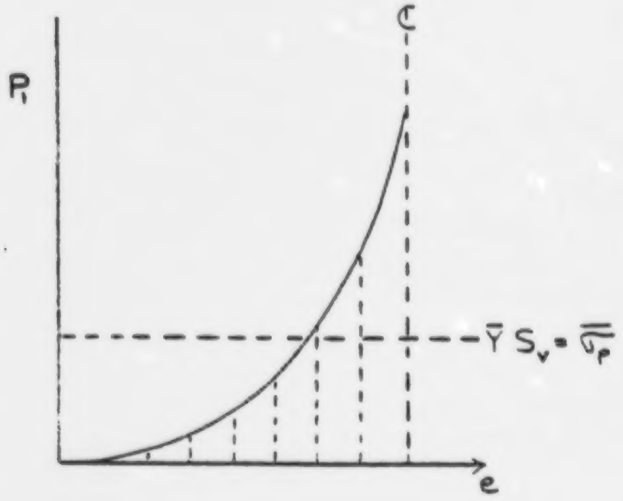
℄
P_1
$\bar{Y} S_v = \bar{\sigma}_P$
e

FIGURE 16: Stress distribution when fracture just reaches the pillar centre

i.e. This equation may be written as:-

$$P_1 = \frac{P_B}{2\ Sin\phi_B}\left\{(1+Sin\phi_B)\ e^{\tan\phi_B\left\{\frac{1+Sin\phi_B}{1-Sin\phi_B}\right\}\left[\frac{e-w}{h}\right]} - (1-Sin\phi_B)\right\} \tag{54}$$

Hence the total load L carried by the pillar when the fracture zone just reaches the centre of the pillar is given by the area under the curve in Figure 16 and is thus given by:-

$$L = \int_{e=w}^{e=w+b} P_1 de = \int_{e=w}^{e=w+b} \frac{P_B}{2\ Sin\phi_B}\left\{(1+Sin\phi_B)e^{\tan\phi_B\left\{\frac{1+Sin\phi_B}{1-Sin\phi_B}\right\}\left[\frac{e-w}{h}\right]} - (1-Sin\phi_B)\right\} de$$

$$= \left[\frac{P_B}{2\ Sin\phi_B}\left\{\frac{(1-Sin\phi_B)\ h}{\tan\phi_B}\ e^{\tan\phi_B\left\{\frac{1+Sin\phi_B}{1-Sin\phi_B}\right\}\left[\frac{e-w}{h}\right]} - (1-Sin\phi_B)\ e\right\}\right]_{e=w}^{e=w+b}$$

$$= \frac{P_B}{2Sin\phi_B}\ (1-Sin\phi_B)\left\{\frac{h}{\tan\phi_B}\left[e^{\tan\phi_B\left\{\frac{1+Sin\phi_B}{1-Sin\phi_B}\right\}\left(\frac{b}{h}\right)} -1\right] -b\right\} \tag{55}$$

and, for unit thickness, the residual mean pillar stress capacity, $\bar{\sigma}_{PR}$ is given by:-

$$\bar{\sigma}_{PR} = \frac{L}{b} = \frac{P_B}{2b\ Sin\phi_B}\ (1-Sin\phi_B)\left\{\frac{h}{\tan\phi_B}\left[e^{\tan\phi_B\left\{\frac{1+Sin\phi_B}{1-Sin\phi_B}\right\}\left(\frac{b}{h}\right)} -1\right] -b\right\} \tag{56}$$

For example: if $P_B = 1$ psi, $\phi_B = 27^\circ$, $h = 5$ ft then Figure 17 and Table 6.1 show the variation of the residual mean pillar stress capacity for different pillar widths.

Table 6.1: Residual mean pillar stress capacity example

semi-pillar width - b ft	$\bar{\sigma}_{PR}$ psi
5	2.8
10	7.7
15	22.1
20	66.2
30	674.3
40	7637.5
50	92,175
60	1.158×10^6
70	14.98×10^6

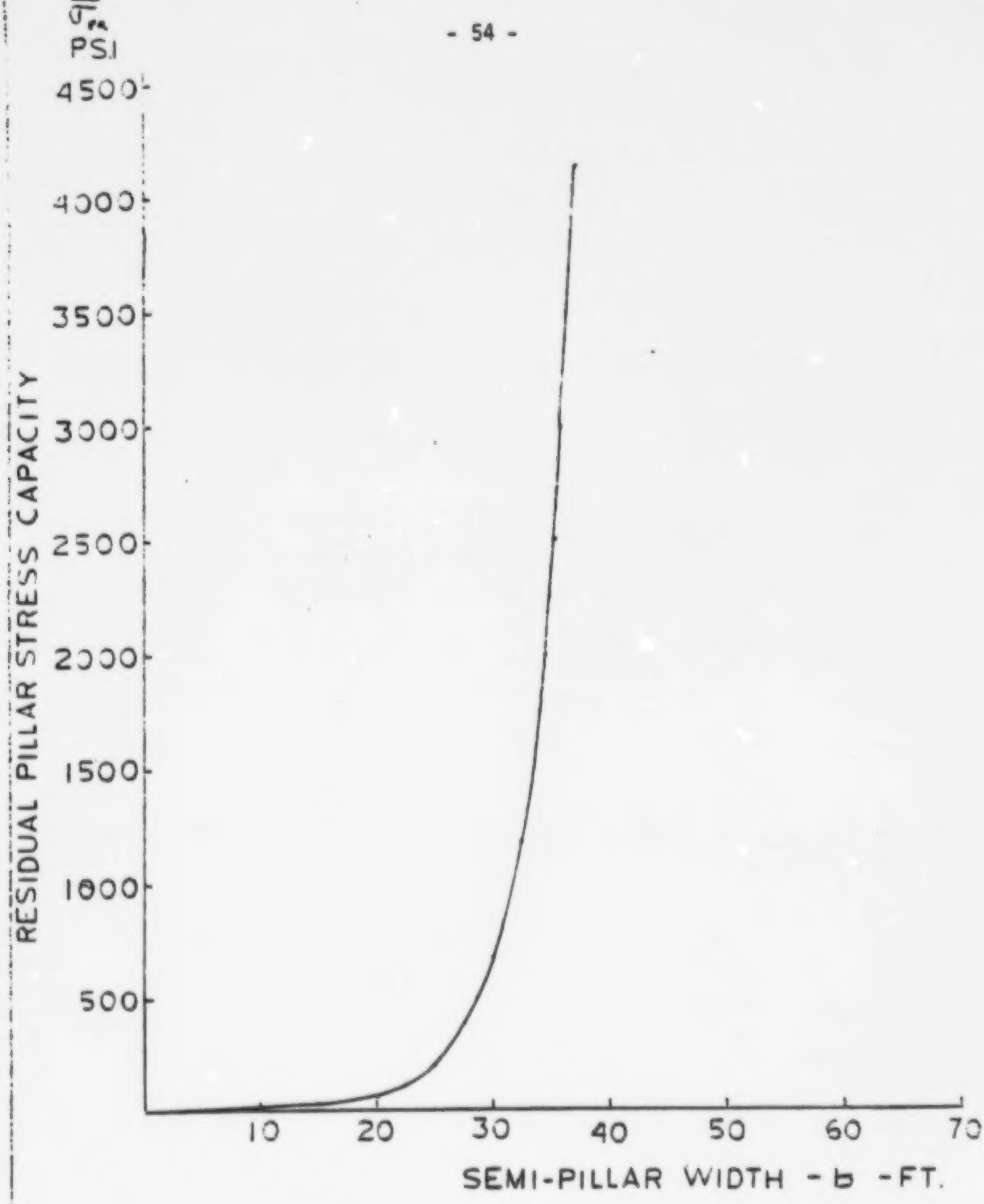

FIGURE 17: Increase in residual pillar stress capacity with pillar width

6.3 Concept of catastrophic fracture

Suppose we have a 20 ft. wide pillar (b = 10 ft.), of height 10 ft. (h = 5 ft.) adjacent to a rectangular room of width 20 ft. (w = 10 ft.) and assuming that the applied stress ratio $k = \frac{S_H}{S_V} = 0$, then from equation 1 using tributary area theory, $\bar{Y} = 2.0$ and, from equation 21, $Y_{mm} = 2.71$. Assume that the uniaxial compressive strength of the solid coal, $\sigma_c = 1000$ psi. Then from equation 53, the mean pillar stress required before fracture can initiate is given by:-

$$\bar{\sigma}_{pmin} = \frac{\bar{Y}}{Y_{mm}} \cdot \sigma_c = 738 \text{ p.s.i.}$$

and, if $P_B = 1$ p.s.i. and $\phi_B = 27^\circ$, the residual mean pillar stress capacity when the pillar has just failed to the centre is calculated from equation 56 (see Figure 17 and Table 6.1) as:-

$$\bar{\sigma}_{PR} = 7.7 \text{ psi}$$

In this case the residual mean pillar stress capacity is much less than the mean pillar stress required to initiate fracture in the pillar. It follows therefore that once fracture has initiated at the boundary of the pillar it must propogate immediately to the center of the pillar, and further load must be shed from the pillar onto the adjacent pillars. This will be called CATASTROPHIC FRACTURE of the pillar.

6.4 Sequence of events as $\bar{\sigma}_p$ increases.

Consider the possible sequence of events as the mean pillar stress, $\bar{\sigma}_p$, increases:-

(i) $\bar{\sigma}_p < \bar{\sigma}_{pmin}$ (Figure 18A) Fracture cannot initiate. The pillar is solid and has a elastic stress distribution as illustrated in Figure 18A. The are under the curve, A_1, must be equal to $\bar{\sigma}_{p.b.}$.

(ii) $\bar{\sigma}_p > \bar{\sigma}_{pmin}$, $\bar{\sigma}_{pmin} > \bar{\sigma}_{pr}$ (Figure 18B) $\bar{\sigma}_p$ increases and is now greater than $\bar{\sigma}_{pmin}$, therefore fracture initiates. In this case $\bar{\sigma}_{pmin}$ is also greater than the residual mean pillar stress capacity $\bar{\sigma}_{PR}$; therefore fracture propogates immediately to the centre causing CATASTROPHIC FRACTURE. The area under the curve, A_1, is less than $\bar{\sigma}_{p.b.}$; consequently load is shed from the

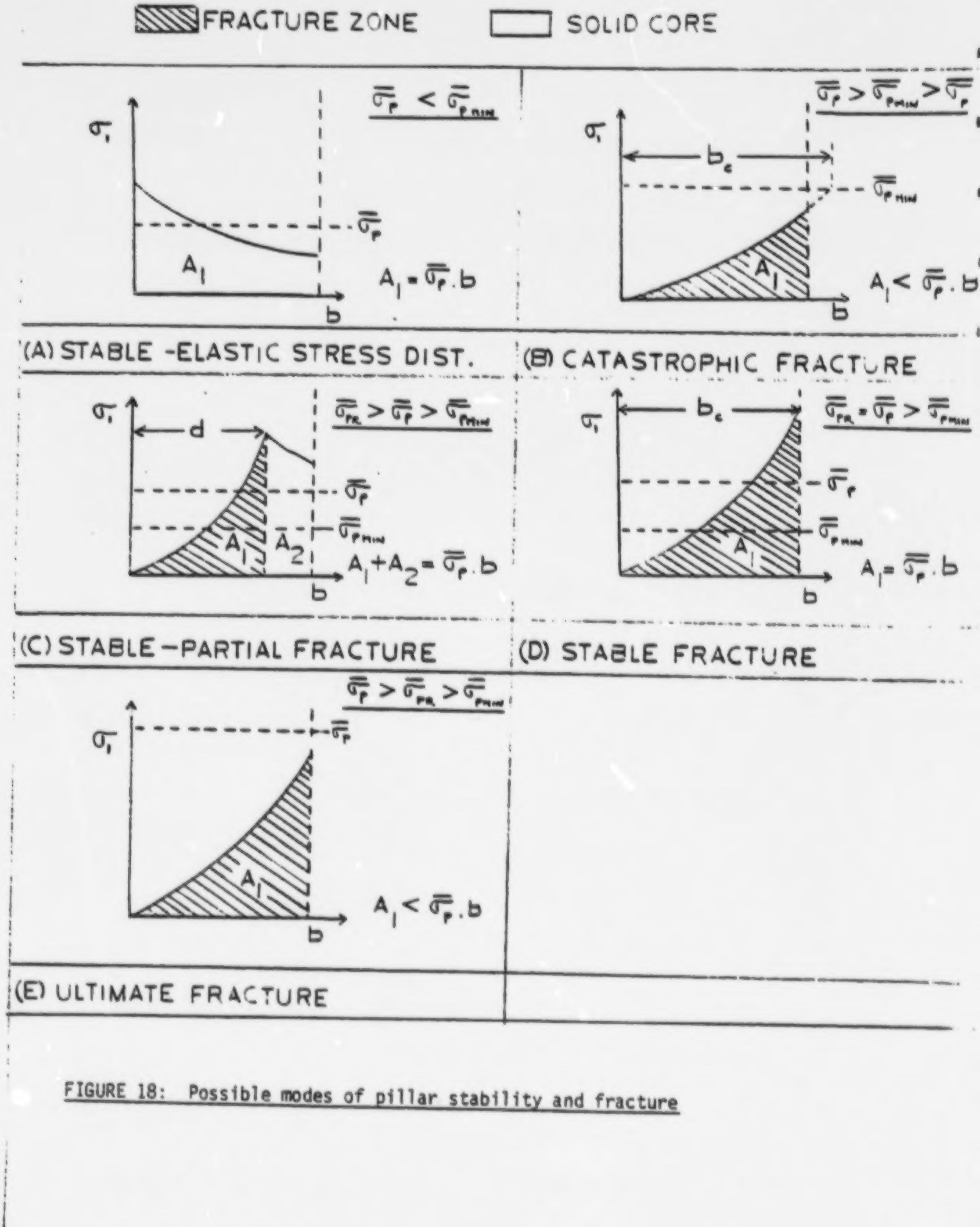
FRACTURE ZONE
SOLID CORE
$\bar{\bar{\sigma}}_p < \bar{\bar{\sigma}}_{p\,min}$
σ_1
$\bar{\bar{\sigma}}_p$
A_1
$A_1 = \bar{\bar{\sigma}}_p . b$
b
(A) STABLE -ELASTIC STRESS DIST.
$\bar{\bar{\sigma}}_p > \bar{\bar{\sigma}}_{p\,min} > \bar{\bar{\sigma}}_f$
σ_1
b_c
$\bar{\bar{\sigma}}_{p\,min}$
A_1
$A_1 < \bar{\bar{\sigma}}_p . b$
b
(B) CATASTROPHIC FRACTURE
$\bar{\bar{\sigma}}_{FR} > \bar{\bar{\sigma}}_p > \bar{\bar{\sigma}}_{p\,min}$
σ_1
d
$\bar{\bar{\sigma}}_p$
$\bar{\bar{\sigma}}_{p\,min}$
A_1
A_2
$A_1 + A_2 = \bar{\bar{\sigma}}_p . b$
b
(C) STABLE—PARTIAL FRACTURE
$\bar{\bar{\sigma}}_{FR} = \bar{\bar{\sigma}}_p > \bar{\bar{\sigma}}_{p\,min}$
σ_1
b_c
$\bar{\bar{\sigma}}_p$
$\bar{\bar{\sigma}}_{p\,min}$
A_1
$A_1 = \bar{\bar{\sigma}}_p . b$
b
(D) STABLE FRACTURE
$\bar{\bar{\sigma}}_p > \bar{\bar{\sigma}}_{FR} > \bar{\bar{\sigma}}_{p\,min}$
σ_1
$\bar{\bar{\sigma}}_p$
A_1
$A_1 < \bar{\bar{\sigma}}_p . b$
b
(E) ULTIMATE FRACTURE

FIGURE 18: Possible modes of pillar stability and fracture

pillar onto the adjacent pillars. The magnitude of this shed load (for the half pillar of width b) is given by:-

$$L_s = b\left\{\bar{\sigma}_{pmin} - \bar{\sigma}_{PR}\right\} \qquad (57)$$

It also follows that $\bar{\sigma}_{pmin}$ must be the minimum strength of the pillar. The mechanism of the re-distribution of this shed load onto the adjacent pillars is beyond the scope of this study and will not be considered further.

(iii) $\bar{\sigma}_p > \bar{\sigma}_{pmin}$ but $\bar{\sigma}_{pmin} < \bar{\sigma}_{PR}$ (Figure 18C) $\bar{\sigma}_p$ has increased and is greater than $\bar{\sigma}_{pmin}$, thus fracture initiates. However in this case the residual load bearing capacity of the broken coal is greater than the mean pillar stress for fracture initiation. Thus fracture propogates to some distance, d, (Figure 18C) into the pillar but cannot propogate further. There is a central solid core with an elastic stress distribution consisting of the initial stress distribution plus the accumulated increments shed from the fractured elements. The pillar is stable. The sum of the areas under the curve $A_1 + A_2$ must equal $\bar{\sigma}_{p}.b$; therefore no load is shed from the pillar.

(iv) $\bar{\sigma}_p > \bar{\sigma}_{pmin}$ and $\bar{\sigma}_p = \bar{\sigma}_{PR}$ (Figure 18D) $\bar{\sigma}_p$ has increased further and is now just equal to $\bar{\sigma}_{PR}$ the residual mean pillar stress capacity. Fracture will then have just propogated to the centre of the pillar. This unique condition will be called "STABLE FRACTURE". The area under the curve, A_1, is equal to $\bar{\sigma}_{p}.b$; thus no load is shed from the pillar despite the fact that it has failed.

(v) $\bar{\sigma}_p > \bar{\sigma}_{pmin}$ and $\bar{\sigma}_p > \bar{\sigma}_{PR}$, $\bar{\sigma}_{pmin} < \bar{\sigma}_{PR}$ (Figure 18E) $\bar{\sigma}_p$ has increased still further, the pillar cannot resist a stress greater than $\bar{\sigma}_{PR}$ thus load must be shed from the pillar onto the adjacent pillars. i.e. the area A_1 under the curve is less that $\bar{\sigma}_{p}.b$. (Note: it is assumed here that this overloading of the pillar does not cause large additional deformation of the pillar and hence a drop in $\bar{\sigma}_{PR}$ the residual stress capacity of the pillar. In practice, some drop in $\bar{\sigma}_{PR}$ is likely to occur. The load shed from the pillar must therefore be regarded as the minimum possible). This will be called "ULTIMATE FRACTURE".

The minimum amount of load shed by the pillar (for the half pillar of width b) is therefore given by:-

$$L_s = b\left(\bar{\sigma}_p - \bar{\sigma}_{PR}\right) \qquad (58)$$

6.5 Critical pillar dimensions to avoid total fracture.

It is seen from the above discussion that there are two potential categories of total fracture illustrated by Figure 18B and E respectively:-

Category 1: when $\bar{\sigma}_p > \bar{\sigma}_{pmin}$ and $\bar{\sigma}_{pmin} > \bar{\sigma}_{PR}$ (Catastrophic Fracture)

and

Category 2: when $\bar{\sigma}_p > \bar{\sigma}_{pmin}$ and $\bar{\sigma}_p > \bar{\sigma}_{PR}$ $(\bar{\sigma}_{pmin} < \bar{\sigma}_{PR})$ (Ultimate Fracture)

It therefore follows that for any given geometry and applied stress there must be some critical pillar dimension above which total fracture cannot occur. Let us determine these critical pillar dimensions.

6.5.1 Critical dimension for Category 1 catastrophic fracture

$\bar{\sigma}_p > \bar{\sigma}_{pmin}$ and $\bar{\sigma}_{pmin} > \bar{\sigma}_{PR}$. Let the critical pillar dimension be equal to b_{c1}. This critical pillar dimension will occur when $\bar{\sigma}_{pmin} = \bar{\sigma}_{PR}$. i.e. At any smaller pillar dimension $\bar{\sigma}_{pmin} > \bar{\sigma}_{PR}$ and catastrophic fracture occurs (Figure 18B) and at any larger pillar dimension the pillar is stable (Figure 18C).

Now from equations 53 and 56 we have, putting $b = b_{c1}$ and $\bar{\sigma}_{pmin} = \bar{\sigma}_{PR}$:-

$$\frac{\bar{Y}}{Y_{mm}}\cdot\sigma_c = \frac{P_B\,(1-\sin\phi_B)}{2\,b_{c1}\,\sin\phi_B}\left\{\frac{h}{\tan\phi_B}\left[e^{\tan\phi_B\left\{\frac{1+\sin\phi_B}{1-\sin\phi_B}\right\}\left[\frac{b_{c1}}{h}\right]}-1\right]-b_{c1}\right\} \quad (59)$$

This equation can be solved for b_{c1} by successive approximation.

For example: if $\bar{Y} = 2.0$, $Y_{mm} = 2.71$, $\sigma_c = 1000$ psi, $P_B = 1$ psi and $\phi_B = 27^\circ$

then $b_{c1} = 29.02$ ft.

It should be noted that this critical dimension is dependent only on the stress concentration factors, the dimensions and the properties of the solid and broken coal. It is independent of the applied vertical stress, S_v, provided that $\bar{\sigma}_p > \bar{\sigma}_{pmin}$.

For example: Table 6.2 and Figure 19 illustrate how $\bar{\sigma}_{pmin}$, $\bar{\sigma}_{PR}$ and the shed load L_s vary as the pillar width is increased. The following important points should be noted:-

TABLE 6.2: - Examples: Shed load and critical pillar dimensions

Semi pillar height - ft. 5
Semi room width - ft. 10
P_B - compressive strength of broken coal - psi 1
ϕ_B - angle of internal friction - broken coal 27°

σ_c - uniaxial compressure strength, solid coal, 1000 psi
Stress ratio k 0
Opening shape Rectangular

Semi-pillar Width b-ft.	Y (Trib. Area)	Y_{mm} Rect.	$\bar{\sigma}_{pmin}$ psi	$\bar{\sigma}_{PR}$ psi	Category 1* Load shed L_s lbs.	S_v = 250 psi		S_v = 1000 psi		S_v = 3000 psi	
						$\bar{Y} S_v$	L_s*	$\bar{Y} S_v$	L_s*	$\bar{Y} S_v$	L_s*
5	3.0	3.164	948	2.8	4747	750	3736	3000	14986	9000	44986
10	2.0	2.714	737	7.7	7292	500	4923	2000	19223	6000	59923
15	1.67	2.604	641	22	9289	418	5990	1674	24780	5022	75000
20	1.50	2.557	587	66	10,420	375	6180	1500	28680	4500	88680
25	1.40	2.531	553	208	8625**	350	3550	1400	29800	4200	99800
30	1.33	2.514	529	674	0	332	0	1330	19680***	3990	99480
35	1.28	2.503	511	2247	0	320	0	1280	0	3840	55755***
40	1.25	2.495	501	7637	0	312	0	1250	0	3750	0
45	1.22	2.489	490	26370	0	305	0	1220	0	3660	0
50	1.20	2.484	483	92175	0	300	0	1200	0	3600	0
60	1.17	14.77	472	1.158×10^6	0	292	0	1170	0	3510	0
70	1.14	2.472	461	14.98×10^6	0	285	0	1140	0	3420	0
Critical Pillar Dimension	b_{c1} = 29.02 ft.					b_{c2} = 27.5 ft.		b_{c2} = 33 ft.		b_{c2} = 37 ft.	

* Load shed from 1/2 pillar.
** b_{c1}
*** b_{c2}

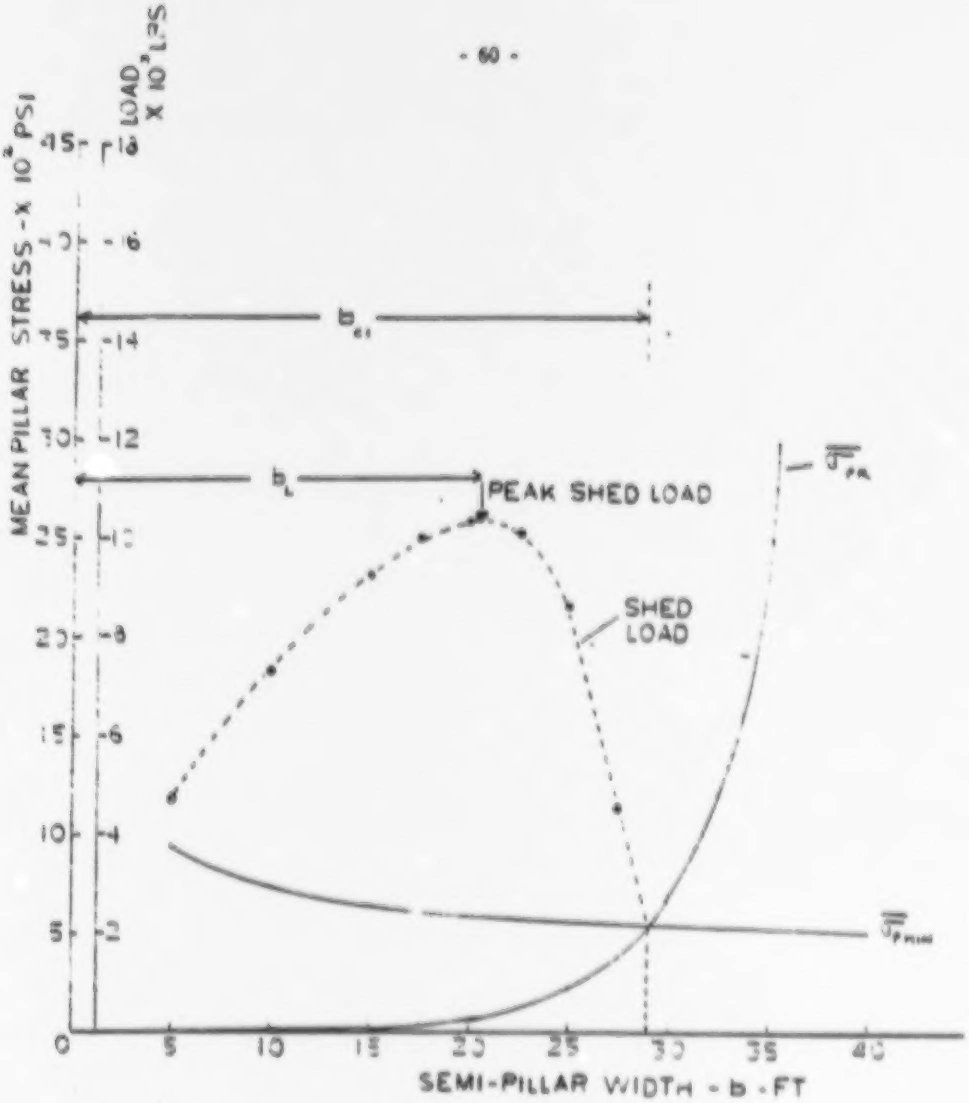

FIGURE 19: Critical pillar dimension b_{c1}, to avoid catastrophic failure (category 1)

(i) $\bar{\sigma}_{pmin}$ diminishes slowly as the pillar size increases. i.e. fracture can initiate earlier in a wider pillar than in a narrower pillar, all other things being equal. At first sight this appears to be somewhat unexpected but nonetheless follows logically from the fact than as the pillar width increases the mean pillar stress concentration fracture $\bar{Y}$ diminishes more rapidly then the maximum stress concentration factor Y_{mm}.

(ii) At some critical pillar dimension, b_{c1}, $\bar{\sigma}_{pmin} = \bar{\sigma}_{PR}$. When this occurs the pillar has fractured to the centre but the failed pillar is able to support the mean pillar stress. This is a point of "stable fracture". For any wider pillars, no load is shed and the pillar has a central solid core.

(iii) The load shed by the pillar is given by equation 57 and, in this example, it is seen from Figure 19 that, during the catastrophic failure zone of pillar widths, the shed load at first increases as b increases, it then peaks and finally decreases to zero when $b = b_{c1}$. The pillar dimension at which the peak load is shed may have some importance in considering load shedding onto adjacent pillars (beyond the scope of this study), direct calculation of this dimension is complex and will not be attempted here (it is probably easier to determine it graphically if needed, as shown in Figure 19).

6.5.2 Critical pillar dimensions for Category 2 ultimate fracture $\bar{\sigma}_p > \sigma_{pmin}$, $\bar{\sigma}_p > \bar{\sigma}_{PR}$ $(\bar{\sigma}_{pmin} < \bar{\sigma}_{PR})$

Let the critical pillar dimension in this case be equal to b_{c2}. This critical dimension will occur when $\bar{\sigma}_p = \bar{\sigma}_{PR}$. i.e. at any smaller pillar dimension $\bar{\sigma}_p = \bar{\sigma}_{PR}$ and ultimate fracture occurs as illustrated in Figure 18E and at a larger pillar dimension the pillar is stable (Figure 18C). Now in this case $\bar{\sigma}_p = \bar{Y}\, S_v$ and $\bar{\sigma}_{PR}$ is given by equation 56, hence putting $b = b_{c2}$ and equating $\bar{\sigma}_p = \bar{\sigma}_{PR}$ gives:-

$$\bar{Y}\, S_v = \frac{P_B}{2b_{c2}} \; \frac{(1-\mathrm{Sin}\phi_B)}{\mathrm{Sin}\phi_B} \left\{ \frac{h}{\tan\phi_B} \left[e^{\tan\phi_B \left\{\frac{(1+\mathrm{Sin}\phi_B)}{(1-\mathrm{Sin}\phi_B)}\right\} \left[\frac{b_{c2}}{h}\right]} - 1 \right] - b_{c2} \right\} \qquad (60)$$

Table 6.3 and Figure 20 show an example for this case for three values of S_v.

TABLE 6.3: Pillar Strength Variation with P_B and ϕ_B

Semi pillar height = 5 ft.

Semi room width = 10 ft.

P_B - uniaxial compressive strength of broken coal = 1, 10, and 100 psi

ϕ_B - angle of internal friction of broken coal = 27°, 30°

σ_c - uniaxial compressive strength - solid coal = 1000 psi

Stress ratio k = 0

Semi Pillar Width b-ft.	$\bar{Y}$ (Trib.) area	Y_{mm} Rect.	$\bar{\sigma}_{pmin}$ psi	P_B = 1.0 psi				P_B = 10 psi				P_B = 100 psi			
				$\phi_B = 27^\circ$		$\phi_B = 30^\circ$		$\phi_B = 27^\circ$		$\phi_B = 30^\circ$		$\phi_B = 27^\circ$		$\phi_B = 30^\circ$	
				$\bar{\sigma}_{PR}$	$\bar{\sigma}_s$	$\bar{\sigma}_{PR}$	$\bar{\sigma}_s$	$\bar{\sigma}_{PR}$	$\bar{\sigma}_s$	$\bar{\sigma}_{PR}$	$\bar{\sigma}_s$	$\bar{\sigma}_{PR}$	$\bar{\sigma}_s$	$\bar{\sigma}_{PR}$	$\bar{\sigma}_s$
5	3.0	3.164	948	2.8	948	3.5	948	28	948	35	948	280	948	350	948
10	2.0	2.714	737	7.7	737	13	737	77	737	130	737	771	771	1300	1300
15	1.67	2.604	641	22	641	51	641	220	641	510	641	2200	2200	5100	5100
20	1.50	2.557	587	66	587	220	587	660	660	2200	2200	6600	6600	2.2×10^4	2.2×10^4
25	1.40	2.531	555	207	555	998	998	2070	2070	9980	9980	2.1×10^4	2.1×10^4	9.9×10^4	9.9×10^4
30	1.33	2.514	529	674	674	4700	4700	6740	6740	4.7×10^4	4.7×10^4	6.7×10^4	6.7×10^4	4.7×10^5	4.7×10^4
35	1.28	2.503	511	2246	2246	2.3×10^4	2.3×10^4	2.2×10^4	2.2×10^4	2.3×10^5	2.3×10^5	2.2×10^5	2.2×10^5	2.3×10^6	2.3×10^4
40	1.25	2.495	501	7637	7637	1.1×10^5	1.1×10^5	7.6×10^4	7.6×10^4	1.1×10^6	1.1×10^6	7.6×10^5	7.6×10^5	1.1×10^7	1.1×10^7
45	1.22	2.489	490	26370	26370	5.6×10^5	5.6×10^5	2.6×10^5	2.6×10^5	5.6×10^6	5.6×10^6	2.6×10^6	2.6×10^6	5.6×10^7	5.6×10^7
50	1.20	2.484	483	92175	92175	1.8×10^6	1.8×10^6	9.2×10^5	9.2×10^5	2.8×10^7	2.8×10^7	9.2×10^6	9.2×10^6	2.8×10^8	2.8×10^8
60	1.17	2.477	472	1.16×10^6	1.16×10^6	7.6×10^7	7.6×10^7	1.1×10^7	1.1×10^7	7.6×10^8	7.6×10^8	1.1×10^8	1.1×10^8	7.6×10^9	7.6×10^9
70	1.14	2.472	461	14.9×10^6	14.9×10^6	2.1×10^{10}	2.1×10^{10}	1.5×10^{10}	1.5×10^{10}	2.1×10^{11}	2.1×10^{11}	1.5×10^9	1.5×10^9	2.1×10^{12}	2.1×10^{12}

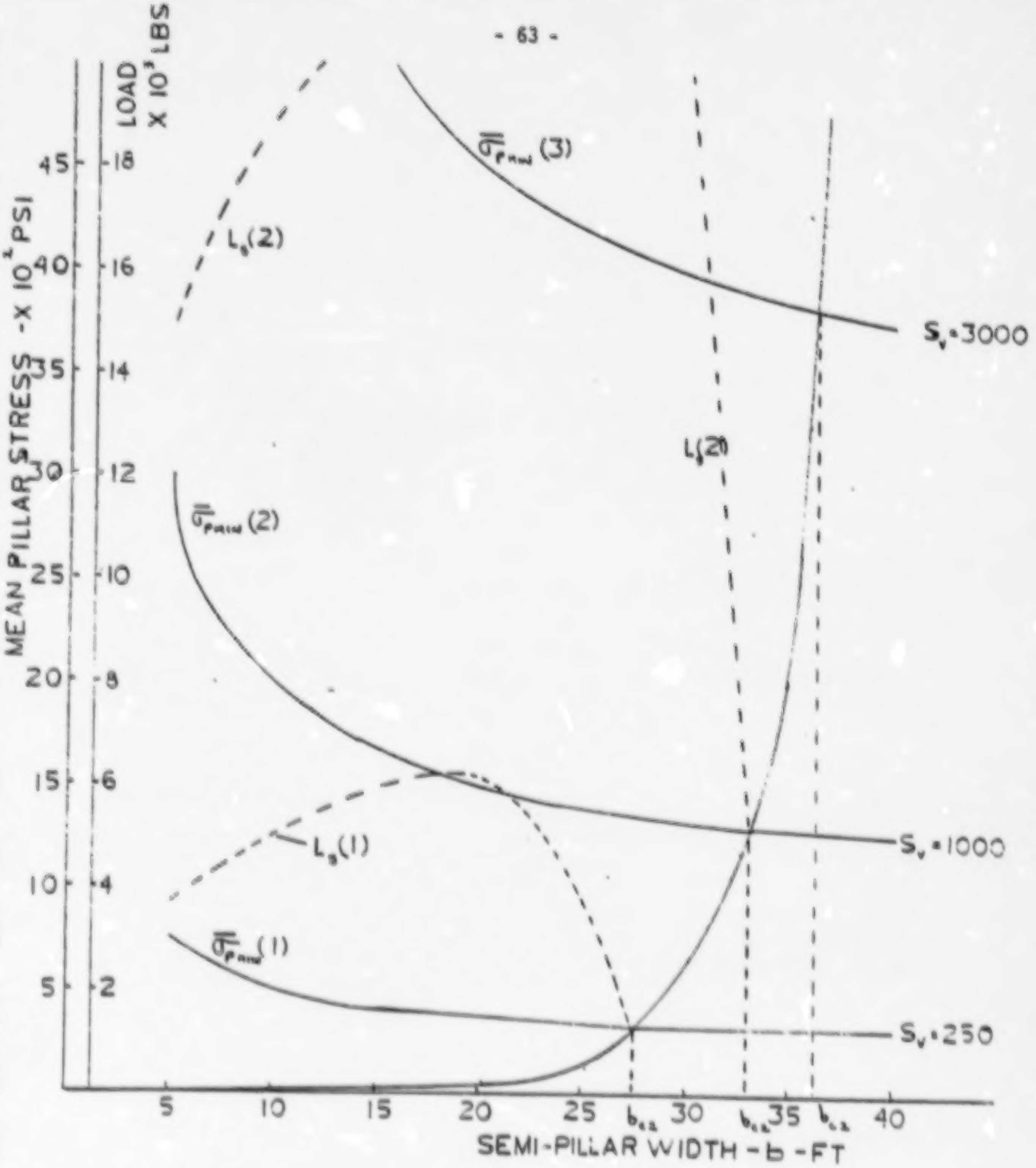

FIGURE 20: Critical pillar dimension, b_{c2}, to avoid ultimate failure (category 2)

The values of b_{c2} for these examples are:

S_v = 250 psi b_{c2} = 27.5 ft.
S_v = 1000 psi b_{c2} = 33 ft.
S_v = 3000 psi b_{c2} = 37 ft.

It is seen that the critical pillar dimension that will be required to totally avoid the possibility of catastrophic or ultimate fracture must be the larger value of b_{c1} or b_{c2}.

when $\bar{\gamma} S_v$ is $< \frac{\bar{\gamma}}{\bar{\gamma}_{mm}} \sigma_c$ then $b_{c1} > b_{c2}$ and the critical dimension is given by equation 59 and L_s is given by equation 57.

whereas when $\bar{\gamma} S_v > \frac{\bar{\gamma}}{\bar{\gamma}_{mm}} \sigma_c$ then $b_{c2} > b_{c1}$ and the critical pillar dimension is given by equation 60 and L_s is given by equation 58.

6.6 Pillar strength and safety factor.

6.6.1 Pillar strength

The pillar strength, $\bar{\sigma}_s$, is defined as that mean pillar stress required to just fracture the pillar to its centre. Now it was shown in Section 6.3 that when $b < b_{c1}$ (i.e. when $\frac{\bar{\gamma}}{\bar{\gamma}_{mm}} \sigma_c > \bar{\gamma} S_v$)

then $\bar{\sigma}_{pmin}$ = the minimum pillar strength. Further, it follows from section 6.4 that when $b > b_{c2}$ (i.e. when $\frac{\bar{\gamma}}{\bar{\gamma}_{mm}} \sigma_c > \bar{\gamma} S_v$) then the pillar strength is equal to $\bar{\sigma}_{PR}$, the mean residual stress capacity, when the fracture just reaches the pillar centre. Hence the pillar strength, $\bar{\sigma}_s$, can be summarized as follows:-

when $b \leq b_{c1}$ (given by equation 59) i.e. when $\frac{\bar{\gamma}}{\bar{\gamma}_{mm}} \sigma_c > \bar{\gamma} S_v$ then

$$\bar{\sigma}_s = \frac{\bar{\gamma}}{\bar{\gamma}_{mm}} \cdot \sigma_c \tag{61}$$

and when $b \geq b_{c2}$ (given by equation 60) i.e. when $\bar{\gamma} S_v > \frac{\bar{\gamma}}{\bar{\gamma}_{mm}} \sigma_c$

$$\bar{\sigma}_s = \frac{P_B\ (1-\mathrm{Sin}\phi_B)}{2b\ \ \mathrm{Sin}\phi_B}\left\{\frac{h}{\tan\phi_B}\left[e^{\tan\phi_B\left(\frac{1+\mathrm{Sin}\phi_B}{1-\mathrm{Sin}\phi_B}\right)\left[\frac{b}{h}\right]}-1\right]-b\right\} \tag{62}$$

The effects of pillar width on pillar strength can therefore be illustrated by the example considered previously as can the influence of P_B and ϕ_B on pillar strength: Table 6.3 gives the parameters for these examples and Figure 21 shows the results in graphical form.

The following points are illustrated in the example:-

(i) The minimum pillar strength, $\bar{\sigma}_{pmin} = \bar{\sigma}_s$, diminishes slowly with increasing pillar width. This is due to the fact that, in this example at least, $\overline{Y}$ decreases more rapidly than Y_{mm} with increase in b.

(ii) Once $\bar{\sigma}_s$, exceeds $\bar{\sigma}_{pmin}$ the strength is very sensitive to the value of both P_B and ϕ_B.

(iii) The pillar strength is only influenced by the solid coal properties (σ_c) for small pillars which fail immediately, fracture is initiated as controlled by σ_c. For larger pillars this is not the case, the strength is solely dependent on the properties of the broken coal!

(iv) The pillar strength $\bar{\sigma}_s$ for the larger pillars, as given by equation 62, increases exponentially with increase of the semi-pillar width. This rapidly leads to pillars of effectively infinite strength. Clearly the vertical applied stress and the corresponding confining stresses rapidly reach values where brittle failure would not be expected but where it might be anticipated that the coal would exhibit ductile or pseudo-ductile yielding.

Consequently the failure criterion (Coulomb-Navier) used in these analyses to this point should be modified to allow for ductile yielding of the pillar in addition to brittle fracture. This development and the criteria for pseudo-ductile yielding are considered in the ensuing sections of this report.

6.6.2 Pillar safety factor

The pillar safety factor, S.F., can be defined as the mean pillar stress at failure divided by the mean applied pillar stress:-

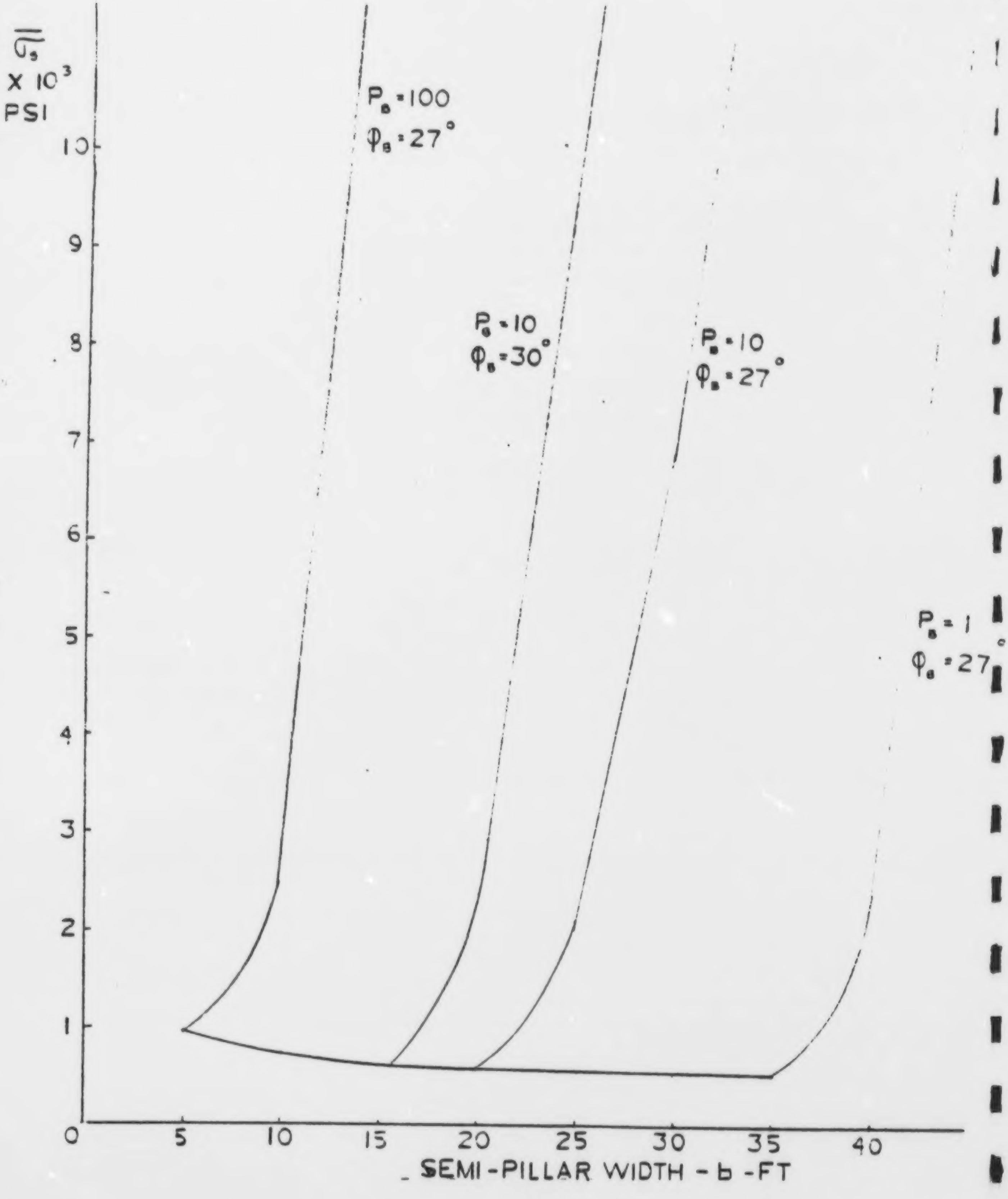

FIGURE 21: Pillar strength variation with P_B and ϕ_B

$$\underline{\text{when } \frac{\bar{\gamma}}{\gamma_{mm}} \sigma_c > \bar{\gamma} S_v \quad (b < b_{c1})} \tag{63}$$

$$\underline{S.F = \frac{\bar{\sigma}_s}{\bar{\gamma} S_v} = \frac{\bar{\gamma} \sigma_c}{\gamma_{mm} \bar{\gamma} S_v} = \frac{\sigma_c}{\gamma_{mm} S_v}}$$

Once fracture initiates, catastrophic failure occurs and the "safety factor" of the residual failed pillar drops to less than unity and load is shed on to adjacent pillars. If this safety factor is > 1, no fracture has occured in the pillar.

$$\text{When } \underline{\bar{\gamma} S_v > \frac{\bar{\gamma}}{\gamma_{mm}} \sigma_c \quad (b > b_c)}$$

$$S.F = \frac{\bar{\sigma}_{PR}}{\bar{\gamma} S_v} = \frac{P_B \quad (1-\text{Sin}\phi_B)}{2b\ \text{Sin}\phi_B \quad \bar{\gamma} S_v} \left\{ \frac{h}{\tan\phi_B} \left[e^{\tan\phi_B \left(\frac{1+\text{Sin}\phi_B}{1-\text{Sin}\phi_B}\right) \left[\frac{b}{h}\right]} - 1 \right] - b \right\} \tag{64}$$

If this safety factor is > unity then the pillar is stable and the stress distribution curve will be as illustrated in Figure 18C. If it is < unity then ultimate failure occurs, load is shed on to adjacent pillars and the stress distribution is as illustrated in Figure 18E.

6.7 Conclusions.

This consideration of pillar stress and safety factor brings to an end the first part of this analysis dealing with brittle fracture development in pillar. Analytical expressions for all steps 1 to 12 given Figure 1 have been derived. The remaining parts of this report will consider the influence of pseudo-ductile behaviour on the pillar and will also describe the computer program developed.

7. Transition from brittle to pseudo-ductile failure and revised failure criteria

7.1 Transition from brittle to pseudo-ductile failure

Consider a triaxial test illustrated in Figure 22. Figure 23 shows how the triaxial specimen deforms as the axial stress is increased; the differential stress $(\sigma_1 - \sigma_3)$ is proportional to the shear stress for any given angle of failure, θ.

At some confining pressure (σ_{33}, Figure 23), the differential stress increases rapidly with relatively little axial strain up to some critical value and then the specimen undergoes large deformation with little or no change in differential (or shear) stress. This type of deformation behaviour is usually called "ductile" failure and is usually defined as :-

either (a) permanent deformation without loss of cohesion

or (b) deformation without change in applied stress

It has been shown (14, 15, 16), as will be explained below, that what is often interpreted as pure plastic or ductile failure in triaxial tests is actually brittle failure and friction along fracture surfaces. Consequently definition (a) above which requires no loss in cohesion does not apply. Hence the second definition, which incidentally says nothing about the mechanism of failure, will be used in this study. Further, to distinguish this failure from pure plastic behaviour the author will use the term "pseudo-ductile" failure to describe this deformation without change in axial stress.

Consider the failure at the different confining pressures illustrated in Figure 23. As the axial stress increases, the shear stress and the normal stress both increase until the shear stress τ on a plane at angle θ° exceeds the shear resistance of the solid rock on that plane and the rock fractures. Following fracture, the normal stress, σ, continues to act across the fracture surface producing a frictional resistance f where:-

$$f = \mu\sigma$$

where *μ is the coefficient of sliding friction on the fracture surface

*Note: Amonton's law of dry friction is assumed where μ is a constant defined as the coefficient of sliding friction. There is a significant body of evidence (14, 15) to indicate that μ is not a constant but decreases as the normal stress increases. Functions such as $f = a\sigma^e$ (14) and $f = a + (^b/\sigma)$, (15), have been used to describe the frictional resistance to sliding. However, for the purposes of this study μ will be assumed to be a constant. If deemed necessary later, the relationship could easily be changed to reflect a variable μ based on experimental results for the sliding of coal surfaces.

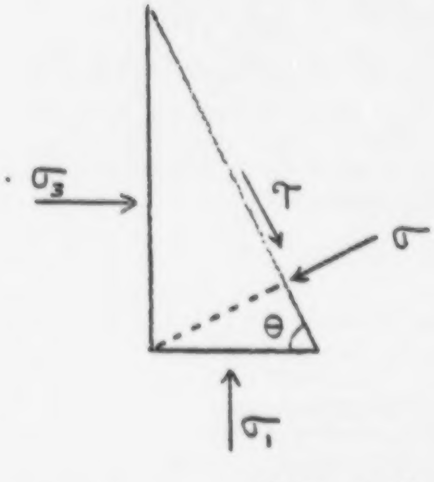
σ_3
τ
σ
θ
σ_1

NORMAL STRESS $\sigma = \left\{\frac{\sigma_1 + \sigma_3}{2}\right\} + \left\{\frac{\sigma_1 - \sigma_3}{2}\right\} \cos 2\theta$

SHEAR STRESS $|\tau| = \left\{\frac{\sigma_1 - \sigma_3}{2}\right\} \sin 2\theta$

FIGURE 22: Triaxial test

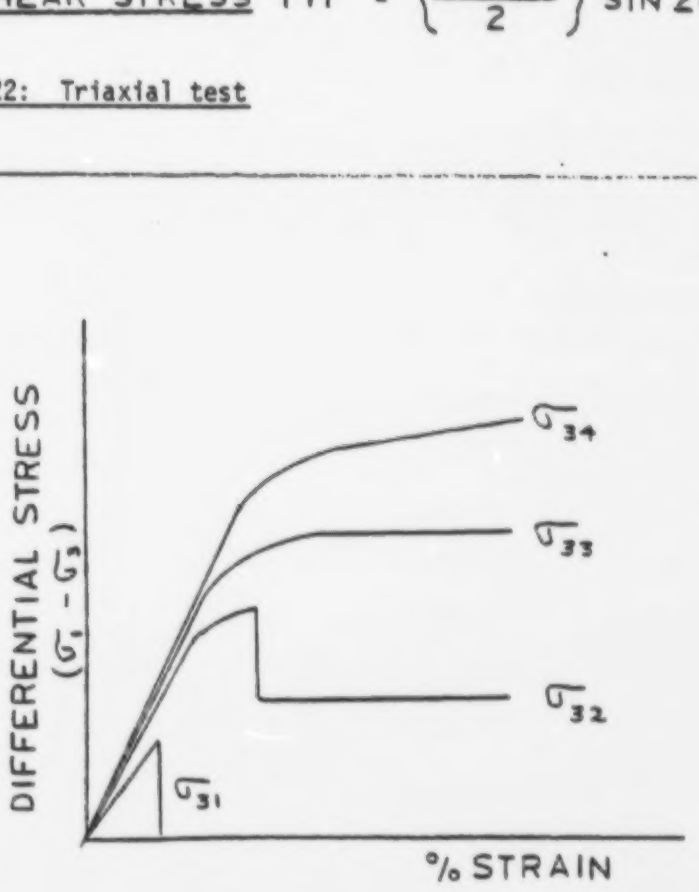

FIGURE 23: Typical differential stress versus strain curves from triaxial tests

At low confining pressures (σ_{31}, σ_{32}, Figure 23) the frictional resistance to sliding is lower than the shear resistance to fracture of the rock and the rock breaks into two or three pieces; when fracture takes place there is a drop of stress to the level of the sliding frictional resistance and deformation continues by sliding on the fractured surface.

At confining pressures greater than σ_{33} (σ_{34}, Figure 23) the frictional resistance to sliding exceeds the shear resistance to fracture of the rock. i.e. the resistance to displacement along the fractured surface is greater than it was before fracture. Consequently it is easier to form new fracture surfaces than to produce displacement along existing fractures as the load is increased. As a result conjugate sets of parallel fractures are formed and the specimens, rather than fracturing into distinct pieces, become barrel shaped. It will be noted that the σ_{34} curve in Figure 23 has a slight positive slope after fracture; this is attributed to some form of strain hardening, but will be ignored in this study.

Hence it is seen that the brittle / pseudo-ductile transition occurs when the shear resistance of the solid rock to failure, τ_s, on the plane at angle θ_s equals the frictional resistance to sliding on that plane.

$$\text{i.e.} \quad \tau_s = \mu\sigma_s \tag{65}$$

It is important to this study to note that this brittle / pseudo-ductile transition cannot take place if we assume that Coulomb-Navier failure of the solid rock. This is illustrated by reference to Figure 24; the Mohr envelope for Coulomb-Navier theory is given by a straight line:-

$$\tau_s = S_o + \mu_A\sigma_s$$

where μ_A is the coefficient of "internal friction" of the solid rock.

and the frictional resistance to sliding, f, is given by,

$$f = \mu_B \sigma_s$$

where μ_B is the coefficient of sliding friction.

The brittle / pseudo-ductile transition occurs when these two curves intersect and:-

$$\mu_B \sigma_s = S_o + \mu_A \sigma_s$$

$$\text{or } \underline{S_o = \sigma_s (\mu_B - \mu_A)}$$

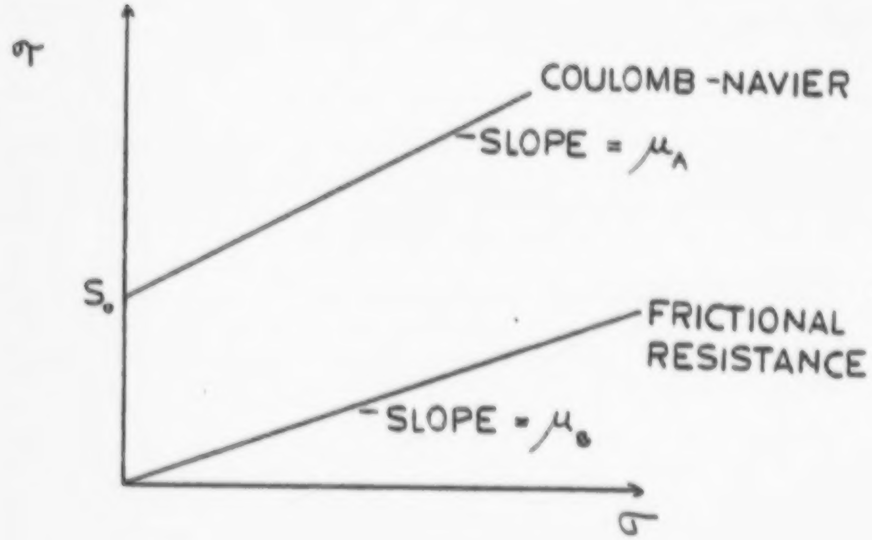
τ
COULOMB -NAVIER
SLOPE = μ_A
S_0
FRICTIONAL RESISTANCE
SLOPE = μ_0
σ

FIGURE 24: Shear resistance versus normal stress; Coulomb-Navier failure and frictional sliding

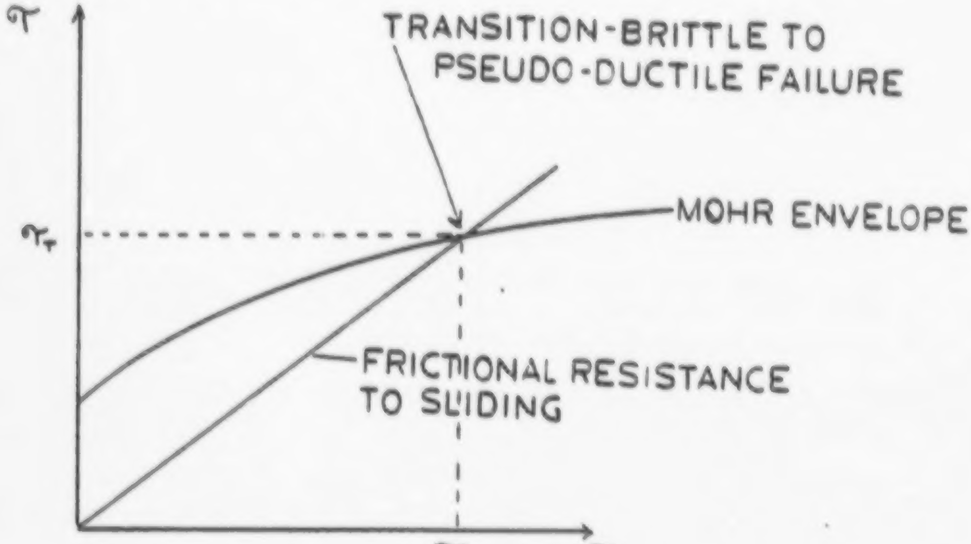
τ
TRANSITION-BRITTLE TO PSEUDO-DUCTILE FAILURE
τ_T
MOHR ENVELOPE
FRICTIONAL RESISTANCE TO SLIDING
σ_T
σ

FIGURE 25: Shear resistance versus normal stress; Mohr failure theory and frictional sliding

Now So must always be a positive finite value, thus this equation will only be satisfied if $\mu_B > \mu_A$.

However the coefficient of internal friction of a rock, μ_A, is always greater than the sliding coefficient of friction μ_B (10). Consequently this equation can never be satisfied. Hence Coulomb-Navier theory for the failure of the solid rock cannot be used if it is necessary to consider, beyond some critical stress value, the pseudo-ductile behaviour of the rock.

|Note: this does not prelude considering the behaviour of the broken rock in terms of Coulomb-Navier theory as was done in Section 5.3.1 when considering the stress build up in the broken rock. This aspect will remain unchanged in the revised analysis.|

However, if a non-linear Mohr envelope is used to describe the rock failure (i.e. Mohr theory rather than Coulomb-Navier theory) then this brittle / pseudo-ductile transition can occur, as illustrated in Figure 25. In Appendix I a non-linear Mohr envelope of parabolic form has been assumed and various stress relationships at failure have been derived. It is also shown in this appendix that this form of Mohr envelope gives an acceptable description of the experimental results for triaxial tests on a number of different coals. Let us therefore assume that the Mohr envelope for failure is as described in Appendix I as is given by :-

$$\underline{\tau_s{}^2 - A\sigma_s - A^2/_4 = 0} \qquad (66)$$

where τ_s and σ_s are the shear and normal stress on the failure plane required to produce failure.

Now the shear resistance due to sliding friction on the failed surface, f, is given by :-

$$\underline{f = \mu_B\ \sigma_s} \qquad (67)$$

Thus brittle / pseudo-ductile transition will occur when $\tau_s = f$. Let $\tau_s = \tau_T$ and $\sigma_s = \sigma_T$ at this transition point. Then from 66 and 67 :-

$$\underline{\mu_B{}^2\ \sigma_T{}^2 - A\sigma_T - A^2/_4 = 0} \qquad (68)$$

Which, solving for σ_T, gives :-

$$\sigma_T = \frac{A}{2\mu_B^2}\left\{1+\left(1+\mu_B^2\right)^{\frac{1}{2}}\right\} \tag{69}$$

and, from 67 and 69 :-

$$\tau_T = \frac{A}{2\mu_B}\left\{1+\left(1+\mu_B^2\right)^{\frac{1}{2}}\right\} \tag{70}$$

and further, using the relationships at failure derived in Appendix I the angle of failure, θ_T, the vertical stress σ_{1T} and the lateral stress σ_{3T} at the transition point can be determined and are given by :-

$$\text{Cos } 2\theta_T = \frac{-\mu_B}{\left\{2\left(1+\mu_B^2\right) + 2\left(1+\mu_B\right)^{\frac{1}{2}}\right\}^{\frac{1}{2}}} \tag{71}$$

$$\begin{aligned}\sigma_{1T} &= \frac{A}{2} + \sigma_T + \left\{\frac{A^2}{2} + A\sigma_T\right\}^{\frac{1}{2}} \\ &= \frac{A}{2} + \frac{A}{2\mu_B^2}\left\{1+\left(1+\mu_B^2\right)^{\frac{1}{2}}\right\} + \left\{\frac{A^2}{2} + \frac{A^2}{2\mu_B^2}\left[1+\left(1+\mu_B^2\right)^{\frac{1}{2}}\right]\right\}^{\frac{1}{2}}\end{aligned} \tag{72}$$

and $$\sigma_{3T} = \frac{A}{2} + \frac{A}{2\mu_B^2}\left\{1+\left(1+\mu_B^2\right)^{\frac{1}{2}}\right\} - \left\{\frac{A^2}{2} + \frac{A^2}{2\mu_B^2}\left[1+\left(1+\mu_B^2\right)^{\frac{1}{2}}\right]\right\}^{\frac{1}{2}} \tag{73}$$

Consider now the behaviour of the material beyond the transition point. If an applied shear stress τ is applied to an element and τ is greater then τ_T then the material will yield and thus τ_T will be the "residual shear stress capacity" of the element, and excess load will be shed onto adjacent, as yet, unfailed slices. i.e. we have a "maximum shear stress" failure criteria. Consequently the angle of failure will remain constant at the value given by equation 71 and both σ_{1T} and σ_{3T} will remain constant. The important consequence of this is that the lateral confining pressure σ_3 remains constant at a value σ_{3T} and does not build up in the yield zone. Further, it follows that σ_{3T} will be equal to the value of P_3, the lateral stress applied by the last fractured slice.

7.2 Revised failure criteria

7.2.1 Requirement for brittle failure.

Let σ_{1s} and σ_{3s} be the vertical and lateral principle stresses to fail the slice by brittle fracture, then using the relationships derived in Appendix I from the Mohr failure envelope we have (from equation 1) :-

$$\left\{\frac{\sigma_{1s} - \sigma_{3s}}{2}\right\}^2 = A\left\{\frac{\sigma_{1s} + \sigma_{3s}}{2}\right\} \qquad (74)$$

$$\text{i.e. } \sigma_{1s}^{\;2} - 2\sigma_{1s}\,(\sigma_{3s} + A) + \sigma_{3s}\,(\sigma_{3s} - A) = 0$$

from which it can be shown that:-

$$\sigma_{1s} = (\sigma_{3s} + A) + (4A\sigma_{3s} + A^2)^{\frac{1}{2}} \qquad (75)$$

and the angle of fracture, θ_s, from equation I 10, is given by:-

$$\text{Cos } 2\theta_s = \frac{-(\sigma_{1s} - \sigma_{3s})}{2\,(\sigma_{1s} + \sigma_{3s})} \qquad (76)$$

and if T_s is the shear stress on this failure plane then, from equation I 12:-

$$T_s = \left\{\frac{\sigma_{1s} - \sigma_{3s}}{2}\right\} \text{Sin } 2\theta_s = \left\{\frac{\sigma_{1s} - \sigma_{3s}}{2}\right\}\left\{\frac{\left[4\,(\sigma_{1s} + \sigma_{3s})^2 - (\sigma_{1s} - \sigma_{3s})^2\right]}{2(\sigma_{1s} + \sigma_{3s})}\right\}^{\frac{1}{2}} \qquad (77)$$

Now the lateral stress σ_{3s} on the first slice is zero and on the remaining slices is P_3, as given by equation 44, which in turn can be determined from the value P_1 of the residual vertical stress capacity of that slice from equation 43.

Hence putting $\sigma_{3s} = P_3$ we have:-

$$\sigma_{1s} = (P_3 + A) + (4AP_3 + A^2)^{\frac{1}{2}} \qquad (78)$$

$$\text{Cos } 2\theta_s = \frac{-(\sigma_{1s} - P_3)}{2(\sigma_{1s} + P_3)} \qquad (79)$$

$$\text{and } \tau_s = \left\{\frac{\sigma_{1s} - P_3}{2}\right\}\left\{\frac{\left[4\,(\sigma_{1s} + P_3)^2 - (\sigma_{1s} - P_3)^2\right]^{\frac{1}{2}}}{2(\sigma_{1s} + P_3)}\right\} \qquad (80)$$

Consequently σ_{1s}, θ_s and τ_s for fracture can be evaluated from these three equations.

Now the applied vertical stress in the i th slice, σ_{1i} is known, as before, from the inital vertical stress plus the accumulated increments shed from previously failed slices. Consequently the applied shear stress acting on this potential fracture plane will be given by τ :-

$$\tau = \frac{(\sigma_{1i} - P_3)}{2}\,\text{Sin } 2\theta_s \qquad (81)$$

Hence brittle fracture will occur if

$$\tau > \tau_s \qquad (82)$$

If $\tau < \tau_s$ brittle fracture will not occur, the slice will be stable and the pillar will have a solid central core with an elastic stress distribution, given as before by the initial stress plus the accumulated stresses shed from the unfailed slices.

If $\tau > \tau_s$, brittle fracture occurs; the residual vertical stress capacity P_1 is determined as before from the properties of the broken coal as:-

$$P_1 = \frac{P_B}{2\,\text{Sin}\phi_B}\left\{(1+\text{Sin}\phi_B)\; e^{\tan\phi_B\left\{\frac{1+\text{Sin}\phi_B}{1-\text{Sin}\phi_B}\right\}\left[\frac{e-w}{h}\right]} - (1-\text{Sin}\phi_B)\right\} \qquad (54)$$

The lateral stress applied to the next adjacent, as yet unfailed, slices is given by:-

$$P_3 = \left\{\frac{1 - \text{Sin}\phi_B}{1 + \text{Sin}\phi_B}\right\}(P_1 - P_B) \qquad (44)$$

and the load shed, Δ_{L1} from this failed slice onto the adjacent slices is given by :-

$$\underline{\Delta L_1 = (\sigma_{1i} - P_1)\ \delta e}$$

where δe is the slice thickness.

Hence the new elastic stress on the remaining slices can be determined, as in Section 5.4, and the new vertical stress $\sigma_{1(i+1)}$ on the next adjacent slice is thus known. Hence this slice can be tested for failure by repeating this sequence of calculations for the $(i + 1)$th slice etc.

7.2.2 Requirements for pseudo-ductile yield

In the previous sequence of steps, having calculated τ_s the shear stress required for brittle fracture, we should then determine τ_T the shear stress at the transition point where τ_T is given by equation 70 as :-

$$\tau_T = \frac{A}{2\mu_B}\left\{1 + (1 + \mu_B{}^2)^{\frac{1}{2}}\right\} \qquad (70)$$

τ_s should then be compared with τ_T.

If $\tau_s < \tau_T$ then the only possible mode of failure for this slice is brittle fracture and the brittle fracture criteria given in Section 7.2.1 above will be considered.

However if $\tau_s > \tau_T$ then the transition point has been passed and the only possible mode for failure of the slice is by pseudo-ductile yield. In this case, the next step is to determine the angle of failure at the transition point, θ_T, which is given by equation 69 as :-

$$\text{Cos } 2\theta_T = \frac{-\mu_B}{\left[2(1+\mu_B{}^2) + 2(1+\mu_B{}^2)^{\frac{1}{2}}\right]^{\frac{1}{2}}} \qquad (69)$$

and the applied sheer stress τ is given, as above, by equation 81:-

$$\underline{\tau = \left\{\frac{\sigma_{1i} - P_3}{2}\right\} \text{Sin } 2\theta_T} \qquad (83)$$

where P_3 is the lateral stress generated by the last slice to have failed by brittle fracture.

Hence pseudo-ductile yield will occur if :-

$$\tau > \tau_T \qquad (84)$$

If $\tau < \tau_T$ then pseudo-ductile yield cannot have taken place, the remaining pillar slices will be stable and this central solid core will have an elastic stress distribution given by the initial stress distribution plus the accumulated increments from each of the previously fractured or yielded slices.

If $\tau > \tau_T$ then the slice will have yielded. The residual vertical stress capacity of this slice will be given by equation 72 as :-

$$\sigma_{1T} = \frac{A}{2} + \frac{A}{2\mu_B^2}\left\{1 + (1+\mu_B^2)^{\frac{1}{2}}\right\} + \left\{\frac{A^2}{2} + \frac{A^2}{2\mu_B^2}\left[1+(1+\mu_B^2)^{\frac{1}{2}}\right]\right\}^{\frac{1}{2}} \qquad (72)$$

The load shed onto the next adjacent, as yet, unyielded slice will be :-

$$\Delta L = (\sigma_{1i} - \sigma_{1T})\,\delta e \qquad (85)$$

where δe is the slice thickness.

Hence the new elastic stress distribution on the remaining slices can be determined as before, thus the new vertical stress $\sigma_{1(i+1)}$ can be calculated. The new lateral stress is still equal to P_3 the lateral stress applied by the last fractured slice, as was shown in Section 7.1 (i.e. the lateral stress remains constant throughout the yield zone). Consequently the next slice can be tested for yield by repeating these steps for the stresses on the (i+1)th slice.

This somewhat complex explanation of the revised failure criteria is more easily envisaged by reference to figure 26 in which the computer logic flow diagram is given for these decisions together with the appropriate equations.

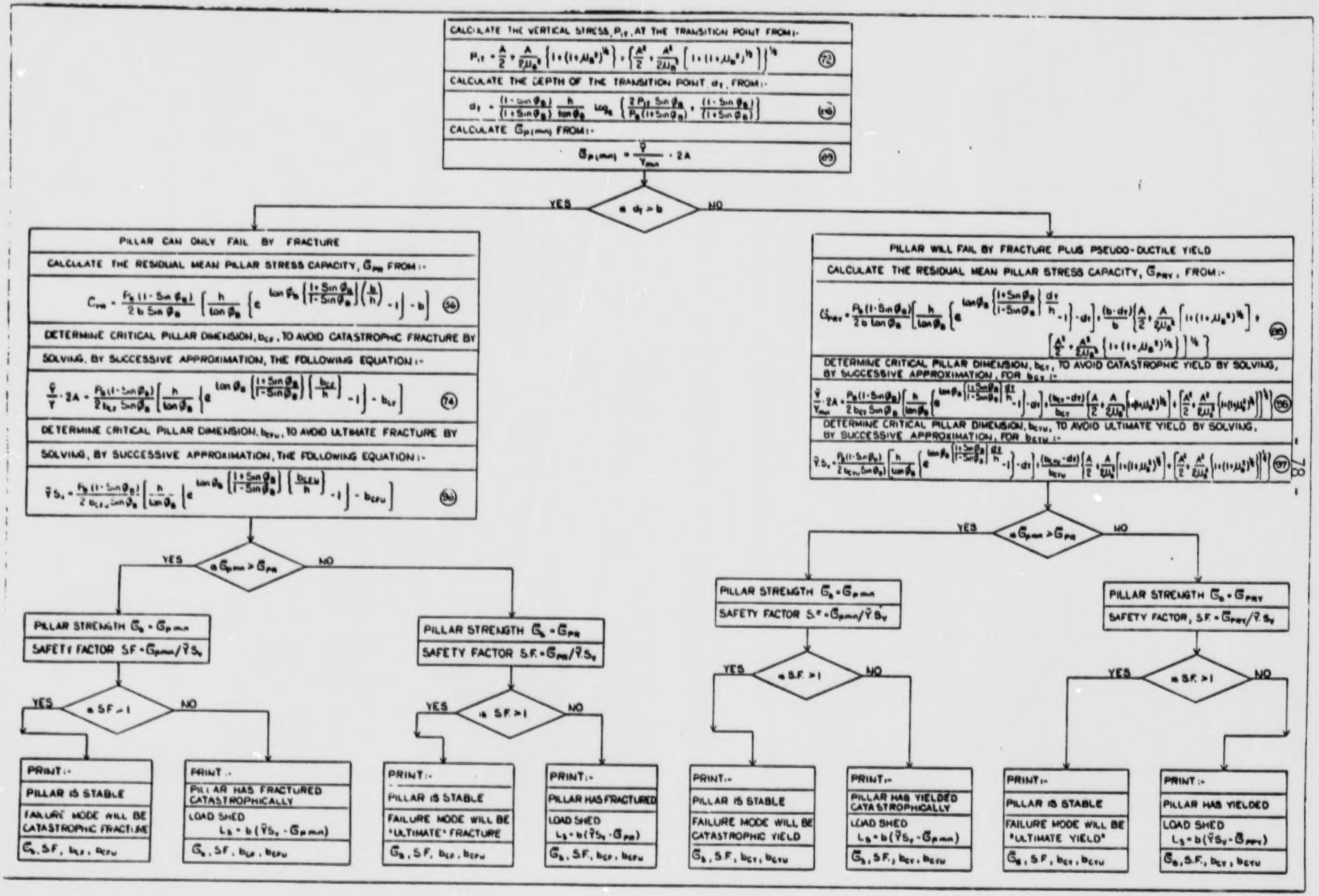
CALCULATE THE VERTICAL STRESS, P_{1T}, AT THE TRANSITION POINT FROM:-
$P_{1T} = \frac{A}{2} + \frac{A}{2\mu_B^2}\left\{1+(1+\mu_B^2)^{1/2}\right\} + \left\{\frac{A^2}{2} + \frac{A^2}{2\mu_B^2}\left[1+(1+\mu_B^2)^{1/2}\right]\right\}^{1/2}$ (72)
CALCULATE THE DEPTH OF THE TRANSITION POINT d_T, FROM:-
$d_T = \frac{(1-\sin\phi_B)}{(1+\sin\phi_B)}\frac{h}{\tan\phi_B}\log_e\left\{\frac{2P_{1T}\sin\phi_B}{P_B(1+\sin\phi_B)} + \frac{(1-\sin\phi_B)}{(1+\sin\phi_B)}\right\}$
CALCULATE $\bar{\sigma}_{p(mn)}$ FROM:-
$\bar{\sigma}_{p(mn)} = \frac{\bar{\gamma}}{\gamma_{mn}} \cdot 2A$
IS $d_T > b$
YES
NO
PILLAR CAN ONLY FAIL BY FRACTURE
CALCULATE THE RESIDUAL MEAN PILLAR STRESS CAPACITY, $\bar{\sigma}_{PR}$ FROM:-
$\bar{\sigma}_{PR} = \frac{P_B(1-\sin\phi_B)}{2b\sin\phi_B}\left[\frac{h}{\tan\phi_B}\left\{e^{\tan\phi_B\left\{\frac{1+\sin\phi_B}{1-\sin\phi_B}\right\}\left(\frac{b}{h}\right)}-1\right\}-b\right]$ (56)
DETERMINE CRITICAL PILLAR DIMENSION, b_{CF}, TO AVOID CATASTROPHIC FRACTURE BY
SOLVING, BY SUCCESSIVE APPROXIMATION, THE FOLLOWING EQUATION:-
$\frac{\bar{\gamma}}{\gamma} \cdot 2A = \frac{P_B(1-\sin\phi_B)}{2b_{CF}\sin\phi_B}\left[\frac{h}{\tan\phi_B}\left\{e^{\tan\phi_B\left\{\frac{1+\sin\phi_B}{1-\sin\phi_B}\right\}\left(\frac{b_{CF}}{h}\right)}-1\right\}-b_{CF}\right]$ (74)
DETERMINE CRITICAL PILLAR DIMENSION, b_{CFU}, TO AVOID ULTIMATE FRACTURE BY
SOLVING, BY SUCCESSIVE APPROXIMATION, THE FOLLOWING EQUATION:-
$\bar{\gamma}S_v = \frac{P_B(1-\sin\phi_B)}{2b_{CFU}\sin\phi_B}\left[\frac{h}{\tan\phi_B}\left\{e^{\tan\phi_B\left\{\frac{1+\sin\phi_B}{1-\sin\phi_B}\right\}\left(\frac{b_{CFU}}{h}\right)}-1\right\}-b_{CFU}\right]$
PILLAR WILL FAIL BY FRACTURE PLUS PSEUDO-DUCTILE YIELD
CALCULATE THE RESIDUAL MEAN PILLAR STRESS CAPACITY, $\bar{\sigma}_{PRY}$, FROM:-
$\bar{\sigma}_{PRY} = \frac{P_B(1-\sin\phi_B)}{2b\tan\phi_B}\left[\frac{h}{\tan\phi_B}\left\{e^{\tan\phi_B\left\{\frac{1+\sin\phi_B}{1-\sin\phi_B}\right\}\frac{d_T}{h}}-1\right\}-d_T\right] + \frac{(b-d_T)}{b}\left\{\frac{A}{2} + \frac{A}{2\mu_B^2}\left[1+(1+\mu_B^2)^{1/2}\right] + \left[\frac{A^2}{2} + \frac{A^2}{2\mu_B^2}\left\{1+(1+\mu_B^2)^{1/2}\right\}\right]^{1/2}\right\}$
DETERMINE CRITICAL PILLAR DIMENSION, b_{CY}, TO AVOID CATASTROPHIC YIELD BY SOLVING, BY SUCCESSIVE APPROXIMATION, FOR b_{CY}:-
$\frac{\bar{\gamma}}{\gamma_{mn}} \cdot 2A = \frac{P_B(1-\sin\phi_B)}{2b_{CY}\sin\phi_B}\left[\frac{h}{\tan\phi_B}\left\{e^{\tan\phi_B\left\{\frac{1+\sin\phi_B}{1-\sin\phi_B}\right\}\frac{d_T}{h}}-1\right\}-d_T\right] + \frac{(b_{CY}-d_T)}{b_{CY}}\left\{\frac{A}{2} + \frac{A}{2\mu_B^2}\left[1+(1+\mu_B^2)^{1/2}\right] + \left[\frac{A^2}{2} + \frac{A^2}{2\mu_B^2}\left\{1+(1+\mu_B^2)^{1/2}\right\}\right]^{1/2}\right\}$ (96)
DETERMINE CRITICAL PILLAR DIMENSION, b_{CYU}, TO AVOID ULTIMATE YIELD BY SOLVING, BY SUCCESSIVE APPROXIMATION, FOR b_{CYU}:-
$\bar{\gamma}S_v = \frac{P_B(1-\sin\phi_B)}{2b_{CYU}\sin\phi_B}\left[\frac{h}{\tan\phi_B}\left\{e^{\tan\phi_B\left\{\frac{1+\sin\phi_B}{1-\sin\phi_B}\right\}\frac{d_T}{h}}-1\right\}-d_T\right] + \frac{(b_{CYU}-d_T)}{b_{CYU}}\left\{\frac{A}{2} + \frac{A}{2\mu_B^2}\left[1+(1+\mu_B^2)^{1/2}\right] + \left[\frac{A^2}{2} + \frac{A^2}{2\mu_B^2}\left\{1+(1+\mu_B^2)^{1/2}\right\}\right]^{1/2}\right\}$ (97)
IS $\bar{\sigma}_{pmn} > \bar{\sigma}_{PR}$
YES
NO
PILLAR STRENGTH $\bar{\sigma}_s = \bar{\sigma}_{pmn}$
SAFETY FACTOR S.F. = $\bar{\sigma}_{pmn}/\bar{\gamma}S_v$
IS S.F. > 1
YES
NO
PRINT:-
PILLAR IS STABLE
FAILURE MODE WILL BE CATASTROPHIC FRACTURE
$\bar{\sigma}_s$, S.F., b_{CF}, b_{CFU}
PRINT:-
PILLAR HAS FRACTURED CATASTROPHICALLY
LOAD SHED $L_s = b(\bar{\gamma}S_v - \bar{\sigma}_{pmn})$
$\bar{\sigma}_s$, S.F., b_{CF}, b_{CFU}
PILLAR STRENGTH $\bar{\sigma}_s = \bar{\sigma}_{PR}$
SAFETY FACTOR S.F. = $\bar{\sigma}_{PR}/\bar{\gamma}S_v$
IS S.F. > 1
YES
NO
PRINT:-
PILLAR IS STABLE
FAILURE MODE WILL BE "ULTIMATE" FRACTURE
$\bar{\sigma}_s$, S.F., b_{CF}, b_{CFU}
PRINT:-
PILLAR HAS FRACTURED
LOAD SHED $L_s = b(\bar{\gamma}S_v - \bar{\sigma}_{PR})$
$\bar{\sigma}_s$, S.F., b_{CF}, b_{CFU}
IS $\bar{\sigma}_{pmn} > \bar{\sigma}_{PR}$
YES
NO
PILLAR STRENGTH $\bar{\sigma}_s = \bar{\sigma}_{pmn}$
SAFETY FACTOR S.F. = $\bar{\sigma}_{pmn}/\bar{\gamma}S_v$
IS S.F. > 1
YES
NO
PRINT:-
PILLAR IS STABLE
FAILURE MODE WILL BE CATASTROPHIC YIELD
$\bar{\sigma}_s$, S.F., b_{CY}, b_{CYU}
PRINT:-
PILLAR HAS YIELDED CATASTROPHICALLY
LOAD SHED $L_s = b(\bar{\gamma}S_v - \bar{\sigma}_{pmn})$
$\bar{\sigma}_s$, S.F., b_{CY}, b_{CYU}
PILLAR STRENGTH $\bar{\sigma}_s = \bar{\sigma}_{PRY}$
SAFETY FACTOR, S.F. = $\bar{\sigma}_{PRY}/\bar{\gamma}S_v$
IS S.F. > 1
YES
NO
PRINT:-
PILLAR IS STABLE
FAILURE MODE WILL BE "ULTIMATE YIELD"
$\bar{\sigma}_s$, S.F., b_{CY}, b_{CYU}
PRINT:-
PILLAR HAS YIELDED
LOAD SHED $L_s = b(\bar{\gamma}S_v - \bar{\sigma}_{PRY})$
$\bar{\sigma}_s$, S.F., b_{CY}, b_{CYU}

Fi[illegible]e 2[illegible] Flo[illegible]iag[illegible] for [illegible] ise[illegible] ilu[illegible] rit[illegible]

7.3 Examples of fracture and yield zone development

The computer program, which will be described in detail in Section 9, has been modified to include the revised failure criteria developed in Section 7.2. The analysis of pillars C1 to C5 has been repeated taking into account the brittle and pseudo-ductile behaviour of the coal using typical coal properties.

7.3.1 Re-analysis of pillars C1 to C5

Table 7.1 gives the input parameters used in this re-analysis. Figure 27 shows the Mohr envelope for coal and the transition point used in the example. Figure 28 shows the resulting stress distribution across these pillars. Figure 29 shows an example computer program output sheet (for pillar C1).

It is of interest to compare the stress distribution given in Figure 28 with that obtained before the possibilities of yield were considered, the results of which were given in Figure 14. Whereas previously only one pillar (C 2) had failed, in this case with the yield parameters chosen the analysis indicates that pillars C 1, C 2, C 4 and C 5 have failed by partial fracture and yielding. The large pillar C 3 is the only pillar which is stable in both analyses and, in this latter analysis shows a fracture zone, a small yield zone and a central solid elastic core.

Previously, when fracture only was considered, the strength of the large pillars built up exponentially due to the rapid build up of the confining pressures in the broken coal and the strength of the large pillars could rapidly approach infinity; this was unrealistic. The introduction of the yield criteria sets some upper limit on the pillar strength so that it can no longer approach an infinite value, whilst at the same time the build up of confining pressure in the broken coal does increase the pillar strength significantly until yield takes place. This model appears to be much more realistic in terms of the observed behaviour of coal pillars underground.

TABLE 7.1 : Input parameters for pillar analyses used for pillar C1 to C5

INPUT PARAMETER	PILLAR								
	C1	C2		C3		C4		C5	
	-	LHS	RHS	LHS	RHS	LHS	RHS	LHS	RHS
Sv - virgin vertical stress psi	1540	1540	1540	1540	1540	1540	1540	1540	1540
R - general extraction ratio	0.254	0.254	0.254	0.254	0.254	0.254	0.254	0.254	0.254
ℓ - semi-length of mining span-ft.	315	315	315	315	315	315	315	315	315
x - coordinate of specific pillar-ft.	255	165	165	5	5	145	145	260	260
w - semi-width of room-ft.	10	10	20	20	10	10	20	20	10
z - overburden depth-ft.	1400	1400	1400	1400	1400	1400	1400	1400	1400
b - semi-pillar width-ft.	40	30	30	90	90	40	40	35	35
h - semi-pillar height-ft.	5	5	5	5	5	5	5	5	5
μ_r - Poisson's ratio of surrounding rock	0.3	0.3	0.3	0.3	0.3	0.3	0.3	0.3	0.3
μ_p - Poisson's ratio of pillar coal	0.3	0.3	0.3	0.3	0.3	0.3	0.3	0.3	0.3
E_r - Youngs modulus of surrounding rock	$5x10^6$	$5x10^6$	$5x10^6$	$5x10^6$	$5x10^6$	$5x10^6$	$5x10^6$	$5x10^6$	$5x10^6$
E_p - Youngs modulus of pillar coal	$1x10^6$	$1x10^6$	$1x10^6$	$1x10^6$	$1x10^6$	$1x10^6$	$1x10^6$	$1x10^6$	$1x10^6$
Opening shape	Rect.	Rect.	Rect.	Rect.	Rect.	Rect.	Rect.	Rect.	Rect.
$k = S_{H}/Sv$	0.33	0.33	0.33	0.33	0.33	0.33	0.33	0.33	0.33
N - number of pillars in span	5	5	5	5	5	5	5	5	5
OUTPUTS									
$\bar{Y}$ - mean pillar stress concentration	1.242	1.260	1.260	1.287	1.287	1.263	1.263	1.241	1.241
Y_{max} - maximum pillar stress concentration	2.192	2.192	2.698	2.582	2.156	2.254	2.650	2.670	2.274
Stress distribution constants k_1	0.4867	0.3756	0.1384	0.6206	3.0530	0.5623	0.1973	0.1488	0.4046
k_2	-0.6086	-0.6999	-0.9192	-0.6235	1.1249	-0.5506	-0.8820	-0.9118	-0.6746
k_3	0.9482	0.9596	0.9848	0.9338	0.7256	0.9405	0.9784	0.9836	0.9566
INPUTS									
n_1 - number of slices in pillar	160	120	120	360	360	160	160	140	140
P_B - uniaxial compressive strength broken coal-psi	1	1	1	1	1	1	1	1	1
ϕ_B - angle of friction of broken coal	27°	27°	27°	27°	27°	27°	27°	27°	27°
μ_B - coefficient of sliding friction	0.51	0.51	0.51	0.51	0.51	0.51	0.51	0.51	0.51
A - Mohr envelope constant	500	500	500	500	500	500	500	500	500
α - load shedding factor	0.5	0.5	0.5	0.5	0.5	0.5	0.5	0.5	0.5

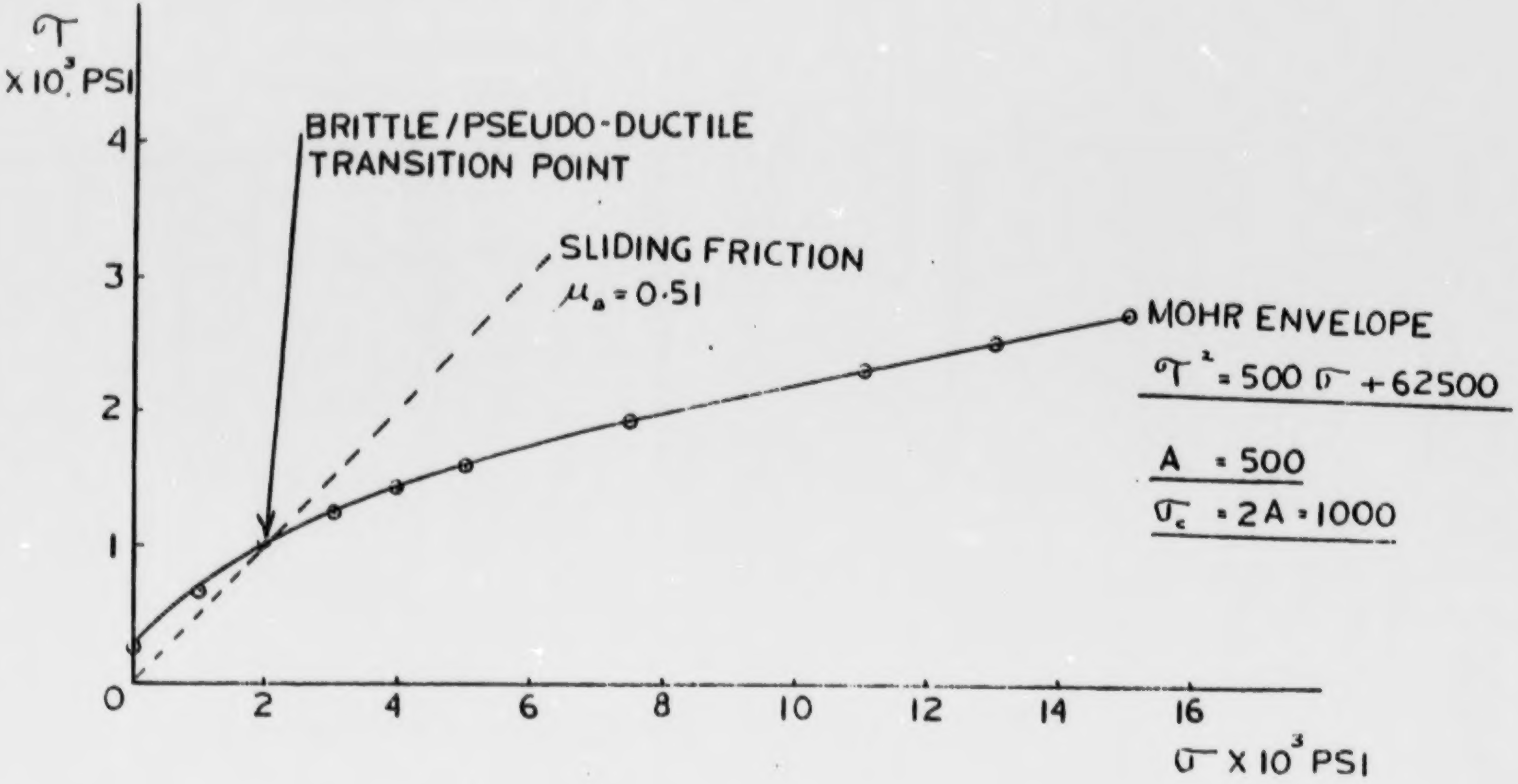

FIGURE 27: Mohr envelope assumed in example analyses

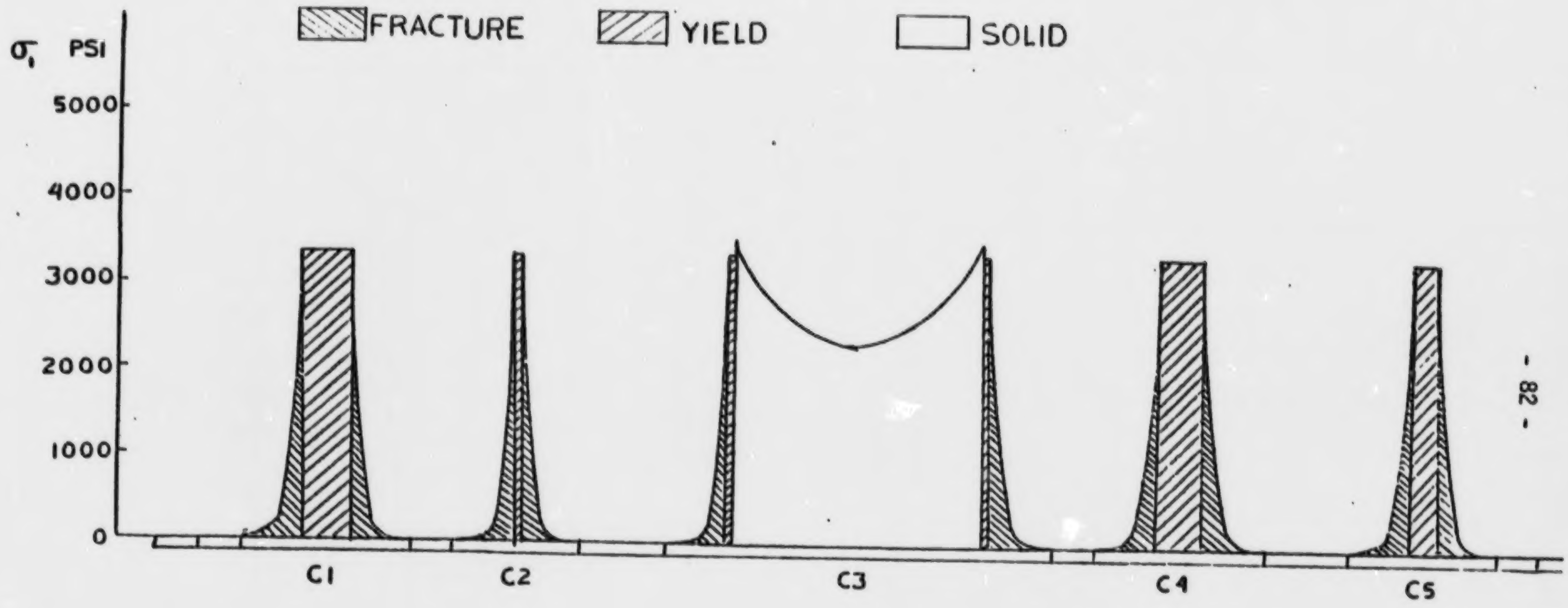

FIGURE 28: Stress distribution across pillars C1 to C5

```
CALCULATION FOR RECTANGULAR OPENING


VIRGIN STRESS=1540.0          EXTRACTION RATIO=0.254
LENGTH OF SPAN= 315.0         SEMI-WIDTH OF PILLAR= 40.0
SEMI-HEIGHT OF PILLAR= 5.0    OVERBURDEN DEPTH= 1400
DISTANCE "X"= 255             SEMI-ROOM WIDTH= 10.0
RATIO "SH/SV"=0.330           NUMBER OF PILLARS IN SPAN= 5
COMPRESSIVE STRENGTH OF BROKEN COAL=  1.
MOHR CONSTANT "A"=  500.00
ANGLE OF INTERNAL FRICTION OF BROKEN COAL=27.
POISSONS RATIO FOR SURROUNDING ROCK=0.30
POISSONS RATIO FOR PILLAR ROCK=0.30
COEFFICIENT OF SLIDING FRICTION FOR BROKEN COAL=0.51
YOUNGS MODULAS FOR SURROUNDING ROCK= 5000000
YOUNGS MODULAS FOR PILLAR ROCK= 1000000
STRESS REDISTRIBUTION COEFFICIENT=0.50
TOTAL NUMBER OF SLICES=  160
SLICE INTERVAL IN PRINTOUT= 5


THE RESULTS ARE

MEAN STRESS CONCENTATION=1.269
MEAN PILLAR STRESS:LHS=1955.
MAXIMUM STRESS CONCENTRATION=      2.19
THE PILLAR HAS YIELDED
THE LOAD SHED          =  26131.35
THE PILLAR STRENGTH =     1301.37
THE SAFETY FACTOR   =        0.67
THE CRITICAL PILLAR DIMENSION TO AVOID
      A) CATASTROPHIC YIELD IS  29.61
      B) ULTIMATE YIELD IS  58.59
            K1= 0.4288
            K2=-0.6536
            K3= 0.9541

  SLICE    (90-0)   TAUS/F    TAU      STATUS       PONE   PTHREE ACCUM STRESS
  -----    ------   ------    ---      ------       ----   ------ ------------
   1( 0.5)  30.00    433.0   1406.1    FAILED        1.1      0.1        0.0
  10( 5.0)  30.01    434.7   1395.8    FAILED        5.2      1.7      950.8
  15( 7.5)  30.03    436.9   1463.2    FAILED       10.9      4.0     1294.7
  20(10.0)  30.07    441.3   1561.5    FAILED       22.0      8.5     1639.5
  25(12.5)  30.13    449.8   1685.7    FAILED       43.9     17.3     2008.6
  30(15.0)  30.23    465.7   1835.7    FAILED       87.1     34.6     2418.1
  35(17.5,  30.42    494.6   2012.5    FAILED      172.2     68.8     2881.3
  40(20.0)  30.74    544.5   2215.5    FAILED      339.9    136.2     3408.2
  45(22.5)  31.29    626.1   2436.5    FAILED      670.4    269.1     3998.6
  50(25.0)  32.21    751.9   2643.7    FAILED     1321.7    530.8     4622.0
  55(27.5)  33.76    938.0   2740.5    FAILED     2605.4   1046.7     5161.0
  60(30.0)  38.24   1040.5   2795.2   YIELDED     3360.2   1373.2     5454.6
  65(32.5)  38.24   1040.5   3129.7   YIELDED     3360.2   1373.2     6156.4
  70(35.0)  38.24   1040.5   3858.1   YIELDED     3360.2   1373.2     7666.9
  75(37.5)  38.24   1040.5   5805.7   YIELDED     3360.2   1373.2    11683.6
  80(40.0)  38.24   1040.5  23699.5   YIELDED     3360.2   1373.2    48499.1

BRITTLE/DUCTILE TRANSITION POINT:TAUF=  1040.5
FRACTURE ZONE ENDED ON  58TH SLICE AND EXTENDED 29.0 FT INTO THE PILLAR.
DEPTH OF FRACTURE ZONE JUST AT FAILURE 28.19
```

<u>Figure 29: Example computer output sheet for pillar C1</u>

8. Pillar strengths and safety factors - revised to include pseudo-ductile yield.

8.1 Depth of the transition point

Consider the depth, d_T, of the transition point in the pillar, as illustrated in Figure 30. Now the build up of the vertical stress in the fractured zone is given by equation 54 as :-

$$P_1 = \frac{P_B}{2\,\mathrm{Sin}\phi_B}\left\{(1+\mathrm{Sin}\phi_B)\; e^{\tan\phi_B\left\{\frac{1+\mathrm{Sin}\phi_B}{1-\mathrm{Sin}\phi_B}\right\}\left[\frac{e-w}{h}\right]} - (1-\mathrm{Sin}\phi_B)\right\} \tag{54}$$

and the transition point occurs when (e-w) = d_T and $P_1 = P_{1T}$ thus from this equation, putting (e-w) = d_T and $P_1 = P_{1T}$ we have

$$d_T = \frac{(1-\mathrm{Sin}\phi_B)}{(1+\mathrm{Sin}\phi_B)}\;\frac{h}{\tan\phi_B}\;\log_e\left\{\frac{2\,P_{1T}\,\mathrm{Sin}\phi_B}{P_B\,(1+\mathrm{Sin}\phi_B)} + \frac{(1-\mathrm{Sin}\phi_B)}{(1+\mathrm{Sin}\phi_B)}\right\} \tag{86}$$

But at the transition point $P_{1T} = \sigma_{1T}$ where σ_{1T} is the vertical stress required to produce yield, which from equation 72, is given by :-

$$\sigma_{1T} = \frac{A}{2} + \frac{A}{2\mu_B^{\,2}}\left\{1 + (1+\mu_B^{\,2})^{\frac{1}{2}}\right\} + \left\{\frac{A}{2}^{2} + \frac{A^2}{2\mu_B^{\,2}}\left[1 + (1+\mu_B^{\,2})^{\frac{1}{2}}\right]\right\}^{\frac{1}{2}} \tag{72}$$

Hence, if we evaluate σ_{1T} from the material properties using equation 72, and put $\sigma_{1T} = P_{1T}$ in equation 86, the depth into the pillar, d_T, at which the transition from fracture to yield takes place can be calculated.

8.2 Load taken by the fracture zone

The load, L_F, taken by the fracture zone is represented by the area A_{1T} in Figure 30.

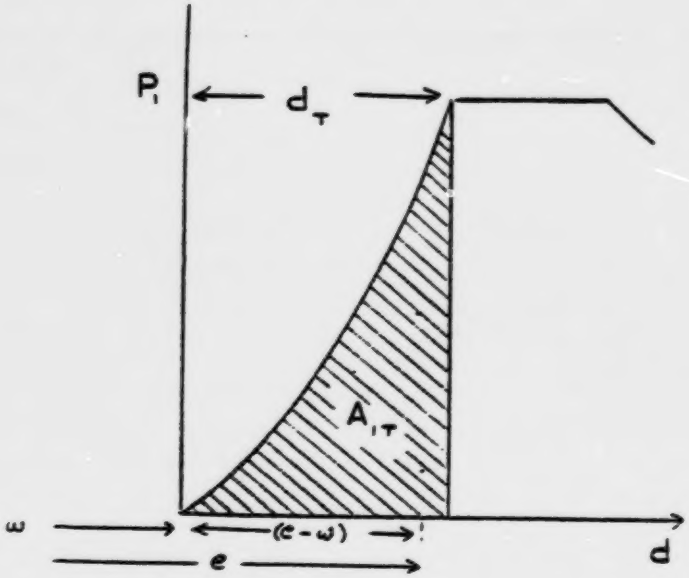
P₁
d_T
A₁T
ω
(e - ω)
e
d

FIGURE 30: Depth of the transition point

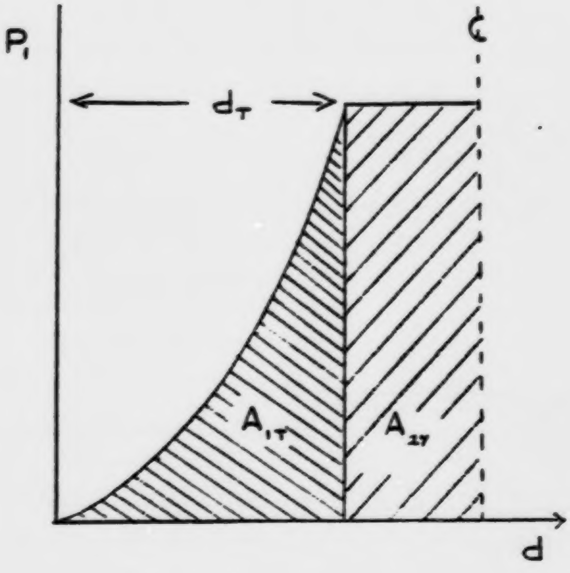
P₁
℄
d_T
A₁T
A₂T
d

FIGURE 31: Pillar that has just failed by yield

$$A_{1T} = L_F = \int_{(e-w)=0}^{(e-w)=d_T} P_1 \, d(e-w)$$ and, substituting from equation 59 for P_1 gives

$$= \int_{(e-w)=0}^{(e-w)=d_T} \frac{P_B}{2\,\mathrm{Sin}\phi_B}\left\{(1+\mathrm{Sin}\phi_B)\, e^{\tan\phi_B\left\{\frac{1+\mathrm{Sin}\phi_B}{1-\mathrm{Sin}\phi_B}\right\}\left(\frac{e-w}{h}\right)} - (1-\mathrm{Sin}\phi_B)\right\}$$

$$= \left[\frac{P_B}{2\,\mathrm{Sin}\phi_B}\left\{\frac{(1+\mathrm{Sin}\phi_B)}{(1+\mathrm{Sin}\phi_B)}\,\frac{(1-\mathrm{Sin}\phi_B).h}{\tan\phi_B}\, e^{\tan\phi_B\left\{\frac{1+\mathrm{Sin}\phi_B}{1-\mathrm{Sin}\phi_B}\right\}\left(\frac{e-w}{h}\right)} - (1-\mathrm{Sin}\phi_B)\,(e-w)\right\}\right]_{0}^{d_T}$$

$$= \left[\frac{P_B}{2\,\mathrm{Sin}\phi_B}\;\frac{(1-\mathrm{Sin}\phi_B)\;.\;h}{\tan\phi_B}\left\{e^{\tan\phi_B\left\{\frac{1+\mathrm{Sin}\phi_B}{1-\mathrm{Sin}\phi_B}\right\}\frac{d_T}{h}} - 1\right\} - (1-\mathrm{Sin}\phi_B)\;d_T\right]$$

i.e.
$$\underline{A_{1T} = L_F = \frac{P_B\,(1-\mathrm{Sin}\phi_B)}{2\,\mathrm{Sin}\phi_B}\left[\frac{h}{\tan\phi_B}\left\{e^{\tan\phi_B\left\{\frac{1+\mathrm{Sin}\phi_B}{1-\mathrm{Sin}\phi_B}\right\}\frac{d_T}{h}} - 1\right\} - d_T\right]} \qquad (87)$$

8.3 Residual mean pillar stress capacity of a pillar that has failed by yield. ($\bar{\sigma}_{PRY}$)

The residual mean pillar stress capacity can be defined as the mean pillar stress required to just fail the pillar to its centre. The stress distribution, when yielding occurs, is illustrated in Figure 31. It is important to note that the stress distribution is solely dependent in the properties of the broken coal and of the yielded coal.

but, with a curved Mohr envelope of the form $\tau^2 = A\sigma + {}^{A^2}/4$ it is shown in Appendix 1 (Equation I 18)

that $\sigma_c = 2A$

Hence $$\bar{\sigma}_{pmin} = \frac{2\bar{Y}}{Y_{mm}} \, . \, A \qquad (89)$$

It also follows, as before (Section 6.3), that $\bar{\sigma}_{pmin}$ is the minimum pillar strength. Further, it also follows that catastrophic fracture or catastrophic yield can occur. i.e. the residual mean pillar stress capacity, be the failure by total fracture or partial fracture plus yield, can be less than the value of σ_{pmin}. In this case the fracture, or the fracture plus yield as the case may be, must propogate immediately to the centre of the pillar and the excess load must be shed onto the adjacent pillars.

8.5 Sequence of events as $\bar{\sigma}_p$ increases

Consider the possible sequence of events as the mean pillar stress, $\bar{\sigma}_p$, increases:-

(i) $\bar{\sigma}_p < \bar{\sigma}_{pmin}$ (Figure 32A) In this case fracture cannot initiate. The pillar is solid and has an elastic stress distribution as illustrated in Figure 32 A. The area under the curve, A_1, must be equal to $\bar{\sigma}_{p.b}$.

(ii) $\bar{\sigma}_p > \bar{\sigma}_{pmin}$; $\bar{\sigma}_{pmin} > \bar{\sigma}_{PR}$ and $d_T > b$ (Figure 32 B1) $\bar{\sigma}_p$ has increased and is now greater than $\bar{\sigma}_{pmin}$; therefore fracture initiates. $d_T > b$ consequently no yielding can take place and only fracture can occur. $\bar{\sigma}_{pmin}$ is > the residual mean pillar stress capacity $\bar{\sigma}_{PR}$; therefore once fracture initiates it must propogate immediately to the centre causing catastrophic fracture. The area under the curve, A_1, is less than $\bar{\sigma}_{p.b}$; consequently load is shed from the pillar onto the adjacent pillars. The magnitude of the shed load (for the half pillar width b) is given by :-

$$L_s = b\left[\bar{\sigma}_{pmin} - \bar{\sigma}_{PR}\right] \qquad (90)$$

(iii) $\bar{\sigma}_p > \bar{\sigma}_{pmin}$; $\bar{\sigma}_{pmin} > \bar{\sigma}_{PRY}$ and $d_T < b$ (Figure 32 B2) This is similar to case (ii) above, $\bar{\sigma}_p$ has increased and is now greater than $\bar{\sigma}_{pmin}$; therefore fracture can initiate. However $d_T < b$ thus the pillar will partially fracture and partially yield. $\bar{\sigma}_{pmin}$ is > the residual mean pillar stress capacity for yielding, $\bar{\sigma}_{PRY}$; therefore once fracture initiates the pillar must fail immediately to the centre by partial fracture and yielding; this will be called "Catastrophic yield".

The total load carried by the pillar $L = L_F + L_Y$ where L_F is the load carried by the fractured coal and L_Y is that carried by the yielded coal.

$L = L_F + L_Y = A_{1T} + A_{2Y}$ when A_{1T} and A_{2Y} are the areas under the stress distribution curve illustrated in Figure 31.

L_F is given by equation 87 above and

$L_Y = \sigma_{1T} (b - d_T)$ where σ_{1T} is the vertical stress for yield given by equation 72.

Hence the residual mean pillar stress capacity is $\bar{\sigma}_{PRY} = \frac{L}{b}$

$$\text{i.e.}\quad \bar{\sigma}_{PRY} = \frac{1}{b}\left[\frac{P_B (1- \mathrm{Sin}\phi_B)}{2\,\mathrm{Sin}\phi_B}\left[\frac{h}{\tan\phi_B}\left\{e^{\tan\phi_B\left\{\frac{1+\mathrm{Sin}\phi_B}{1-\mathrm{Sin}\phi_B}\right\}\frac{d_T}{h}} - 1\right\} - d_T\right]\right.$$

$$\left. + (b - d_T)\left\{\frac{A}{2} + \frac{A}{2\mu_B{}^2}\left[1+ (1+\mu_B{}^2)^{\frac{1}{2}}\right] + \left(\frac{A^2}{2} + \frac{A^2}{2\mu_B{}^2}\left[1+ (1+\mu_B{}^2)^{\frac{1}{2}}\right]\right)^{\frac{1}{2}}\right\}\right] \qquad (88)$$

8.4 Mean pillar stress for initiation of fracture

As before, Section 6.1, there must be some minimum value of the mean pillar stress below which fracture cannot initiate in the pillar. Let S_{vc} be the critical value of the vertical virgin stress at which fracture can just initiate in the first slice. Then the stress acting at the mid height of this slice on the pillar edge is initially the maximum stress on any pillar element and is equal to $Y_{mm} . S_v$ and, for fracture to be able to initiate at this point, this stress must be equal to the uniaxial compressive strength of the solid coal, σ_c. i.e. fracture will initiate when:-

$$Y_{mm} S_{vc} = \sigma_c \qquad (51)$$

and the mean pillar stress acting on the pillar when this occurs is given by:-

$$\bar{\sigma}_p \text{ (min)} = \bar{Y} . S_{vc} \qquad (52)$$

Thus, eliminating S_{vc} from 51 and 52 gives

$$\bar{\sigma}_p \text{ min} = \frac{\bar{Y}}{Y_{mm}} . \sigma_c \qquad (53)$$

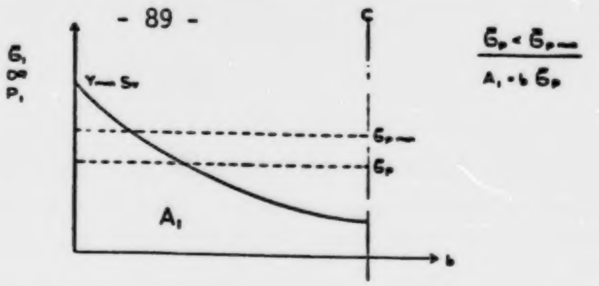
σ1 or P1
Y = Sv
σp min
σp
A1
b
℄
σp < σp min
A1 = b σp

(A) STABLE PILLAR - ELASTIC STRESS DISTRIBUTION

b < dr

b > dr

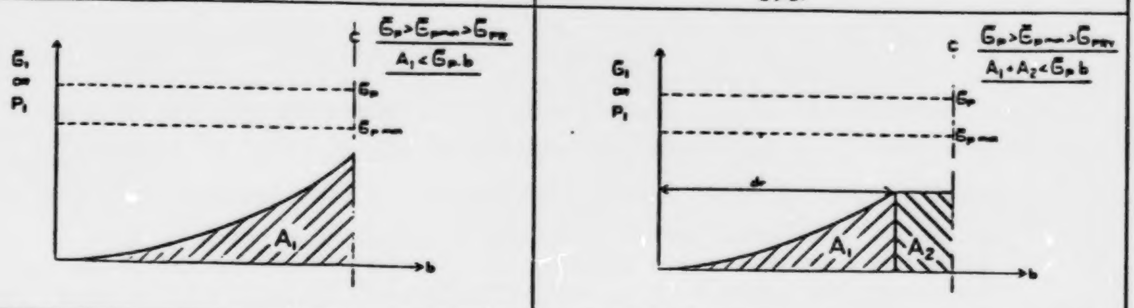
σ1 or P1
σp > σp min > σFR
A1 < σp.b
σp
σp min
A1
b
σp > σp min > σPRY
A1 + A2 < σp.b
dr
A2

(B.1) CATASTROPHIC FRACTURE

(B.2) CATASTROPHIC YIELD

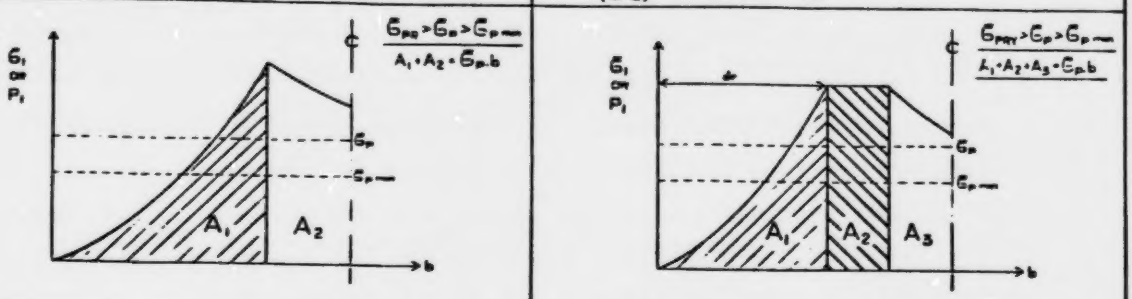
σ1 or P1
σFR > σp > σp min
A1 + A2 = σp.b
σp
σp min
A1
A2
b
σPRY > σp > σp min
A1 + A2 + A3 = σp.b
dr
A3

(C.1) STABLE PILLAR - PARTIAL FRACTURE

(C.2) STABLE PILLAR - PARTIAL FRACTURE, PARTIAL YIELD

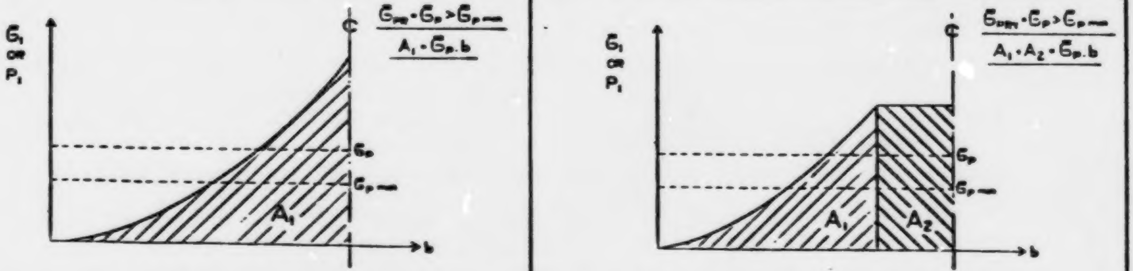
σ1 or P1
σFR = σp > σp min
A1 = σp.b
σp
σp min
A1
b
σPRY = σp > σp min
A1 + A2 = σp.b
A2

(D.1) STABLE FRACTURE

(D.2) STABLE YIELD

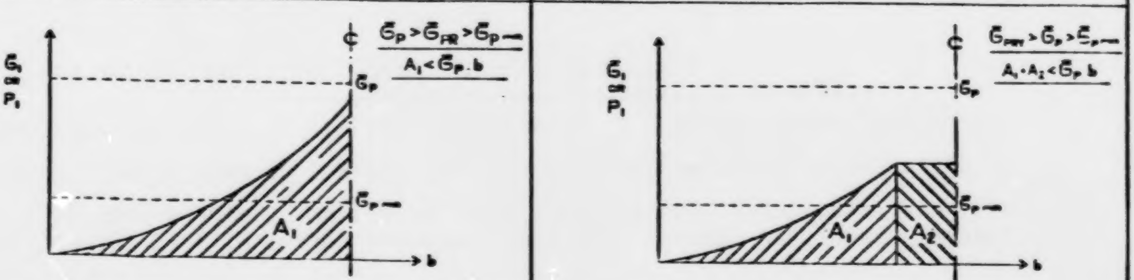
σ1 or P1
σp > σFR > σp min
A1 < σp.b
σp
σp min
A1
b
σPRY > σp > σp min
A1 + A2 < σp.b
A2

(E.1) ULTIMATE FRACTURE

(E.2) ULTIMATE YIELD

▨ FRACTURE ZONE ▧ YIELD ZONE ☐ SOLID ELASTIC CORE

FIGURE 32: POSSIBLE MODES OF PILLAR STABILITY AND FAILURE

The area, $A_1 + A_2$, under the curve (Figure 32 B2) is less than $\bar{\sigma}_p b$; consequently load is shed from the pillar onto the adjacent pillars. The magnitude of the shed load (from the half pillar under consideration) is given by :-

$$L_s = b\left[\bar{\sigma}_{pmin} - \bar{\sigma}_{PRY}\right] \tag{91}$$

(iv) $\bar{\sigma}_p > \bar{\sigma}_{pmin}$; $\bar{\sigma}_p < \bar{\sigma}_{PR}$ and $d_T > b$ (Figure 32 C1) $\bar{\sigma}_p$ has increased and is greater than $\bar{\sigma}_{pmin}$, therefore fracture initiates. $d_T > b$ thus yield cannot take place. In this case the residual stress capacity at fracture, $\bar{\sigma}_{PR}$ is greater than $\bar{\sigma}_p$. Then fracture propogates to some distance into the pillar but cannot propogate further, and yield cannot take place. There is therefore a central solid elastic core to the pillar and the pillar is stable. The sum of the areas $A_1 + A_2$ under the curve (Figure 32 C1) is equal to $\bar{\sigma}_p b$ and no load is shed from the pillar.

(v) $\bar{\sigma}_p > \bar{\sigma}_{pmin}$; $\bar{\sigma}_p < \bar{\sigma}_{PRY}$ and $d_T < b$ (Figure 32 C2) This is the yield case equivalent to (iv) above. $\bar{\sigma}_p$ has increased and is greater than $\bar{\sigma}_{pmin}$; therefore fracture initiates. d_T is $< b$ and thus yielding will take place in the pillar. The residual stress capacity of the pillar, $\bar{\sigma}_{PRY}$, is greater than $\bar{\sigma}_p$. Thus fracture propogates some distance into the pillar, yielding then commences but cannot continue to the pillar centre. There is an elastic central solid pillar core and the pillar is stable. The sum of the areas $A_1 + A_2 + A_3$ (Figure 32 C2) under this curve is equal to $\bar{\sigma}_p b$ and no load is shed from the pillar.

(vi) $\bar{\sigma}_p > \bar{\sigma}_{pmin}$, $\bar{\sigma}_p = \bar{\sigma}_{PR}$, $d_T > b$ (Figure 32 D1) $\bar{\sigma}_p$ has increased further and is now just equal to $\bar{\sigma}_{PR}$ the residual mean pillar stress capacity. $d_T > b$ thus yield cannot occur in the pillar. Hence fracture will have just propogated to the centre of the pillar. This unique condition is called "Stable Fracture". The area under the curve, A_1 (Figure 32 D1) is equal to $\bar{\sigma}_p b$; thus no load is shed onto other pillars despite the fact that the pillar has failed.

(vii) $\bar{\sigma}_p > \bar{\sigma}_{pmin}$, $\bar{\sigma}_p = \bar{\sigma}_{PRY}$, $d_T < b$ (Figure 32 D2) This is the yield case equivalent to (vi) above. $\bar{\sigma}_p$ is now just equal to $\bar{\sigma}_{PRY}$ the residual mean pillar stress capacity for yielding. $d_T < b$ thus yield does does occur. Hence fracture will have propogated some distance into the pillar, yielding then occurs and just reaches the pillar centre. The area under the curve, $A_1 + A_2$ (Figure 32 D2) is equal to $\bar{\sigma}_{p.b}$; thus no load is shed onto other pillars despite the fact that the pillar has failed by yielding. This unique condition is called "Stable Yield".

(viii) $\bar{\sigma}_p > \bar{\sigma}_{pmin}$; $\bar{\sigma}_p > \bar{\sigma}_{PR}$; $\bar{\sigma}_{PR} > \bar{\sigma}_{pmin}$, $d_T > b$ (Figure 32 E1) $\bar{\sigma}_p$ has increased still further, the pillar cannot resist a stress greater than $\bar{\sigma}_{PR}$; $d_T > b$ thus yield cannot take place. Hence the pillar fails by fracture and the area under the curve, A_1 (Figure 32 E1) is less than $\bar{\sigma}_{p.}$ b and load will be shed onto adjacent pillars. This case will be called "Ultimate Fracture". The load shed onto other adjacent pillars from the half pillar under consideration is given by:-

$$L_s = b\,(\bar{\sigma}_p - \bar{\sigma}_{PR}) \qquad (92)$$

Note: it is assumed here that this "overloading" of the pillar does not cause large additional deformation of the pillar and hence a drop in $\bar{\sigma}_{PR}$ the residual stress capacity of the pillar. In practice, some drop of $\bar{\sigma}_{PR}$ might be expected in which case the shed load L_s given above is a minimum value.

(ix) $\bar{\sigma}_p > \bar{\sigma}_{pmin}$; $\bar{\sigma}_p > \bar{\sigma}_{PRY}$; $\bar{\sigma}_{PRY} > \bar{\sigma}_{pmin}$, $d_T < b$ (Figure 32 E2) This is the yield case equivalent to (viii) above. $\bar{\sigma}_p$ is now greater than the residual stress capacity of the pillar, $\bar{\sigma}_{PRY}$, and $d_T < b$ thus yield takes place. Hence the pillar fails by partial fracture and yield and the area under the curve, $A_1 + A_2$ (Figure 32 E2) is less than $\bar{\sigma}_{p.}$ b and load will be shed onto adjacent pillars. This case will be called "Ultimate Yield". The load shed from the half pillar under consideration is given by :-

$$L_s = b\,(\bar{\sigma}_p - \bar{\sigma}_{PRY}) \qquad (93)$$

Note: as with case (viii) it is assumed that there is no drop in $\bar{\sigma}_{PRY}$ due to additional pillar deformation caused by this overloading.

8.6 Critical pillar dimensions to avoid Catastrophic Fracture, Catastrophic Yield, Ultimate Fracture and Ultimate Yield

8.6.1 Critical pillar dimension to avoid Catastrophic Fracture.

It is seen from the above discussion that there must be some critical pillar dimension, b_{cF}, above which catastrophic fracture cannot occur. This critical pillar dimension will be the semi pillar width b_{cF} such that $\bar{\sigma}_{pmin} = \bar{\sigma}_{PR}$ (i.e. at a smaller value of b then $\bar{\sigma}_{pmin} > \bar{\sigma}_{PR}$ and catastrophic fracture occurs as illustrated in Figure 32 B1, and at any larger value of b then $\bar{\sigma}_{PR} > \sigma_{pmin}$ and the pillar is stable as illustrated in Figure 32 C1).

Now from equation 89 and 56, putting $b = b_{cF}$ and $\bar{\sigma}_{pmin} = \bar{\sigma}_{PR}$ then :-

$$\frac{\bar{Y}}{\bar{Y}_{mm}} \cdot 2A = \frac{P_B\,(1-\sin\phi_B)}{2\,b_{cF}\,\sin\phi_B}\left\{\frac{h}{\tan\phi_B}\left[e^{\tan\phi_B\left\{\frac{1+\sin\phi_B}{1-\sin\phi_B}\right\}\frac{b_{cF}}{h}} - 1\right] - b_{cF}\right\} \qquad (94)$$

This equation can be solved for b_{cF} by successive approximation.

8.6.2 Critical pillar dimension to avoid Catastrophic Yield.

It also follows that there must be some critical pillar dimension b_{cy} above which catastrophic yield cannot occur. This critical pillar dimension will occur when $\bar{\sigma}_{pmin} = \bar{\sigma}_{PRY}$ thus, from equations 89 and 88, putting $b = b_{cy}$ and $\bar{\sigma}_{pmin} = \bar{\sigma}_{PRY}$ we have:-

$$\begin{aligned}\frac{\bar{Y}}{\bar{Y}_{mm}} \cdot 2A = {} & \frac{P_B\,(1-\sin\phi_B)}{2\,b_{cy}\,\sin\phi_B}\left\{\frac{h}{\tan\phi_B}\left[e^{\tan\phi_B\left\{\frac{1+\sin\phi_B}{1-\sin\phi_B}\right\}\frac{d_T}{h}} - 1\right] - d_T\right\} \\ & + \frac{(b_{cy} - d_T)}{b_{cy}}\left\{\frac{A}{2} + \frac{A}{2\mu_B^{\,2}}\left[1 + (1+\mu_B^{\,2})^{\frac{1}{2}}\right] + \left[\frac{A^2}{2} + \frac{A^2}{2\mu_B^{\,2}}\left\{1 + (1+\mu_B^{\,2})^{\frac{1}{2}}\right\}\right]^{\frac{1}{2}}\right\}\end{aligned} \qquad (95)$$

where d_T is given by equation 72 and 86.

Likewise it is also possible to solve this equation by successive approximation.

8.6.3 Critical pillar dimension to avoid ultimate fracture

Let this critical pillar dimension be b_{cFu}. It will occur when $\bar{\sigma}_p = \bar{\sigma}_{PR}$. (i.e. at any smaller semi pillar width $\bar{\sigma}_p > \bar{\sigma}_{PR}$ and ultimate fracture will occur as illustrated in Figure 32 E1 and at a larger value of b the pillar will be stable as illustrated in Figure 32 C1).

Now in this case $\bar{\sigma}_p = \bar{Y} . S_v$ and $\bar{\sigma}_{PR}$ is given by equation 56, thus putting $b = b_{cFu}$ and equating $\sigma_{PR} = \bar{\sigma}_p$:-

$$\bar{Y} . S_v = \frac{P_B}{2\, b_{cFu}} \; \frac{(1-\sin\phi_B)}{\sin\phi_B} \left\{ \frac{h}{\tan\phi_B} \left[e^{\tan\phi_B \left\{ \frac{1+\sin\phi_B}{1-\sin\phi_B} \right\} \frac{d_T}{h}} - 1 \right] - b_{cFu} \right\} \qquad (96)$$

This equation can be solved for b_{cFu} by successive approximation.

8.6.4 Critical pillar dimension to avoid ultimate yield

Let this critical pillar dimension be b_{cYu}. It will occur when $\bar{\sigma}_p = \bar{\sigma}_{PRY}$. Hence we have from equation $\bar{\sigma}_p = \bar{Y}\ S_v$ and equation 88, putting $b = b_{cYu}$:-

$$\bar{Y} . S_v = \frac{P_B}{2\, b_{cYu}} \; \frac{(1-\sin\phi_B)}{\sin\phi_B} \left\{ \frac{h}{\tan\phi_B} \left[e^{\tan\phi_B \left\{ \frac{1+\sin\phi_B}{1-\sin\phi_B} \right\} \frac{d_T}{h}} - 1 \right] - d_T \right\}$$

$$+ \frac{(b_{cYu} - d_T)}{b_{cYu}} \left\{ \frac{A}{2} + \frac{A}{2\mu_B{}^2} \left[1 + (1+\mu_B{}^2)^{\frac{1}{2}} \right] + \left[\frac{A^2}{2} + \frac{A^2}{2\mu_B{}^2} \left\{ 1 + (1+\mu_B{}^2)^{\frac{1}{2}} \right\} \right]^{\frac{1}{2}} \right\} \qquad (97)$$

when d_T is given by equations 72 and 86.

Likewise it is possible to solve this equation for b_{cYu} by successive approximation.

Hence it is possible to evaluate the various critical pillar dimensions required to avoid the various categories of failure by fracture or yield.

8.7 Pillar strength and safety factors

The pillar strength, $\bar{\sigma}_s$, is defined as the mean pillar stress required which will just fail the pillar to the centre, whether it be by fracture or by partial fracture plus yield. The pillar safety factor is defined as the ratio of the pillar strength, $\bar{\sigma}_s$, to the mean applied pillar stress = $\bar{Y}\, S_v$. Figure 33 gives the necessary computer program logic and the various equations required to evaluate the pillar strengths, the safety factor, and the various critical pillar dimensions using the equations derived in the above analyses. It is believed that this diagram is self explanatory.

8.8 Variation of pillar strengths with P_B, ϕ_B, μ_B, A, W, b and h

The variation of pillar strength with semi-pillar width b has been determined in order to investigate the sensitivity of the strength to the variables P_B, ϕ_B, μ_B, A, w and h. This has been done for the range of variables given in Table 8.1. The results are briefly discussed below.

8.8.1 Influence of P_B

Figure 34 shows the variation of the pillar strength $\bar{\sigma}_s$ with semi-pillar width when the uniaxial compressive strength of broken rock, P_B, is varied from 0.1 to 10 psi. It will be noted that:-

(i) Below a certain pillar width, the pillar fails catastrophically, this portion of the curve is uninfluenced by P_B. However, the higher the value of P_B the smaller becomes the pillar which will fail catastrophically.

(ii) For the larger pillars (beyond catastrophic failure), the strength increases with increasing P_B.

(iii) The curves become relatively flat as the pillar becomes larger; so that for any P_B value the rate of change of strength with pillar width diminishes gradually.

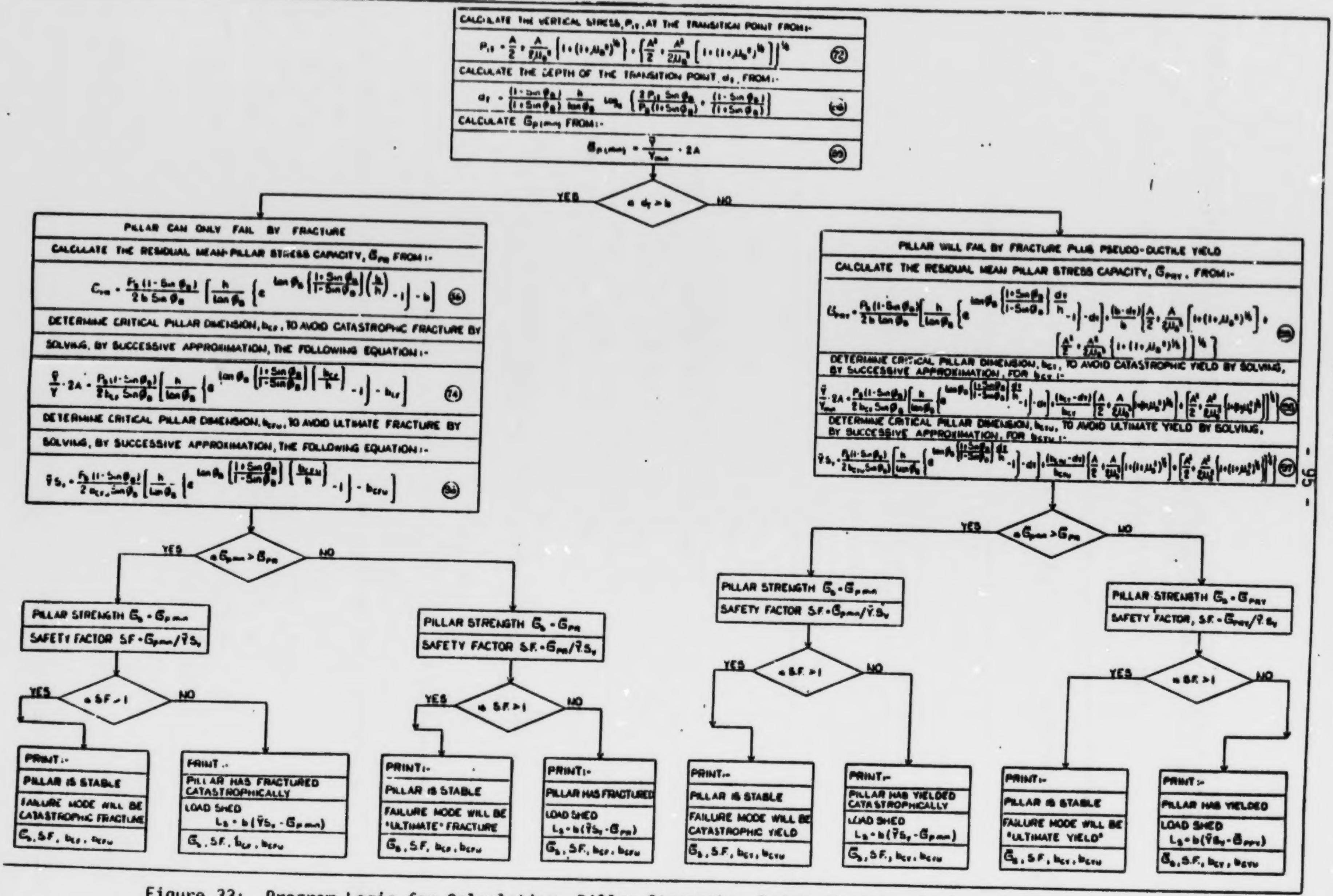
CALCULATE THE VERTICAL STRESS, P_{it}, AT THE TRANSITION POINT FROM:-
(72)
CALCULATE THE DEPTH OF THE TRANSITION POINT, d_t, FROM:-
CALCULATE $\sigma_{p(min)}$ FROM:-
$\sigma_{p(min)} = \frac{\bar{\gamma}}{\gamma_{max}} \cdot 2A$
$d_t > b$
YES
NO
PILLAR CAN ONLY FAIL BY FRACTURE
CALCULATE THE RESIDUAL MEAN-PILLAR STRESS CAPACITY, σ_{pe} FROM:-
DETERMINE CRITICAL PILLAR DIMENSION, b_{cf}, TO AVOID CATASTROPHIC FRACTURE BY
SOLVING, BY SUCCESSIVE APPROXIMATION, THE FOLLOWING EQUATION:-
(74)
DETERMINE CRITICAL PILLAR DIMENSION, b_{cfu}, TO AVOID ULTIMATE FRACTURE BY
SOLVING, BY SUCCESSIVE APPROXIMATION, THE FOLLOWING EQUATION:-
PILLAR WILL FAIL BY FRACTURE PLUS PSEUDO-DUCTILE YIELD
CALCULATE THE RESIDUAL MEAN PILLAR STRESS CAPACITY, σ_{pry}, FROM:-
DETERMINE CRITICAL PILLAR DIMENSION, b_{cy}, TO AVOID CATASTROPHIC YIELD BY SOLVING, BY SUCCESSIVE APPROXIMATION, FOR b_{cy}:-
DETERMINE CRITICAL PILLAR DIMENSION, b_{cyu}, TO AVOID ULTIMATE YIELD BY SOLVING, BY SUCCESSIVE APPROXIMATION, FOR b_{cyu}:-
(97)
$\sigma_{pmin} > \sigma_{pe}$
YES
NO
PILLAR STRENGTH $\sigma_s = \sigma_{pmin}$
SAFETY FACTOR $S.F. = \sigma_{pmin}/\bar{\gamma}S_v$
PILLAR STRENGTH $\sigma_s = \sigma_{pe}$
SAFETY FACTOR $S.F. = \sigma_{pe}/\bar{\gamma}S_v$
$S.F. > 1$
YES
NO
PRINT:-
PILLAR IS STABLE
FAILURE MODE WILL BE CATASTROPHIC FRACTURE
σ_s, S.F., b_{cf}, b_{cfu}
PRINT:-
PILLAR HAS FRACTURED CATASTROPHICALLY
LOAD SHED $L_s = b(\bar{\gamma}S_v - \sigma_{pmin})$
σ_s, S.F., b_{cf}, b_{cfu}
PRINT:-
PILLAR IS STABLE
FAILURE MODE WILL BE 'ULTIMATE' FRACTURE
σ_s, S.F., b_{cf}, b_{cfu}
PRINT:-
PILLAR HAS FRACTURED
LOAD SHED $L_s = b(\bar{\gamma}S_v - \sigma_{pe})$
σ_s, S.F., b_{cf}, b_{cfu}
$\sigma_{pmin} > \sigma_{pe}$
PILLAR STRENGTH $\sigma_s = \sigma_{pmin}$
SAFETY FACTOR $S.F. = \sigma_{pmin}/\bar{\gamma}S_v$
PILLAR STRENGTH $\sigma_s = \sigma_{pry}$
SAFETY FACTOR, $S.F. = \sigma_{pry}/\bar{\gamma}S_v$
PRINT:-
PILLAR IS STABLE
FAILURE MODE WILL BE CATASTROPHIC YIELD
σ_s, S.F., b_{cy}, b_{cyu}
PRINT:-
PILLAR HAS YIELDED CATASTROPHICALLY
LOAD SHED $L_s = b(\bar{\gamma}S_v - \sigma_{pmin})$
σ_s, S.F., b_{cy}, b_{cyu}
PRINT:-
PILLAR IS STABLE
FAILURE MODE WILL BE "ULTIMATE YIELD"
σ_s, S.F., b_{cy}, b_{cyu}
PRINT:-
PILLAR HAS YIELDED
LOAD SHED $L_s = b(\bar{\gamma}S_v - \sigma_{pry})$
σ_s, S.F., b_{cy}, b_{cyu}

Figure 33: Program Logic for Calculating, Pillar Strengths, Safety Factors, Failure Mode and Critical Pillar Dimensions

Table 8.1 : Input parameters for investigation of influence of these parameters on pillar strength.

Semi-pillar width b varied from 5 to 120 ft. in all cases

Data Set #	Variable	P_B psi	ϕ_B	μ_B	A psi	w ft.	h ft.
1	P_B 0.1 psi 1.0 psi 10.0 psi		30°	0.577	500	10	5
2	ϕ_B 27° 30° 33°	1.0	-	0.577	500	10	5
3	μ_B 0.51 0.577 0.65	1.0	30°	-	500	10	5
4	A 250 psi 500 psi 1000 psi	1.0	30°	0.577	-	10	5
5	w 5 ft. 10 ft. 15 ft.	1.0	30°	0.577	500	-	5
6	h 2.5 ft. 5 ft. 10 ft.	1.0	30°	0.577	500	10	-

Note: These examples were run with the "short program" for rib pillars given in Section 10.

FIGURE 35· Strength variation with pillar width for a range of angles of internal friction of broken coal

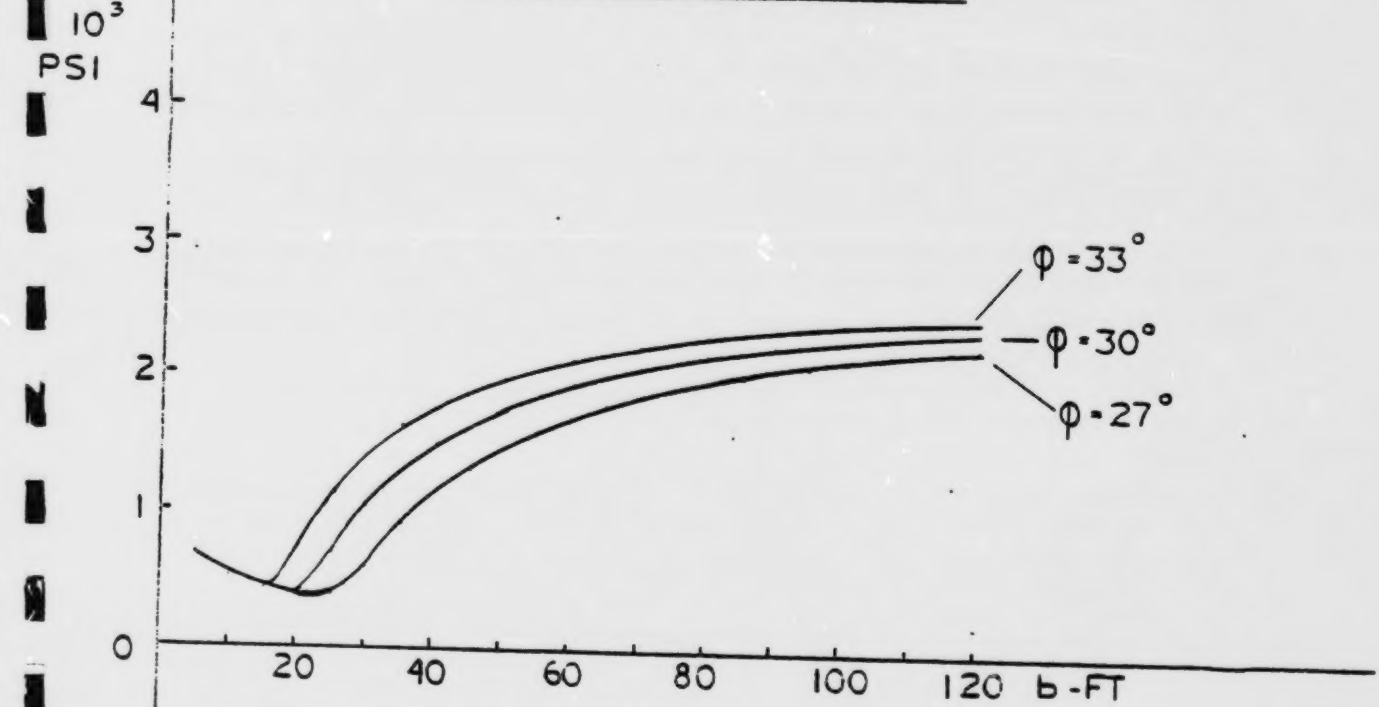

FIGURE 34: Strength variation with pillar width for a range of uniaxial compressive strengths of broken coal

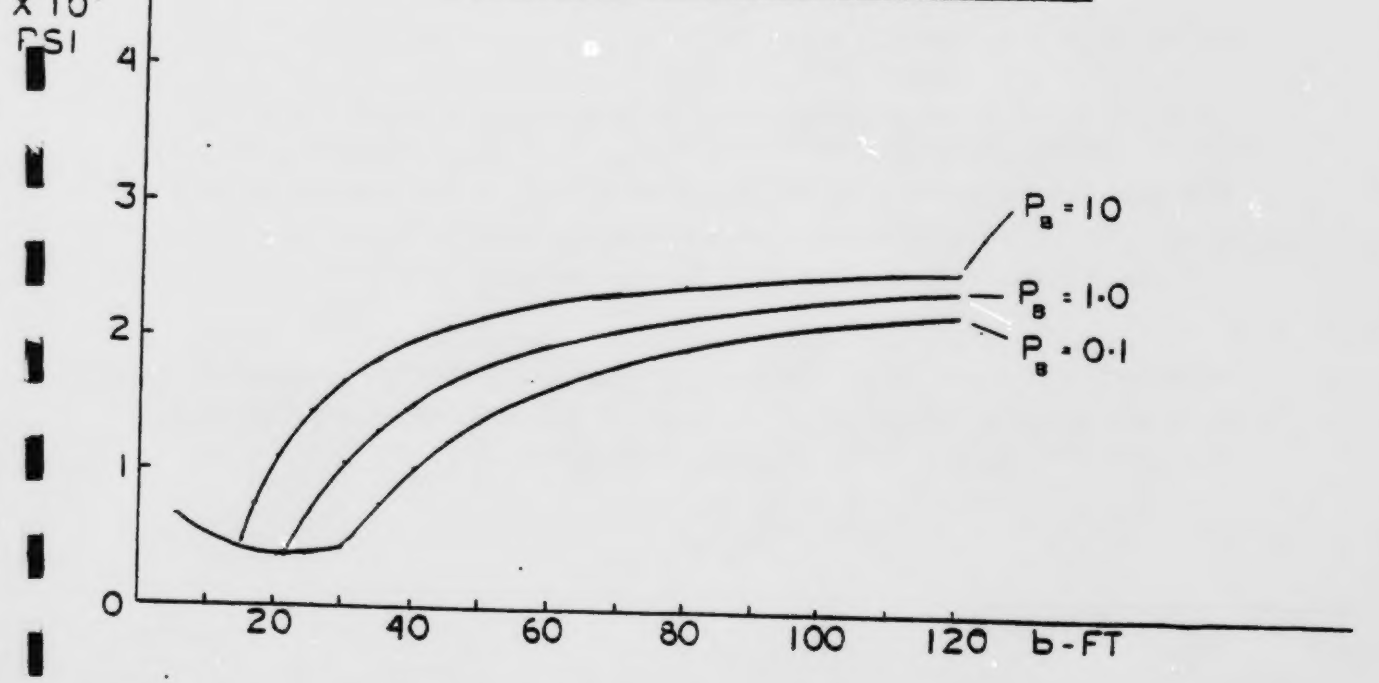

8.8.2 Influence of ϕ_B

Figure 35 shows the variation of pillar strength $\bar{\sigma}_s$ with semi-pillar width when the angle of internal friction of broken coal, ϕ_B, is varied from 27° to 33° . The influence of ϕ_B is very similar to that of P_B and the following points are noted:-

(i) Below a certain pillar width, the pillar fails catastrophically and this portion of the curve is uninfluenced by ϕ_B. However, the higher the value of ϕ_B the smaller becomes the pillar which will fail catastrophically.

(ii) For the larger pillars (beyond catastrophic failure), the strength increases with increasing ϕ_B.

(iii) The curves become relatively flat as the pillar becomes larger; so that for any ϕ_B value the rate of change of strength with pillar width diminishes gradually.

8.8.3 Influence of μ_B

Figure 36 shows the variation of pillar strength with semi-pillar width for a range of sliding coefficients of friction of broken coal, μ_B, from 0.51 to 0.65. The following points are noted:-

(i) Below a certain pillar width, regardless of the value of μ_B, the pillar fails catastrophically and the strength is uninfluenced by μ_B.

(ii) For the larger pillars (beyond catastrophic failure), then the pillar strength decreases with increasing μ_B. It is thus interesting to note that the influence of μ_B in the larger pillars is the opposite of that of ϕ_B. Now it could be argued (but not necessarily established) that $\mu_B = \tan^{-1} (\phi_B)$. If this were the case then we would have:-

$\tan^{-1} 33° = 0.65$, $\tan^{-1} 30° = 0.577$ and $\tan^{-1} 27° = 0.51$.

Consequently it would follows that, if $\mu_B = \tan^{-1}\phi_B$, then the combined influence of μ_B and ϕ_B would tend to cancel out and the pillar strength would be very insensitive to changes in the combination of μ_B and ϕ_B.

FIGURE 36: Strength variations with pillar width for a range of sliding coefficients of friction

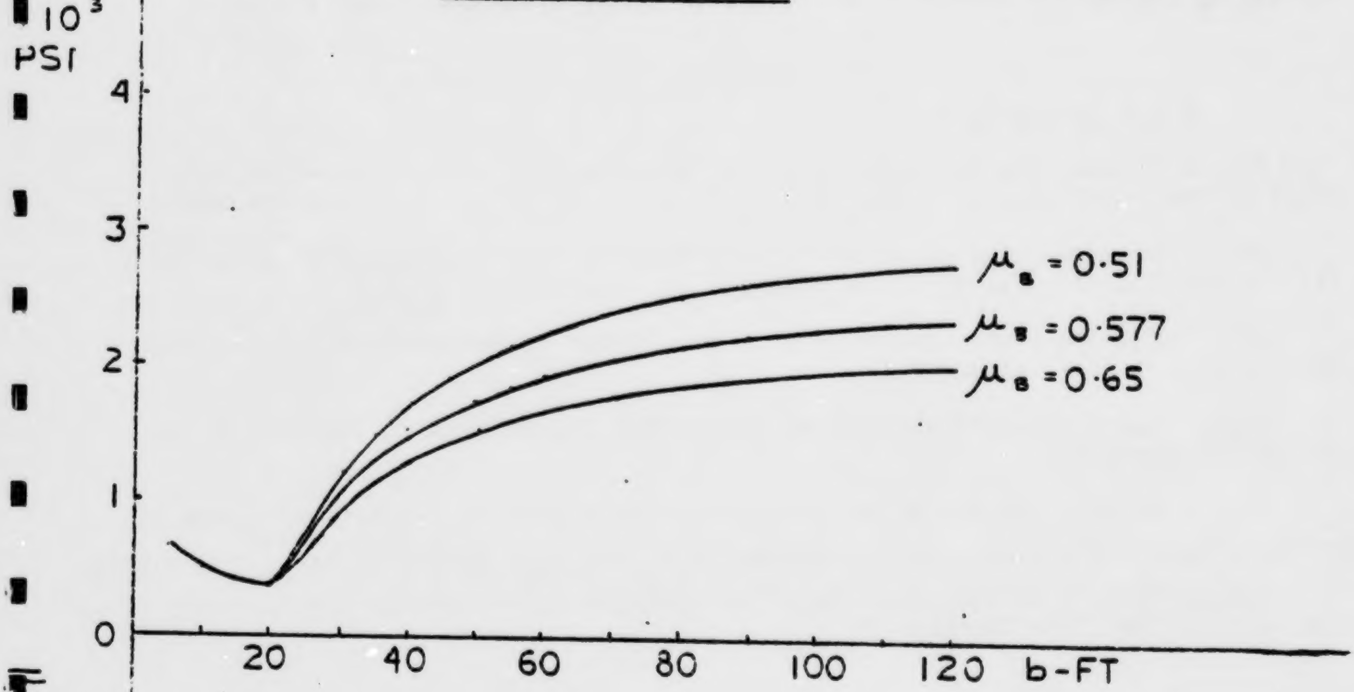

FIGURE 37: Strength variation with pillar width for a range of "Mohr" constants

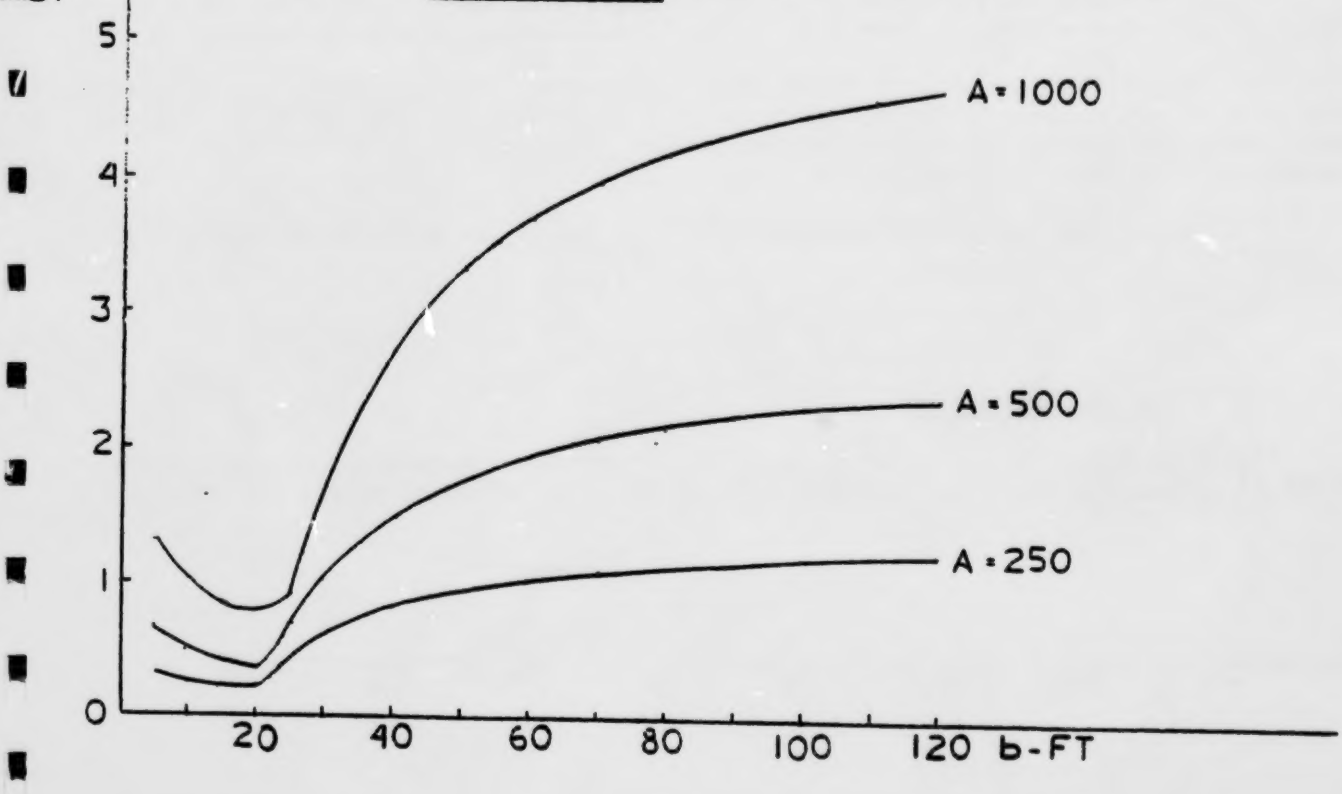

(iii) The curves become relatively flat as the pillar becomes larger; so that for any μ_B the rate of change of strength with pillar width diminishes gradually.

8.8.4 Influence of A

Figure 37 shows the variation of pillar strength with semi-pillar width for a range of "Mohr constants", A from 250 to 1000 psi. The following points are noted:-

(i) The higher the value of A, the greater is the stress required to initiate failure and thus the greater is the strength for catastrophic failure.

(ii) Also the higher the value of A the greater is the pillar width for which catastrophic failure can occur.

(iii) Beyond catastrophic failure, the higher the value of A, the greater is the pillar strength.

(iv) Further, the higher the value of A, the greater is the rate of change of pillar strength with size. i.e. the greater is A, the less rapidly do the curves flatten.

Consequently it is seen that the pillar strength is exceedingly sensitive to the value of the "Mohr constant" A.

8.8.5 Influence of w

Figure 38 shows the variation of pillar strength with semi-pillar width for a range of semi-room widths, w, from 5 to 15 ft. The following points are noted:-

(i) In the range of small b values when catastrophic failure occurs, the greater the value of w, the lower is the stress at which catastrophic failure can occur. On the other hand, the greater the value of w, the smaller is the pillar width for which catastrophic failure is possible.

(ii) Beyond the region of catastrophic failure the pillar strength is completely insensitive to the value of w.

8.8.6 Influence of h

Figure 39 shows the variation of the pillar strength with semi-pillar width for a range of semi-pillar heights, h, from 2.5 to 10 ft. The following points are noted:-

FIGURE 38: Strength variation with pillar width for a range of semi-pillar widths

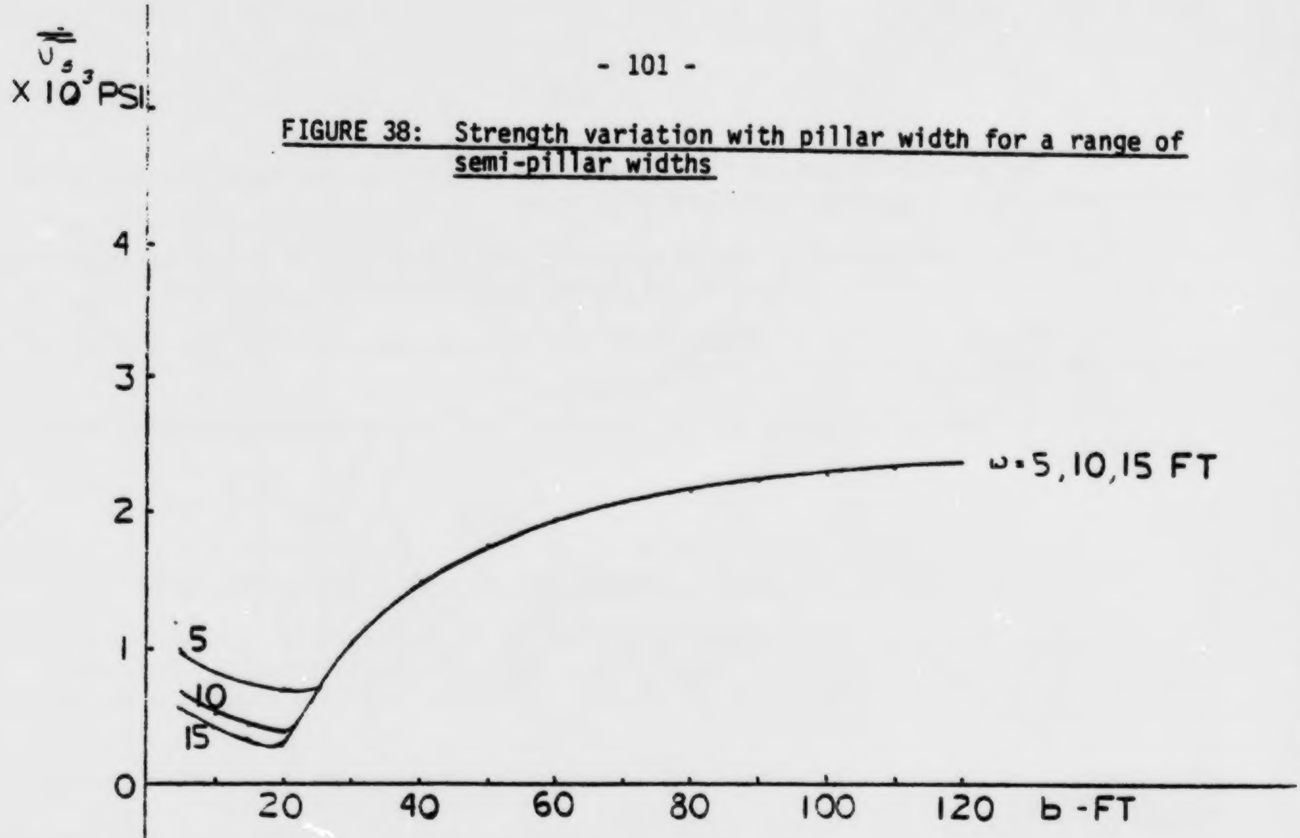

FIGURE 39: Strength variation with pillar width for a range of semi-pillar heights

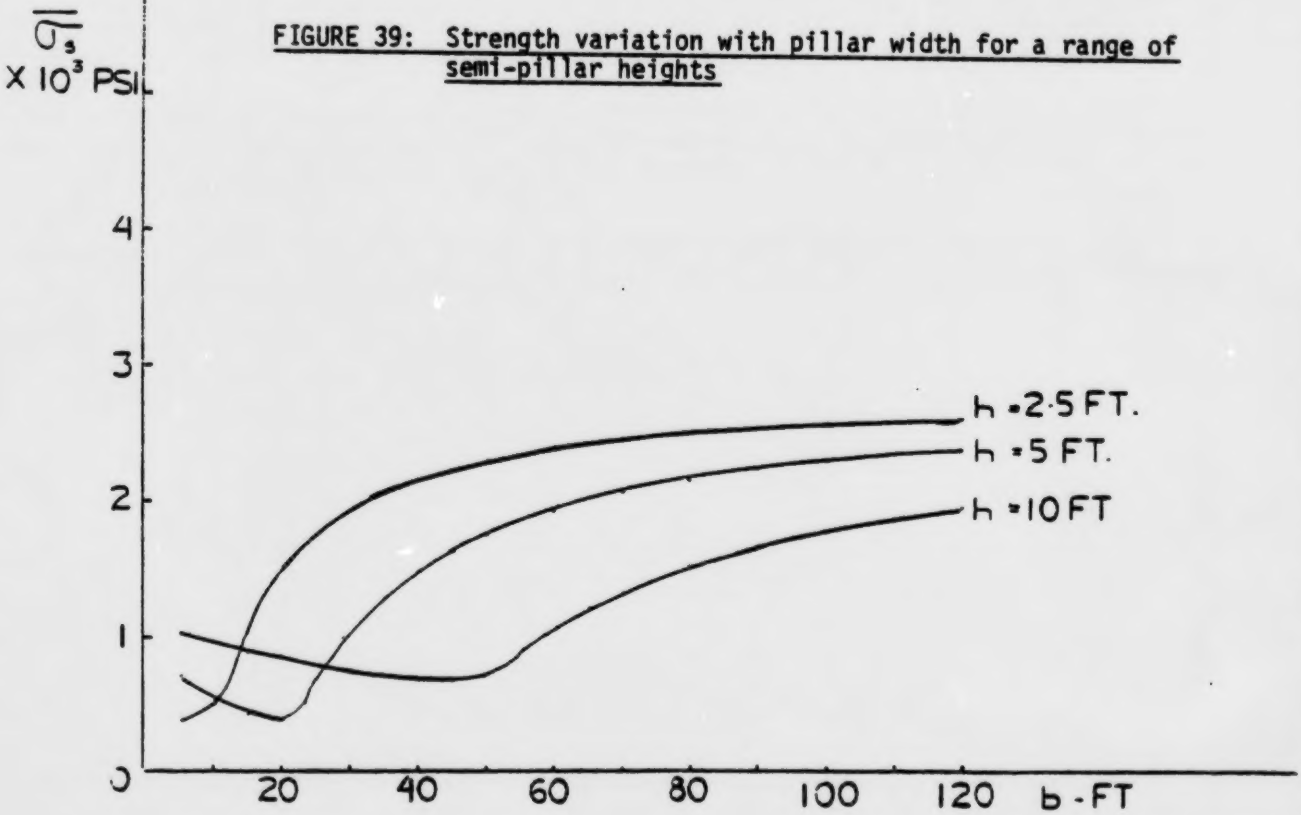

(i) The greater is semi-pillar height, the greater is the range of semi-pillar widths over which catastrophic failure will occur.

(ii) Also, the greater is the value of h, the higher is the stress at which fracture will initiate and the higher is the stress for catastrophic failure.

(iii) Beyond the range of catastrophic failure, the greater the semi-pillar height, the lower is the pillar strength.

(iv) The rate of change of pillar strength with pillar width diminishes with diminishing h.

8.9 General form of the pillar strength versus semi-pillar width curve

From the results of the preceeding section it is now possible to sketch a "general form" graph of pillar strength versus semi-pillar width curve. This has been done in Figure 40. The curve splits into up to three zones, depending on the mode of failure:-

Zone 1. At small pillar widths catastrophic fracture occurs. In this zone the pillar strength decreases with pillar size. This is caused by the fact that (as explained in Section 6.5.1) mean pillar stress concentration $\bar{Y}$ diminishes more rapidly as the pillar width increases than does the maximum stress concentration factor Y_{mm}. Consequently the mean pillar stress required to initiate fracture at the boundary diminishes over this range and, in this range, this mean pillar stress for fracture initiation is equal to the strength. (Sections 6.3 and 8.4)

Zone 2. In this zone catastrophic yield occurs. This zone may or may not occur depending on the parameters used in the analysis. As with catastrophic fracture, and for the same reasons, the pillar strength may diminish with increasing pillar width in this zone.

Zone 3. In this zone the mode of failure is one of "ultimate yield". The pillar strength increases with the semi-pillar width at a gradually diminishing rate.

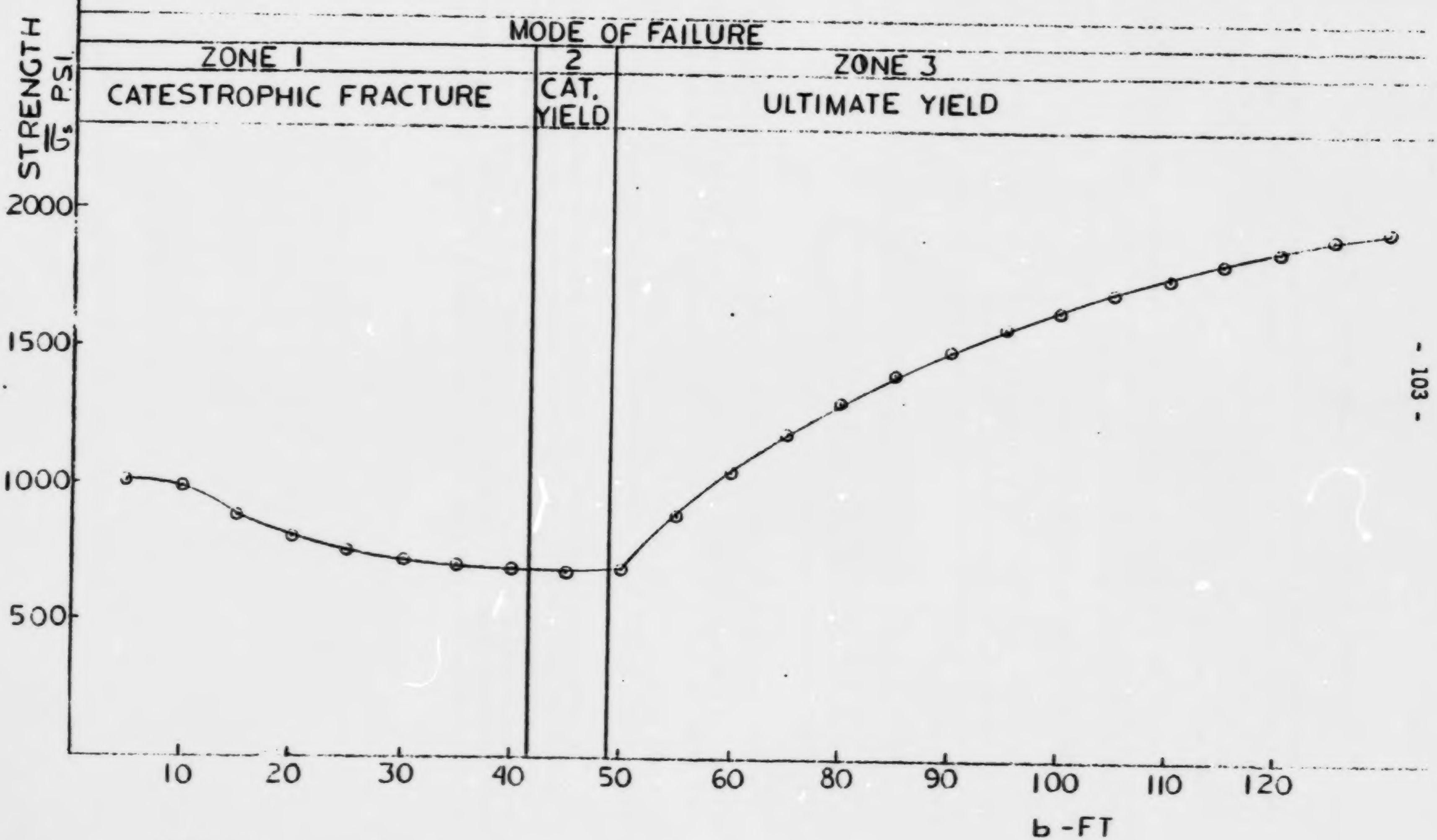

FIGURE 40: General form of the pillar strength versus semi-pillar width curve

8.10 Effect of the choice of the number of slices.

One other aspect of this pillar analysis program should be investigated and that is the effect of the choice of the number of slices into which the pillar is split. Clearly the larger the number of slices chosen the more accurate will be the resulting stress distribution in the pillar, on the other hand the longer will be time taken for the program to run.

The tables in Figure 41 give the input parameters and results for an example case in which n_1 is equal to 36, 180 and 540 slices. Figure 42 shows the resulting stress distribution for each of these cases.

The following points will be noted:-

(i) When $n_1 = 540$, it is seen that there is a fracture zone, a yield zone and a central solid elastic core in the pillar. There is a slight discontinuity in the stress distribution curve when the transition from the yield zone to the elastic core occurs.

(ii) When $n_1 = 180$. The yield zone is missed and there is a transition from fracture directly to the solid core. Otherwise, the stress distribution in the fracture zone and the stress distribution in the elastic core compares very favourably with that when $n_1 = 540$.

(iii) When $n_1 = 36$, not only is the yield zone missed but there is a significant difference between the stress distribution in the fracture zone and that given by the $n_1 = 180$ and $n_1 = 360$ solutions. Within the elastic core the stress distributions compare quite well. In addition the depth in the pillar at which the solid core commences is also significantly different.

The conclusion is obvious, for accurate determination of the stress distribution curve and of the transition depths from fracture to yield and yield to elastic it is essential that a large number of slices be selected. It is suggested that a slice width of not greater than 0.25 ft. be selected for most practical cases. Fortunately the additional computer time and costs involved due to the selection of a larger number of slices is almost insignificant.

```
CALCULATION FOR RECTANGULAR OPENING

VIRGIN STRESS=1540.0          EXTRACTION RATIO=0.254
LENGTH OF SPAN= 315.0         SEMI-WIDTH OF PILLAR= 90.0
SEMI-HEIGHT OF PILLAR= 5.0  OVERBURDEN DEPTH= 1400
DISTANCE "X"=    5            SEMI-ROOM WIDTH= 20.0
RATIO "SH/SV"=0.330           NUMBER OF PILLARS IN SPAN= 5
COMPRESSIVE STRENGTH OF BROKEN COAL=  1.
MOHR CONSTANT "A"=  500.00
ANGLE OF INTERNAL FRICTION OF BROKEN COAL=27.
POISSONS RATIO FOR SURROUNDING ROCK=0.30
POISSONS RATIO FOR PILLAR ROCK=0.30
COEFFICIENT OF SLIDING FRICTION FOR BROKEN COAL=0.51
YOUNGS MODULAS FOR SURROUNDING ROCK= 5000000
YOUNGS MODULAS FOR PILLAR ROCK= 1000000
STRESS REDISTRIBUTION COEFFICIENT=0.50
TOTAL NUMBER OF SLICES=   36
SLICE INTERVAL IN PRINTOUT= 1


THE RESULTS ARE

MEAN STRESS CONCENTATION=1.312
MEAN PILLAR STRESS:LHS=2021
MAXIMUM STRESS CONCENTRATION=     2.58
THE PILLAR IS STABLE
THE FAILURE MODE WILL BE ULTIMATE YIELD
THE PILLAR STRENGTH =    2445.16
THE SAFETY FACTOR   =        1.21
THE CRITICAL PILLAR DIMENSION TO AVOID
       A) CATASTROPHIC YIELD IS  28.88
       B) ULTIMATE YIELD IS  61.49
             K1= 0.3654
             K2=-0.7747
             K3= 0.9604

  SLICE   (90-O)  TAUS/F   TAU      STATUS     PONE   PTHREE ACCUM STRESS
  -----   ------  ------   ---      ------     ----   ------ ------------
  1( 5.0)  30.00   433.0  1336.0    FAILED       2.8     1.7      0.0
 2(10.0)   30.02   435.0  1239.4    FAILED      11.7     8.5    446.4
 3(15.0)   30.10   442.6  1247.7    FAILED      47.0    34.6    743.5
 4(20.0)   30.38   470.2  1290.6    FAILED     184.3   136.2   1002.6
 5(25.0)   31.36   558.0  1332.6    FAILED     717.5   530.8   1238.3
 6(30.0)   34.48   783.7  1260.9    FAILED    2788.3  2063.4   1402.1
 7(35.0)   42.32  1271.7   460.6  NOT FAILED  3010.8  2063.4   1227.7
 8(40.0)   42.81  1271.7   362.6  NOT FAILED  2809.3  2063.4   1062.4
 9(45.0)   43.15  1271.7   296.7  NOT FAILED  2673.6  2063.4    955.2
10(50.0)   43.43  1271.7   247.3  NOT FAILED  2572.1  2063.4    876.7
11(55.0)   43.65  1271.7   208.4  NOT FAILED  2492.1  2063.4    815.6
12(60.0)   43.84  1271.7   176.6  NOT FAILED  2426.7  2063.4    766.2
13(65.0)   44.00  1271.7   150.0  NOT FAILED  2371.9  2063.4    724.9
14(70.0)   44.15  1271.7   127.2  NOT FAILED  2325.1  2063.4    689.8
15(75.0)   44.27  1271.7   107.5  NOT FAILED  2284.6  2063.4    659.5
16(80.0)   44.38  1271.7    90.3  NOT FAILED  2249.1  2063.4    632.8
17(85.0)   44.48  1271.7    75.0  NOT FAILED  2217.6  2063.4    609.2
18(90.0)   44.56  1271.7    61.3  NOT FAILED  2189.4  2063.4    586.1
 BRITTLE/DUCTILE TRANSITION POINT:TAUF=  1040.5
 FRACTURE ZONE ENDED ON   7TH SLICE AND EXTENDED 35.0 FT INTO THE PILLAR
 DEPTH OF FRACTURE ZONE JUST AT FAILURE 28.19
```

```
CALCULATION FOR RECTANGULAR OPENING

VIRGIN STRESS=1540.0          EXTRACTION RATIO=0.254
LENGTH OF SPAN= 315.0         SEMI-WIDTH OF PILLAR= 90.0
SEMI-HEIGHT OF PILLAR= 5.0  OVERBURDEN DEPTH= 1400
DISTANCE "X"=    5            SEMI-ROOM WIDTH= 20.0
RATIO "SH/SV"=0.330           NUMBER OF PILLARS IN SPAN= 5
COMPRESSIVE STRENGTH OF BROKEN COAL=  1
MOHR CONSTANT "A"=  500.00
ANGLE OF INTERNAL FRICTION OF BROKEN COAL=27
POISSONS RATIO FOR SURROUNDING ROCK=0.30
POISSONS RATIO FOR PILLAR ROCK=0.30
COEFFICIENT OF SLIDING FRICTION FOR BROKEN COAL=0.51
YOUNGS MODULAS FOR SURROUNDING ROCK= 5000000
YOUNGS MODULAS FOR PILLAR ROCK= 1000000
STRESS REDISTRIBUTION COEFFICIENT=0.50
TOTAL NUMBER OF SLICES=  180
SLICE INTERVAL IN PRINTOUT= 5


THE RESULTS ARE

MEAN STRESS CONCENTATION=1.312
MEAN PILLAR STRESS:LHS=2021
MAXIMUM STRESS CONCENTRATION=     2.58
THE PILLAR IS STABLE
THE FAILURE MODE WILL BE ULTIMATE YIELD
THE PILLAR STRENGTH =    2445.16
THE SAFETY FACTOR   =        1.21
THE CRITICAL PILLAR DIMENSION TO AVOID
       A) CATASTROPHIC YIELD IS  28.88
       B) ULTIMATE YIELD IS  61.49
             K1= 0.3654
             K2=-0.7747
             K3= 0.9604

  SLICE   (90-O)  TAUS/F   TAU      STATUS     PONE   PTHREE ACCUM STRESS
  -----   ------  ------   ---      ------     ----   ------ ------------
  1( 1.0)  30.00   433.0  1613.9    FAILED       1.2     0.2      0.0
 10(10.0)  30.07   440.2  1385.1    FAILED      20.5     8.5    918.2
 15(15.0)  30.26   461.7  1416.3    FAILED      81.3    34.6   1209.0
 20(20.0)  30.97   532.4  1461.8    FAILED     317.5   136.2   1469.1
 25(25.0)  33.32   722.5  1423.7    FAILED    1235.0   530.8   1639.3
 30(30.0)  40.06  1144.4   798.1  NOT FAILED  3214.5  1572.9   1404.6
 35(35.0)  40.66  1144.4   661.0  NOT FAILED  2932.6  1572.9   1165.0
 40(40.0)  41.06  1144.4   578.3  NOT FAILED  2762.3  1572.9   1027.6
 45(45.0)  41.36  1144.4   519.4  NOT FAILED  2641.2  1572.9    932.6
 50(50.0)  41.60  1144.4   474.3  NOT FAILED  2548.4  1572.9    861.0
 55(55.0)  41.80  1144.4   438.1  NOT FAILED  2474.0  1572.9    804.3
 60(60.0)  41.98  1144.4   408.3  NOT FAILED  2412.6  1572.9    757.8
 65(65.0)  42.13  1144.4   383.1  NOT FAILED  2360.8  1572.9    718.7
 70(70.0)  42.26  1144.4   361.4  NOT FAILED  2316.3  1572.9    685.2
 75(75.0)  42.37  1144.4   342.6  NOT FAILED  2277.5  1572.9    656.0
 80(80.0)  42.48  1144.4   326.0  NOT FAILED  2243.3  1572.9    630.4
 85(85.0)  42.58  1144.4   311.2  NOT FAILED  2213.0  1572.9    607.5
 90(90.0)  42.66  1144.4   298.0  NOT FAILED  2185.8  1572.9    587.0
 BRITTLE/DUCTILE TRANSITION POINT:TAUF=  1040.5
 FRACTURE ZONE ENDED ON  30TH SLICE AND EXTENDED 30.0 FT INTO THE PILLAR.
 DEPTH OF FRACTURE ZONE JUST AT FAILURE 28.19
```

```
CALCULATION FOR RECTANGULAR OPENING

VIRGIN STRESS=1540.0          EXTRACTION RATIO=0.254
LENGTH OF SPAN= 315.0         SEMI-WIDTH OF PILLAR= 90.0
SEMI-HEIGHT OF PILLAR= 5.0  OVERBURDEN DEPTH= 1400
DISTANCE "X"=    5            SEMI-ROOM WIDTH= 20.0
RATIO "SH/SV"=0.330           NUMBER OF PILLARS IN SPAN= 5
COMPRESSIVE STRENGTH OF BROKEN COAL=  1
MOHR CONSTANT "A"=  500.00
ANGLE OF INTERNAL FRICTION OF BROKEN COAL=27
POISSONS RATIO FOR SURROUNDING ROCK=0.30
POISSONS RATIO FOR PILLAR ROCK=0.30
COEFFICIENT OF SLIDING FRICTION FOR BROKEN COAL=0.51
YOUNGS MODULAS FOR SURROUNDING ROCK= 5000000
YOUNGS MODULAS FOR PILLAR ROCK= 1000000
STRESS REDISTRIBUTION COEFFICIENT=0.50
TOTAL NUMBER OF SLICES=  540
SLICE INTERVAL IN PRINTOUT=15


THE RESULTS ARE

MEAN STRESS CONCENTATION=1.312
MEAN PILLAR STRESS:LHS=2021
MAXIMUM STRESS CONCENTRATION=     2.58
THE PILLAR IS STABLE
THE FAILURE MODE WILL BE ULTIMATE YIELD
THE PILLAR STRENGTH =    2445.16
THE SAFETY FACTOR   =        1.21
THE CRITICAL PILLAR DIMENSION TO AVOID
       A) CATASTROPHIC YIELD IS  28.88
       B) ULTIMATE YIELD IS  61.48
             K1= 0.3654
             K2=-0.7747
             K3= 0.9604

  SLICE   (90-O)  TAUS/F   TAU      STATUS     PONE   PTHREE ACCUM STRESS
  -----   ------  ------   ---      ------     ----   ------ ------------
   1( 0.3) 30.00   433.0  1683.3    FAILED       1.1     0.1      0.0
 30(10.0)  30.08   441.7  1437.1    FAILED      22.5     8.5   1057.5
 45(15.0)  30.30   467.1  1472.6    FAILED      88.1    34.6   1351.1
 60(20.0)  31.11   548.9  1515.5    FAILED     347.7   136.2   1609.1
 75(25.0)  33.79   762.3  1439.9    FAILED    1352.0   530.8   1737.3
 90(30.0)  38.95  1068.9   921.9  NOT FAILED  3208.7  1312.5   1401.9
105(35.0)  39.51  1068.9   785.3  NOT FAILED  2927.8  1312.5   1162.7
120(40.0)  39.88  1068.9   703.6  NOT FAILED  2759.7  1312.5   1026.9
135(45.0)  40.17  1068.9   645.3  NOT FAILED  2639.8  1312.5    932.7
150(50.0)  40.40  1068.9   600.6  NOT FAILED  2547.8  1312.5    861.6
165(55.0)  40.59  1068.9   564.7  NOT FAILED  2473.9  1312.5    805.2
180(60.0)  40.75  1068.9   535.0  NOT FAILED  2412.9  1312.5    758.9
195(65.0)  40.90  1068.9   509.9  NOT FAILED  2361.3  1312.5    720.0
210(70.0)  41.02  1068.9   488.4  NOT FAILED  2317.0  1312.5    686.6
225(75.0)  41.14  1068.9   469.6  NOT FAILED  2278.3  1312.5    657.5
240(80.0)  41.24  1068.9   453.0  NOT FAILED  2244.3  1312.5    631.9
255(85.0)  41.33  1068.9   438.3  NOT FAILED  2214.0  1312.5    609.1
270(90.0)  41.41  1068.9   425.1  NOT FAILED  2186.9  1312.5    588.6
BRITTLE/DUCTILE TRANSITION POINT:TAUF=  1040.5
FRACTURE ZONE ENDED ON  86TH SLICE AND EXTENDED 28.7 FT INTO THE PILLAR
DEPTH OF FRACTURE ZONE JUST AT FAILURE 28.19
```

Figure 41: Example cases for n_1 = 36, 180 and 360 slices

FIGURE 42: Effect of the number of slices on the vertical stress distribution

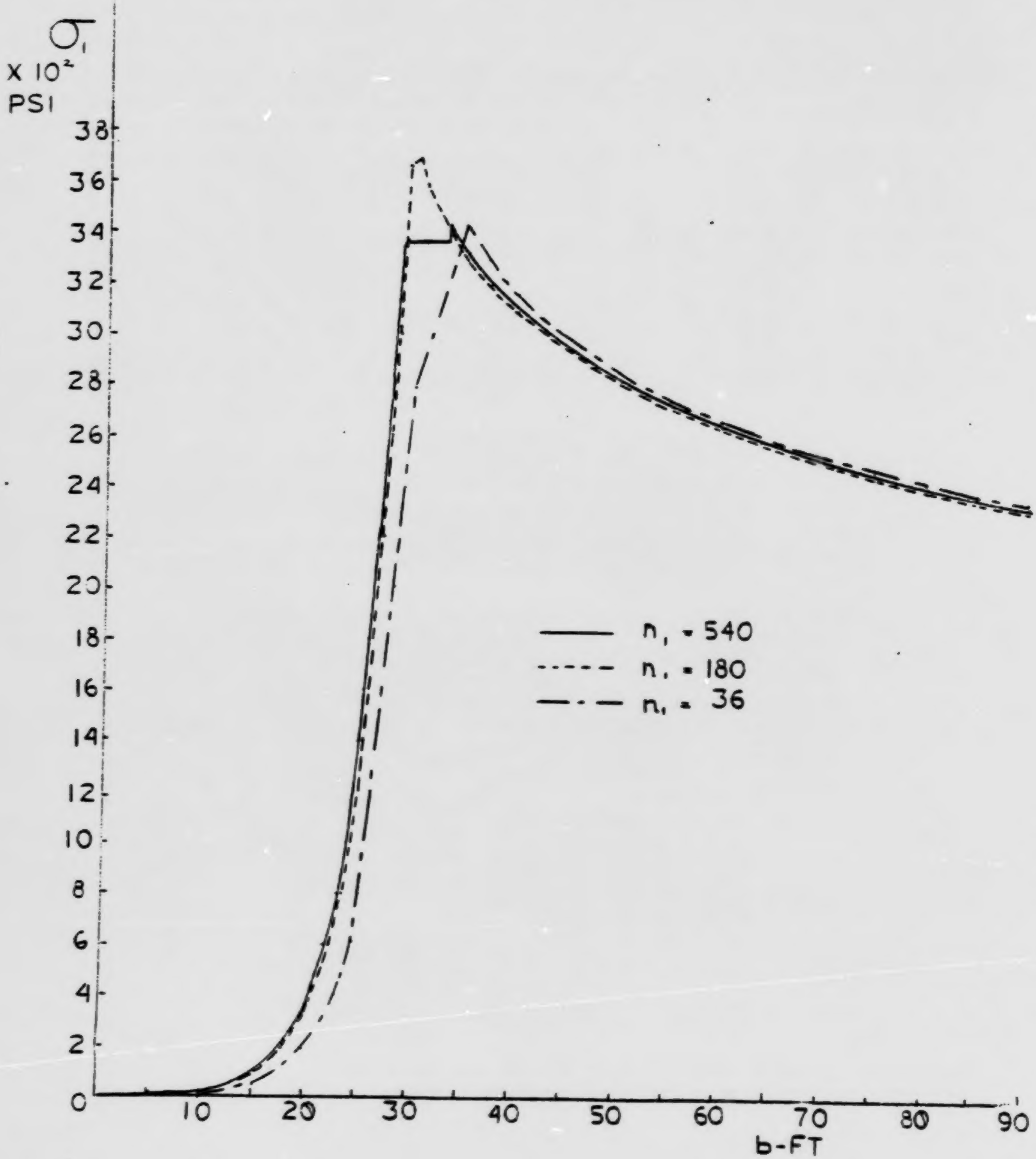

9. Pillar Program

By: Stephen Thornton and Gary Boehm

9.1 Program Flow

9.1.1 Main Program

The pillar program was written as a design tool for underground mining. All equations and assumptions used in the program can be found in the theory contained in this text. This section will explain the steps which the program goes through in order to derive the results. Numbers in brackets refer to the step numbers in the program listing.

Reading and initiallizing of all the necessary data is first done. (1-34) A title is written into the output describing the type of opening which will be used. (35-40) The program can analyse eliptical, rectangular, or ovoidal openings. If requested, all input data is printed as well. (44-68)

Before any calculations are begun the program checks that the width to height ratio lies between 0.25 and 4 and that the horizontal virgin stress to vertical virgin stress ratio is less than 1.5 . (74-75) These restrictions are placed on the program by theory and a warning will be printed if they are exceeded.

There are three methods which can be used to determine the mean pillar stress concentration. The first is by inputting it directly, and the second is by calculation using the tributary area theory, and the third is by use of Coates' equations. (77-118) The result is then used to calculate the mean pillar stress. (119)

As explained in Appendix C there are varying equations, depending upon the opening shape, for determining the maximum stress concentrations (Y_{mm}). (126-132) If the value which is calculated for Y_{mm} is less than the mean pillar stress concentration, the two values are equated. (133-134) This will also envoke a uniform stress distribution.

When the values are not equated, values for k_1, k_2 and k_3 or the characteristic constants used in the evaluation of the vertical stress, must be calculated. K_2 is calculated using the subroutine NEWT2 (See Section on Newton's Method) K_1 and K_3 use the value of K_2 for solutions.

The main program can now call the subroutine for determining the strength of the pillar, the transition point, the safety factor, the mode of failure, and the shed load. (155-156) (See Section on Strength Subroutines)

If the entire printout is requested, table headings are printed into the output file. (171-173) The program now enters the main loop. First the depth to the i th slice is calculated by :-

$$X = 1 + \frac{2Bi}{nW} \qquad (174)$$

If i is found to be greater than $\frac{X}{2}$ the program is referenced around the calculations to the evaluation of τ_S with respect to τ_F. When this is not met then the stress distribution will be calculated as uniform as previously stated or by the equation :-

$$\sigma_{1i} = \left\{ \frac{K_1}{K_2 + 1 + \frac{(2i - 1)B}{Wn}} \right\} + K_3 \qquad (175\text{-}178)$$

The values for τ_F, 2θ , τ, σ_1 and τ_S are all calculated at this time. (179-189)

The failure criteria can now be checked. If τ_F is greater than τ_S the program enters the fracture criteria loop. A value τ greater than τ_S indicates failure by fracture. (195-197)

The values of P_3 and P_1 can now be calculated. P_3 is calculated at the edge of the slice for a horizontal stress and P_1 is calculated at the midpoint for the vertical stress. (199-211)

An accumulated stress distribution function is included at this point in the program. If a uniform stress distribution is being used the function appears as:-

$$\Delta\sigma_{1i} = \frac{(\sigma_{1i} - P_1)}{(\frac{n}{2} - 1)}$$

When a non-uniform stress distribution is being used the equation is :-

$$\Delta\sigma_{1i} = \frac{(\sigma_{1i} - P_1)\ (j - i)^{\alpha}}{\sum_{j=i+1}^{n/i} \frac{1}{(j - i)^{\alpha}}} \qquad (212\text{-}242)$$

A τ_F value less than a τ_S value will put the program into a pseudo-ductile loop. (247) Once the program enters this loop it cannot return to the other. The values for σ_1 and σ_3 are calculated using "s" and "r" values of

$$s = \frac{A}{2} + \sigma$$

$$r = \left\{\frac{A}{2} + A\sigma\right\}^{\frac{1}{2}}$$

The accumulated load distribution is calculated the same here as in the failure loop. (248-272)

Conditions of τ less than τ_F or τ less than τ_S will indicate an unfailed

pillar with a solid core. P_1 is then calculated and the results are printed. A table is printed out if it is requested. (290-300) The values that are printed are :
I, (90-θ), τ_S, τ, FAIL(I), PONE, and PTHREE, ACCUMULATED STRESS.

The transition points are the last to be calculated and printed. The points are between yield-fracture, fracture-stable, and yield-stable.

9.1.2 Subroutines

Three subroutines are used in the pillar program. They are called "STRETH" (401-610), "NEWT" (611-654) and "NEWT2" (655-700). The method by which the first two work are covered in APPENDIX K. NEWT2 follows the same steps as NEWT. It is simply used for deriving the value of K_2 instead of a critical pillar dimension.

9.2 Flow Diagram

Figure 43 gives the flow diagram for this pillar analysis program. The numbers on this figure indicate the relevant program steps in the program listing.

Figure 43: Flow Diagram - Main Program

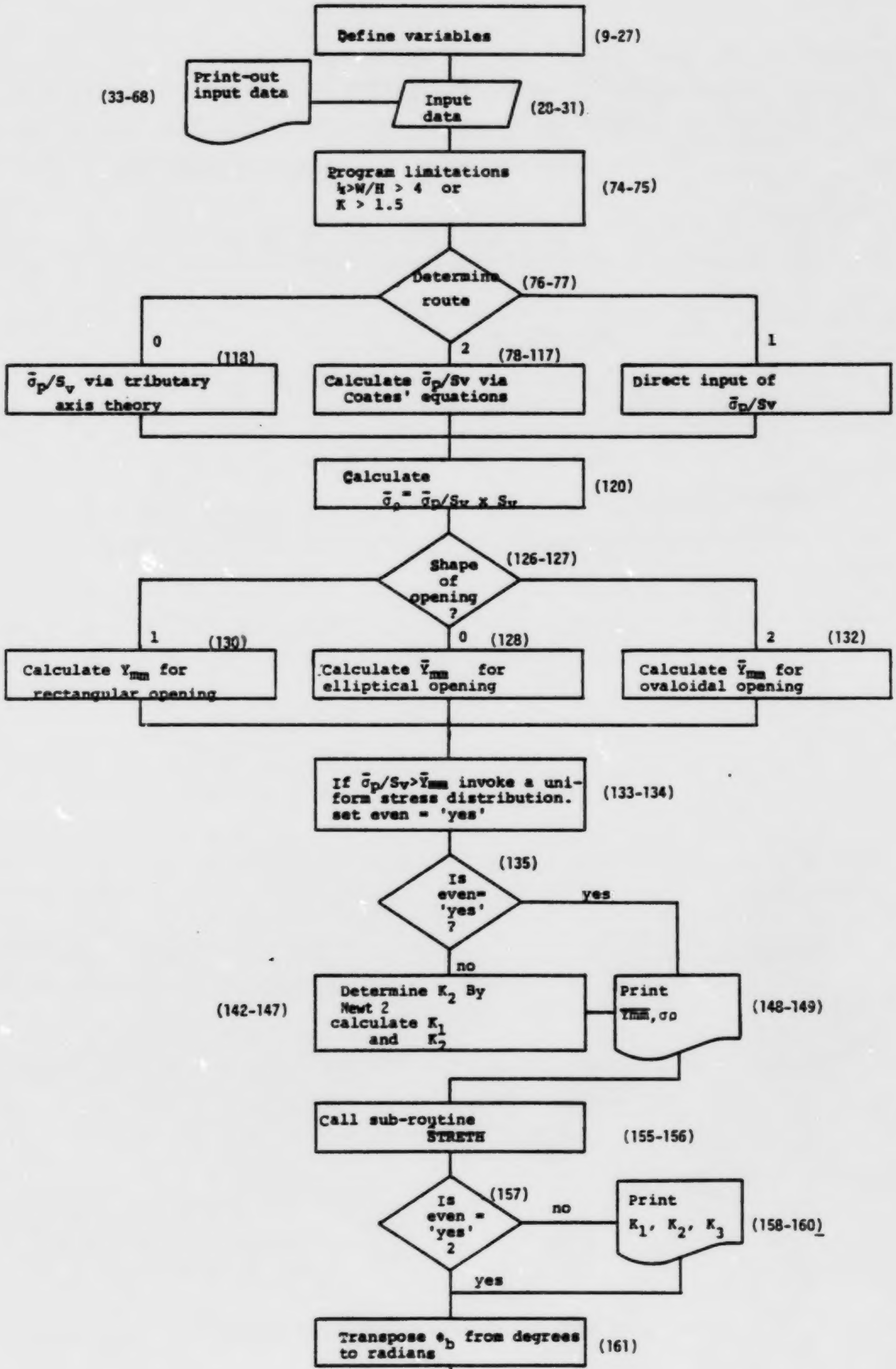
Define variables
(9-27)
Print-out input data
(33-68)
Input data
(28-31)
Program limitations
¼>W/H > 4 or
K > 1.5
(74-75)
Determine route
(76-77)
0
(113)
$\bar{\sigma}_p/S_v$ via tributary axis theory
2
(78-117)
Calculate $\bar{\sigma}_p/Sv$ via Coates' equations
1
Direct input of $\bar{\sigma}_p/Sv$
Calculate $\bar{\sigma}_p = \bar{\sigma}_p/Sv \times Sv$
(120)
Shape of opening ?
(126-127)
1
(130)
Calculate Y_{mm} for rectangular opening
0
(128)
Calculate $\bar{Y}_{mm}$ for elliptical opening
2
(132)
Calculate $\bar{Y}_{mm}$ for ovaloidal opening
If $\bar{\sigma}_p/Sv>\bar{Y}_{mm}$ invoke a uniform stress distribution. set even = 'yes'
(133-134)
Is even= 'yes' ?
(135)
yes
no
Determine K_2 By Newt 2 calculate K_1 and K_2
(142-147)
Print Ymm, σp
(148-149)
Call sub-routine STRETH
(155-156)
Is even = 'yes' ?
(157)
no
Print K_1, K_2, K_3
(158-160)
yes
Transpose ϕ_b from degrees to radians
(161)
Set array of shed loads to zero
(168-169)

Figure 43 (cont.)

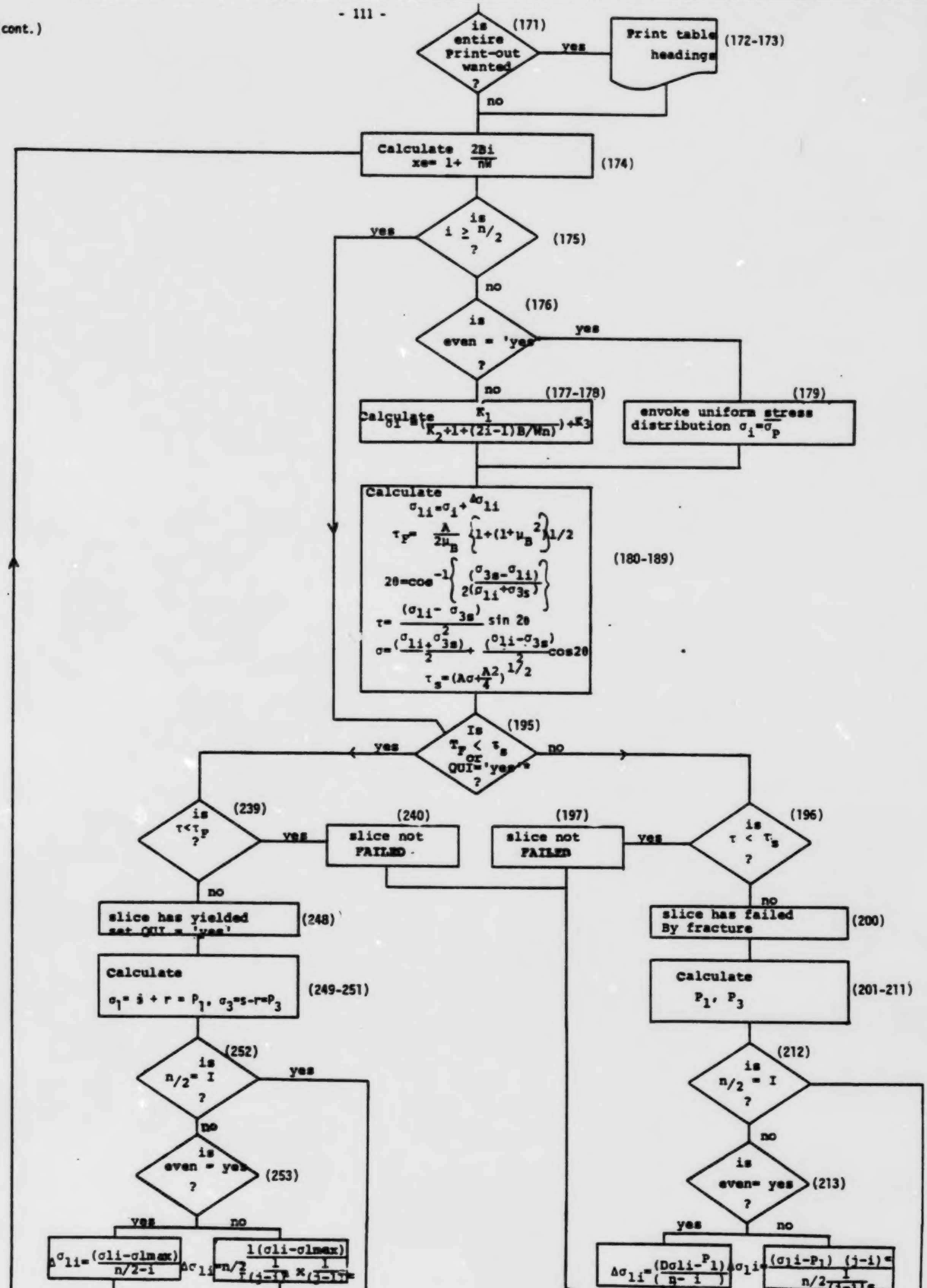
is entire Print-out wanted ?
(171)
yes
Print table headings
(172-173)
no
Calculate xe= 1+ 2Bi/nW
(174)
is i ≥ n/2 ?
(175)
yes
no
is even = 'yes' ?
(176)
yes
no
(177-178)
Calculate σi = (K1/(K2+1+(2i-1)B/Wn)) + K3
(179)
envoke uniform stress distribution σi=σP
Calculate
σ1i=σi+Δσ1i
τF= A/2μB {1+(1+μB²)}1/2
2θ=cos⁻¹{(σ3s-σ1i)/2(σ1i+σ3s)}
τ= (σ1i- σ3s)/2 sin 2θ
σ=(σ1i+σ3s)/2 + (σ1i-σ3s)/2 cos2θ
τs=(Aσ+A²/4)1/2
(180-189)
Is τF < τs or QUI='yes' ?
(195)
yes
no
is τ<τF ?
(239)
yes
(240)
slice not FAILED
(197)
slice not FAILED
yes
is τ < τs ?
(196)
no
slice has yielded set QUI = 'yes'
(248)
no
slice has failed By fracture
(200)
Calculate σ1= s + r = P1, σ3=s-r=P3
(249-251)
Calculate P1, P3
(201-211)
is n/2= I ?
(252)
yes
no
is n/2 = I ?
(212)
no
is even = yes ?
(253)
is even= yes ?
(213)
yes
no
yes
no
Δσ1i=(σ1i-σ1max)/(n/2-i)
Δσ1i=n/2 1(σ1i-σ1max)/(1/(j-1) × 1/(j-1))
Δσ1i=(Dσ1i-P1)/(n- i)
Δσ1i=(σ1i-P1)(j-i)/(n/2 Σ 1/(j-i)) j=i+1
(254-272)
(217-222)

Figure 43 (cont.)

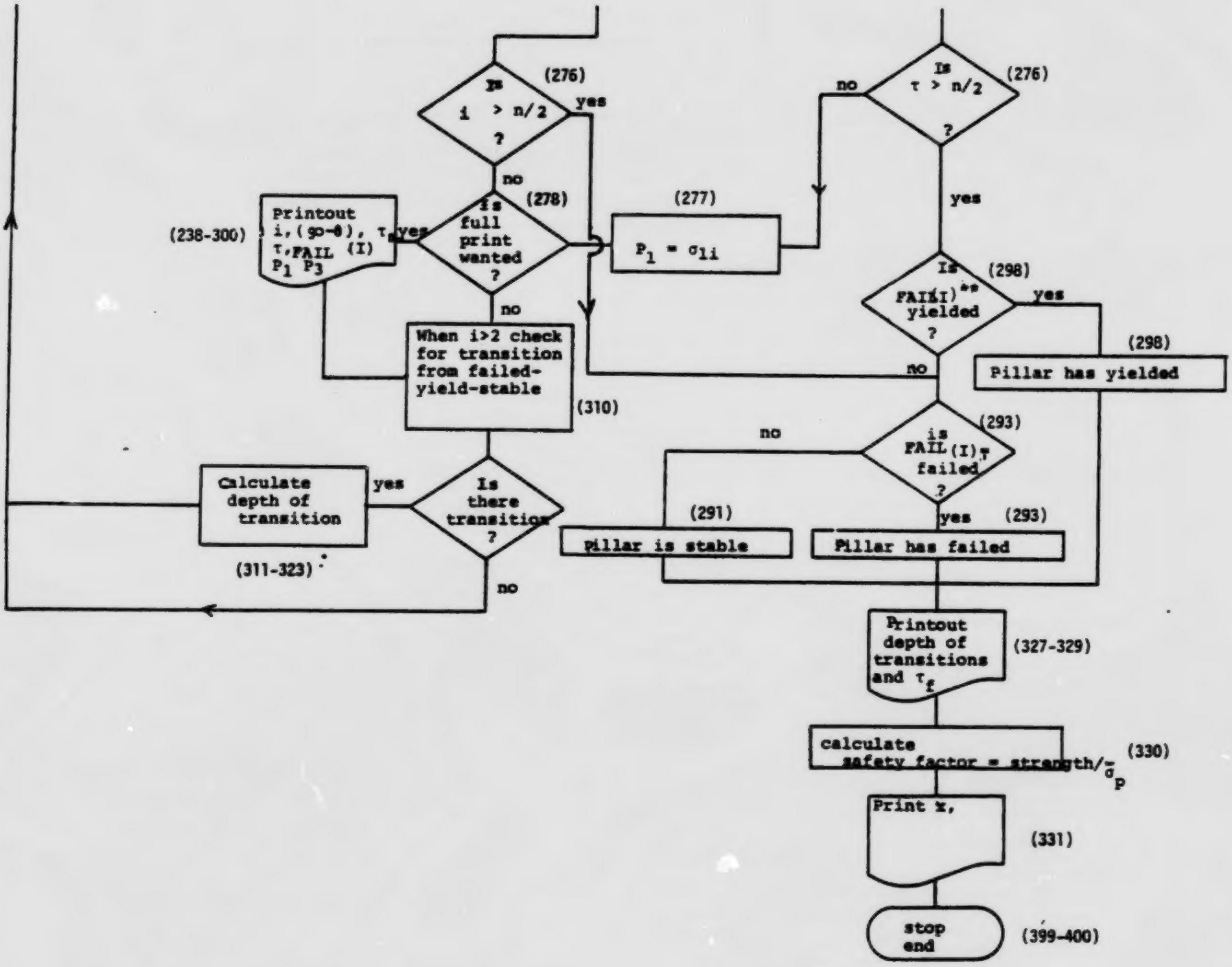
Is i > n/2 ?
(276)
yes
no
Is full print wanted ?
(278)
yes
Printout i,(90-θ), τ, τ,FAIL (I) P1 P3
(238-300)
no
When i>2 check for transition from failed-yield-stable
(310)
Is there transition ?
yes
Calculate depth of transition
(311-323)
no
(277)
$P_1 = \sigma_{1i}$
no
Is τ > n/2 ?
(276)
yes
Is FAIL(I) yielded ?
(298)
yes
(298)
Pillar has yielded
no
is FAIL(I),τ failed ?
(293)
no
yes
(291)
Pillar is stable
(293)
Pillar has failed
Printout depth of transitions and τ_f
(327-329)
calculate safety factor = strength/$\bar{\sigma}_p$
(330)
Print x,
(331)
stop end
(399-400)

9.3 Program Listing

```
PPPPPPPPPPP    IIIIIIIIII   LL            LL             AAAAAAAAAA   RRRRRRRRRRR
PPPPPPPPPPPP   IIIIIIIIII   LL            LL            AAAAAAAAAAAA  RRRRRRRRRRRR
PP        PP       II       LL            LL            AA        AA  RR        RR
PP        PP       II       LL            LL            AA        AA  RR        RR
PP        PP       II       LL            LL            AA        AA  RR        RR
PPPPPPPPPPPP       II       LL            LL            AAAAAAAAAAAA  RRRRRRRRRRRR
PPPPPPPPPPP        II       LL            LL            AAAAAAAAAAAA  RRRRRRRRRRR
PP                 II       LL            LL            AA        AA  RR   RR
PP                 II       LL            LL            AA        AA  RR     RR
PP                 II       LL            LL            AA        AA  RR      RR
PP             IIIIIIIIII   LLLLLLLLLLLL  LLLLLLLLLLLL  AA        AA  RR       RR
PP             IIIIIIIIII   LLLLLLLLLLLL  LLLLLLLLLLLL  AA        AA  RR        RR


 8888888888        11                          11        2222222222                  3333333333     00000000
888888888888      111                         111       222222222222                333333333333   0000000000
88        88     1111                        1111       22        22                33        33  00        00
88        88       11                          11                 22                          33  00        00
 88      88        11                          11                 22                          33  00        00
  88888888         11                          11                22                        3333   00        00
  88888888         11                          11              22                          3333   00        00
88        88       11                          11            22                               33  00        00
88        88       11                          11          22                                 33  00        00
88        88       11                          11        22                         33        33  00        00
888888888888   1111111111                  1111111111   222222222222                333333333333   0000000000
 8888888888    1111111111                  1111111111   222222222222                 3333333333     00000000
```

```
C    ***********************************
C    *     PILLAR FAILURE PROGRAM      *
C    *   AS PART OF CMRC TASK 81/15    *
C    *      WRITTEN BY G. BOEHM        *
C    *      AND S. THORNTON FOR        *
C    *         DR. K. BARRON           *
C    ***********************************
       LOGICAL*1 FREE(1)/'*'/
       INTEGER  ROUTE,LER,N,X,Z,ER,EP,SHAPE,I,G,NNN,
     1   P,J,C,LI,NT,T,S,E,COUNT,INTVAL,II,YES,NO,FAIL(1000),
     1   EVEN,PRINT,QUI,DON,MODE,IJ,JK,IJJ,IJK
       REAL  W,B,H,NU,NUP,MUR,MUP,R,XPR,WPR,ZPR,HPR,BPR,NN,L,
     1       RR,INTA,INTB,INTC,INTD,INTE,K,KBPR,DSPSV,INKA,DQ,
     1       DIS,STREN,PONE,SV,DIST,MUB,A,AREA,AREB,ALPHA,
     1       SP,F,INKB,INKC,INTF,YMM,ALOG,LM,XM,SONES,
     1       XX,YPT,DIFF,Y,D,SPSV,XE,PHIB,PHIS,PHIBD,PHISD,
     1       PTHREE,DSONE(1000),SI,SONEI,STHS,SIN,PB,SCS,
     1       TAN,KTWO,KONE,KTHREE,XBC1,XBC2,XBC3,XBC4,
     1       DL,TOT,PPONE(10,1000),
     1       BCY,BCYU,BCF,BCFU,CANTA,CANTB,RPR,RPRY,
     1       AA,BB,CC,DD,EE,FF,GG,FTOL,BTOL
C
C    INITIALLIZATION OF ALL DATA
C
       EXTERNAL FC3,D03
       IJ=1
 888   READ(5,FREE,END=999) ROUTE,SV,R,L,X,W,Z,B,H,MUR,MUP,
     1    ER,EP,LER,K,N,ALPHA
       READ(5,FREE,END=999) NNN,PB,SCS,A,MUB,PHIBD,SPSV,
     1    SHAPE,PRINT,INTVAL
C
       JK=1
       NO=0
       YES=1
       IF (SHAPE.EQ.0)WRITE(6,111)
       IF (SHAPE.EQ.1)WRITE(6,112)
       IF (SHAPE.EQ.2)WRITE(6,113)
 111   FORMAT('1','CALCULATION FOR ELIPTICAL OPENING',/,/)
 112   FORMAT('1','CALCULATION FOR RECTANGULAR OPENING',/,/)
 113   FORMAT('1','CALCULATION FOR OVALOIDAL OPENING',/,/)
C
C    PRINT OUT ALL INPUT DATA IF REQUESTED
C
       IF (PRINT .EQ. NO) GO TO 2
         AREA=0
         AREB=0
         QUI=NO
         SUMM=0
         PHIB=PHIBD*3.14159/180
         DON=YES
         WRITE(6,1040) SV,R
         WRITE(6,1045) L,B
         WRITE(6,1050) H,Z
         WRITE(6,1055) X,W
         WRITE(6,1060) K,N
         WRITE(6,1065) PB
```

University of Alberta

```
            WRITE(6,1067) A
            WRITE(6,1075) PHIBD
            WRITE(6,1080) MUR
            WRITE(6,1085) MUP
            WRITE(6,1090) MUB
            WRITE(6,1105) ER
            WRITE(6,1110) EP
            WRITE(6,1115) ALPHA
            WRITE(6,1116) NNN
            WRITE(6,1120) INTVAL
            WRITE(6,1100)
     2  CONTINUE
C
C      DETERMINE IF THE INPUT DATA MEETS THE RESTRICTIONS
C        PUT ON THE PROGRAM BY THEORY AND CALCULATE
C                THE STRESS CONCENTRATION.
C
        IF(W/H .LT. 0.25 .OR. W/H .GT. 4) WRITE(6,1010)
           IF(K .GE. 1.5) WRITE(6,1005)
               IF (ROUTE .EQ. 0) GO TO 25
                   IF (ROUTE .EQ. 1) GO TO 30
                   XPR=X/L
                   ZPR=Z/L
                   BPR=B/L
                   HPR=H/L
                   AREA=O
                   AREB=O
C
C
                 NU=MUR/(1-MUR)
                 NUP=MUP/(1-MUP)
                 NN=ER*(1-MUP**2)/EP/(1-MUR**2)
C
C
                      IF(ZPR .LT. 0.8) GO TO 10
                      INTA=2*R*(1-XPR/5+HPR)-K*HPR*(1-NU+NUP*NN)
                      INTB=1+HPR/(1-XPR/5)
                      INTC=2*R*BPR*(1-NU)/3.14159
                 IF(LER .EQ. O) GO TO 5
                 RR=1-(1/(1+W/B))
                 DSPSV=INTA/(HPR*NN+1.8*(1-RR)*INTB+INTC)
                 GO TO 20
    5        DSPSV=INTA/(HPR*NN+1.8*(1-R)*(1+1.00/N)*INTB+INTC)
             GO TO 20
   10        INKA=(1-XPR**2)/2*ZPR**3+1.2*(1+NU)*(1-XPR**2)/ZPR
             F=1-1/(2.26/ZPR+1)
             INKB=13-2*NU*(12*(1-XPR**2)/ZPR**2+1.-8/ZPR**2-3*NU)
             INKC=0.884*F*(1-XPR**2)/ZPR**2
             KBPR=INKA+ZPR/32*INKB+INKC
         INTA=2*R*(1-XPR/5+2*HPR)+R*KBPR
         INTB=K*HPR*(1-NU-NUP*2*NN)
         INTC=2*HPR*NN
         INTD=1.8*(1+HPR/(1-XPR/5))+2*KBPR/3*(1+HPR/(1-XPR**2))
         INTE=4*R*BPR*(1-NU)/3.14159
            IF(LER .EQ. O) GO TO 15
            RR=1-(1/(1+W/B))
```

University of Alberta

```
            DSPSV=(INTA-INTB)/(INTC+INTD*(1-RR)+INTE)
            GO TO 20
  15          DSPSV=(INTA-INTB)/(INTC+INTD*(1-R)*(1+1.00/N)+INTE)
  20           SPSV=(DSPSV+1)
               GO TO 30
  25         SPSV=(W+B)/B
  30         SP=SPSV*SV
             WRITE(6,1070) SPSV
             INTF=0.09*((W/B+1)**2-1)
C
C       CALCULATE THE VALUE OF YMM FOR THE PARTICULAR
C          SHAPE OF OPENING WHICH HAS BEEN CHOSEN.
C
                IF(SHAPE .EQ. 1) GO TO 35
                IF(SHAPE .EQ. 2) GO TO 40
                  YMM=(1-K)+2*W/H+INTF
                  GO TO 45
  35              YMM=(2.048-0.919*K)+0.572*ALOG(W/H)+INTF
                  GO TO 45
  40              YMM=(2.97-1.044*K)+1.327*ALOG(W/H)+INTF
  45              IF(YMM .GE. SPSV) GO TO 3000
                  YMM=SPSV
                  EVEN=YES
                  GO TO 58
  3000            CONTINUE
C
C        CALCULATE THE VALUES FOR K1, K2, AND K3. K2 IS FOUND
C                 USING THE SUBROUTINE NEWT2.
C
             EVEN=NO
             KTWO=-0.6
             I=0
             CALL NEWT2(FC3,DO3,KTWO,YMM,I)
  60          KONE=(YMM-1)*(1+KTWO)*(10+KTWO)/9
              KTHREE=((10-YMM)-KTWO*(YMM-1))/9
  58          WRITE(6,1000) SP
              WRITE(6,1015) YMM
C
C    THE STRENGTH SUBROUTINE IS USED TO DETERMINE THE
C    STRENGTH OF THE PILLAR, THE TRANSITION POINT, THE
C    SAFETY FACTOR, THE MODE OF FAILURE, AND THE SHED LOAD
C
            CALL STRETH(B,W,PHIB,MUB,A,PB,H,YMM,SV,SPSV,STREN,MODE,
     1        K,XBC,SHEDDO,SF)
               IF(EVEN .EQ. YES) GO TO 62
  64           WRITE(6,1019) KONE
               WRITE(6,1021) KTWO
               WRITE(6,1022) KTHREE
  62           PHIB=3.14159*PHIBD/180
C
C   CALCULATE THE VALUES FOR TAU,TAUS,TAUF, AND THETA.
C
                 I=1
                 PTHREE=0
                 DO 3010 J=1,NNN
                 DSONE(J)=0.0
```

University of Alberta

```
 3010              CONTINUE
                 COUNT=1
                 IF(PRINT .EQ. NO) GO TO 65
                 WRITE(6,1031)
                 WRITE(6,1032)
   65            XE=1+(2*B*I/NNN/W)
               IF(I .GT. NNN/2) GO TO 70
               IF(EVEN .EQ. YES) GO TO 71
               SI=(KONE/(1.0+KTWO+(2.0*I-1.0)/NNN*B/W)+KTHREE)*SV
               GO TO 72
   71            SI=SP
   72            SONEI=SI+DSONE(I)
                 STHS=PTHREE
                 TAUF=A/2/MUB*(1.0+SQRT(1+MUB**2))
                 DEL=-1*(SONEI-STHS)/(2*(SONEI+STHS))
                 TWOTH=ARCOS(DEL)
                 THETA=90*(1-TWOTH/3.14159)
                 TAU=(SONEI-STHS)/2*SIN(TWOTH)
                 SIGMA=(A+STHS)+SQRT(4*A*STHS+A**2)
                 TAUS=((SIGMA-STHS)/2)*(SQRT((4*(SIGMA+STHS)**2)-
     1                 ((SIGMA-STHS)**2)))/(2*(SIGMA+STHS))
C
C     DETERMINE IF THE FAILURE MODE IS FRACTURE OR YIELD.
C     NOTE: ONCE THE PILLAR ENTERS THE YIELDING SOLUTION
C               IT CANNOT RETURN TO A FAILURE MODE.
C
                   IF(TAUF .LT. TAUS .OR. QUI .EQ. YES) GO TO 75
   70              IF(TAU .GT. TAUS) GO TO 3020
                   FAIL(I)=1
                   GO TO 85
 3020              CONTINUE
            FAIL(I)=2
            INTA=PB/2/SIN(PHIB)
            INTB=TAN(PHIB)*(1+SIN(PHIB))/(1-SIN(PHIB))*W/H*(XE-1)
            INTC=1-SIN(PHIB)
            PONE=INTA*((1+SIN(PHIB))*EXP(INTB)-INTC)
            PTHREE=(1-SIN(PHIB))/(1+SIN(PHIB))*(PONE-PB)
            NT=NNN/2-I
            XE=XE-B/NNN/W
            INTA=PB/2/SIN(PHIB)
            INTB=TAN(PHIB)*(1+SIN(PHIB))/(1-SIN(PHIB))*W/H*(XE-1)
            INTC=1-SIN(PHIB)
            PONE=INTA*((1+SIN(PHIB))*EXP(INTB)-INTC)
            IF(NNN/2 .EQ. I) GO TO 80
            IF(EVEN .EQ. YES) GO TO 76
            TOT=0
            NT=I+1
            LI=I
 3022             CONTINUE
                  IF(NT .GT. NNN/2) GO TO 3021
                  TOT=TOT+1.0/((NT-LI)**ALPHA)
                  NT=NT+1
                  GO TO 3022
 3021             CONTINUE
   76             NT=I+1
 3024        CONTINUE
```

University of Alberta

```
              IF(NT .GT. NNN/2)GO TO 3023
              IF(EVEN .EQ. YES) GO TO 77
              DL=(SONEI-PONE)/TOT*1.0/((NT-LI)**ALPHA)
              GO TO 78
   77         DL=(SONEI-PONE)/(NNN/2-I)
   78         DSONE(NT)=DSONE(NT)+DL
              NT=NT+1
              GO TO 3024
 3023         CONTINUE
              GO TO 80
   75    DELT=-1*MUB/(SQRT(2*(1+MUB**2)+2*(SQRT(1+MUB**2))))
         TWOTHT=ARCOS(DELT)
         TAU=((SONEI-PTHREE)/2)*SIN(TWOTHT)
         THETAT=90*(1-TWOTHT/3.14159)
               IF(TAU .GE. TAUF) GO TO 3030
               FAIL(I)=1
               GO TO 85
 3030          CONTINUE
C
C     THIS IS THE SECTION WHICH CALCULATES THE VALUES FOR
C                    A YIELDING PILLAR.
C
              FAIL(I)=3
              QUI=YES
         SIMAX=(A/2)*(1+(1/MUB**2)*(1+SQRT(1+MUB**2)))+
     1      SQRT((A**2/2)*(1+(1/MUB**2)*(1+SQRT(1+MUB**2))))
         IF(I .GE. NNN/2) GO TO 30
         PONE=SIMAX
         IF(EVEN .EQ. YES) GO TO 81
         TOT=0
         NT=I+1
         LI=I
 3032       CONTINUE
             IF (NT .GT. NNN/2) GO TO 3031
             TOT=TOT+1.0/((NT-LI)**ALPHA)
             NT=NT+1
            GO TO 3032
 3031       CONTINUE
   81       NT=I+1
 3034           CONTINUE
                IF(NT .GT. NNN/2) GO TO 3033
                IF(EVEN .EQ. YES) GO TO 82
                DL=(SONEI-SIMAX)/TOT*1.0/((NT-LI)**ALPHA)
                GO TO 83
   82           DL=(SONEI-SIMAX)/(NNN/2-I)
   83           DSONE(NT)=DSONE(NT)+DL
                NT=NT+1
                GO TO 3034
 3033           CONTINUE
              IF(I .GT. NNN/2) GO TO 95
              GO TO 90
   85         IF(I .GT. NNN/2) GO TO 95
              PONE=SONEI
   90         IF(PRINT .EQ. NO) GO TO 91
              IF(I .EQ. COUNT*INTVAL .OR. I .EQ. 1)GO TO 3050
              GO TO 3051
```

University of Alberta

```
 3050        DIS=I*B/NNN*2
C
C   THE FOLOWING IF STATEMENTS ARE USED TO DETERMINE IF THE
C     FAILURE IS:  1. NOT FAILED
C                  2. FAILED
C                  3. YIELDED
C    AND PRINT OUT THE APPROPRIATE RESPONSE IN A TABLE FORM.
C
        IF (QUI.EQ.YES) GO TO 6000
        IF (FAIL(I).EQ.1)WRITE(6,1035) I,DIS,THETA,TAUS,TAU,
     1        PONE,PTHREE,DSONE(I)
        IF (FAIL(I).EQ.2)WRITE(6,1036) I,DIS,THETA,TAUS,TAU,
     1        PONE,PTHREE,DSONE(I)
        GO TO 6001
 6000   IF (FAIL(I).EQ.1)WRITE(6,1035) I,DIS,THETAT,TAUF,TAU,
     1        PONE,PTHREE,DSONE(I)
        IF (FAIL(I).EQ.3)WRITE(6,1037) I,DIS,THETAT,TAUF,TAU,
     1        PONE,PTHREE,DSONE(I)
 6001   CONTINUE
C
C         THESE VARIABLES GATHER THE INFORMATION IN ARRAY
C             FORM FOR THE GRAPH OF P1 VERSUS B.
C
        PPONE(IJ,JK)=PONE
        IF (IJ .EQ. 1) PDIS=DIS
        JK=JK+1
            . COUNT=COUNT+1
 3051         CONTINUE
   31       IF(I .LT. 2) GO TO 4020
            IF(FAIL(I) .NE. 2 .AND. FAIL(I-1) .EQ. 2)GO TO 4000
            GO TO 4001
 4000       DIST=I*B/NNN*2
            II=I
            AREA=1
 4001       CONTINUE
          IF (FAIL(I) .EQ. 1 .AND. FAIL(I-1) .EQ. 3) GO TO 4003
              GO TO 4004
 4003         DUST=I*B/NNN*2
              III=I
              AREB=1
 4004         CONTINUE
 4020   CONTINUE
        I=I+1
        GO TO 65
   95   QQ=NNN/2
             WRITE(6,1024) TAUF
           IF(AREA .EQ. 1) WRITE(6,1023) II,DIST
           IF(AREB .EQ. 1) WRITE(6,1026) III,DUST
           SF=STREN/SP
  110 WRITE(6,1125) XBC
C
C   THE FOLLOWING IF STATEMENTS DETERMINE IF THE MODE OF
C     FAILURE IS 1. UNSTABLE YIELD
C                2. CONTROLLED FRACTURE
C                3. CATASTROPHIC FRACTURE
```

University of Alberta

```
C     AND PRINTS OUT THE APPROPRIATE REPLY.
C
C
 1005 FORMAT(' ','WARNING:VALUES OF K EXCEED RECOMMENDED VALUE OF',
     1   ' K .LT. 1.5')
 1010  FORMAT(' ','WARNING:VALUE OF W/H IS NOT WITHIN RECOMENDED',
     1   ' RANGE OF 0.25 GT W/H LT 4')
 1015  FORMAT(' ','MAXIMUM STRESS CONCENTRATION=',F8.2)
 1019 FORMAT(' ',12X,'K1=',F7.4)
 1021  FORMAT(' ',12X,'K2=',F7.4)
 1022  FORMAT(' ',12X,'K3=',F7.4,/,/)
 1023 FORMAT(' ','FRACTURE ZONE ENDED ON ',I3,'TH SLICE AND',
     1 ' EXTENDED',F5.1,' FT INTO THE PILLAR.')
 1024 FORMAT(' ',/,'BRITTLE/DUCTILE TRANSITION POINT:TAUF=',
     1 F8.1)
 1026 FORMAT(' ','YEILD ZONE ENDED ON ',I3,'TH SLICE AND ',
     1 'EXTENDED',F5.1,' FT INTO THE PILLAR.')
 1031 FORMAT(' ',' SLICE   (90-0)  TAUS/F   TAU     STATUS     PONE',
     1 '   PTHREE ACCUM STRESS')
 1032 FORMAT(' ',' -----   ------  ------   ---     ------     ----',
     1 '   ------ ------------')
 1035 FORMAT(' ',I3,'(',F4.1,')',2X,F5.2,2(1X,F7.1),
     1  1X,' NOT FAILED',3(1X,F7.1))
 1036 FORMAT(' ',I3,'(',F4.1,')',2X,F5.2,2(1X,F7.1),
     1  1X,'   FAILED  ',3(1X,F7.1))
 1037 FORMAT(' ',I3,'(',F4.1,')',2X,F5.2,2(1X,F7.1),
     1  1X,'  YIELDED  ',3(1X,F7.1))
 1000 FORMAT(' ','MEAN PILLAR STRESS:LHS=',F5.0)
 1040 FORMAT(' ','VIRGIN STRESS=',F6.1,8X,'EXTRACTION RATIO=',
     1 F5.3)
 1045 FORMAT(' ','LENGTH OF SPAN=',F6.1,7X,'SEMI-WIDTH OF PILLAR=',
     1 F5.1)
 1050 FORMAT(' ','SEMI-HEIGHT OF PILLAR=',F4.1,2X,'OVERBURDEN DEPTH=',
     1 I5)
 1055 FORMAT(' ','DISTANCE "X"=',I4,11X,'SEMI-ROOM WIDTH=',F5.1)
 1060 FORMAT(' ','RATIO "SH/SV"=',F5.3,9X,'NUMBER OF PILLARS',
     1 ' IN SPAN=',I2)
 1065 FORMAT(' ','COMPRESSIVE STRENGTH OF BROKEN COAL=',F4.0)
 1067 FORMAT(' ','MOHR CONSTANT "A"=',F8.2)
 1070 FORMAT(' ','MEAN STRESS CONCENTATION=',F5.3)
 1075 FORMAT(' ','ANGLE OF INTERNAL FRICTION OF BROKEN COAL=',F3.0)
 1080 FORMAT(' ','POISSONS RATIO FOR SURROUNDING ROCK=',F4.2)
 1085 FORMAT(' ','POISSONS RATIO FOR PILLAR ROCK=',F4.2)
 1090 FORMAT(' ','COEFFICIENT OF SLIDING FRICTION FOR BROKEN',
     1 ' COAL=',F4.2)
 1125 FORMAT(' ','DEPTH OF FRACTURE ZONE JUST AT FAILURE',F6.2)
 1100 FORMAT('0','THE RESULTS ARE',/)
 1105 FORMAT(' ','YOUNGS MODULAS FOR SURROUNDING ROCK=',I8)
 1110 FORMAT(' ','YOUNGS MODULAS FOR PILLAR ROCK=',I8)
 1115 FORMAT(' ','STRESS REDISTRIBUTION COEFFICIENT=',F4.2)
 1116 FORMAT(' ','TOTAL NUMBER OF SLICES= ',I4)
 1120 FORMAT(' ','SLICE INTERVAL IN PRINTOUT=',I2,/,/)
      IJ=IJ+1
      GO TO 888
  999 IJ=IJ-1
      JK=JK-1
```

University of Alberta

```
      DO 55 IJJ=1,IJ
      DO 56 IJK=1,JK
      WRITE(7,5566)PPONE(IJJ,IJK),IJJ,IJK
5566  FORMAT(' ','PONE = ',F12.2,/,'IJJ = ',I3,'IJK = ',I3)
  56  CONTINUE
  55  CONTINUE
      STOP
      END
```

University of Alberta

```
C
C                         STRENGTH SUBROUTINE
C                             CHAPTER 8
C
      SUBROUTINE STRETH(B,W,PHIB,MUB,A,PB,H,YMM,SV,SPSV,STREN,MODE,
     1   K,XBC,SHEDDO,SF)
C
C
      EXTERNAL FC1,DO1,FC2,DO2
      REAL MUB,K
C
C    BLOCK 1 - CALCULATE THE VERTICAL STRESS, DEPTH OF THE
C          TRANSITION  POINT AND MINIMUM PILLAR CAPACITY
C
      C=SIN(PHIB)
      D=TAN(PHIB)
      ANTA=A/2+A/2/(MUB**2)*(1+SQRT(1+MUB**2))
      ANTB=A*SQRT(0.5+0.5/MUB**2*(1+SQRT(1+MUB**2)))
      PONE=ANTA+ANTB
      XBC1=(1-C)/(1+C)
      XBC2=H/D
      XBC3=((1-C)/(1+C))
      XBC4=2*PONE*C/(PB*(1+C))
      XBC=XBC1*XBC2*ALOG(XBC3+XBC4)
      RBX=XBC
      STREO=2*A*SPSV/YMM
C
C    THESE ARE OTHER NECESSARY VARIABLES WHICH WILL NEEDED IN
C         THE NEWTONIAN SUBROUTINE.
              AA=PB*(1-C)/2/C
              BB=H/D
              CC=D/H*((1+C)/(1-C))
              DD=2*A*SPSV/YMM
              EE=SPSV*SV
              FF=ANTA+ANTB
              GG=XBC
              BCF=2*B
              BCFU=2*B
              TT=(BB*(EXP(CC*GG)))-BB-GG-FF*GG/AA
C
C
      IF(XBC.LE.B)GO TO 100
C
C    BLOCK 2 - CALCULATE RESIDUAL MEAN STRESS CAPACITY AND
C          CRITICAL PILLAR DIMENSIONS FOR FRACTURED PILLARS
C
      BANTA=PB*(1-C)/(2*B*C)
      BANTB=D*((1+C)/(1-C))*B/H
      RPR=BANTA*((H/D)*(EXP(BANTB)-1)-B)
      I = 0
      CALL NEWT(FC1,DO1,BCF,AA,BB,CC,DD,EE,FF,GG,TT,I)
      I = O
      CALL NEWT(FC2,DO2,BCFU,AA,BB,CC,DD,EE,FF,GG,TT,I)
      WRITE(6,1222)BCF,BCFU
 1222 FORMAT(' ','THE CRITICAL PILLAR DIMENSION TO AVOID ',
     1      /,'         A) CATASTROPHIC FRACTURE IS ',F6.2,
```

University of Alberta

```
457.000           1          /,'        B) ULTIMATE FRACTURE IS ',F6.2)
458.000   36              IF (STREO.LE.RPR)GO TO 80
459.000        C
460.000        C    BLOCK 3 - CALCULATE PILLAR STRENGTH AND SAFETY FACTOR
461.000        C
462.000   37              STREN=STREO
463.000   38              SF=STREO/(SPSV*SV)
464.000        C
465.000   39            IF (SF.LE.1) GO TO 70
466.000        C
467.000        C    BLOCK 4 - PRINT OUT RESULTS - STABLE (CATASTROPHIC FRACTURE)
468.000        C
469.000   40            WRITE(6,6000)
470.000   41    6000     FORMAT(' ','PILLAR IS STABLE.')
471.000   42            WRITE(6,6001)
472.000   43    6001     FORMAT(' ','FAILURE MODE IS CATASTROPHIC FAILURE.')
473.000   44            WRITE(6,6002) STREN, SF
474.000   45    6002     FORMAT(' ','THE PILLAR STRENGTH = ', F9.2,
475.000           1              /,'THE SAFETY FACTOR    = ',F5.2)
476.000   46            WRITE(6,7001)BCF,BCFU
477.000   47   7001     FORMAT(' ','THE CRITICAL PILLAR DIMENSION TO AVOID ',
478.000           1          /,'        A) CATASTROPHIC FRACTURE IS ',F6.2,
479.000           1          /,'        B) ULTIMATE FRACTURE IS ',F6.2)
480.000   48            GO TO 10
481.000        C
482.000        C    BLOCK 5 - PRINT OUT RESULTS - FRACTURED CATASTROPHICALLY
483.000        C
484.000   49     70     WRITE(6,6003)
485.000   50    6003     FORMAT(' ','PILLAR HAS FRACTURED CATASTROPHICALLY')
486.000   51               SHEDDO=B*(SPSV*SV-STREN)
487.000   52            WRITE(6,6004) SHEDDO
488.000   53    6004     FORMAT(' ','THE SHED LOAD = ',F9.2)
489.000   54            WRITE(6,6005) STREN,SF
490.000   55    6005     FORMAT(/,'THE PILLAR STRENGTH = ', F9.2,
491.000           1              /,'THE SAFETY FACTOR    = ',F9.2)
492.000   56            WRITE(6,7002)BCF,BCFU
493.000   57   7002     FORMAT(' ','THE CRITICAL PILLAR DIMENSION TO AVOID ',
494.000           1          /,'        A) CATASTROPHIC FRACTURE IS ',F6.2,
495.000           1          /,'        B) ULTIMATE FRACTURE IS ',F6.2)
496.000   58            GO TO 10
497.000        C
498.000        C    BLOCK 6 - CALCULATE PILLAR STRENGTH AND SAFETY FACTOR
499.000        C
500.000   59     80     STREN=RPR
501.000   60            SF=RPR/(SPSV*SV)
502.000        C
503.000   61            IF (SF.LE.1)GO TO 60
504.000        C
505.000        C    BLOCK 7 - PRINT OUT RESULTS - STABLE (ULTIMATE FRACTURE)
506.000        C
507.000   62            WRITE(6,6006)
508.000   63    6006     FORMAT(' ','PILLAR IS STABLE')
509.000   64            WRITE(6,6007)
510.000   65    6007     FORMAT(' ','FRACTURE MODE WILL BE ULTIMATE FRACTURE')
511.000   66            WRITE(6,6008) STREN, SF
512.000   67    6008     FORMAT(' ','THE PILLAR STRENGTH = ', F9.2,

                    SUBROUTINE STRETH
```

University of Alberta

```
     1           /,'THE SAFETY FACTOR    = ',F5.2)
           WRITE(6,7003)BCF,BCFU
 7003      FORMAT(' ','THE CRITICAL PILLAR DIMENSION TO AVOID ',
     1          /,'          A) CATASTROPHIC FRACTURE IS ',F6.2,
     1          /,'          B) ULTIMATE FRACTURE IS ',F6.2)
           GO TO 10
C
C     BLOCK 8 - PRINT OUT RESULTS - FRACTURED
C
   60      WRITE(6,6009)
 6009       FORMAT(' ','PILLAR HAS FRACTURED')
             SHEDDO=B*(SPSV*SV-STREN)
           WRITE(6,6010) SHEDDO
 6010       FORMAT(' ','THE SHED LOAD        = ',F9.2)
           WRITE(6,6011) STREN, SF
 6011       FORMAT(' ','THE PILLAR STRENGTH = ', F9.2,
     1           /,'THE SAFETY FACTOR    = ',F5.2)
           WRITE(6,7003)BCF,BCFU
           GO TO 10
C
C     BLOCK 9 - CALCULATE RESIDUAL MEAN STRESS CAPACITY AND
C             CRITICAL PILLAR DIMENSIONS FOR YIELDING PILLARS
C
  100      CANTA=PB*(1-C)/(2*B*C)
           CANTB=D*((1+C)/(1-C))*XBC/H
           RPRY=CANTA*((H/D)*(EXP(CANTB)-1)-XBC)+(1-XBC/B)*PONE
           BCY=(TT*AA)/(DD-FF)
           BCYU=(TT*AA)/(EE-FF)
          IF (STREO.LE.RPRY)GO TO 50
C
C     BLOCK 10 - CALCULATE PILLAR STRENGTH AND SAFETY FACTOR
C
          STREN=STREO
          SF=STREO/(SPSV*SV)
C
          IF (SF.LE.1) GO TO 40
C
C     BLOCK 11 - PRINT OUT RESULTS - STABLE (CATASTROPHIC YIELD)
C
           WRITE(6,6012)
 6012       FORMAT(' ','THE PILLAR IS STABLE')
           WRITE(6,6013)
 6013       FORMAT(' ','FAILURE MODE WILL BE CATATROPHIC YIELD')
           WRITE(6,6014) STREN,SF
 6014       FORMAT(' ','THE PILLAR STRENGTH = ', F9.2,
     1           /,'THE SAFETY FACTOR    = ',F9.2)
           WRITE(6,7004)BCY,BCYU
 7004      FORMAT(' ','THE CRITICAL PILLAR DIMENSION TO AVOID ',
     1          /,'          A) CATASTROPHIC YIELD IS ',F6.2,
     1          /,'          B) ULTIMATE YIELD IS ',F6.2)
           GO TO 10
C
C     BLOCK 12 - PRINT OUT RESULTS - CATASTROPHIC YIELD
C
   40       WRITE(6,6015)
 6015      FORMAT(' ','THE PILLAR HAS YIELDED CATASTROPHICALLY')
```

University of Alberta

```
           SHEDDO=B*(SPSV*SV-STREN)
       WRITE(6,6016) SHEDDO
 6016   FORMAT(' ','THE SHED LOAD        =',F9.2)
       WRITE(6,6017)STREN,SF
 6017   FORMAT(' ','THE PILLAR STRENGTH = ', F9.2,
     1         /,'THE SAFETY FACTOR    = ',F9.2)
       WRITE(6,7004)BCY,BCYU
       GO TO 10
C
C     BLOCK 13 - CALCULATE PILLAR STRENGTH AND SAFETY FACTOR
C
   50  STREN=RPRY
       SF=RPRY/(SPSV*SV)
C
       IF (SF.LE.1)GO TO 30
C
C     BLOCK 14- PRINT OUT RESULTS - STABLE (ULTIMATE YIELD)
C
       WRITE(6,6018)
 6018   FORMAT(' ','THE PILLAR IS STABLE')
       WRITE(6,6019)
 6019   FORMAT(' ','THE FAILURE MODE WILL BE ULTIMATE YIELD')
       WRITE(6,6020) STREN,SF
 6020   FORMAT(' ','THE PILLAR STRENGTH = ', F9.2,
     1         /,'THE SAFETY FACTOR    = ',F9.2)
       WRITE(6,7004)BCY,BCYU
       GO TO 10
C
C     BLOCK 15 - PRINT OUT RESULTS - YIELDED
C
   30  WRITE(6,6021)
 6021   FORMAT(' ','THE PILLAR HAS YIELDED')
           SHEDDO=B*(SPSV*SV-STREN)
       WRITE(6,6022) SHEDDO
 6022   FORMAT(' ','THE LOAD SHED        = ',F9.2)
       WRITE(6,6023) STREN, SF
 6023   FORMAT(' ','THE PILLAR STRENGTH = ', F9.2,
     1         /,'THE SAFETY FACTOR    = ',F9.2)
       WRITE(6,7004)BCY,BCYU
       GO TO 10
   10  RETURN
       END




       SUBROUTINE STRETH
```

University of Alberta

University of Alberta

```
C
C
C     THIS SUBROUTINE USES NEWTONS METHOD TO DETERMINE THE
C           ROOTS FOR THE CRITICAL PILLAR DIMENSIONS.
C
        SUBROUTINE NEWT(FCN,FDER,B,AA,BB,CC,DD,EE,FF,GG,TT,I)
        LOGICAL PRINT
        LOGICAL*1 FREE(1)/'*'/
        PRINT=.TRUE.
        REAL B,AA,BB,CC,DD,EE,FF,GG,TT,BERR,FERR,DER,TRIAL
        INTEGER I,J,MAX
        IF (I .NE. O) PRINT=.FALSE.
        BERR=.05
        FERR=.1
        MAX=50
        FB=FCN(B,AA,BB,CC,DD,EE,FF,GG,TT)
C
        DO 2000 J=1,MAX
        DER=FDER(B,AA,BB,CC,DD,EE,FF,GG,TT)
        TRIAL=FB/DER
        B=B-TRIAL
        FB=FCN(B,AA,BB,CC,DD,EE,FF,GG,TT)
    5   IF (ABS(TRIAL).LE.BERR) GO TO 60
        IF (ABS(FB).LE.FERR)GO TO 70
 2000   CONTINUE
C
C    THE VALUE OF B HAS NOT BEEN FOUND WITHIN THE ERROR
C                    RANGE GIVEN.
C
        I=-1
        WRITE (6,200)
  200   FORMAT (' ','THE VALUE OF "B" HAS NOT BEEN FOUND.')
        RETURN
C
C         THE B ERROR TOLERANCE HAS BEEN MET.
C
   60   I=1
        RETURN
C
C      THE FUNCTION ERROR TOLERANCE HAS BEEN MET.
C
   70   I=2
        RETURN
        END
```

```
C
C
C   THIS SUBROUTINE USES NEWTONS METHOD TO DETERMINE THE
C                 VALUE OF THE VARIABLE KTWO
C
      SUBROUTINE NEWT2(FCN,FDER,KTWO,YMM,I)
      LOGICAL PRINT
      LOGICAL*1 FREE(1)/'*'/
      PRINT=.TRUE.
      EXTERNAL FC3,DO3
      REAL KTWO,KERR,FERR,DER,TRIAL,YMM
      INTEGER I,J,MAX
      IF (I .NE. 0) PRINT=.FALSE.
      KERR=.005
      FERR=.001
      MAX=50
      FKTWO=FCN(KTWO,YMM)
C
      DO 2000 J=1,MAX
      DER=FDER(KTWO,YMM)
      TRIAL=FKTWO/DER
      KTWO=KTWO-TRIAL
      IF(KTWO.LE.-1) KTWO=-0.9999
      FKTWO=FCN(KTWO,YMM)
    5 IF (ABS(TRIAL).LE.KERR) GO TO 60
      IF (ABS(FKTWO).LE.FERR) GO TO 70
 2000 CONTINUE
C
C   THE VALUE OF KTWO HAS NOT BEEN FOUND WITHIN THE ERROR
C                      RANGE GIVEN.
C
      I=-1
      WRITE (6,200)
  200 FORMAT (' ','THE VALUE OF "KTWO" HAS NOT BEEN FOUND.')
      RETURN
C
C      THE KTWO ERROR TOLERANCE HAS BEEN MET.
C
   60 I=1
      RETURN
C
C    THE FUNCTION ERROR TOLERANCE HAS BEEN MET.
C
   70 I=2
      RETURN
      END
```

SUBROUTINE NEWT2

University of Alberta

```
C
C     THE FUNCTIONS NEEDED FOR THE NEWTON PROGRAM FOR THE
C             DETERMINATION OF THE VALUES OF BCF
C                        AND BCFU.
C
C    THE FUNCTION FOR CATASTROPHIC FRACTURE IS:
C
        FUNCTION FC1(B,AA,BB,CC,DD,EE,FF,GG,TT)
        REAL TT
        FC1=AA*BB/B*(EXP(CC*B)-1)-AA-DD
        RETURN
        END
```

University of Alberta

```
C
C     THE DERIVATIVE FOR CATASTROPHIC FRACTURE IS:
C
      FUNCTION DO1(B,AA,BB,CC,DD,EE,FF,GG,TT)
      REAL TT
      DO1=(AA*BB/B**2)*(CC*B*EXP(CC*B)-EXP(CC*B)+1)
      RETURN
      END
```

FUNCTION DO1

University of Alberta

```
C
C    THE FUNCTION FOR ULTIMATE FRACTURE IS:
C
        FUNCTION FC2(B,AA,BB,CC,DD,EE,FF,GG,TT)
        REAL TT
        FC2=AA*BB/B*(EXP(CC*B)-1)-AA-EE
        RETURN
        END
```

University of Alberta

```
C
C     THE DERIVATIVE FOR ULTIMATE FRACTURE IS:
C
      FUNCTION DO2(B,AA,BB,CC,DD,EE,FF,GG,TT)
      REAL TT
      DO2=(AA*BB/B**2)*(CC*B*EXP(CC*B)-EXP(CC*B)+1)
      RETURN
      END
```

FUNCTION DO2

University of Alberta

```
C
C   THESE FUNCTIONS ARE USED FOR THE SOLUTION OF THE
C                  VARIABLE KTWO.
C
C    THE FUNCTION FOR KTWO IS:
C
        FUNCTION FC3(KTWO,YMM)
        REAL KTWO,YMM,C1,C2,C3,FC11,FC22
        C1=(YMM-1)/9
        C2=YMM-1
        C3=YMM
        FC11=C1*(10 + 11*KTWO + KTWO**2)
        FC22=ALOG( (10+KTWO) / (1+KTWO) )
        FC3=FC11*FC22 - C2*KTWO - C3
        RETURN
        END
```

University of Alberta

```
C
C    THE DERIVATIVE OF THE KTWO FUNCTION IS:
C
      FUNCTION DO3 (KTWO,YMM)
      REAL KTWO,YMM,C1,C2,C3,DO11,DO22
      C1=(YMM-1)/9
      C2=YMM-1
      C3=YMM
      DO11=C1*(11+2*KTWO)*ALOG(1+9/(KTWO+1))
      DO22=C1*(10+11*KTWO+KTWO**2)*(-9/((KTWO+1)**2))
      DO3=DO11+DO22/(1+9/(KTWO+1))-C2
      RETURN
      END
```

University of Alberta

9.4 Variables and Constants

1. Route = input parameter which will determine which method will be used to determine the stress concentration. One of the numbers 0, 1, or 2 is typed in which represent the methods of tributary axis theory, direct input, and Coates' theory respectively.
2. SV = (S_v) virgin stress in (psi)
3. R = general extraction ratio
4. L = semi length of the mining span
5. X = x co-ordinate of the specific pillar (centre of span to centre of pillar)
6. W = semi room width
7. Z = overburden depth
8. B = semi pillar width
9. H = semi pillar height
10. MUR (μ_r) = Poisson's ratio for surrounding rock
11. MUP (μ_p) = Poisson's ratio for pillar rock
12. ER = modulus of the surrounding rock
13. EP = modulus of the pillar rock
14. LER = an input parameter which determines if the local extraction ratio is known. The numbers 0 or 1 are used for extraction ratio available or not, respectively.
15. K = ratio of horizontal to vertical virgin stress (SH/SV)
16. N = number of pillars in a span
17. ALPHA (α) = Load shedding factor
18. NNN = number of slices desired over the entire pillar
19. PB (P_B) = uniaxial compressive strength of broken coal
20. SCS = uniaxial compressive strength of solid coal
21. A = constant used to describe the shape of the Mohr envelope
22. MUB (μ_B) = coefficient of sliding friction for the broken coal
23. PHIBD (ϕ_B) = angle of internal friction for broken coal
24. SPSV ($\frac{\bar{\sigma}_p}{S_v}$) = $1 + \frac{\Delta\bar{\sigma}_p}{S_v}$ = stress concentration, input as 0 or desired value when the Route is 1
25. SHAPE = an input data to describe the shape of the opening. 0 for an elliptical opening; 1 for a rectangular opening; and 2 for an ovaloidal opening
26. PRINT = describes which form of output is desired. 'YES' or 1 for printout input and output and 'NO' or 0 for summary only wanted
27. INTVAL = the interval of slices desired in the output
28. AREA = is initially set to zero. If a transition occurs from failure to yielding or failure to stability, AREA is equated to 1 to enable the program to print out the depth of the transition after the main table is finished
29. AREB = works identically to AREA except is equated to 1 when there is a transition from yielding to stability
30. QUI = is initially set to 'N'. When the program comes to the failure yield criteria and the criterian for yield is met, then QUI is equated to 'Y'. This will enable the program to remain in the yield loop and not fluctuate between failure and yield

31. PHIB (ϕ_B) = is the angle of internal friction for broken coal in radians

32. XPR = X' = $\frac{X}{L}$

33. ZPR = Z' = $\frac{Z}{L}$

34. BPR = B' = $\frac{B}{L}$

35. HPR = H' = $\frac{H}{L}$

36. NU = $\nu = \frac{\mu_r}{1-\mu_r}$

37. NUP = $\nu = \frac{\mu_p}{1-\mu_p}$

38. NN = $\frac{E_r(1-\mu_p)}{E_p(1-\mu_r)}$

39. INTA, INTB, INTC, INKA, INKB, INTD, INTE = are all intermediate calculations leading up to the evaluation of $\frac{\Delta\bar{\sigma}_p}{S_v}$

40. RR = is the general extraction ratio if the local extraction ratio in not known

41. DSPSV = $\frac{\Delta\bar{\sigma}_p}{S_v}$ is the increase of mean pillar stress concentration due to mining the rooms

42. F = is used to calculate K'_B

43. KBPR (K'_B) = is the dimensionless number that varies with depth of the seam below surface and the length of the mining span. Used to calculate $\frac{\Delta\bar{\sigma}_p}{S_v}$ if local extraction ratio not available

44. SP ($\bar{\sigma}_p$) = is the mean pillar stress

45. INTF = is an intermediary calculation used to determine $\overline{Y}_{mm}$.

46. YMM ($\overline{Y}_{mm}$) = is the maximum stress concentration applied to the edge of the pillar

47. EVEN = is 'YES' if $\overline{Y}_{mm} < \frac{\bar{\sigma}_p}{S_v}$ to invoke a uniform stress distribution. If $\overline{Y}_{mm} > \frac{\bar{\sigma}_p}{S_v}$ then EVEN will equal 'NO'

48. KONE, KTWO, KTHREE (k_1 , k_2, k_3) are the three characteristic-constants used to evaluate vertical stress at any point in the pillar

49. LM XM Y = are intermediate calculations in the iteration of k_2

50. STREN = is the calculated strength of the pillar

51. MODE = is the mode of failure when the pillar has failed to the centre, for determination of strength
52. XBC = is the depth of the fracture zone when the pillar has failed to the centre.
53. SHEDDO = is the load shed onto other pillars by a pillar which has failed catastrophically
54. I and J = are counters from 1 to NNN
55. NNN (n) = is the number of slices being considered
56. DSONE (I) ($\Delta\sigma_{1i}$) = is the array of $\frac{n}{2}$ in dimension carrying the cummulative shed load onto an i^{th} slice
57. XE (x) = is the current depth of fracture zone at any period of time

$$x = 1 + \frac{2Bi}{nW}$$

58. SI (σ_{1i}) = is the vertical stress acting on the i^{th} slice as

$$Yi = \left[\frac{K_1}{K_2+1+(\frac{2i-1}{n})\ (\frac{B}{W})} + K_3\right]S_v$$

59. SONEI (σ_{1i}) = is the vertical stress acting on the i^{th} slice taking into account the shed stress and applied stress
60. STHS (σ_{3s}) = is the horizontal stress which is applied to the adjacent unfractured slice
61. PTHREE (P_3) = is the horizontal stress acting on one side of the element
62. PONE (P_1) = is the vertical stress acting on the element of broken coal
63. TAUF (τ_F) = is the shear resistance of the solid rock to failure on the plane at an angle of 2θ by pseudo-ductile failure
64. DEL = is an intermediate calculation equivalent to the cos 2θ
65. TWOTH = (2θ) is the angle of the plane of failure for the rock under a set of stresses σ_1 and σ_3
66. THETA (θ) = is actually the value of $90-\theta$ given in degrees and used as output

$$(90-\theta) = 90(1 - \frac{2\theta}{3.14159})$$

67. TAUS (τ_s) = is the shear resistance to failure of the solid coal on the plane an angle of 2θ failure will occur by brittle fracture if $\tau > \tau_s$
68. TAU (τ) = is the shear stress on the potential failure plane
69. SIGMA (σ) = is the normal stress acting on the potential failure plane
70. FAIL (I) = is a character variable * which shows the failure state of the i^{th} slice

    * ALPHA-NUMERIC
71. TOT = is the

$$\sum_{j=i+1}^{\frac{n}{2}} \frac{1}{(j-i)^{\alpha}}$$

where i and α are previously defined, and j is every subsequent slice after the i th onto which load is to be shed

72. NT = is a counter carrying initially the value of i+1 up to $\frac{n}{2}$
73. LI = has the value of i
74. SIMAX (σ_{imox}) = is the maximum vertical stress which can be resisted by the elemental slice
75. DIS = is the depth into pillar corresponding to i given in feet

$$DIS = \frac{2i\ B}{n}$$

76. DIST = if there is a transition between failure to yield, DIST is the depth into the pillar at which this transition takes place
77. II = is the slice at which the transition takes place
78. DUST = is the depth into pillar at which, with a transition between yield and stability, this transition occurs
79. III = is the slice at which the transition between yield and stability takes place
80. D = sin (ϕ_b)
81. C = tan (ϕ_b)
82. RBX = XBC
83. STREO = is the strength of a pillar which has failed catastrophically

   - built in functions used in the program were
     SQRT, EXP, ALOG, ARCOS, COS, SIN, TAN
     (square root, exponential, natural log, $\cos^{-1}$, cos, sin)

84. BCY (b_{cy}) = the calculated "B" value for catastrophic yield
85. BCYU (b_{cyu}) = the calculated "B" value for ultimate yield
86. BCF (b_{cF}) = the calculated "B" value for catastrophic fracture
87. BCFY (b_{cFu}) = the calculated "B" value for ultimate fracture
88. SF = the safety factor
89. RPR (σ_{pr}) = the calculated residual mean pillar stress capacity
90. BERR, FERR, KERR = tolerance for B and KTWO subroutines
91. MAX = the total number of iterations attempted in the subroutines
92. FB = FC1 or FC2 = functions used to determine the value of BCF and BCFU respectively
93. FKTWO = function used to determine the value of K_2
94. DER = DO1, DO2, or DO3 = the derivations of the functions for BCF, BCFU and K_2, respectively
95. XBC1, XBC2, XBC3, XBC4, AA, BB, CC, DD, EE, FF, BANTA, BANTB, CANTA, CANTB = intermediate calculations

9.5 User's Manual

9.5.1 Required Input

Table 9.1 gives an "Input data sheet" listing all the data required for input to run the program.

9.5.2 Program Use

* To Run Program

1. Create a testfile (anyname can be used which is not already in use)
2. Input data (using the file description given previously)

Example:

```
     #Ed Testfile
     : i
     ? 2, 1540, 1254, 315, 5, 10, 1400, 20, 5, .3, .3, 5000000, 1000000
       1, .33, 5, .5
     ? 350, 1, 1000, 500, .51, .27, 1.241, 'YES', 5
**   ? (blankline)
     : MTS
```

3. Compile the main program

```
#$RUN *fortg SCARDS=PILLAR  T=2
```

4. Run program

```
#$RUN -LOAD#  5=testfile  6=outputfile (-a)  7=plotfile (-aa)
```

5. a) Obtain output on terminal

```
#$COPY -a
```

b) Obtain page printer output

```
#$CONTROL *PRINT* format=fmtl1  PRINTON=oneside  Paper=x3
#$COPY -a *PRINT*
#$RELEASE *PRINT*
```

(Obtain print number to obtain printout from I/O room, 2nd Floor, General Services Building)

Notes:

* These steps are followed when using the MTS system at the University of Alberta. Other installations may vary these steps.

** It should be noted that if more than one set of test data is being used, enter them at this point. See end for example.

TABLE 9.1: INPUT DATA SHEET

First Line - Insert as listed, seperated by commas only

1 ROUTE;
    a. For Tributary Axis Theory (0)
    b. For Direct Input of Stress Concentration (1)
    c. For Coates' Analysis (2)
2. SV - Virgin Stress (psi) ....
3. R - General Extraction Ratio ....
4. L - Semi Length of Mining Span ....
5. X - X co-ordinate of Specific Pillar (centre of span to centre of pillar) ....
6. W - Semi Room Width ....
7. Z - Overburden Depth ....
8. B - Semi Pillar Width ....
9. H - Semi Pillar Height ....
10. MUR - Poisson's Ratio for Surrounding Rock ....
11. MUP - Poisson's Ratio for Pillar Rock ....
12. ER - Modulus of the Surrounding Rock ....
13. EP - Modulus of the Pillar Rock ....
14. LER - Route Taken; ....
    a. 0 when Local Extraction Ratio is Available
    b. 1 when not available
15. k = SH/SV ....
16. N - Number of Pillars in Span ....
17. ALPHA - Load shedding factor ....

....

Second Line - Insert as listed, Seperated by commas only

1. NNN - Number of Slices Desired over Entire Pillar
2. PB - Uniaxial Compressive Strength of Broken Coal ....
3. SCS - Uniaxial Compressive Strength of Solid Coal ....
4. A - Constant which describes shape of Mohr Envelope ....
5. MUB - Coefficient of sliding friction for the broken coal ....
6. PHIBD - Angle of Internal Friction for Broken Coal ....
7. SPSV - Stress Concentration, Input as 0 or Desired Value when Route is 1 ....
8. SHAPE; ....
    a. 0 for Elliptical Opening ....
    b. 1 for Rectangular
    c. 2 for Ovaloidal
9. PRINT; ....
    a. 'YES' if entire output wanted
    b. 'NO' if only summary wanted
10. INTVAL - Interval of Slices to be Printed Out ....

....

9.6 Examples

Table 9.2 gives 9 example sets of input data.

Table 9.3 gives the results of the first example in the full output format.

Table 9.4 gives the results of this example in the summary format.

Table 9.2 - 9 example sets of input data

```
1       2,1540,.254,315,255,10,1400,40,5,.3,.3,5000000,1000000,1,.33,5,.5
2        160,1.,1000,500,.510,27,1.241,1,'YES',5
3       2,1540,.254,315,165,10,1400,30,5,.3,.3,5000000,1000000,1,.33,5,.5
4        120,1.,1000,500,.510,27,1.241,1,'YES',5
5       2,1540,.254,315,165,20,1400,30,5,.3,.3,5000000,1000000,1,.33,5,.5
6        120,1.,1000,500,.510,27,1.241,1,'YES',5
7       2,1540,.254,315,5,20,1400,90,5,.3,.3,5000000,1000000,1,.33,5,.5
8        360,1.,1000,500,.510,27,1.241,1,'YES',5
9       2,1540,.254,315,5,10,1400,90,5,.3,.3,5000000,1000000,1,.33,5,.5
10       360,1.,1000,500,.510,27,1.241,1,'YES',5
11      2,1540,.254,315,145,10,1400,40,5,.3,.3,5000000,1000000,1,.33,5,.5
12       160,1.,1000,500,.510,27,1.241,1,'YES',5
13      2,1540,.254,315,145,20,1400,40,5,.3,.3,5000000,1000000,1,.33,5,.5
14       160,1.,1000,500,.510,27,1.241,1,'YES',5
15      2,1540,.254,315,260,20,1400,35,5,.3,.3,5000000,1000000,1,.33,5,.5
16       140,1.,1000,500,.510,27,1.241,1,'YES',5
17      2,1540,.254,315,260,10,1400,35,5,.3,.3,5000000,1000000,1,.33,5,.5
18       140,1.,1000,500,.510,27,1.241,1,'YES',5
```

Table 9.3 - Example output - 1st data set - full format

```
CALCULATION FOR RECTANGULAR OPENING


VIRGIN STRESS=1540.0          EXTRACTION RATIO=0.254
LENGTH OF SPAN= 315.0         SEMI-WIDTH OF PILLAR= 40.0
SEMI-HEIGHT OF PILLAR= 5.0  OVERBURDEN DEPTH= 1400
DISTANCE "X"= 255             SEMI-ROOM WIDTH= 10.0
RATIO "SH/SV"=0.330           NUMBER OF PILLARS IN SPAN= 5
COMPRESSIVE STRENGTH OF BROKEN COAL=  1.
MOHR CONSTANT "A"=  500.00
ANGLE OF INTERNAL FRICTION OF BROKEN COAL=27.
POISSONS RATIO FOR SURROUNDING ROCK=0.30
POISSONS RATIO FOR PILLAR ROCK=0.30
COEFFICIENT OF SLIDING FRICTION FOR BROKEN COAL=0.51
YOUNGS MODULAS FOR SURROUNDING ROCK= 5000000
YOUNGS MODULAS FOR PILLAR ROCK= 1000000
STRESS REDISTRIBUTION COEFFICIENT=0.50
TOTAL NUMBER OF SLICES=  160
SLICE INTERVAL IN PRINTOUT= 5



THE RESULTS ARE

MEAN STRESS CONCENTATION=1.269
MEAN PILLAR STRESS:LHS=1958.
MAXIMUM STRESS CONCENTRATION=     2.19
THE PILLAR HAS YIELDED
THE LOAD SHED         =  26131.35
THE PILLAR STRENGTH =    1301.37
THE SAFETY FACTOR     =      0.67
THE CRITICAL PILLAR DIMENSION TO AVOID
       A) CATASTROPHIC YIELD IS  28.61
       B) ULTIMATE YIELD IS  58.59
            K1= 0.4288
            K2=-0.6536
            K3= 0.9541


 SLICE   (BO-O)  TAUS/F   TAU      STATUS     PONE   PTHREE ACCUM STRESS
 -----   ------  ------   ---      ------     ----   ------ ------------
 1( 0.5)  30.00   433.0  1406.1    FAILED       1.1     0.1      0.0
10( 5.0)  30.01   434.7  1385.8    FAILED       5.2     1.7    850.8
15( 7.5)  30.03   436.9  1463.2    FAILED      10.9     4.0   1284.7
20(10.0)  30.07   441.3  1561.5    FAILED      22.0     8.5   1639.5
25(12.5)  30.13   449.8  1685.7    FAILED      43.9    17.3   2006.6
30(15.0)  30.23   465.7  1835.7    FAILED      87.1    34.6   2418.1
35(17.5)  30.42   494.6  2012.5    FAILED     172.2    68.8   2881.3
40(20.0)  30.74   544.5  2215.5    FAILED     339.9   136.2   3408.2
45(22.5)  31.29   626.1  2436.5    FAILED     670.4   269.1   3998.6
50(25.0)  32.21   751.9  2643.7    FAILED    1321.7   530.8   4622.0
55(27.5)  33.76   938.0  2740.5    FAILED    2605.4  1046.7   5161.0
60(30.0)  38.24  1040.5  2795.2   YIELDED    3360.2  1373.2   5454.6
65(32.5)  38.24  1040.5  3129.7   YIELDED    3360.2  1373.2   6156.4
70(35.0)  38.24  1040.5  3858.1   YIELDED    3360.2  1373.2   7666.9
75(37.5)  38.24  1040.5  5805.7   YIELDED    3360.2  1373.2  11683.6
80(40.0)  38.24  1040.5 23699.5   YIELDED    3360.2  1373.2  48499.1

BRITTLE/DUCTILE TRANSITION POINT:TAUF=  1040.5
FRACTURE ZONE ENDED ON  58TH SLICE AND EXTENDED 29.0 FT INTO THE PILLAR.
DEPTH OF FRACTURE ZONE JUST AT FAILURE 28.19
```

Table 9.4 - Example output - 1st data set - short format

```
CALCUL.:ION FOR RECTANGULAR OPENING


MEAN STRESS CONCENTATION=1.269
MEAN PILLAR STRESS:LHS=1958.
MAXIMUM STRESS CONCENTRATION=     2.19
THE PILLAR HAS YIELDED
THE LOAD SHED         =  26131.35
THE PILLAR STRENGTH =    1301.37
THE SAFETY FACTOR     =      0.67
THE CRITICAL PILLAR DIMENSION TO AVOID
       A) CATASTROPHIC YIELD IS  28.61
       B) ULTIMATE YIELD IS  58.59
            K1= 0.4288
            K2=-0.6536
            K3= 0.9541


BRITTLE/DUCTILE TRANSITION POINT:TAUF=  1040.5
FRACTURE ZONE ENDED ON  58TH SLICE AND EXTENDED 29.0 FT INTO THE PILLAR.
DEPTH OF FRACTURE ZONE JUST AT FAILURE 28.19
```

10. Short program for pillar strengths, safety factors and shed load, assuming tributary area theory with rectangular pillars and rooms

10.1 Purpose of the short program

It will already have been noted that the pillar strengths, safety factors and the shed load can be calculated directly from specific equations without having to utilize the "slice by slice" analysis technique. The "slice by slice" technique gives a complete stress distribution across a pillar and if this is required or desired then it is necessary to make use of the main program given in Section 9. However, often the main interest will be in determining the pillar strength and the safety factor only; in this case it is unneccessary to operate the main program and a "short program" has been written to derive these required outputs.

Further, in many underground coal mining situations rooms are rectangular in shape, pillars are often rectangular or square and the pillar layout is often quite uniform and extensive. For uniform pillar layouts and wide mining spans there is very little difference between the mean pillar stresses predicted by tributary area theory and by Coates' hypothesis, particularly for those pillars in the centre of the mining span. Consequently, the short program has been written, assuming rectangular rooms, rectangular (rib, square, or rectangular) pillars using tributary area theory. This short program is therefore limited by these assumptions and is only applicable to uniform, extensive pillar layouts. Nonetheless this short program is believed to be quite useful for the quick analysis of many cases that occur in practice, and will be most useful in analysing a number of practical cases considered in Phase 2 of this report.

The types of pillars, the appropriate mean stress concentration, $\overline{Y}$, and the extraction ratio R that can be used in this program are defined by Figure 44 and the equations on this figure.

The program logic for this program and the appropriate equation are given in the flow diagram shown in Figure 45 . Table 10.1 shows the input parameters required for operating this program and also lists the outputs obtained, and gives an two example analysis.

Appendix K, gives the program operating instructions, the program description and the program listing.

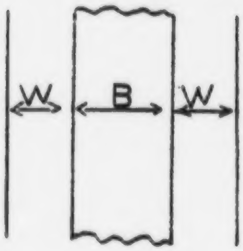

$$\bar{Y} = \frac{W+B}{B}$$

$$R = \frac{W}{W+B}$$

(A) RIB PILLARS

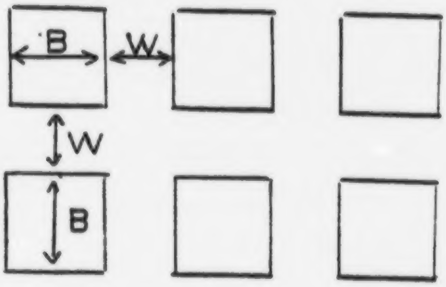

$$\bar{Y} = \frac{(W+B)^2}{B^2}$$

$$R = \frac{\omega(\omega+B)}{(\omega+b)^2}$$

(B) SQUARE PILLARS

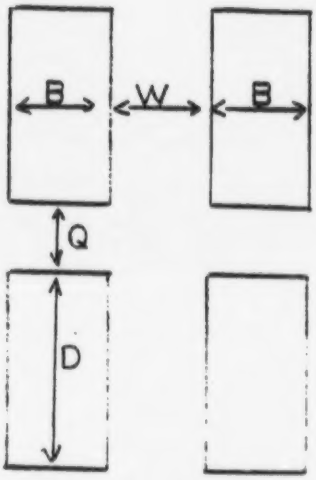

$$\bar{Y} = \frac{(W+B)(D+Q)}{BD}$$

$$R = \frac{(\omega d+\omega q+bq)}{(\omega+b)(d+q)}$$

$B = 2b$
$W = 2\omega$
$D = 2d$
$Q = 2q$

(C) RECTANGULAR PILLARS

Figure 44: Rectangular pillar types & dimensions

Figure 45:

PILLAR STRENGTHS SAFETY FACTORS FOR UNIFORM PILLAR LAYOUTS WITH RECTANGULAR ROOMS

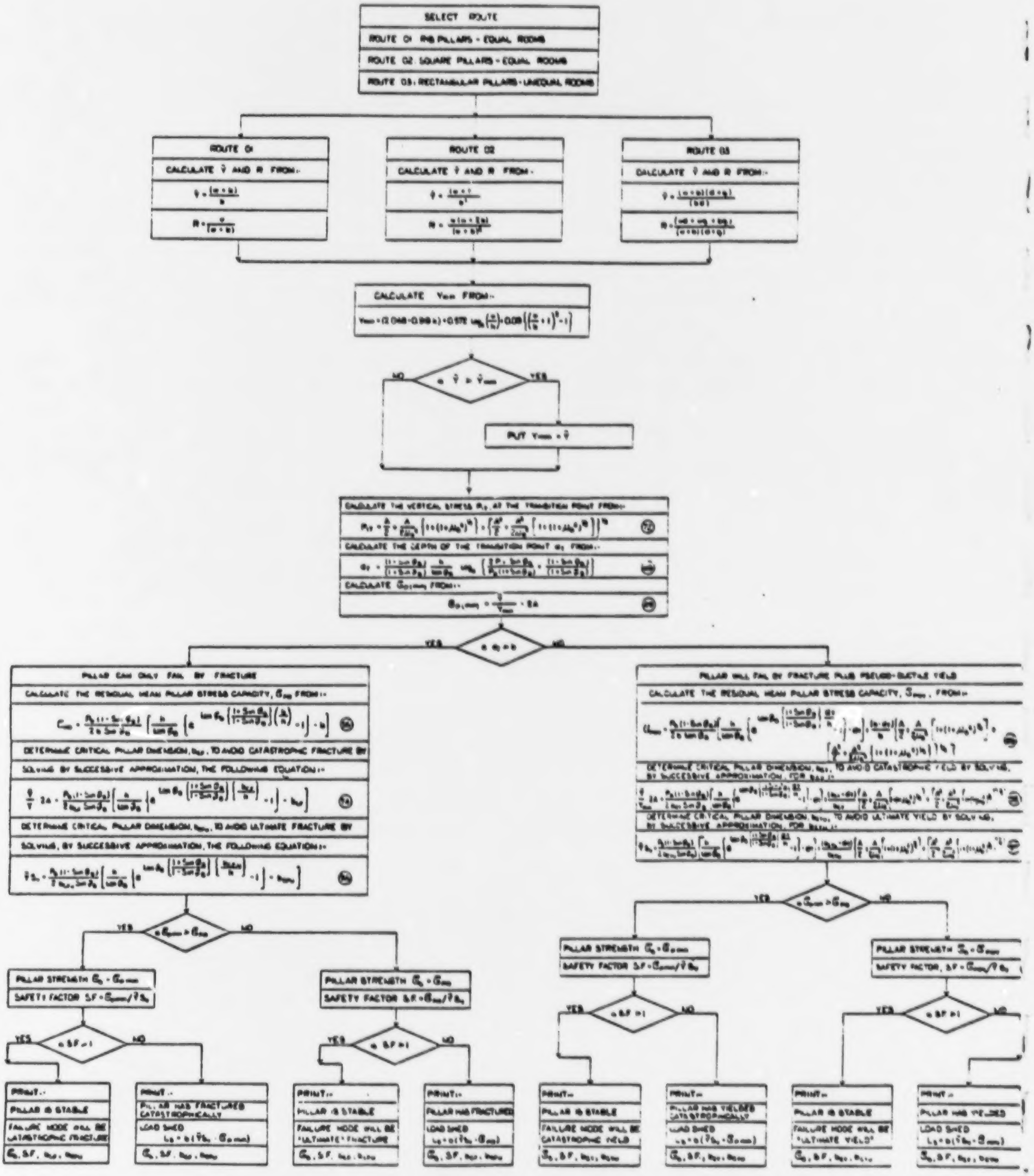
SELECT ROUTE
ROUTE 01 RIB PILLARS - EQUAL ROOMS
ROUTE 02 SQUARE PILLARS - EQUAL ROOMS
ROUTE 03: RECTANGULAR PILLARS - UNEQUAL ROOMS
ROUTE 01
CALCULATE AND R FROM:-
ROUTE 02
CALCULATE AND R FROM:-
ROUTE 03
CALCULATE AND R FROM:-
CALCULATE FROM:-
NO
YES
PUT
CALCULATE THE VERTICAL STRESS AT THE TRANSITION POINT FROM:-
CALCULATE THE DEPTH OF THE TRANSITION POINT FROM:-
CALCULATE FROM:-
YES
NO
PILLAR CAN ONLY FAIL BY FRACTURE
CALCULATE THE RESIDUAL MEAN PILLAR STRESS CAPACITY, FROM:-
DETERMINE CRITICAL PILLAR DIMENSION, TO AVOID CATASTROPHIC FRACTURE BY
SOLVING BY SUCCESSIVE APPROXIMATION, THE FOLLOWING EQUATION:-
DETERMINE CRITICAL PILLAR DIMENSION, TO AVOID ULTIMATE FRACTURE BY
SOLVING, BY SUCCESSIVE APPROXIMATION, THE FOLLOWING EQUATION:-
PILLAR WILL FAIL BY FRACTURE PLUS PSEUDO-DUCTILE YIELD
CALCULATE THE RESIDUAL MEAN PILLAR STRESS CAPACITY, FROM:-
DETERMINE CRITICAL PILLAR DIMENSION, TO AVOID CATASTROPHIC YIELD BY SOLVING, BY SUCCESSIVE APPROXIMATION, FOR
DETERMINE CRITICAL PILLAR DIMENSION, TO AVOID ULTIMATE YIELD BY SOLVING, BY SUCCESSIVE APPROXIMATION, FOR
YES
NO
PILLAR STRENGTH
SAFETY FACTOR SF
YES
NO
PRINT:-
PILLAR IS STABLE
FAILURE MODE WILL BE CATASTROPHIC FRACTURE
PILLAR HAS FRACTURED CATASTROPHICALLY
LOAD SHED
FAILURE MODE WILL BE "ULTIMATE" FRACTURE
PILLAR HAS FRACTURED
FAILURE MODE WILL BE CATASTROPHIC YIELD
PILLAR HAS YIELDED CATASTROPHICALLY
FAILURE MODE WILL BE "ULTIMATE YIELD"
PILLAR HAS YIELDED

```
RIB PILLAR CALCULATION-EQUAL ROOMS

SEMI-ROOM WIDTH   =  10.00
SEMI-PILLAR WIDTH =  25.00
VIRGIN STRESS RATIO =     0.33
SEMI-PILLAR HEIGHT  =     2.50
MOHR ENVELOPE CONSTANT =     500.00
COEFFICIENT OF SLIDING FRICTION FOR COAL =  0.5770
ANGLE OF INTERNAL FRICTION FOR BROKEN COAL =    30.00
APPLIED VIRGIN VERTICAL STRESS =    1000.00
UNIAXIAL COMPRESSIVE STRENGTH OF BROKEN COAL =       1.00

THE RESULTS ARE:

MEAN PILLAR STRESS CONCENTRATION =   1.40
MAXIMUM PILLAR STRESS CONCENTRATION =   2.62
EXTRACTION RATIO =  0.2857
THE PILLAR IS STABLE.
THE FAILURE MODE WILL BE ULTIMATE YIELD.
THE PILLAR STRENGTH =    1763.10
THE SAFETY FACTOR   =          1.26
THE CRITICAL PILLAR DIMENSION TO AVOID:
       A) CATASTROPHIC YIELD IS  11.64
       B) ULTIMATE YIELD IS INFINITY.
DEPTH OF TRANSITION POINT =  10.89
```

```
RIB PILLAR CALCULATION-EQUAL ROOMS

SEMI-ROOM WIDTH   =  10.00
SEMI-PILLAR WIDTH =  30.00
VIRGIN STRESS RATIO =     0.33
SEMI-PILLAR HEIGHT  =     2.50
MOHR ENVELOPE CONSTANT =     500.00
COEFFICIENT OF SLIDING FRICTION FOR COAL =  0.5770
ANGLE OF INTERNAL FRICTION FOR BROKEN COAL =    30.00
APPLIED VIRGIN VERTICAL STRESS =    1000.00
UNIAXIAL COMPRESSIVE STRENGTH OF BROKEN COAL =       1.00

THE RESULTS ARE:

MEAN PILLAR STRESS CONCENTRATION =   1.33
MAXIMUM PILLAR STRESS CONCENTRATION =   2.61
EXTRACTION RATIO =  0.2500
THE PILLAR IS STABLE.
THE FAILURE MODE WILL BE ULTIMATE YIELD.
THE PILLAR STRENGTH =    1941.63
THE SAFETY FACTOR   =          1.46
THE CRITICAL PILLAR DIMENSION TO AVOID:
       A) CATASTROPHIC YIELD IS  11.53
       B) ULTIMATE YIELD IS INFINITY.
DEPTH OF TRANSITION POINT =  10.89
```

Table 10.1: Example outputs - short program

11. References

1. Wilson, A. H. - "Research into the Determination of Pillar Size. Part 1: An hypothesis concerning pillar stability". The Mining Engineer, pp.409-417, Vol.131, June 1972

2. Coates, D. F. - "Pillar loading - Part 1: Literature survey and new hypothesis". Dept. E.M.R., Ottawa, Mines Branch Research Report R168, October 1965

3. Coates, D. F. - "Pillar loading - Part 2: Model Studies". Dept. E.M.R, Ottawa, Mines Branch Research Report R170, November 1965

4. Coates, D. F. - "Pillar loading - Part 3: Field Measurements". Dept. E.M.R., Ottawa, Mines Branch Research Report R180, February 1966

5. Duvall, W. I. - "Stress analysis applied to underground mining problems"- Part 1: Stress analysis applied to single openings. U.S. Bureau of Mines, R.I. 4192 March 1948

   Part 2: Stress analysis applied to multiple openings and pillars. U.S. Bureau of Mines, R.I. 4387 November 1948

6. Savin, G. N. - "Stress concentration around holes". Pergammon Press Ltd., London 1961

7. Greenspan, M. - "Effect of a small hole on the stresses in a uniformly loaded plate". Quarterly Appl. Math, Vol. 2, pp. 60-71. 1944

8. Obert L. and Duvall W. I. - "Rock Mechanics and the design of rock structures"., John Wiley and Sons Inc., New York, 1967

9. Hiramatsu Y. and Oka Y. - "Stress on the wall surface of levels with cross sections of various shapes"., Int. J. Rock Mechanics Mining Science Vol. 1, pp. 199-216, 1964

10. Barron K. - "Fracture of brittle rock around mine excavations"., Ph. D thesis, University of London, 1969

11. Logie C. V. - "Photoelastic study into ground stress in bord and pillar coal mining"., Council for Scientific and Industrial Research, Pretira, S. Africa, CSIR Report MEG 439, April 1966

12. Yu, Y.S. and Toews, N. A. - "Three dimensional stress distribution in a pillar for a typical room and pillar system of mining "., CANMET, Dept. of Energy Mines and Resources, Mining Research Laboratories, Report MRP/MRL 79/102 (TR), Dec. 1979

13. Walker, Lister - "The theory of strata control"., Mine and Quarry Engineering, pp. 291-296, July 1955

14. Orawin, E. - "Mechanism of Seismic Faulting"., Rock Deformation, Geological Science Am. Mem. 79, pp. 323-345, 1960

15. Maurer, W. C. - "Shear failure of rock under compression"., Soc. Petrol. Engres Journal 5, pp. 167-175, 1965

16. Byerlee, J. D. - "Fractional characteristics of granite under high confining pressure"., J. Geophysical Research, 14, pp. 3634-3648, July 1967

17. Hobbs, D.W. - "The strength and the stress - strain characteristics of coal in triaxial compression" J. Geol. V.72, pp. 214-231, 1964

12. Acknowledgements

The author gratefully acknowledges the funding received for this project from the Canada Centre for Mineral and Energy Technology, Dept. Energy, Mines and Resources, Canada via the Department of Supply and Services. Mr. Gilles Mongeau was Science Procurement Manager for D.S.S. on this contract and Dr. D.F.G. Hedley acted as Scientific Authority on behalf on CANMET. Dr. Hedley's constructive comments during the progress of this work were much appreciated.

Many of the ideas and concepts developed in this study resulted originally from discussion between the author and Dr. Declan B. Livesey (formerly with CANMET now with Texaco Ltd.). The author gratefully acknowledges the contributions made by Dr. Livesey to the basic thinking behind this study.

The computer programs given in this study were developed by Mr. Gary Boehm, Mining student, University of Alberta and by Mr. Stephen Thornton, Engineer, Coal Mining Research Centre; to them goes the credit for much patience and perseverance.

Finally the author would like to thank the several typists who transcribed the text and struggled with the equations; in particular thanks to Miss Christine Rousseau of C.M.R.C. who shouldered the bulk of this load.

Appendix A

Nomenclature for Coates' Pillar Stress Hypothesis

S_v is the virgin pre-mining stress perpendicular to the seam

S_H is the virgin pre-mining stress parallel to the seam

$k = \frac{S_H}{S_v}$

R is the general extraction ratio (= ratio of roof area extracted to the total roof area)

$H = 2h$ is the height of the room

$L = 2\ell$ is the total mining span

$W = 2w$ is the room width

$B = 2b$ is the pillar width

x is the X coordinate of the specific pillar (measured from the centre of the mining span)

Z is the depth below surface

$x' = \frac{x}{\ell}$ the dimensionless x coordinate of the pillar

$w' = \frac{w}{\ell}$ the dimensionless room width

$Z' = \frac{Z}{\ell}$ the dimensionless depth below the seam

$b' = \frac{b}{\ell}$ the dimensionless pillar width

$h' = \frac{h}{\ell}$ the dimensionless pillar height

$\overline{\Delta\sigma_p}$ is the increase of mean pillar stress due to mining the rooms

$1 + \frac{\Delta\sigma_p}{S_v}$ = mean pillar stress concentration

$\nu = \frac{\mu_r}{(1-\mu_r)}$ where μ_r is the Poisson's ratio of the surrounding rocks

$\nu_p = \frac{\mu_p}{(1-\mu_p)}$ where μ_p is the Poisson's ratio of the pillar rock

$n = \frac{M}{M_p}$ where $M = \frac{E_r}{(1-\mu_r^2)}$ and E_r is the modulus of the surrounding rock

and $M_p = \frac{E_p}{(1-\mu_p^2)}$ and E_p is the modulus of the pillar rock.

r is the local extraction ratio based on the area tributary to the pillar in question.

where $(1-r) = \frac{1}{(1+w/b)}$

K_b' is a dimensionless parameter that varies with the ratio of the depth of the seam below the surface to the span of the mining zone.

For horizontal workings K_b' is given by:-

$$K_b' = \left\{\frac{1-x'^2}{2Z'^3}\right\} + \left\{\frac{1.2(1+\nu)(1-x'^2)}{Z'}\right\} + \left\{13 - \left[2\nu \frac{12(1-x'^2)}{Z'^2} + 1 - \frac{8}{Z'^2} - 3\nu\right]\right\}\frac{Z'}{32}$$

$$+ \frac{0.884\ F(1-x'^2)}{Z'^2}$$

where $F = 1 - \left\{\frac{1}{\frac{2.26}{Z'} + 1}\right\}$

N is the number of pillars (across the span).

Appendix B: Example of the Use of Coates' Pillar Formulae

Figure B1 shows a plan of a portion of an undergound coal mine in a flat lying seam in Western Canada. The total overburden is 1400 ft. The vertical stress S_V is assumed to be 1.1 x 1400 = 1540 psi. It is also assumed that the stress ratio $k = \frac{S_H}{S_V} = 0.33$; $\mu_r = \mu_p = 0.3$; $E_r = 5 \times 10^6$ psi and $E_p = 1 \times 10^6$ psi.

The mean stress concentration on pillars A, B and each of the five pillars in the CC cross section will be determined. The cross section, AA, BB and CC marked on Figure B1 are shown on Figure B2. Coates' Equation 7 was used in each of these determinations.

Table B1 lists the parameters used in this calculation and gives the mean pillar stress concentrations and the mean pillar stresses determined using the equation.

Figure B3 shows a comparision of the pillar stress concentrations determined using Coates' formulae, for the pillars on the CC cross section, with tributary area theory. This illustrates clearly the differences between the two theories and how Coates' formulae takes into account the position of the pillar in the mining span.

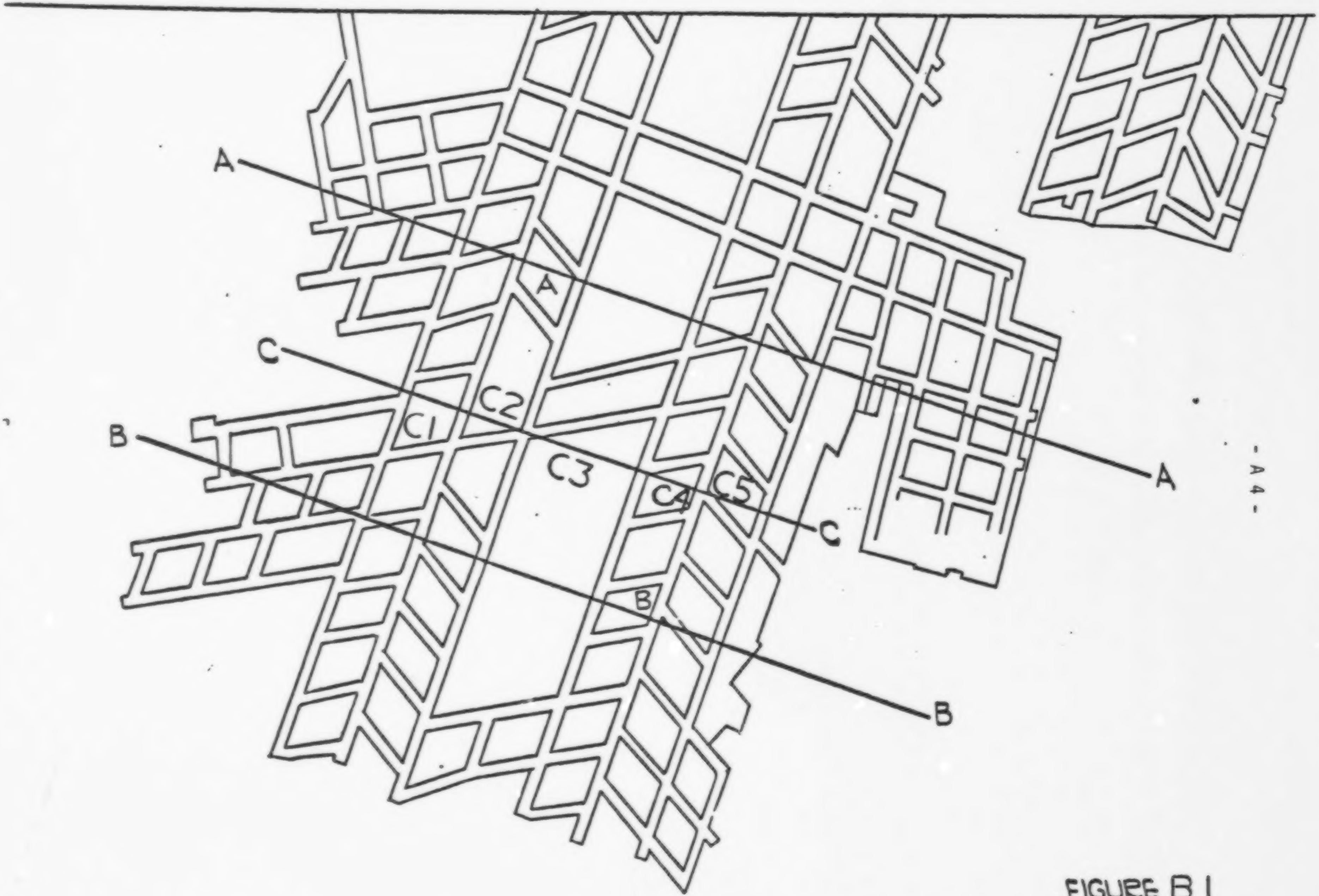
A
A
C
C2
C1
B
C3
C4
C5
C
A
B
B

FIGURE B1

Plan of a Coal Mine in Western Canada

Figure B2: Cross Sections through Test Pillars A, B and C

SECTION A-A: At Time of Tests - Prior to Pillar Splitting and Extraction

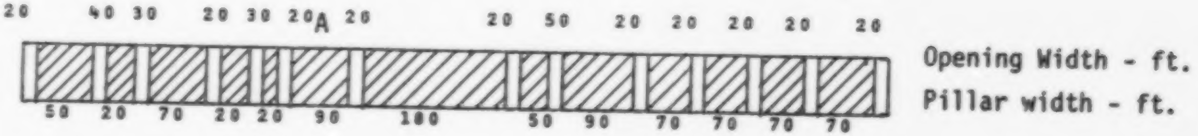
20 40 30 20 30 20 A 20 20 50 20 20 20 20 20
Opening Width - ft.
Pillar width - ft.
50 20 70 20 20 90 180 50 90 70 70 70 70

L = 1120 ft. Z = 1400 ft. $\frac{Z}{\ell} = 2.29$ $R = \frac{350}{1220} = 0.287$ ℓ = 610 ft. B = 26 = 90 ft. x = 225 ft. N = 13
h = 5 ft.

SECTION B-B: At Time of Tests - Prior to Pillar Splitting and Extraction

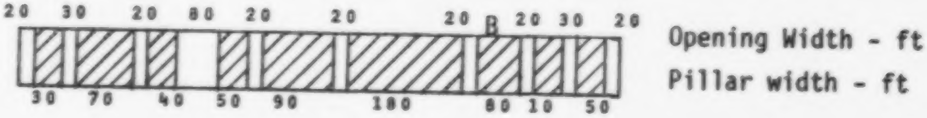
20 30 20 80 20 20 20 B 20 30 20
Opening Width - ft
Pillar width - ft
30 70 40 50 90 180 80 10 50

L = 880 ft. Z = 1400 ft. $\frac{Z}{\ell} = 3.18$ $R = \frac{280}{880} = 0.318$ ℓ = 440 ft. B = 26 = 80 ft. x = 270 ft. N = 9
h = 5 ft.

SECTION C-C: At Time of Tests - Prior to Pillar Splitting and Extraction

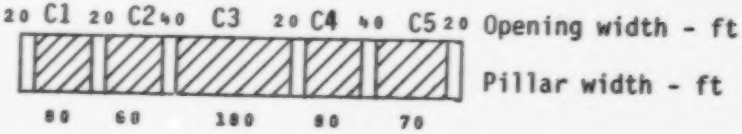
20 C1 20 C2 40 C3 20 C4 40 C5 20
Opening width - ft
Pillar width - ft
80 60 180 80 70

L = 630 ft. Z = 1400 ft. $\frac{Z}{\ell} = 4.44$ $R = \frac{160}{630} = 0.254$ ℓ = 315 ft. B = 26=80 ft. x = 145 ft. N = 5
h = 5 ft.

NOTE: Height of section not drawn to scale.

Table B1: Parameters and Results for Example Use of Coates' Pillar Formulae

PARAMETER	PILLAR						
	A	B	C1	C2	C3	C4	C5
R	0.287	0.318	0.254	0.254	0.254	0.254	0.254
x - ft	225	270	255	165	5	145	260
h - ft	5	5	5	5	5	5	5
ℓ - ft	610	440	315	315	315	315	315
b - ft	45	40	40	30	90	40	35
k	.33	.33	.33	.33	.33	.33	.33
μ_r	.3	.3	.3	.3	.3	.3	.3
μ_p	.3	.3	.3	.3	.3	.3	.3
E_r-psi	$5\text{x}10^6$	$5\text{x}10^6$	$5\text{x}10^6$	$5\text{x}10^6$	$5\text{x}10^6$	$5\text{x}10^6$	$5\text{x}10^6$
E_p-psi	$1\text{x}10^6$	$1\text{x}10^6$	$1\text{x}10^6$	$1\text{x}10^6$	$1\text{x}10^6$	$1\text{x}10^6$	$1\text{x}10^6$
N	13	9	5	5	5	5	5
$\frac{\overline{\sigma_p}}{S_v}$	1.367	1.383	1.242	1.260	1.287	1.263	1.241
$\overline{\sigma_p}$-psi*	2104	2130	1913	1940	1982	1945	1912

* assuming S_v = 1.1 x Z = 1.1 x 1400 = 1540 psi where Z = overburden depth - ft.

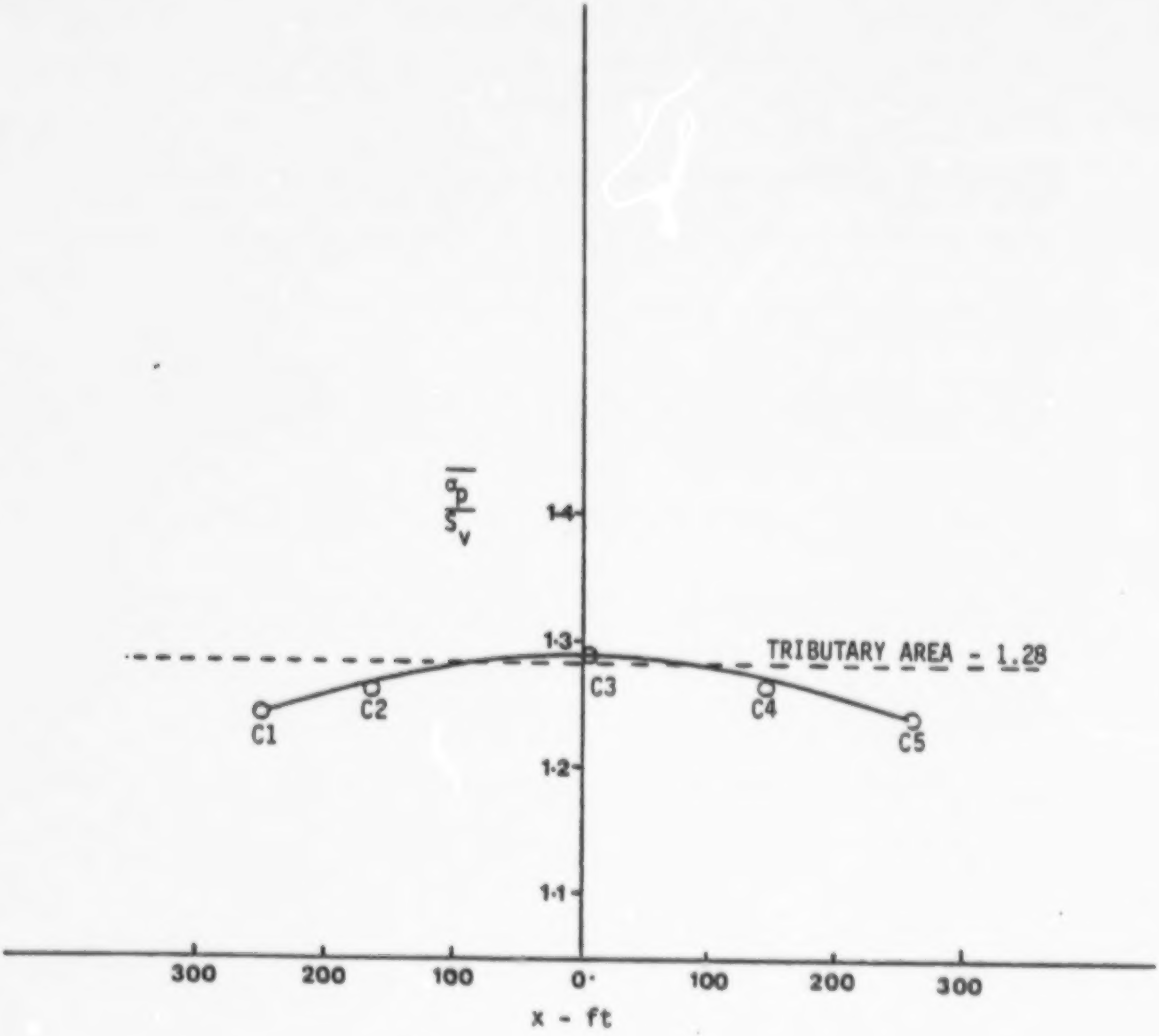

Figure B3: Comparison of Tributary Area Theory with Coates' Hypothesis for Pillars on Section C-C

Appendix C

Approximate analytical expressions for the maximum stress concentration, at the mid height of the side wall on the horizontal axis, for a single opening of various shapes, under a range of stress conditions.

(a) For a single elliptical opening. For this case an exact theoretical solution exists (5) and is given by:

$$\frac{\sigma_{p\,max}}{S_V} = Y_m = (1-k) + 2\left(\frac{w}{h}\right) \qquad (11a)$$

where $k = \frac{S_H}{S_V}$ and $\frac{w}{h}$ is the width/height ratio of the opening.

(b) For rectangular openings. Stress concentration on the boundaries of single rectangular openings have been determined analytically by Savin (6) and Greenspan (7) and photoelastically by Duvall (5), Obert and Duvall (8) and Hiramatsu and Oka (9). Table C1 lists the stress concentrations at the mid height of the side wall obtained from these sources for stress ratios of k ranging from 0 to 1 and a range of width/height ratios.

Figure C1 shows this data plotted against (w/h) for $k = 0$, $k = 1/3$ and $k = 1$. A correlation of the form $Y_m = a' + b' \log_e(\frac{w}{h})$ has been assumed for each curve and the parameters a' and b' determined. Figure C2 shows that the parameter b' is a constant for all values of k, and the parameter a' is related linearly to k by $a' = (2.048-.919k)$.

Hence the following equation gives a general approximation to all the data:-

$$Y_m = (2.048-0.919k) + 0.572 \log_e\left(\frac{w}{h}\right) \qquad (11b)$$

Table C1 also lists the stress concentrations determined using the approximate formula and gives the percentage difference from the real data. In some instances the differences are quite high; this is as much a reflection of the wide variation between the experimental and the analytical results (which are sensitive to the degree of rounding the corners of the rectangle) as it is of the accuracy of the approximation.

Nonetheless it is thought that this equation gives a reasonable approximation of the stress concentration at the mid height on the boundary of a rectangular opening, within the range k from 0 to 1, and $0.25 < w/h < 4$.

TABLE C.1: Stress Concentrations, Y_m at the Mid Height of the Boundary of Rectangular Holes

Applied Stress Ratio k	Ratio $(\frac{w}{h})$	Stress Concentration Y_m	Source Reference Number	Calculated from Equation C2	% Difference
0	1.0	1.616	6	2.05	-21.2
1/3	1.0	1.328	6	1.741	-23.7
1	1.0	0.745	6	1.129	-34.0
0	0.67	1.342	6	1.818	-26.1
1/3	0.67	1.018	6	1.513	-32.7
1	0.67	0.362	6	0.900	-59.7
0	1.5	2.152	6	2.280	-5.6
1/3	1.5	1.898	6	1.974	-3.8
1	1.5	1.382	6	1.361	+1.5
0	0.2	1.192	6	1.127	+5.7
1/3	0.2	0.882	6	0.82	+7.6
1	0.2	0.252	6	.208	+21.1
0	5.0	2.42	6	2.968	-18.4
1/3	5.0	2.166	6	2.662	-18.6
1	5.0	1.652	6	2.049	-19.3
0	1.0	1.644	7	2.05	-19.8
1/3	1.0	1.371	7	1.741	-21.2
1	1.0	0.817	7	1.129	-27.6
0	3.0	3.60	9	2.676	+34.5
1/3	3.0	3.30	9	2.370	+39.2
1	3.0	2.60	9	1.757	+47.9
0	2.0	2.80	9	2.444	+14.5
1/3	2.0	2.40	9	2.138	+12.2
1	2.0	1.80	9	1.525	+18.0
0	1.0	2.10	9	2.05	+2.4
1/3	1.0	1.80	9	1.741	+3.3
1	1.0	1.10	9	1.129	+2.6
0	0.5	1.7	9	1.651	+2.9
1/3	0.5	1.3	9	1.345	-3.3
1	0.5	0.7	9	0.732	-4.4
0	0.33	1.6	9	1.414	+13.1
1/3	0.33	1.3	9	1.107	+17.4
1	0.33	0.6	9	0.495	+21.2
0	3.92	3.56	5	2.829	+25.8
0	4.0	2.98	5	2.841	+4.8
0	4.0	2.79	5	2.841	+1.8
0	2.0	2.55	5	2.444	+4.3
0	2.0	2.11	5	2.444	-13.7
0	1.0	1.70	5	2.05	-17.1
0	1.0	1.99	5	2.05	-2.9
0	1.0	1.73	5	2.05	-15.6
0	1.0	1.93	5	2.05	-5.8
0	1.0	2.01	5	2.05	-1.9
0	0.5	1.76	5	1.651	+6.6
0	0.25	1.61	5	1.255	+28.3
0	0.25	1.47	8	1.255	+17.1
1/3	0.25	1.26	8	0.948	+32.9
1	0.25	0.65	8	0.336	+93.4
0	0.50	1.74	8	1.651	+5.3
1/3	0.50	1.53	8	1.345	+13.7
1	0.50	1.0	8	0.732	+36.6
0	1.0	1.95	8	2.05	-4.8
1/3	1.0	1.63	8	1.741	-6.3
1	1.0	0.97	8	1.129	-14.1
0	2.0	2.44	8	2.444	-0.1
1/3	2.0	1.95	8	2.138	-8.7
1	2.0	1.46	8	1.525	-4.3
0	4.0	3.0	8	2.841	+5.6
1/3	4.0	2.67	8	2.534	+5.4
1	4.0	2.0	8	1.922	+4.1

Mean |%| = 16.4%

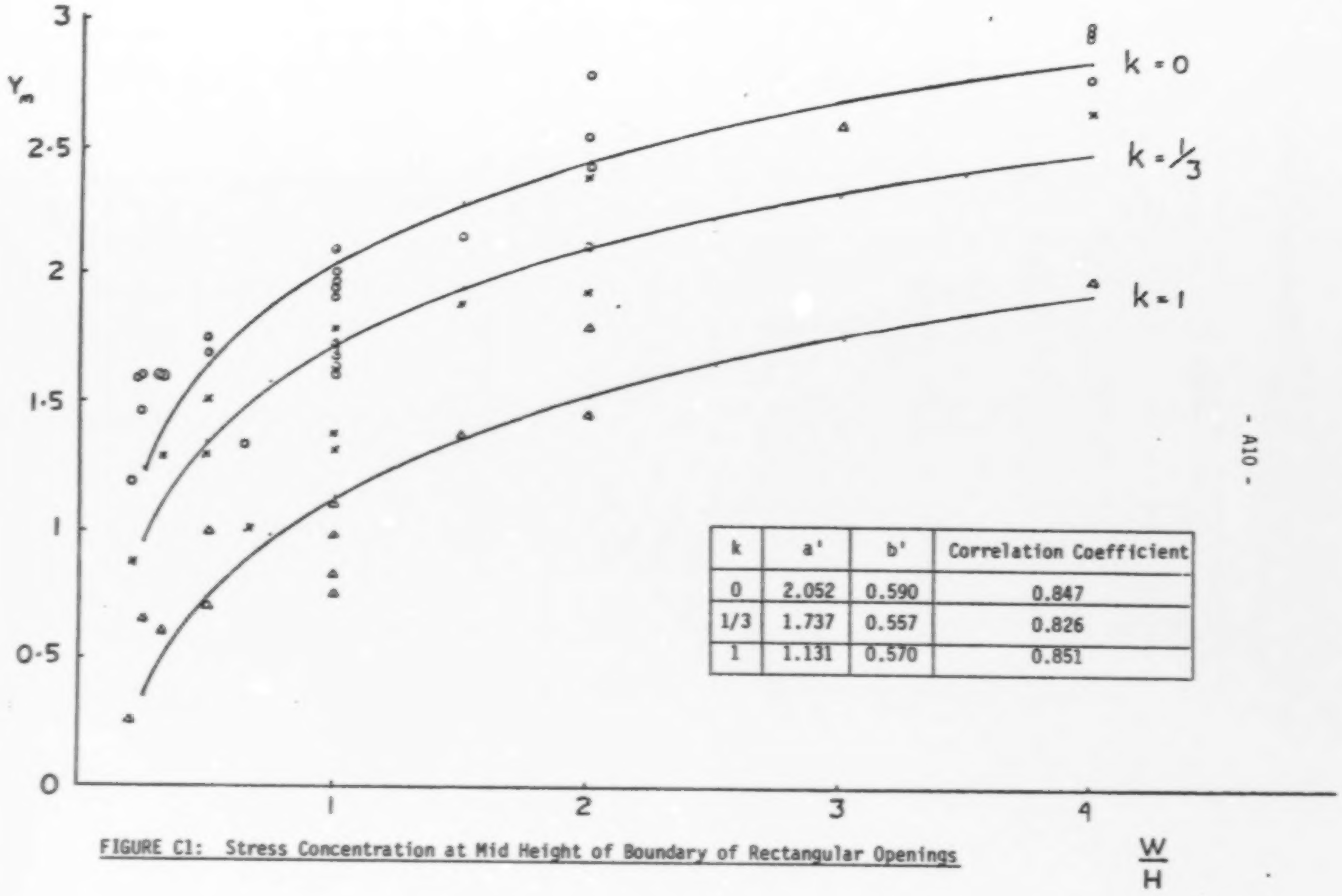

k	a'	b'	Correlation Coefficient
0	2.052	0.590	0.847
1/3	1.737	0.557	0.826
1	1.131	0.570	0.851

FIGURE C1: Stress Concentration at Mid Height of Boundary of Rectangular Openings

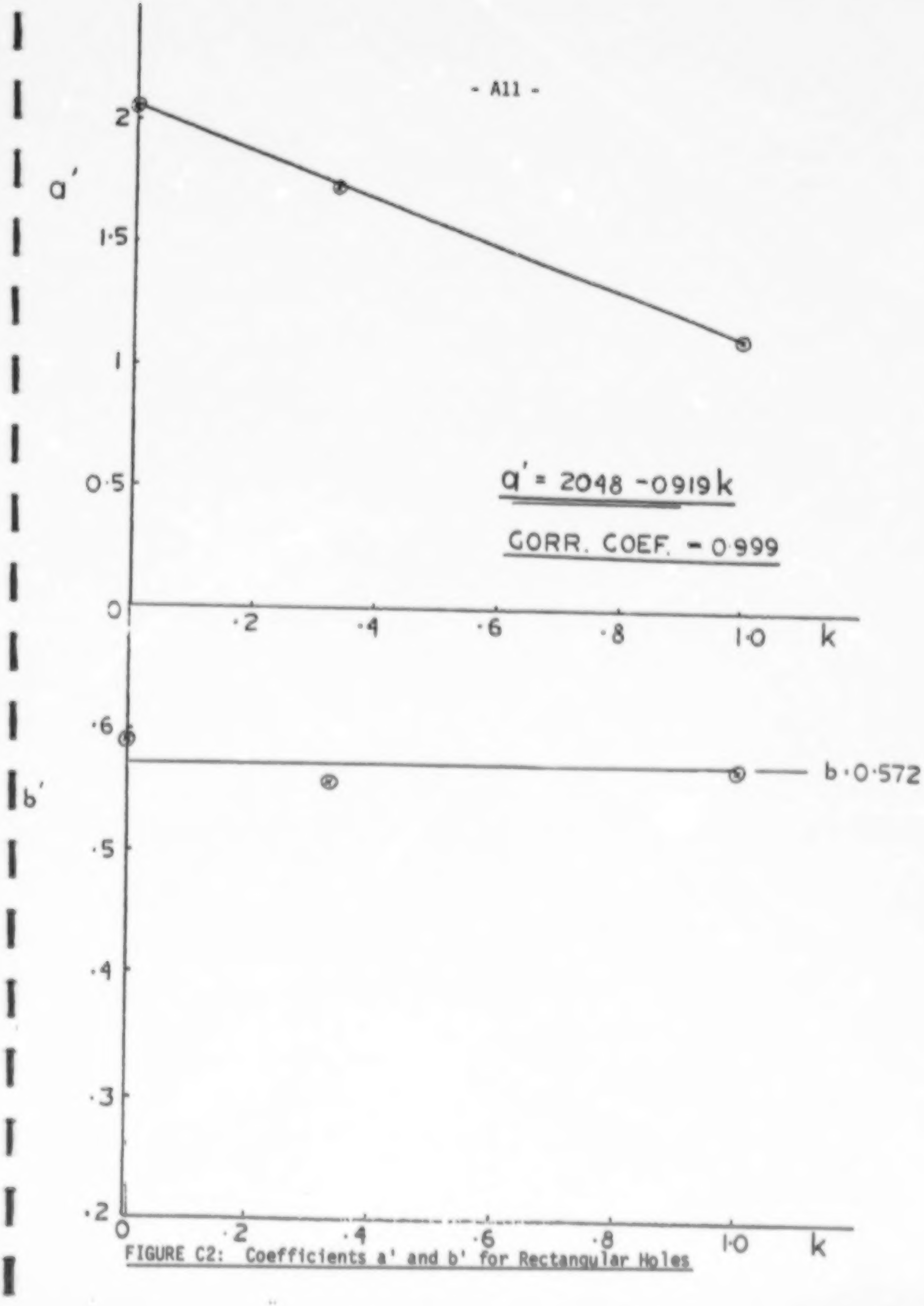

FIGURE C2: Coefficients a' and b' for Rectangular Holes

(c) For ovaloidal openings. Table C2 lists the stress concentrations obtained from the same data sources for ovaloidal openings. Figure C3 shows the data plotted against (w/h) for $k = 0$, $k = 1/3$ and $k = 1$. Once again a correlation of the form $Y_m = a' + b' \log_e (w/h)$ has been assumed for each curve and the parameters a' and b' determined. Figure C4 shows that the parameter b' is a constant for all values of k and the parameter a' is related to k by $a' = (2.97-1.044k)$. Hence the following equation gives a general approximation to all the data:-

$$\underline{Y_m = (2.97-1.044k) + 1.327 \log_e\left(\frac{w}{h}\right)} \qquad (11c)$$

Table C2 also lists the stress concentrations determined using the approximate formula and gives the percentage difference from the real data. The differences in this case are smaller than for the rectangular openings and it is believed that this equation gives a most acceptable approximation to the stress concentration at the mid height of the boundary of the opening, within the range k from 0 to 1, and $0.25 < \frac{w}{h} < 4.0$.

TABLE C2: Stress Concentrations, Y_m, at the Mid Height of the Boundary of Ovaloidal Holes

Applied Stress Ratio k	Ratio $(\frac{w}{h})$	Stress Concentration Y_m	Source Reference Number	Calculated from Equation C3	% Difference
0	1.0	3.0	7	2.97	+1.0
1/3	1.0	2.67	7	2.62	+1.9
1	1.0	2.0	7	1.97	+1.5
0	2.0	3.395	7	3.889	-12.7
1/3	2.0	3.095	7	3.542	-12.6
1	2.0	2.487	7	2.889	-13.9
0	4.0	4.80	7	4.809	-0.2
1/3	4.0	4.50	7	4.462	+0.8
1	4.0	3.89	7	3.809	+2.1
0	3.876	5.35	5	4.768	+12.2
0	2.932	4.75	5	4.397	+8.0
0	1.965	4.14	5	3.866	+7.1
0	1.953	4.02	5	3.858	+4.2
0	1.0	3.17	5	2.97	+6.7
0	1.0	3.05	5	2.97	+2.7
0	0.505	1.90	5	2.063	-7.9
0	0.338	1.72	5	1.531	+12.3
0	0.254	1.65	5	1.151	+43.3
0	0.254	1.65	5	1.151	+43.3
1.0	1.0	2.10	5	1.97	+6.5
1.0	1.0	1.98	5	1.97	+0.5
1.0	1.96	2.95	5	2.863	+3.0
1.0	2.94	3.68	5	3.401	+8.2
1.0	3.89	4.28	5	3.772	+13.4
0	0.25	1.18	8	1.130	+4.4
0	0.50	1.58	8	2.050	-22.9
0	1.0	3.0	8	2.97	-1.0
0	2.0	3.6	8	3.889	-7.4
0	4.0	4.8	8	4.809	-0.2
1/3	0.25	0.91	8	0.782	+16.4
1/3	0.50	1.26	8	1.703	-26.0
1/3	1.0	2.67	8	2.622	+1.8
1/3	2.0	3.10	8	3.542	-12.5
1/3	4.0	4.46	8	4.462	0
1	0.25	0.36	8	0.130	+176.9
1	0.50	0.71	8	1.050	-32.0
1	1.0	2.0	8	1.97	+1.5
1	2.0	2.48	8	2.889	-14.1
1	4.0	3.84	8	3.809	+0.8

Mean |%| = 13.9%

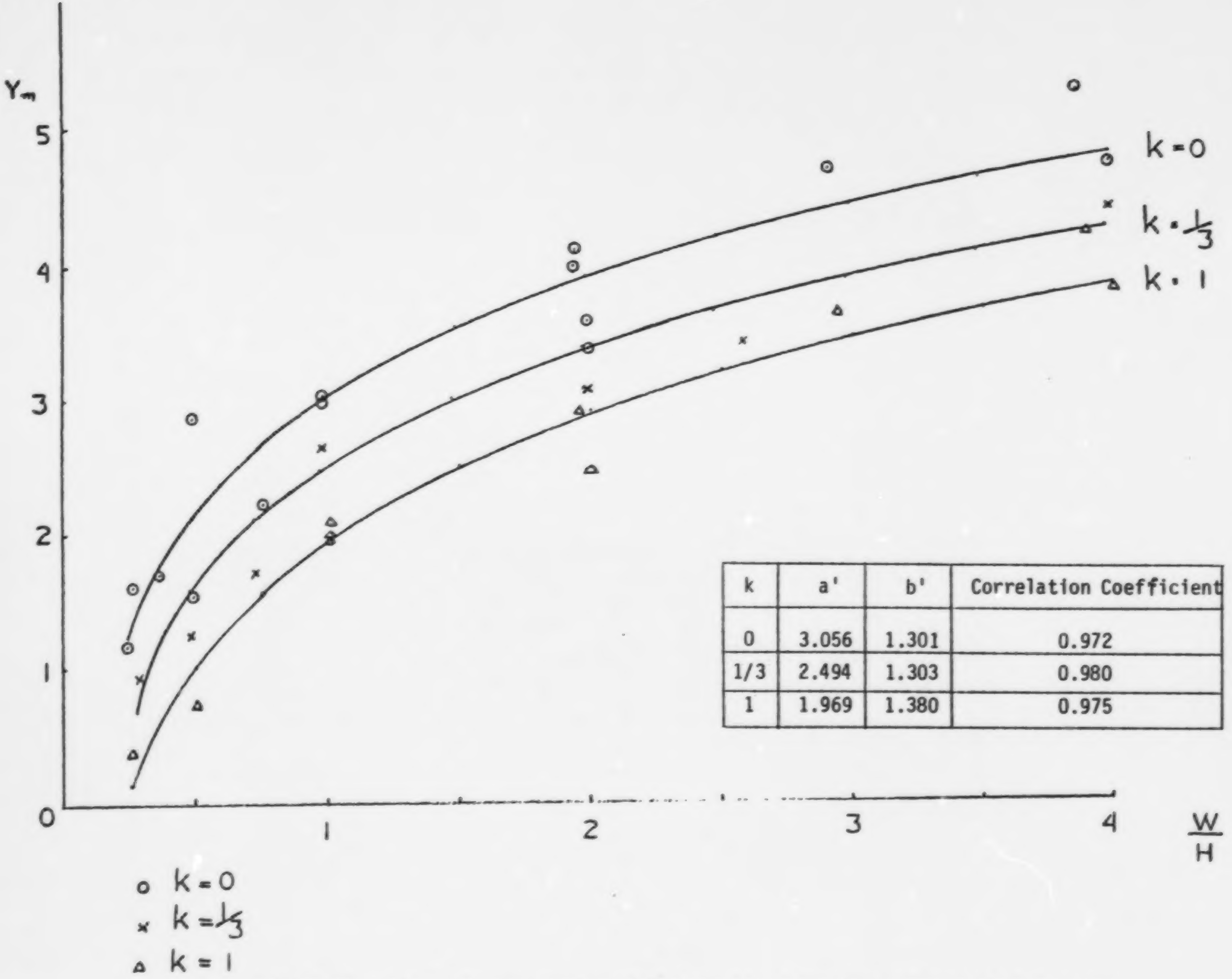

k	a'	b'	Correlation Coefficient
0	3.056	1.301	0.972
1/3	2.494	1.303	0.980
1	1.969	1.380	0.975

FIGURE C3: Stress Concentration at Mid Height of Boundary of Ovaloidal Openings

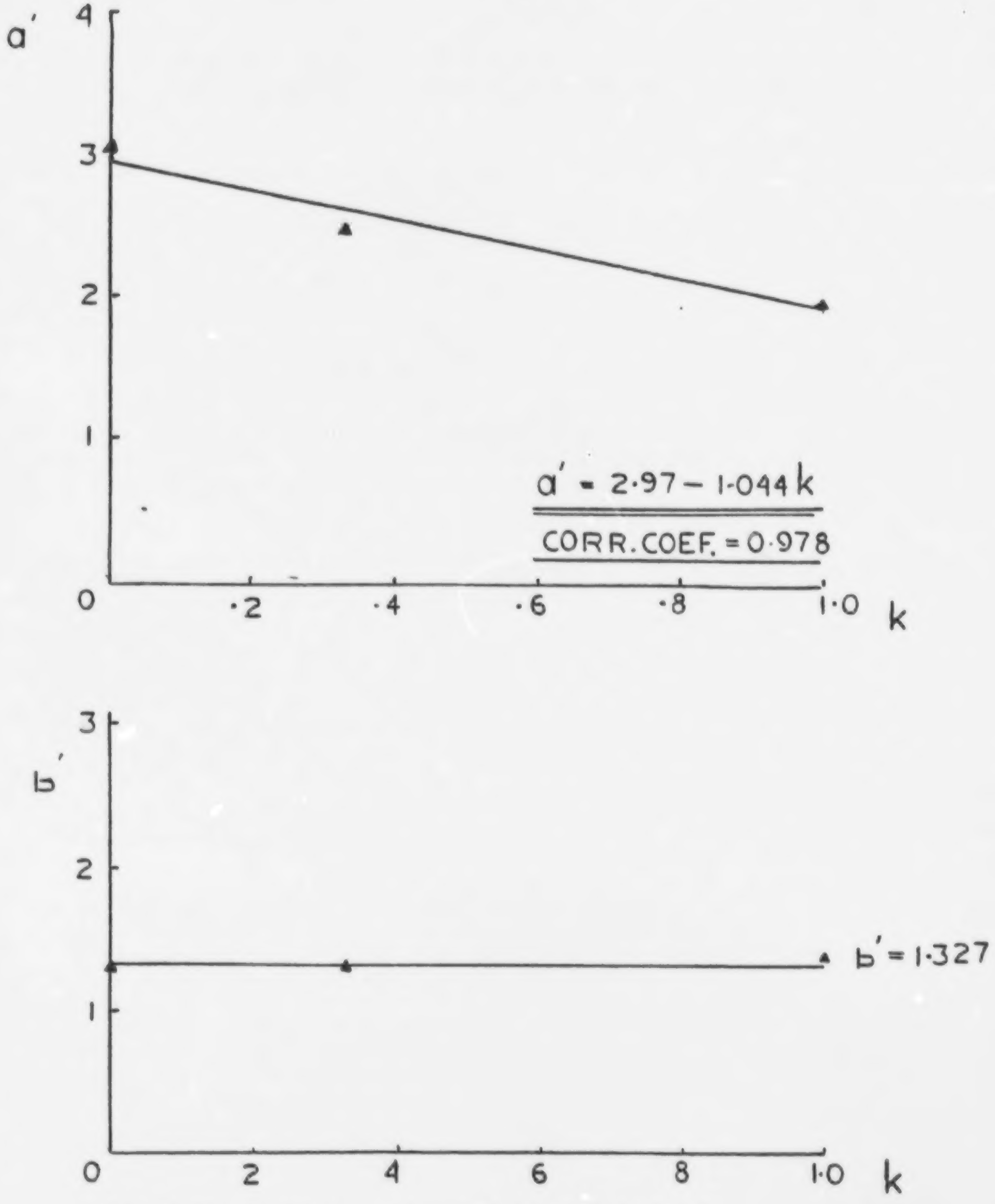

FIGURE C4: Coefficients a' and b' for Ovaloidal Holes

Appendix D

Maximum Stress Concentration at the Mid Height of Side Wall, on the Horizontal Axis, of Multiple Openings

(a) Finite Row of Circular and Ovaloidal Openings

Duvall (5) and Obert and Duvall (7) report results of photoelastic studies for rows of multiple ovaloidal and circular openings under an uniaxial stress field. Tables D1 and D2 give Duvall's results for the stress concentrations at the points A,B,C,D and E for five circular and five ovaloidal openings for a range of openings to pillar width ratio ($\frac{W}{B}$)(see Figure D1). It is seen from these tables that at points D and E the stress concentrations have almost the same value, hence it is concluded that:-

(i) For a row of five or more openings all but the two openings at the end of the row will have the same value for the maximum boundary stress concentration on the horizontal axis at the mid height.

Figure D2 shows the maximum stress concentrations for a row of 2,3 and 5 circular openings with various W/B ratios (8). It is seen that as the number of circular openings increases the maximum stress concentration asymptotically approaches an upper limit which corresponds to that for an infinite row of openings; further, the value given for five openings can be assumed to be equal to that for an infinite number of openings in a row. It seems reasonable to assume that this conclusion will also obtain for openings of other shapes, i.e. it is assumed:-

(ii) that the maximum stress concentration for an infinite row of holes of any shape is the same as that obtained for five or more holes of the same shape.

One final point should be noted from these results; it is seen from the tables that the stress concentrations at positions B and C are always less than that at position E. Hence if an expression is derived which approximates the stress concentration at position E and is then applied to the first pillar in the row, then B and C will be slightly overestimated. However, this would lead to a more conservative (safe) pillar design and consequently it is safe to assume that the stress concentration E can be used for all pillars in the row.

TABLE D.1: Maximum Stress Concentration for a Row of Five Circular Openings (k=0)

W/B	A	B	C	D	E
1.07	3.29	3.29	3.29	3.29	3.29
2.21	3.63	3.72	3.89	4.03	4.03
2.96	3.53	4.08	4.22	4.39	4.39
4.35	3.96	5.12	5.22	5.28	5.28

TABLE D.2: Maximum Stress Concentration for a Row of Five Ovaloidal Openings, $\frac{W}{H} = 2.0$, $k = 0$

W/B	A	B	C	D	E
1.03	3.90	3.90	3.90	4.05	4.17
2.09	4.09	4.50	4.61	4.70	4.79
3.40	4.41	5.02	5.40	5.47	5.56
4.28	4.66	5.67	5.93	6.10	6.10

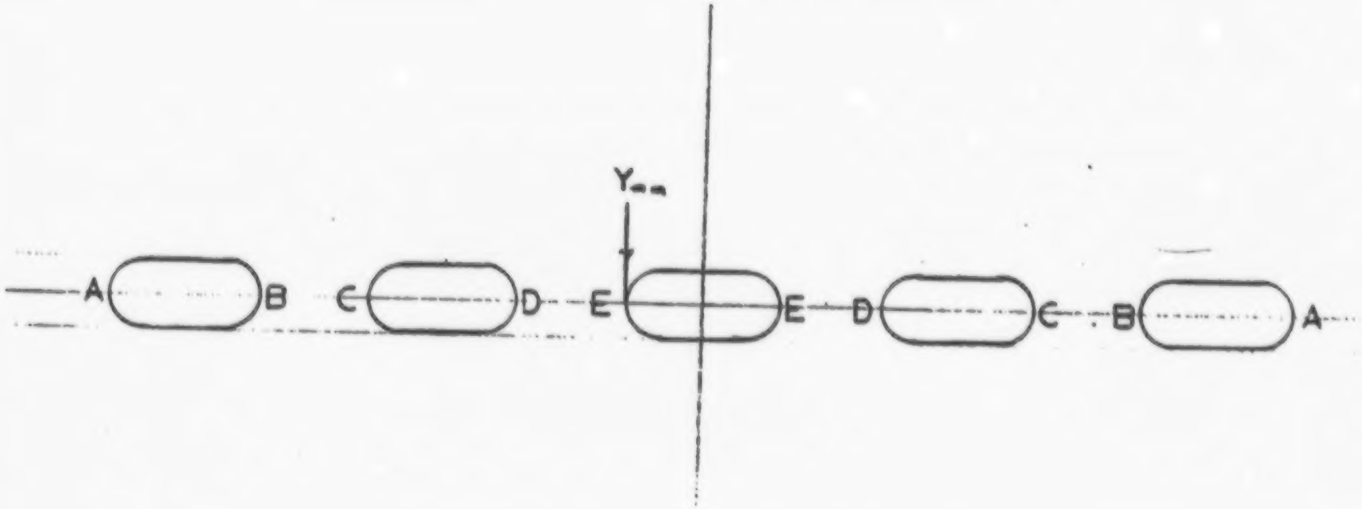
Y
A
B
C
D
E
E
D
C
B
A

FIGURE D1: Multiple openings with pillars between them

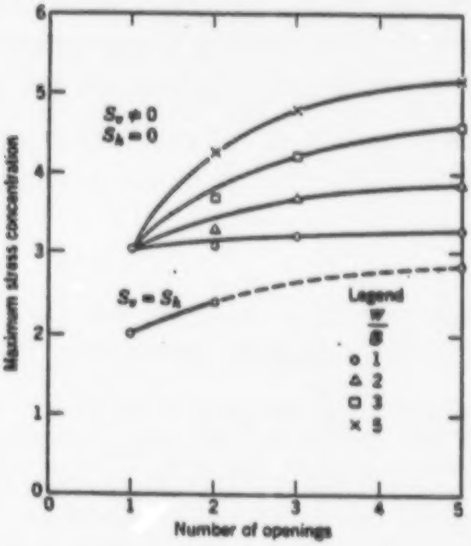

FIGURE D2: Maximum stress concentration for a row of 2, 3, and 5 circular openings for a range of w/b ratios, k = 0

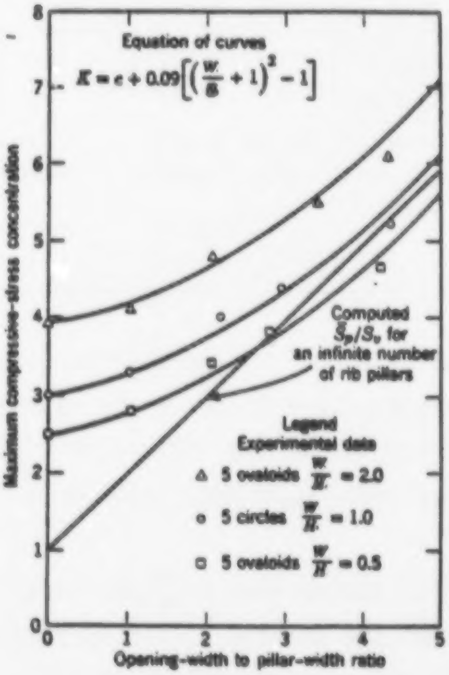

FIGURE D3: Maximum stress concentration for a row of circular and ovaloidal holes

(b) Maximum Stress Concentration at Position E for an Infinite Row of Ovaloidal Openings

Let Y_{mm} be the maximum stress concentration at the position E. Obert and Duvall (8) and Duvall (5) derived the following empirical formula for the maximum stress concentration, Y_{mm}, for multiple ovaloidal openings whose height/width ratios range from 0.5 to 2.0.

$$Y_{mm} = c + 0.09\left[\left(\frac{1}{1-R}\right)^2 - 1\right] \qquad (D.1)$$

Where R is the extraction ratio. Further, for the two dimensional case $R = \frac{W}{W+B}$; then in this case:-

$$Y_{mm} = c + 0.09\left[\left(\frac{W}{B} + 1\right)^2 - 1\right] \qquad (D.2)$$

Where c is stated by Duvall (5) to be "the maximum stress concentration around a single opening" but is stated in Obert and Duvall (8) to be "the maximum stress concentration around a single opening of the same shape in a unidirectional stress field". Clearly this latter statement cannot be correct since when the pillar is very wide relative to the opening width, ($(\frac{W}{B})$ is small), then the stress distribution must approach that around a single hole which, as seen from Appendix C, is very dependent on the stress ratio k. Thus c is taken to be the stress concentration around a single hole under the applied stress ratio k. i.e. c = Ym which is given in Appendix C, Equation 11c, for ovaloidal openings.

Hence for the two dimensional case, Equation D2 above can be combined with equation 11c to give:-

$$\underline{Y_{mm} = (2.97-1.044k) + 1.327 \log_e\left(\frac{W}{H}\right) + 0.09 \left\{\left(\frac{W}{B} + 1\right)^2 - 1\right\}} \qquad (D3)$$

However it should also be borne in mind that as $\frac{W}{B}$ increases, i.e. the pillar becomes small, then the effects of the lateral stress S_H on the pillar will be diminished due to the "shielding" effect of the adjacent openings. There must therefore be some value of $\frac{W}{B}$ above which this equation will not apply.

Now Obert and Duvall (8) showed that as $\frac{W}{B}$ increases then the average pillar stress approaches the maximum pillar stress (Note: the average pillar stress, $\frac{\sigma_p}{S_v} = \bar{Y}$, was determined by them using tributary area theory and not Coates' hypothesis; this however does not affect the conclusion).

This effect is illustrated in Figures D3 and D4. Further it will be noted that the average stress in some cases is greater than the maximum stress calculated by the above equations. (e.g. Figure D3, when $\frac{W}{B}>$ approximately 3,. for 5 ovaloids with $\frac{W}{H}=0.5$). Clearly this cannot be possible. Consequently it will be assumed that Y_{mm} is the maximum given by either the above equation or that given by the average stress $\overline{Y}$. i.e. when W/B > some value, i say

$$Y_{mm}=\overline{Y}=\frac{R}{1-R}$$

which for the two dimensional case is $= 1+\frac{W}{B}$ (D4)

Obert and Duvall also noted that as the average pillar stress concentration increases, the stress distribution across the mid plane of the pillar becomes more uniform. For example, for an infinite row of circular openings with a W/B ratio of 4, the average pillar stress concentration is 5.0, and the maximum concentration is approximately 5.28 (8). Hence the stress distribution curve on the mid plane would be approximately as shown in Figure D5.

Summarizing, therefore, when W/B < i Equation D3 can be used to estimate the maximum stress concentration at the mid height of the boundary for multiple ovaloidal openings but when W/B > i then the maximum stress concentration is closely approximated by the mean pillar stress concentration. Clearly it follows that in this latter case the stress distribution across the pillar must be uniform and equal to the average stress concentration.

It therefore remains to determine the value of i at which the change over occurs from one equation to the other.

This change over must occur when:-

$$(2.97-1.044k)+1.327\log_e\left(\frac{W}{H}\right)+0.09\left\{\left(\frac{W}{B}+1\right)^2-1\right\}=1+W/B$$

re-arranging and solving for W/B = i

$$\underline{W/B=i=4.555-\left\{11.6k-14.74\log_e\left(\frac{W}{H}\right)-1.1425\right\}^{\frac{1}{2}}} \qquad \text{(D5)}$$

now this equation will only have real roots when the expression in the brackets is positive.

i.e. when $11.6k-14.74\log_e\left(\frac{W}{H}\right)-1.1425>0$

i.e. when $\underline{k>0.0985+1.271\log_e(W/H)}$ (D6)

when k is less than this value the maximum stress concentration calculated using Equation D3 will always be the greatest and should always be used.
when k is > than this value then either equation will be used depending on whether W/B is > or < i given by Equation D5.

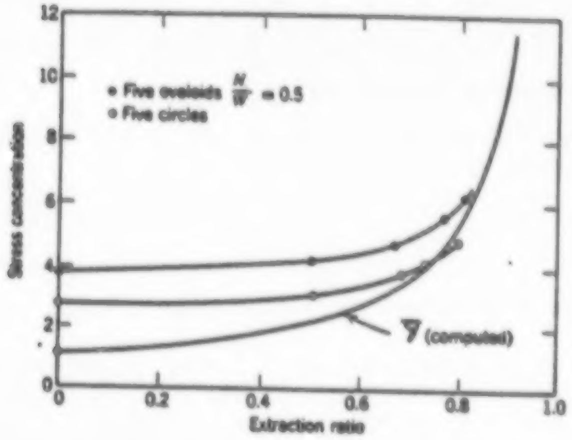

FIGURE D4: Average and maximum stress concentration for different extraction ratios

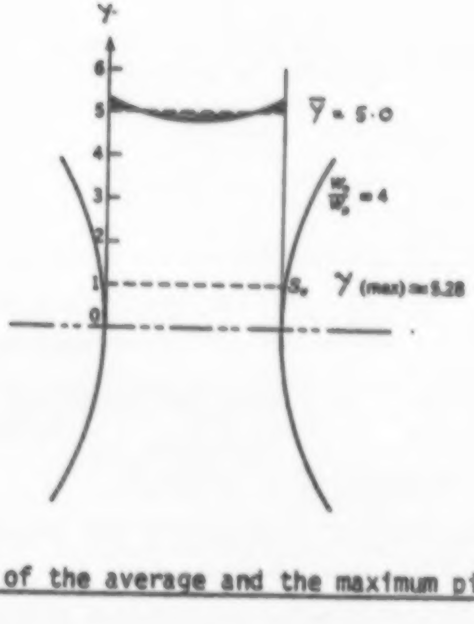
γ
6
5
4
3
2
1
0
$\bar{\gamma} = 5 \cdot 0$
$\frac{W_o}{W_p} = 4$
S_o
γ (max) = 5.28

FIGURE D5: Comparison of the average and the maximum pillar stress concentration

(c) Summary for Ovaloidal Openings.

(i) when $k < 0.0985 + 1.271 \log_e(W/H)$

then

$$Y_{mm} = (2.97 - 1.044k) + 1.327 \log_e(W/H) + 0.09 \{ (W/H+1)^2 - 1 \} \quad (18)$$

(ii) when $k > 0.0985 + 1.327 \log_e(W/H)$

and $W/B < 1 = 4.55 - \{ 11.6k - 14.74 \log_e(W/H) - 1.425 \}^{\frac{1}{2}}$

then Y_{mm} is also given by Equation (18).

(iii) when $k > 0.0985 + 1.271 \log_e(W/H)$

and $(W/B) > 1 = 4.55 - \{ 11.6k - 14.74 \log_e (W/H) - 1.1425 \}^{\frac{1}{2}}$

then
$$Y_{mm} = \frac{1}{1-R} = 1 + \frac{W}{B} \quad (19a)$$

(d) Comparison with Experimental Data.

Figure D6 compares the results obtained by Obert and Duvall (8) for five ovaloidal openings of W/H ratios of 2,1 and 0.5 with the curves calculated from the above equations when $k=0$. There is relatively good agreement between the experimentally derived points and the curves given by these equations; although there is some difference between them when $W/H=0.5$.

These equations will therefore be used in the text to define Y_{mm} for multiple ovaloidal openings.

Further the same principles will be applied for multiple elliptical and multiple rectangular openings in the sections below. The only differences will arise out of derivation of different "cut-off" values for W/B = 1 where the change occurs from one equation to the other.

(e) Multiple Elliptical Openings.

In this case, when $W/B<1$, then it follows from the above and from Equation 11a that:-

$$Y_{mm} = (1-k) + 2\left(\frac{W}{H}\right) + 0.09 \left\{ \left(\frac{W}{B}+1\right)^2 - 1 \right\} \quad (D7)$$

and when $W/B>1$ then

$$Y_{mm} = \frac{1}{1-R} = 1 + \frac{W}{B} \quad (D8)$$

FIGURE D6: Maximum stress concentration at the boundary of multiple ovaloidal openings-comparison of approximation with experimental results

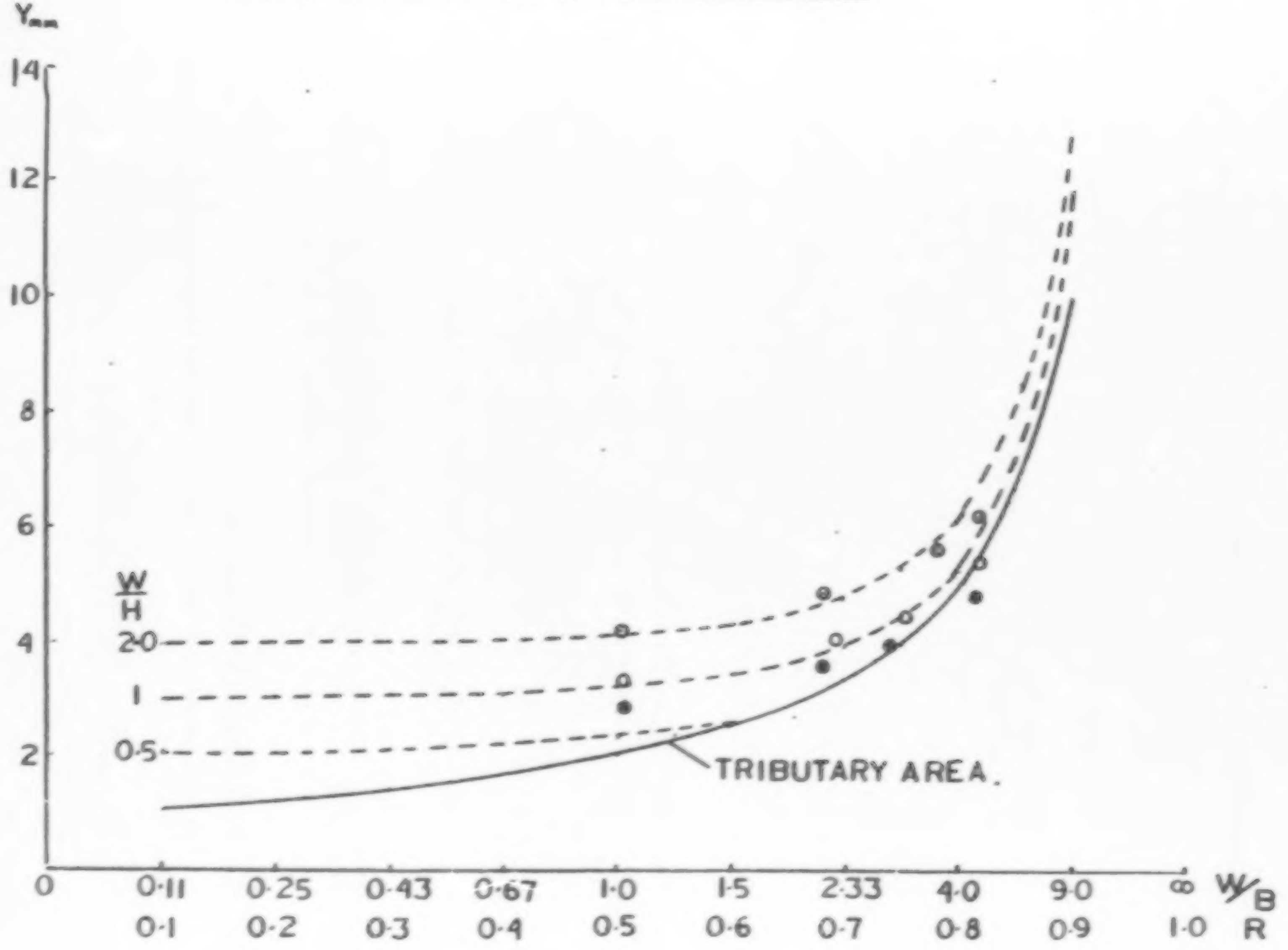

and the change from one equation to the other will occur when $W/B=1$:-

$$(1-k) + 2(\frac{W}{H}) + 0.09 \{ (\frac{W}{B}+1)^2 - 1 \} = 1 + W/B$$

re-arranging and solving for $\frac{W}{B} = 1$ gives:-

$$\underline{\frac{W}{B} = 4.555 - \{ 20.747 - 22.22(\frac{W}{H}) + 11.11k \}^{\frac{1}{2}}} \qquad \text{(D9)}$$

now this equation will only have real roots when the expression in brackets is positive:-

i.e. when $k > 2(\frac{W}{H}) - 1.886$ (D10)

Thus, summarizing for the elliptical openings case we have:-

$\underline{\text{(i)} \quad \text{when } k < 2(\frac{W}{H}) - 1.866}$

then $\underline{Y_{mm} = (1-k) + 2(\frac{W}{H}) + 0.09 \{ (\frac{W}{B}+1)^2 - 1 \}}$ (20)

$\underline{\text{(ii)} \quad \text{when } k > 2(\frac{W}{H}) - 1.866}$

$\underline{\text{and } \frac{W}{B} < 1 = 4.55 - \{20.75 - 22.22(\frac{W}{H}) + 11.11k\}^{\frac{1}{2}}}$

then Y_{mm} is also given by Equation (20).

$\underline{\text{(iii)} \text{ when } k > 2(\frac{W}{H}) - 1.866}$

$\underline{\text{and } \frac{W}{B} > 1 = 4.55 - \{20.75 - 22.22(\frac{W}{H}) + 11.11k\}^{\frac{1}{2}}}$

$\underline{\text{then } Y_{mm} = \frac{1}{(1-R)} = 1 + (\frac{W}{B})}$ (19a)

(f) For Multiple Rectangular Openings

Following the same principles it follows that for multiple rectangular openings,

when $\frac{W}{B} < 1$ then:-

$$Y_{mm} = (2.048 - 0.919k) + 0.572 \log_e(\frac{W}{H}) + 0.09 \{ (\frac{W}{B}) + 1)^2 - 1 \} \qquad \text{(D11)}$$

and when $\frac{W}{B} > 1$ then

$$Y_{mm} = \frac{1}{(1-R)} = 1 + \frac{W}{B} \qquad \text{(D12)}$$

and the change from one equation to the other will occur when $\frac{W}{B} = 1$:-

$$(2.048 - 0.919k) + 0.572 \log_e(\frac{W}{H}) + 0.09 \{ (\frac{W}{B}) + 1)^2 - 1 \} = 1 + \frac{W}{B}$$

re-arranging and solving for W/B=1 gives:-

$$\left(\frac{W}{B}\right) = 4.555 - \{9.11 + 10.21k - 6.536 \log_e\left(\frac{W}{H}\right)\}^{\frac{1}{2}} \qquad \text{(D13)}$$

and this equation will have real roots when:-

$$k > -0.892 + 0.64 \log_e\left(\frac{W}{H}\right) \qquad \text{(D14)}$$

Thus summarizing for multiple rectangular openings we have:-

(i) $\underline{\text{when } k < -0.892 + 0.64 \log_e\left(\frac{W}{H}\right)}$

then $Y_{mm} = (2.048 - 0.919k) + 0.572 \log_e\left(\frac{W}{H}\right) + 0.09\{\left(\frac{W}{B} + 1\right)^2 - 1\}$ (21)

and

(ii) $\underline{\text{when } k > -0.892 + 0.64 \log_e\left(\frac{W}{H}\right)}$

$\underline{\text{and } \frac{W}{B} < 4.555 - \{9.21 + 10.21k - 6.536 \log_e\left(\frac{W}{H}\right)\}^{\frac{1}{2}}}$

Y_{mm} is also given by Equation (21).

(iii) $\underline{\text{when } k > -0.892 + 0.69 \log_e\left(\frac{W}{H}\right)}$

$\underline{\text{and } \frac{W}{B} > 4.555 - \{9.21 + 10.21k - 6.536 \log_e\left(\frac{W}{H}\right)\}^{\frac{1}{2}}}$

$\underline{\text{then } Y_{mm} = \frac{1}{(1-R)} = 1 + \left(\frac{W}{B}\right)}$ (19a)

Unfortunately the author has nct been able to locate experimental data against which to check these approximations for multiple elliptical and rectangular openings.

(g) Summary and use of these equations in the text

It has been shown above that the maximum stress concentration at the mid height of the boundary of multiple openings of various shapes can be approximated by either of two equations for each opening shape. In each case the second of these two equations is the "average" pillar stress, $\frac{\sigma_p}{S_v} = Y$. In the above analysis the average pillar stress used was that determined by tributary area theory; however as pointed out in Section 2 the average pillar stress is best determined using Coates' pillar formulae. Consequently it is the value determined using Coates' equations which will be applied in the text. Summarizing therefore, we have:-

For Ovaloidal Openings

The maximum stress concentration Y_{mm} at the mid height of the opening boundary is given by either

$$Y_{mm} = (2.97-1.044k) + 1.327 \log_e (\frac{W}{H}) + 0.09 ((\frac{W}{H} + 1)^2 - 1) \qquad (18)$$

or by

$$Y_{mm} = \overline{Y} \qquad (19)$$

which ever be the larger value.

where $\overline{Y}$ is the average pillar concentration determined from Coates' pillar formulae.

For Elliptical Openings

The maximum stress concentration Y_{mm} of the mid height of the opening boundary is given by either:-

$$Y_{mm} = (1-k) + 2(\frac{W}{H}) + 0.09 ((\frac{W}{B} + 1)^2 - 1) \qquad (18)$$

or by

$$Y_{mm} = \overline{Y} \qquad (19)$$

whichever is the larger value.

where $\overline{Y}$ is the average pillar stress given by Coates' pillar formulae.

For Rectangular Openings

The maximum stress concentration Y_{mm} at the mid height of the opening boundary is given by either:-

$$Y_{mm} = (2.048-0.919k) + 0.572 \log_e (\frac{W}{H}) + 0.09 ((\frac{W}{B} + 1)^2 - 1) \qquad (20)$$

or by

$$Y_{mm} = \overline{Y} \qquad (19)$$

whichever is the larger value.

Further, it follows that for each case when the equation 19 is applicable then the stress distribution across the pillar must be uniform.

This therefore accomplishes step 2 of the logic diagram shown in Figure 1 of the text.

Appendix E: Example Elastic Stress Distributions Across a Series of Pillars.

This example will be based on the cross sections, CC, illustrated in Figure B1 and B2 of Appendix B.

It is shown in section 5.1 that the stress concentration on the i th slice of the pillar, prior to any failure occuring is given by:-

$$Y_i = \frac{k_1}{\{k_2 + 1 + \frac{(2i - 1)}{n_1} (\frac{B}{W})\}} + k_3 \qquad (29)$$

where n_1 is the number of slices into which the pillar is arbitrarily split. The constants k_1, k_2, k_3, have been determined for each pillar in the manner described in section 4, using the maximum stress concentration Y_{mm} obtained for the appropriate room shape from equations 21 and the mean pillar stress $\overline{Y}$ determined from Coates' pillar formulae and derived in Appendix B.

It will be noted in this case the rooms on either side of the pillar do not have the same dimensions; in these cases each pillar has been treated as two separate half pillars with the dimensions adjacent to each half pillar being used to determine the stress concentration for that half pillar. This leads to a slight discontinuity in the stress distribution at the centre of the pillar, however the differences are extremely small in this example and will suffice, pending the derivation of approximation for the solution of the vertical stress distribution across a pillar with different size and shape rooms on either side.

Table E1 gives the parameters derived for each of the pillars C1 to C5 on this cross section and determines the stress concentration on each slice. Figure E1 shows the resulting stress distribution across the pillars.

TABLE E1: Stress Distribution Across Pillars - Example Section CC From Appendix B

ITEM	PILLAR								
	C1	C2		C3		C4		C5	
		LHS	RHS	LHS	RHS	LHS	RHS	LHS	RHS
Shape of Opening	Rect	Rect	Rect	Rect	Rect	Rect	Rect	Rect	Rect
$\overline{Y}$ (from Coates)	1.242	1.260	1.260	1.287	1.287	1.263	1.263	1.241	1.241
W ft	20	20	40	40	20	20	40	40	20
B ft	80	60	60	180	180	80	80	70	70
H ft	10	10	10	10	10	10	10	10	10
k	.33	.33	.33	.33	.33	.33	.33	.33	.33
Y_{mm} from (21)	2.192	2.192	2.6977	2.5821	2.186	2.254	2.6502	2.6699	2.274
k_1	.4854	.3806	.1391	.6206	2.9393	.5407	.1971	.1480	.3867
k_2	-.6097	-.6913	-.9188	-.6235	1.0234	-.5877	-.8821	-.9122	-.7061
k_3	.9483	.9591	.9487	.9338	.7334	.9426	.9784	.9837	.9584
n slices	16	12	12	18	18	16	16	14	14
slice width ft	5	5	5	10	10	5	5	5	5
i	Yi								
1	1.7064	1.6403	1.6233	1.9244	1.8982	1.7590	1.7898	1.6792	1.6694
2	1.3740	1.3186	1.2536	1.4847	1.5676	1.4078	1.3783	1.3035	1.3288
3	1.2442	1.2033	1.1457	1.3154	1.3832	1.2679	1.2437	1.1913	1.2089
4	1.1751	1.1440	1.0942	1.2256	1.2656	1.1927	1.1769	1.1374	1.1476
5	1.1321	1.1078	1.0640	1.1701	1.1840	1.1457	1.1370	1.1057	1.1104
6	1.1029	1.0835	1.0442	1.1323	1.1241	1.1136	1.1104	1.0849	1.0854
7	1.0816	-	-	1.1049	1.0783	1.0902	1.0915	1.0701	1.0675
8	1.0655	-	-	1.0842	1.0420	1.0725	1.0773	-	-
9	-	-	-	1.0679	1.0127	-	-	-	-

FIGURE E1: Elastic stress distribution across pillars in Section C-C, Figure B1, Appendix B

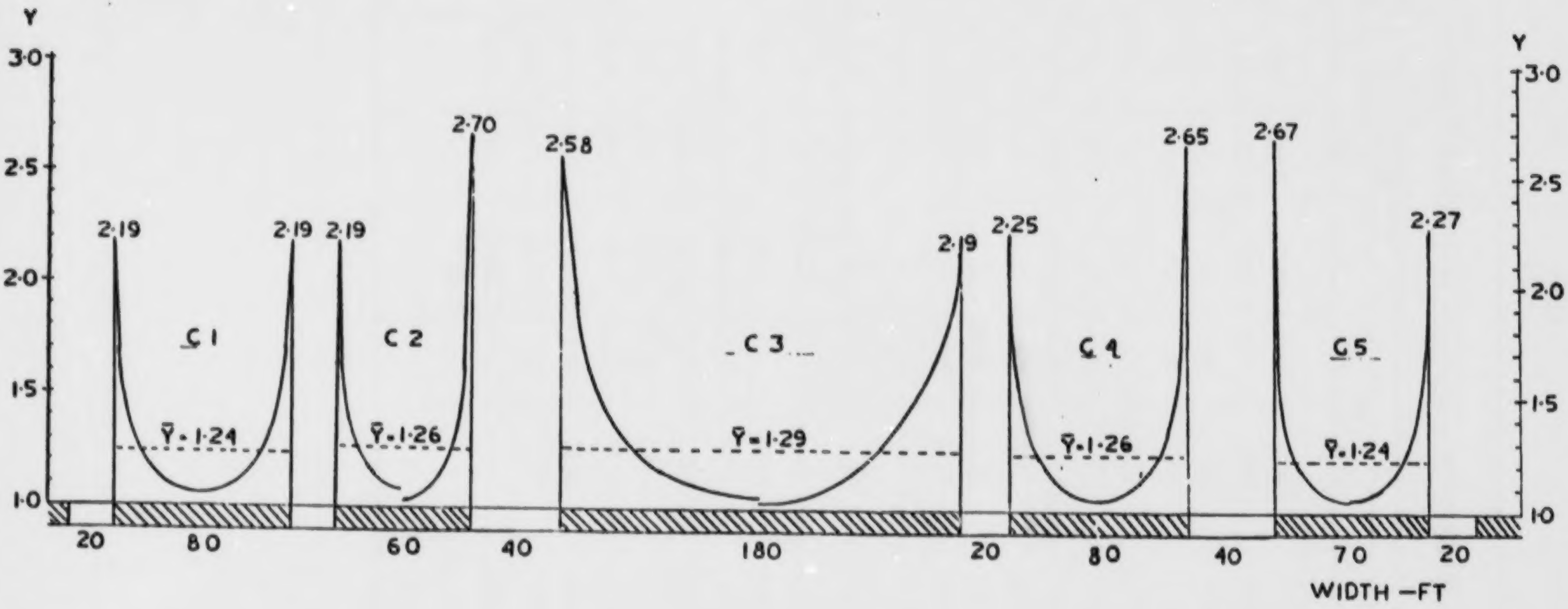

Appendix F: Coulomb - Navier failure theory expressed in different forms

Coulomb assumed that fracture takes place across a plane over which the shear stress reaches a constant value S_o; Navier modified this by assuming that the shear strength is increased by an amount μ times the normal stress across the failure plane.

μ is called the "coefficient of internal friction" of the material and, putting $\mu = \tan \phi$, ϕ is called the "angle of internal friction".

If τ and σ are the shear and normal stresses on the failure plane then the Coulomb-Navier failure criterion states that failure takes place on the plane at which $|\tau|$ first becomes equal to $S_o + \mu\sigma$:-

$$\underline{\text{i.e. } |\tau| = S_o + \mu\sigma} \qquad \text{(F 1)}$$

Figure F 1 expresses Coulomb-Navier failure theory in the form of a Mohr envelope.

Now σ and τ may be expressed in terms of the major and minor principal stresses, σ_1 and σ_3, as follows:-

$$\sigma = \left\{\frac{\sigma_1 + \sigma_3}{2}\right\} + \left\{\frac{\sigma_1 - \sigma_3}{2}\right\} \cos 2\theta \qquad \text{(F 2)}$$

$$\text{and } |\tau| = \left\{\frac{\sigma_1 - \sigma_3}{2}\right\} \sin 2\theta \qquad \text{(F 3)}$$

Figure F 2 illustrates the relationship between the principal stresses and the stresses on the failure plane.

Hence from equations F 1, F 2, and F 3, at failure:-

$$S_o = |\tau| - \mu\sigma = \left\{\frac{\sigma_1 - \sigma_3}{2}\right\}\left\{\sin 2\theta - \mu \cos 2\theta\right\} - \mu\left\{\frac{\sigma_1 + \sigma_3}{2}\right\} \qquad \text{(F 4)}$$

Now S_o will reach a maximum when $\frac{\partial S_o}{\partial \theta} = 0$

Thus, differentiating and putting $\frac{\partial S_o}{\partial \theta} = 0$ gives:-

$$0 = 2 \cos 2\theta + 2\mu \sin 2\theta$$

$$\underline{\text{i.e. } \tan 2\theta = -\frac{1}{\mu}} \qquad \text{(F 5)}$$

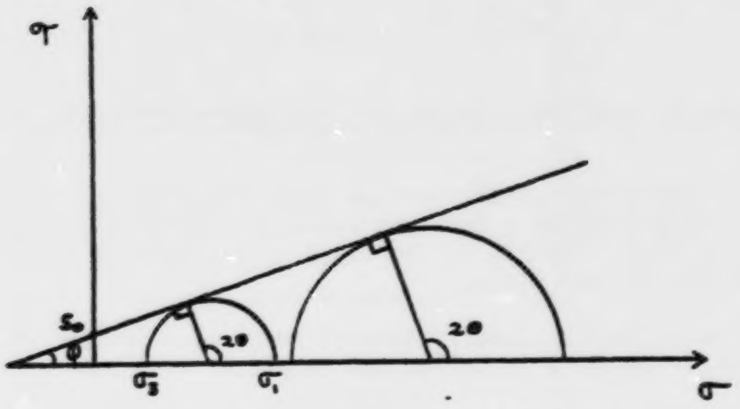
τ
S_0
ϕ
2θ
2θ
σ_3
σ_1
σ

FIGURE F1: Coulomb-Navier failure theory expressed as a Mohr's envelope

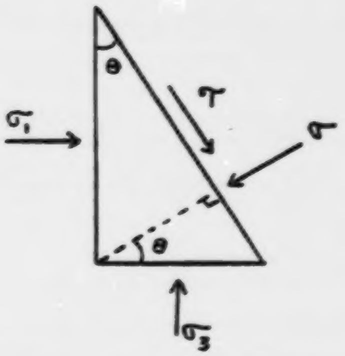
θ
τ
σ_1
σ
θ
σ_3

FIGURE F2: Relationship between the principal stresses and the stresses on the failure plane

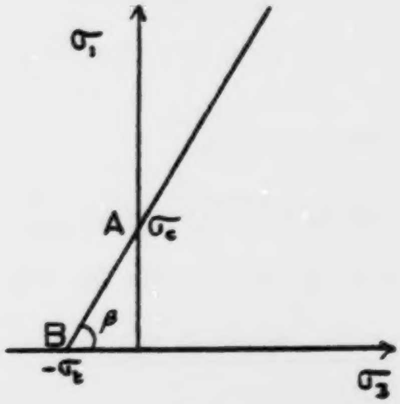
σ_1
A
σ_c
B
β
$-\sigma_t$
σ_3

FIGURE F3: Coulomb-Navier failure theory expressed as a straight line relationship between σ_1 and σ_3

from which it follows that :-

$$\text{Sin } 2\theta = \frac{1}{(1+\mu^2)^{\frac{1}{2}}} \qquad \text{and} \qquad \text{Cos } 2\theta = \frac{-\mu}{(1+\mu^2)^{\frac{1}{2}}} \qquad \text{(F 6)}$$

Hence, substituting from equation F 6 into equation F 4 gives the maximum value of S :-

$$So = \left\{\frac{\sigma_1 - \sigma_3}{2}\right\}\left\{\frac{1}{(1+\mu^2)^{\frac{1}{2}}} + \frac{\mu^2}{(1+\mu^2)^{\frac{1}{2}}}\right\} - \mu\left\{\frac{\sigma_1 + \sigma_3}{2}\right\}$$

$$\text{i.e. } 2\ So = \sigma_1\left\{(1+\mu^2)^{\frac{1}{2}} - \mu\right\} - \sigma_3\left\{(1+\mu^2)^{\frac{1}{2}} + \mu\right\} \qquad \text{(F 7)}$$

This is the "fracture criterion" and So is called the "cohesion".

Under uniaxial compression, then $\sigma_1 = \sigma_c$ the unixial compressive strength, and $\sigma_3 = 0$

$$\text{Hence } \sigma_c = \frac{2\ So}{\left[(1+\mu^2)^{\frac{1}{2}} - \mu\right]} \qquad \text{(F 8)}$$

and under uniaxial tension, $\sigma_1 = 0$ and $\sigma_3 = -\sigma_t$ where σ_t is the uniaxial tensile strength, then

$$\sigma_t = \frac{2\ So}{\left[(1+\mu^2)^{\frac{1}{2}} + \mu\right]} \qquad \text{(F 9)}$$

and the ratio σ_c/σ_t is given by:

$$\frac{\sigma_c}{\sigma_t} = \left\{\frac{(1+\mu^2)^{\frac{1}{2}} + \mu}{(1+\mu^2)^{\frac{1}{2}} - \mu}\right\} \qquad \text{(F10)}$$

The above equations expressing the Coulomb-Navier failure criterion are not necessarily the most convenient for all purposes. Hence the equations will also be expressed in other, sometimes unusual, forms:-

By geometry, from Figure F1, it is seen that: -

$$90 - \phi = 180 - 2\theta$$

$$\text{i.e. } 2\theta = (90 + \phi)$$

Hence $\underline{\text{Sin } 2\theta = \text{Sin } (90 + \phi) = \text{Cos}\phi \text{ and Cos } 2\theta = \text{Cos } (90 + \phi) = - \text{Sin } \phi}$ (F11)

Thus substituting from equation F11 into equation F 4, and putting $\mu = \tan \phi$, gives:-

$$2 \text{ So} = (\sigma_1 - \sigma_3) \text{ Cos}\phi - \mu(\sigma_1 + \sigma_3) + \mu(\sigma_1 - \sigma_3) \text{ Sin}\phi$$

$$= \sigma_1 \left\{ \text{Cos}\phi - \frac{\text{Sin}\phi}{\text{Cos}\phi} + \frac{\text{Sin}^2\phi}{\text{Cos}\phi} \right\} - \sigma_3 \left\{ \text{Cos}\phi + \frac{\text{Sin}\phi}{\text{Cos}\phi} + \frac{\text{Sin}^2\phi}{\text{Cos}\phi} \right\}$$

$$\text{i.e. } 2 \text{ So Cos}\phi = \sigma_1 (\text{Cos}^2\phi + \text{Sin}^2\phi - \text{Sin}\phi) - \sigma_3 (\text{Cos}^2\phi + \text{Sin}^2\phi + \text{Sin}\phi)$$

$$= \sigma_1 (1-\text{Sin}\phi) - \sigma_3 (1+\text{Sin}\phi)$$

$$\text{i.e. } \underline{\sigma_1 = \frac{2 \text{ So Cos}\phi}{(1-\text{Sin}\phi)} + \frac{\sigma_3 (1+\text{Sin}\phi)}{(1-\text{Sin}\phi)}} \qquad \text{(F12)}$$

This equation represents a straight line relationship between σ_1 and σ_3 at failure, as illustrated in Figure F 3.

Further, if tan β is the slope of this line, then

$$\underline{\tan \beta = \frac{(1+ \text{Sin}\phi)}{(1- \text{Sin}\phi)}} \qquad \text{(F13)}$$

The intercept, A, on the σ_1 axis occurs when $\sigma_3 = 0$, i.e. when $\sigma_1 = \sigma_c$ Hence

$$\sigma_c = \frac{2\,S_o \cos\phi}{(1 - \sin\phi)} \tag{F14}$$

and the intercept, B on the σ_3 axis occurs when $\sigma_1 = 0$; i.e. when $\sigma_3 = -\sigma_t$ Hence

$$\sigma_t = \frac{2\,S_o \cos\phi}{(1 + \sin\phi)} \tag{F15}$$

and also

$$\tan\beta = \frac{\sigma_c}{\sigma_t} = \frac{(1 + \sin\phi)}{(1 - \sin\phi)} \tag{F16}$$

Thus from equation F16 and equation F10 :-

$$\tan\beta = \frac{\sigma_c}{\sigma_t} = \frac{(1 + \sin\phi)}{(1 - \sin\phi)} = \left\{\frac{(1 + \mu^2)^{\frac{1}{2}} + \mu}{(1 + \mu^2)^{\frac{1}{2}} - \mu}\right\} \tag{F17}$$

These various forms of the Coulomb-Navier failure criterion will be used as appropriate in the main text.

Appendix G : Example of the build up of the residual stress capacity and the confining pressure in the fractured coal at a pillar edge

It is shown in the text (Sections 5.3.1 and 5.3.2) that the "residual stress capacity of a slice", P_1, and the confining stress P_3 are given respectively by the following two equations:-

$$P_1 = \frac{P_B}{2\,\mathrm{Sin}\phi_B}\left\{(1+\mathrm{Sin}\phi_B)\; e^{\tan\phi_B\left\{\frac{1+\mathrm{Sin}\phi_B}{1-\mathrm{Sin}\phi_B}\right\}\frac{W}{H}(X-1)} - (1-\mathrm{Sin}\phi_B)\right\} \qquad (43)$$

and

$$P_3 = \left\{\frac{1-\mathrm{Sin}\phi_B}{1+\mathrm{Sin}\phi_B}\right\}\left[P_1 - P_B\right] \qquad (44)$$

Assume a rectangular opening, height H = 10 ft. and width W = 20 ft. The manner in which P_1 and P_3 build up in the fractured coal at the edge of the pillar will be examined. $X = {}^{e}/w$. For fractured coal, ϕ_B the angle of internal friction is usually in the range of 27° to 36°. The uniaxial compressive strength of the fractured coal will be small; values of P_B = 10 psi., 1 psi and 0.1 psi will be considered.

Table G1 lists the parameters and the results calculated using the above equations. Figure G1 and G3 show the build up of the residual stress capacity P_1 and the influence of changes in ϕ_B and P_B respectively. Figure G2 shows the build up of the confining stress P_3 and the influence of ϕ_B. It is clearly seen that both P_1 and P_3 are very sensitive to the values of P_B and ϕ_B.

It should be noted that P_1 and P_3 are dependent only on the properties of the fractured coal and on the width / height ratio of the slice. Thus the rate of build up of P_1 and P_3 in the fractured coal will be the same for all pillars in the same coal and adjacent to rooms of the same size and shape. i.e. provided that fracture occurs, then the stress build up in the fractured periphery of the coal pillar is independent of the stress applied to that pillar.

TABLE G 1 : Examples of build up of residual stress capacity and confining pressure in fractured coal at a pillar edge

P_B - p.s.i.	10			10			10		
ϕ_B	36°			30°			27°		
X	P_1	P_3	P_3/P_1	P_1	P_3	P_3/P_1	P_1	P_3	P_3/P_1
1.0	10	0	0	10	0	0	10	0	0
1.1	20.1	2.6	0.13	16.2	2.1	0.128	15	1.9	0.125
1.2	37.9	7.2	0.19	25.0	5.0	0.20	21.5	4.3	0.20
1.3	68.9	15.3	0.222	37.4	9.13	0.244	30.1	7.6	0.25
1.4	123.2	29.4	0.24	54.9	14.9	0.273	41.4	11.8	0.28
1.5	218.3	54.1	0.248	79.8	23.3	0.292	56.2	17.3	0.31
1.6	384.6	97.3	0.253	114.9	34.9	0.304	75.6	24.6	0.33
1.7	675.8	172.7	0.256	164.5	51.5	0.313	101.0	34.2	0.338
1.8	1185.4	305.1	0.257	234.7	74.9	0.319	134.4	46.7	0.348
1.9	2077.3	536.7	0.258	333.9	107.9	0.323	178.1	63.2	0.354
2.0	3638.3	941.9	0.259	474.2	154.7	0.326	235.5	84.7	0.359

P_B - p.s.i.	10			1			5		
ϕ_B	33°			33°			33°		
X	P_1	P_3	P_3/P_1	P_1	P_3	P_3/P_1	P_1	P_3	P_3/P_1
1.0	10	0	0	1	0	0	5	0	0
1.1	17.85	2.31	0.129	1.78	0.23	0.129	8.9	1.16	0.13
1.2	30.0	5.91	0.197	3.00	0.59	0.197	15.0	2.95	0.197
1.3	49.0	11.5	0.235	4.90	1.15	0.23	24.5	5.7	0.235
1.4	78.4	20.2	0.257	7.84	2.02	0.257	39.2	10.1	.257
1.5	124.1	33.6	0.271	12.42	3.36	0.271	62.1	16.8	0.271
1.6	195.2	54.6	0.279	19.5	5.46	0.279	97.6	27.3	0.279
1.7	305.6	87.1	0.285	30.6	8.71	0.285	152.8	43.6	0.285
1.8	477.1	137.7	0.289	47.71	13.8	0.288	238.5	68.9	0.288
1.9	743.5	216.2	0.291	74.3	21.6	0.291	371.8	108.1	0.291
2.0	1157.4	338.2	0.292	115.7	33.8	0.292	578.7	169.1	0.292

FIGURE G1: Build up of residual stress capacity in broken rock-variation with ϕ_B

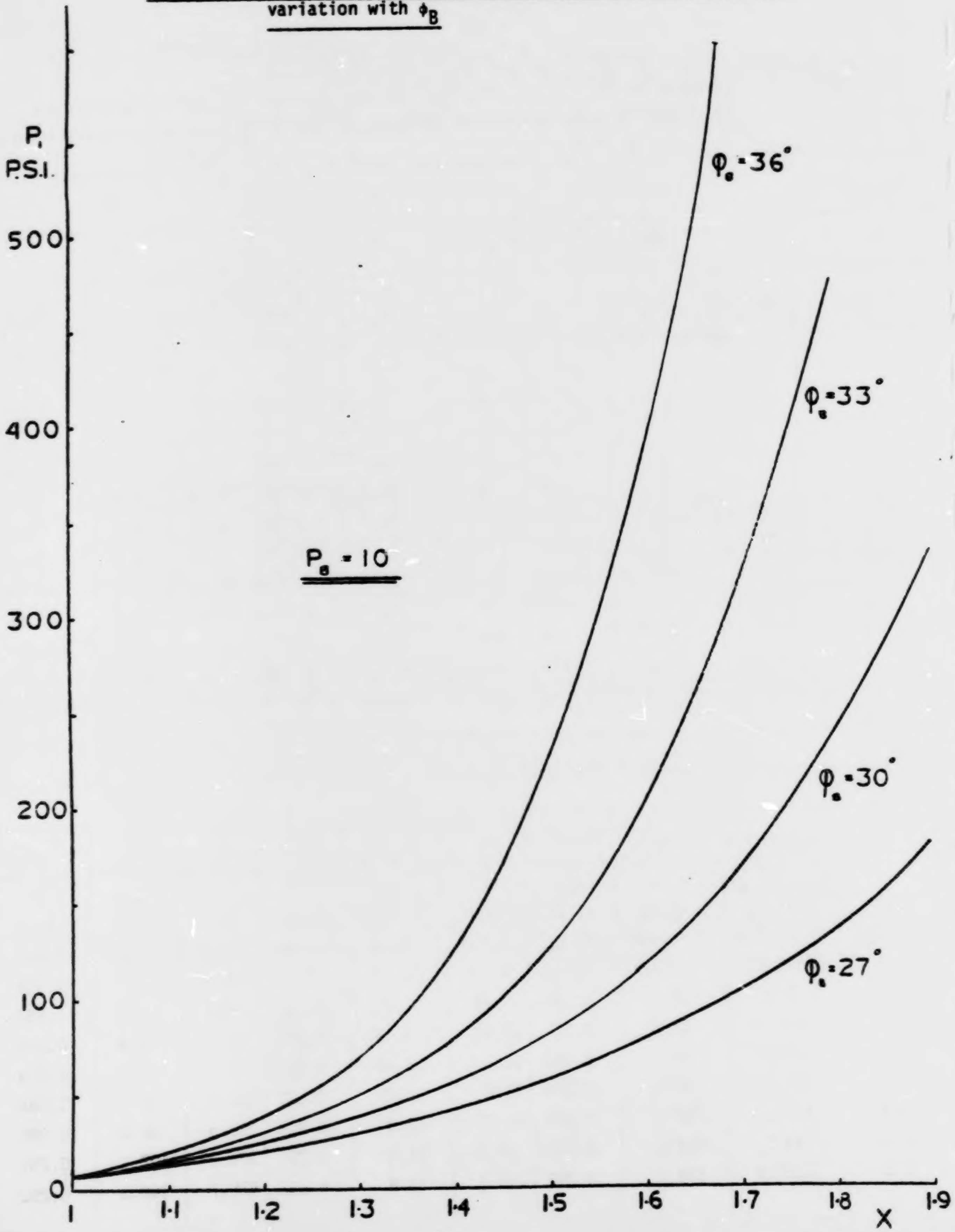

FIGURE G2: Build up of confining pressure in broken rock- variation with ϕ_B

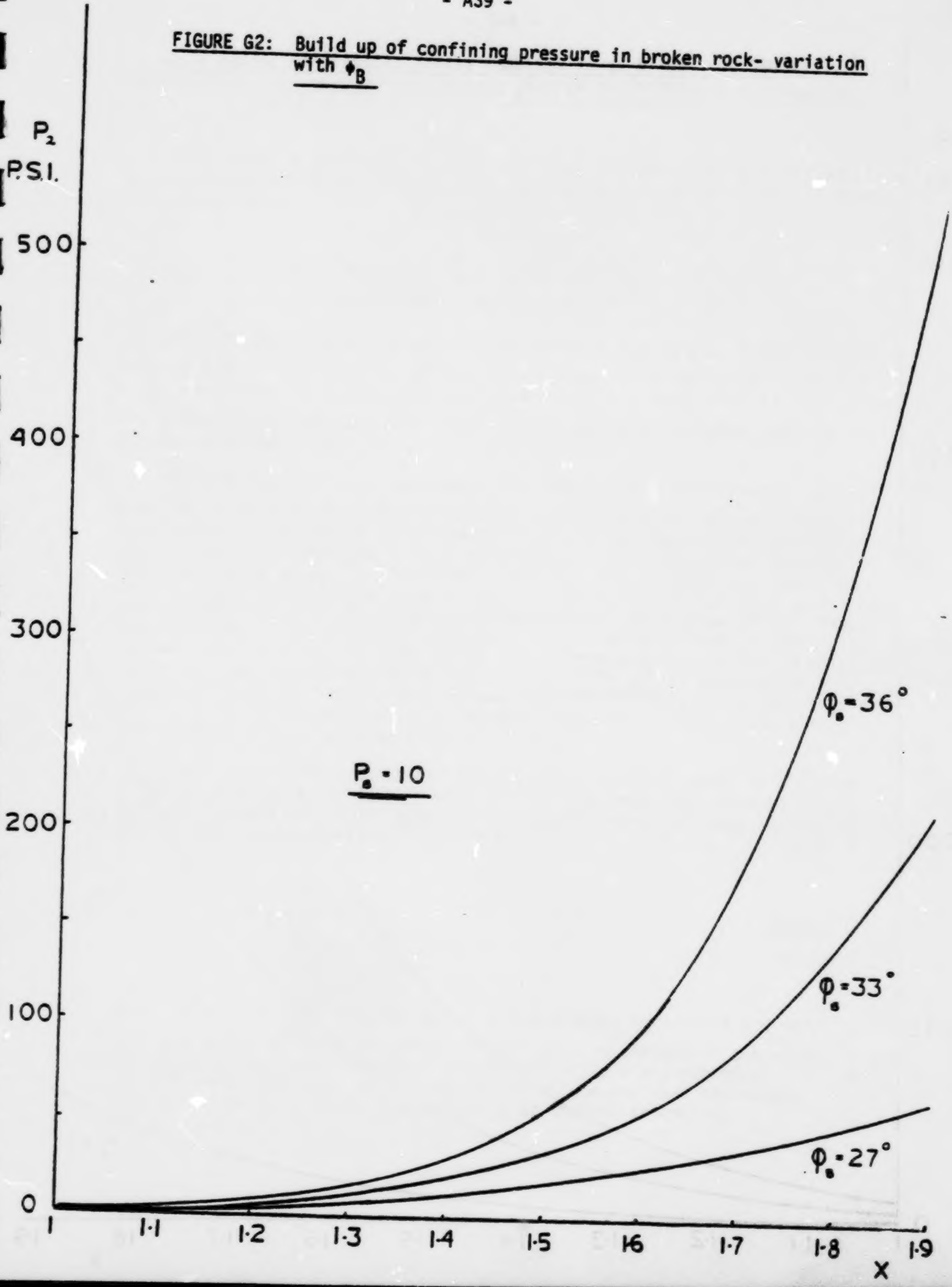

FIGURE G3: Build up of residual stress capacity in broken rock-variation with P_B

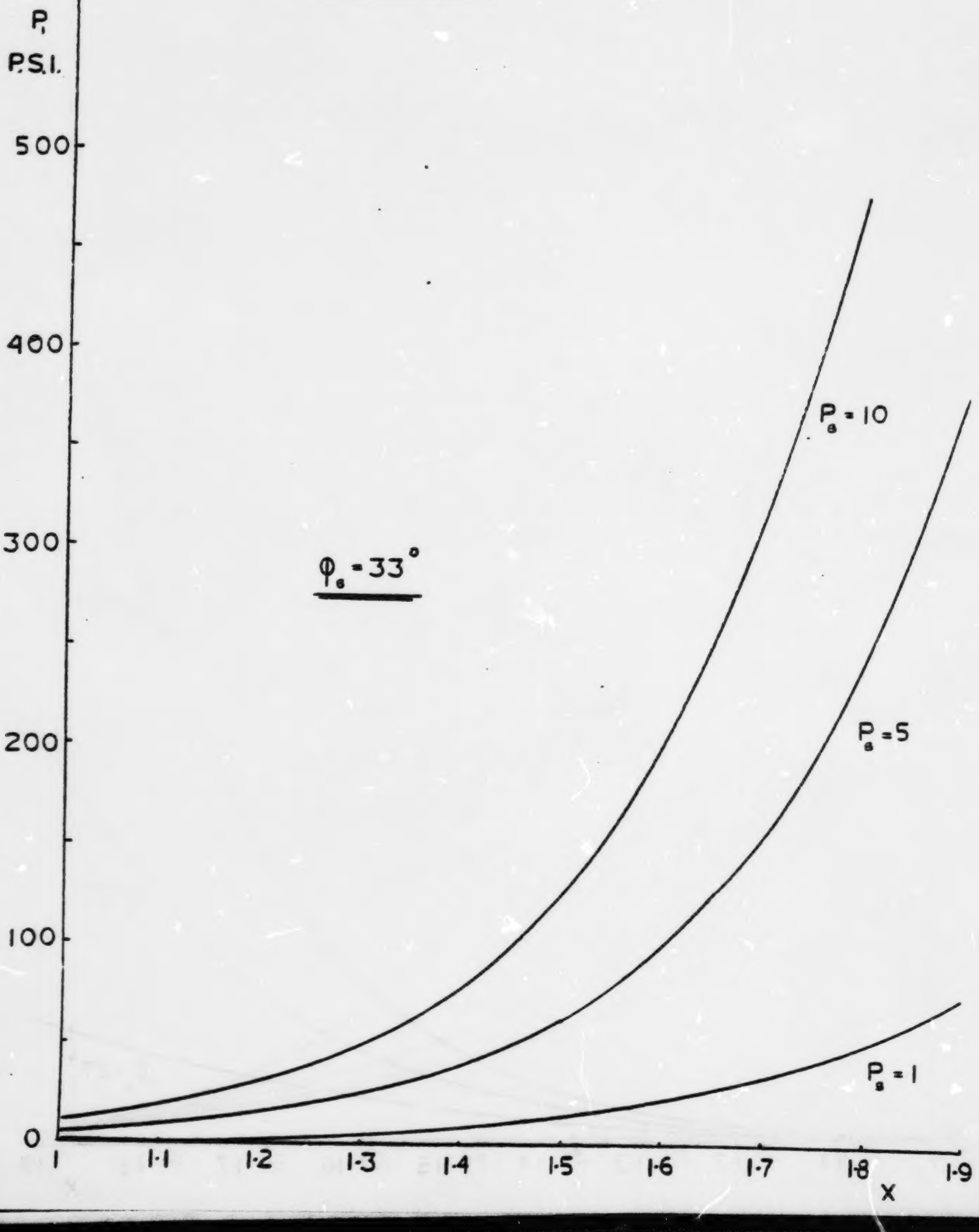

Appendix H : Load re-distribution from the failed slice onto the remaining unfailed slices

It is shown in the text, Section 5.4, that the load shed by a failed slice and which must be re-distributed onto the remaining unfailed slices is given by equation 46 :-

$$\Delta L = (\sigma_{1i} - P_1) \left(\frac{B}{n_1}\right) \qquad \text{(H1)}$$

where σ_{1i} is the vertical stress applied to the slice before fracture, P_1 is the residual stress capacity of the failed slice, B is the pillar width, n_1 is the number of slices into which the pillar has been split and (B/n_1) is the slice width. How does this shed load become re-distributed onto the remaining unfailed slices?

(a) when $Y_{mm} = \overline{Y}$ It has been shown (Section 4.2 and Appendix D) that when the maximum stress concentration in the pillar along the horizontal axis at the mid height is approximately equal to the mean pillar stress concentration, $\overline{Y}$, then the stress distribution across the pillar must be constant and equal to $\overline{Y}$. This stems from the work of Obert and Duvall (8) on the stress distribution in solid pillars which showed that as a pillar gets smaller than the average pillar stress approaches the maximum pillar stress and consequently the stress distribution across the mid plane of the pillar becomes more uniform. The same effect probably occurs in a pillar in which the central core is getting smaller due to fracturing of its perepheries. Consequently it is reasonable to assume that in this case, when the original distribution on the solid core is uniform, then the re-distributed stress distribution must also be uniform.

i.e. it will be assumed in this case that the load shed by a failed slice is re-distributed equally onto each of the remaining unfailed slices. Thus the incremental stress added to the elastic stress already applied to each of the remaining slices is given by :-

$$\Delta\sigma_1 = \frac{\sigma_{1i} - P_1}{(n_{1/2} - i)} \qquad \text{(H2)}$$

Note: $(^{n}1/_{2})$ is used here and not n_1 since symetry is assumed and only half the pillar will be analysed. Clearly this is correct if the width, height and shape of the rooms on either side of the pillars are identical. If they are different then each half of the pillar wll be analysed separately- this will lead to a slight discontinuity at the pillar centre.

The total new vertical stress applied to the next adjacent slice is thus given by :-

$$\sigma_1 = \sigma_{1(i+1)} + \left\{ \frac{\sigma_{1i} - P_1}{(n_{1/2} - i)} \right\} \qquad \text{(H3)}$$

and the lateral stress σ_3 applied to this next slice will be the confining pressure P_3 generated in the fractured coal of the adjacent failed slice and given by equation 44.

Consequently the stresses σ_1 and σ_3 applied to this next unfailed slice are known and can be compared with the failure criterion. If this slice fails then the residual stress capacity of this slice can again be determined and the incremental stress added to each of the remaining slices can be determined as above. If failure does not occur then the final vertical stress distribution in the unfailed core (which is in this case uniform) can be determined. The above steps can be readily combined in a computer loop to consider each slice in turn.

(b) when $Y_{mm} > \overline{Y}$ In this case the initial stress distribution across the pillar is non-uniform and has been approximated by a hyperbola. It would seem unlikely that the re-distribution of stress would be uniform in this case; it would appear more likely that the re-distribution would follow some function which is inversely proportional to the distance from the failed slice i.e. a larger portion of the total shed load would be applied to the immediately adjacent unfailed slice than would be applied to the next most adjacent slice etc. However the precise form of this function is unknown and requires further investigation.

Consider the pillar illustrated in Figure H1; it is divided into n_1 slices (=14). i.e. The half pillar which we are analysing is divided into $n_{1/2}$ slices, each of width B/n_1 .

Let us assume that when a slice fails the excess stress is shed onto the remaining slices as described by a general functional relationship given by:-

$$\Delta\sigma = f\left(\frac{1}{x^{\alpha}}\right) \qquad \text{(H4)}$$

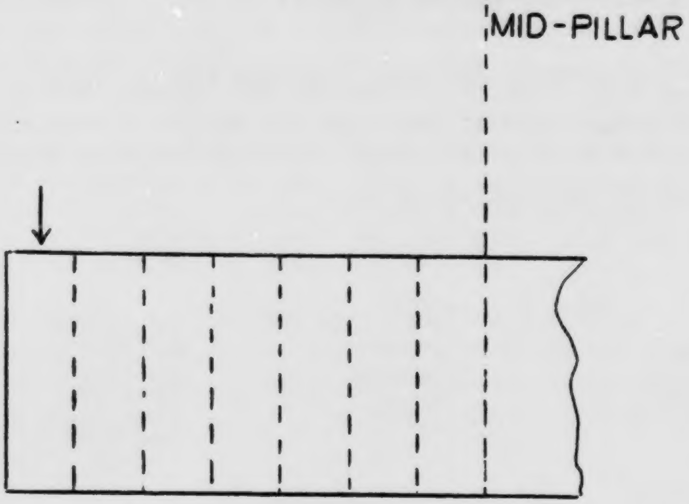

FIGURE H1: Pillar divided into n_1 slices (n_1 = 14)

where x is the distance from the failed slice and α is some unknown constant.

Consider the first slice, let σ_{1i} be the initial vertical stress applied to the first slice, assume it fails and now has a reduced stress capacity of P_1. Therefore the total stress to be shed from this failed slice to the adjacent unfailed slices is given by :-

$$\Delta\sigma = (\sigma_{1i} - P_1) \qquad \text{(H5)}$$

and thus the portion of this total incremental stress that will be shed onto the immediately adjacent (2nd) unfailed slice will be; from equation H4, given by :-

$$\Delta\sigma_2 = \frac{\frac{1}{1^\alpha}(\sigma_{1i} - P_1)}{\left\{\frac{1}{1^\alpha} + \frac{1}{2^\alpha} + \frac{1}{3^\alpha} + \frac{1}{4^\alpha} + \frac{1}{5^\alpha} + \frac{1}{6^\alpha}\right\}} \qquad \text{(H6)}$$

similarly the stress shed from this first failed slice onto the third slice will be given by :-

$$\Delta\sigma_3 = \frac{\frac{1}{2^\alpha}(\sigma_{1i} - P_1)}{\left\{\frac{1}{1^\alpha} + \frac{1}{2^\alpha} + \frac{1}{3^\alpha} + \frac{1}{4^\alpha} + \frac{1}{5^\alpha} + \frac{1}{6^\alpha}\right\}} \qquad \text{(H7)}$$

Hence a general relationship for the stress shed from the 1st slice onto the j th slice is given by :-

$$\Delta\sigma_j = \frac{\left\{\frac{1}{(j-1)^\alpha}\right\}\left[\sigma_{1i} - P_1\right]}{\displaystyle\sum_{j=(i+1)}^{j=({}^{n}1/_{2})} \left\{\frac{1}{(j-1)^\alpha}\right\}} \qquad \text{(H8)}$$

The new vertical stress distribution can therefore be determined by adding the incremental stress $\Delta\sigma_j$ to the original stress applied, for each slice in turn. The failure of the second slice under the new applied vertical stress can therefore be examined and, if this slice fails then the total shed stress can again be determined and the additional stress increments for the remaining slices can again be determined following the above procedures. This procedure is repeated successively for each slice in turn until a slice no longer fails in which case the final stress distribution on the central core is given by the initial stress acting on each unfailed slice plus the accumulated increments from each failed slice.

It now remains to consider what might be the value of ∝ . Unfortunately there is no information in the literature to allow us to empirically derive ∝ . An example analysis has therefore been run, for a typical coal pillar with typical coal properties; in these analyses ∝ has been varied from 0 to 1. The following parameters were used in this analysis (the pillar considered was C5 Appendix B)

S_v = overburden stress - varied
R = general extraction ratio = 0.254
l = semi width of mining span = 315 ft.
x = coordinate of the pillar in the mining span = 315 ft.
w = semi width of room = 20 ft.
b = semi width of pillar = 35 ft.
h = semi height of pillar = 5 ft.
μ_r = Poisson's ratio of surrounding rock = 0.3
μ_p = Poisson's ratio of coal pillar = 0.3
E_r = Young's modulus of surrounding rock - 5×10^6 psi
E_p = Young's modulus of pillar rock = 1×10^6 psi
k = applied stress ratio $= \frac{S_H}{S_v} = 0.33$
N = number of pillars in span = 5
Opening shape - rectangular
Calculated mean pillar stress concentration (from Coates' formulae) = 1.241
n_1 = number of slices over total pillar width = 70
P_B = uniaxial compressive strength of broken coal = 1 psi
ϕ_B = angle of friction of broken coal = 27°
σ_c = uniaxial compressive strength of solid coal = 1000 psi
ϕ_s = angle of internal friction of solid coal = 27°
∝ = load shedding constant - varied : 0: 0.1:0.2:0.3:0.4:0.5:1.0

Table H1 gives a typical computer print out for this pillar analysis where S_v = 650 psi and ∝ = = 0.5

```
MEAN PILLAR STRESS:LHS= 807.
MAXIMUM STRESS CONCENTRATION=2.6689
            K1= 0.1484
            K2=-0.9120
            K3= 0.9837
FRACTURE ZONE ENDED ON  53TH SLICE AND EXTENDED 26.5FT INTO THE PILLAR.
STRESS CONCENTRATION FOR GIVEN INPUT PARAMETERS=   806.6
PILLAR IS STABLE.
 SLICE  SIGMA I  SIGMA II SIGMA IS  STATUS          PONE     PTHREE SHED LOAD
 =====  =======  ======== ========  ======          ====     ====== =========
   1.   1589.1   1589.1   1000.0 FAILED              1.2       0.1      0.0
   2.   1408.0   1513.0   1000.3 FAILED              1.5       0.2    105.0
   3.   1280.3   1454.7   1000.6 FAILED              1.8       0.3    174.4
   4.   1189.0   1417.5   1000.9 FAILED              2.2       0.4    228.5
   5.   1120.5   1394.7   1001.3 FAILED              2.6       0.6    274.3
   6.   1067.1   1382.2   1001.8 FAILED              3.0       0.8    315.0
   7.   1024.4   1377.0   1002.3 FAILED              3.5       1.0    352.5
   8.    989.5   1377.4   1002.9 FAILED              4.1       1.2    387.9
   9.    960.4   1382.2   1003.5 FAILED              4.8       1.4    421.8
  10.    935.7   1390.5   1004.3 FAILED              5.6       1.7    454.8
  11.    914.6   1401.8   1005.2 FAILED              6.5       2.1    487.2
  12.    896.3   1415.5   1006.2 FAILED              7.6       2.5    519.2
  13.    880.2   1431.4   1007.4 FAILED              8.7       2.9    551.2
  14.    866.1   1449.2   1008.7 FAILED             10.1       3.4    583.1
  15.    853.5   1468.8   1010.3 FAILED             11.7       4.0    615.3
  16.    842.2   1490.0   1012.0 FAILED             13.4       4.7    647.7
  17.    832.1   1512.7   1014.0 FAILED             15.5       5.4    680.6
  18.    822.9   1536.9   1016.3 FAILED             17.8       6.3    713.9
  19.    814.6   1562.4   1018.9 FAILED             20.5       7.3    747.8
  20.    807.0   1589.4   1022.0 FAILED             23.6       8.5    782.4
  21.    800.0   1617.8   1025.4 FAILED             27.1       9.8    817.6
  22.    793.6   1647.3   1029.4 FAILED             31.1      11.3    853.7
  23.    787.7   1678.2   1033.9 FAILED             35.7      13.0    890.6
  24.    782.2   1710.6   1039.1 FAILED             41.0      15.0    928.4
  25.    777.1   1744.2   1045.0 FAILED             47.0      17.3    967.1
  26.    772.3   1778.3   1051.8 FAILED             53.9      19.9   1006.9
  27.    767.9   1815.7   1059.6 FAILED             61.8      22.8   1047.8
  28.    763.8   1853.5   1068.5 FAILED             70.9      26.3   1089.8
  29.    759.9   1892.8   1078.8 FAILED             81.3      30.2   1132.9
  30.    756.2   1933.5   1090.5 FAILED             93.2      34.6   1177.3
  31.    752.8   1975.6   1103.9 FAILED            106.8      39.7   1222.8
  32.    749.6   2019.3   1119.2 FAILED            122.5      45.6   1269.7
  33.    746.5   2064.3   1136.8 FAILED            140.3      52.3   1317.8
  34.    743.6   2110.8   1157.0 FAILED            160.8      60.0   1367.2
  35.    740.9   2158.8   1180.1 FAILED            184.3      68.8   1417.9
  36.    738.3   2208.1   1206.5 FAILED            211.2      78.9   1469.8
  37.    735.8   2258.7   1236.8 FAILED            241.9      90.5   1522.9
  38.    733.4   2310.4   1271.4 FAILED            277.2     103.7   1577.0
  39.    731.2   2363.3   1311.1 FAILED            317.5     118.9   1632.1
  40.    729.1   2417.0   1356.6 FAILED            363.8     136.2   1688.0
  41.    727.0   2471.4   1408.7 FAILED            416.7     156.1   1744.3
  42.    725.1   2526.0   1468.3 FAILED            477.4     178.9   1801.0
  43.    723.2   2580.6   1536.7 FAILED            546.8     205.0   1857.4
  44.    721.4   2634.5   1614.9 FAILED            626.4     234.8   1913.1
  45.    719.7   2687.1   1704.5 FAILED            717.5     269.1   1967.4
  46.    718.1   2737.6   1807.2 FAILED            821.8     308.2   2019.8
  47.    716.5   2784.8   1924.7 FAILED            941.3     353.1   2068.3
  48.    715.0   2827.4   2059.4 FAILED           1078.2     404.5   2112.4
  49.    713.6   2863.7   2213.6 FAILED           1235,0     463.4   2150.1
  50.    712.2   2891.4   2390.2 FAILED           1414.6     530.8   2179.3
  51.    710.8   2907.9   2592.5 FAILED           1620.2     608.1   2197.1
  52.    709.5   2909,7   2824.2 FAILED           1855.7     696.5   2200.2
  53.    708.3   2892.3   3089.5 NOT FAILED       2892.3     696.5   2184.0
  54.    707.1   2738.9   3089.5 NOT FAILED       2738.9     696.5   2031.8
  55.    705.9   2634.4   3089.5 NOT FAILED       2634.4     696.5   1928.5
  56.    704.8   2552.5   3089.5 NOT FAILED       2552.5     696.5   1847.7
  57.    703.7   2484.4   3089.5 NOT FAILED       2484.4     696.5   1780.8
  58.    702.6   2425.9   3089.5 NOT FAILED       2425.9     696.5   1723.3
  59.    701.6   2374.4   3089.5 NOT FAILED       2374.4     696.5   1672.8
  60.    700.6   2328.4   3089.5 NOT FAILED       2328.4     696.5   1627.8
  61.    699.7   2286.9   3089.5 NOT FAILED       2286.9     696.5   1587.2
  62.    698.7   2248.9   3089.5 NOT FAILED       2248.9     696.5   1550.2
  63.    697.8   2214.0   3089.5 NOT FAILED       2214.0     696.5   1516.2
  64.    697.0   2181.7   3089.5 NOT FAILED       2181.7     696.5   1484.7
  65.    696.1   2151.7   3089.5 NOT FAILED       2151.7     696.5   1455.5
  66.    695.3   2123.6   3089.5 NOT FAILED       2123.6     696.5   1428.3
  67.    694.5   2097.2   3089.5 NOT FAILED       2097.2     696.5   1402.7
  68.    693.7   2072.4   3089.5 NOT FAILED       2072.4     696.5   1378.7
  69.    693.0   2049.0   3089.5 NOT FAILED       2049.0     696.5   1356.1
  70.    692.2   2026.8   3089.5 NOT FAILED       2026.8     696.5   1334.6
```

Table H1: Vertical stress distribution across a pillar for S_v = 650 p.s.i. and α = 0.5

Figure H2 shows the vertical stress distribution across the pillar for S_v = 650 and 850 psi for α = 0:0.2; 0.3:0.4; 0.5 and 1.0.

Consider the influence of increasing the applied virgin stress S_v on (i) the fracture zone depth and (ii) on the stress distribution in the central unfailed core.

(I) Influence of S_v on the fracture zone development for variation of α

Table H2 gives the depth of the fracture zone for these cases.

It will be noted from this table that when α=1 the fracture zone develops exceptionally rapidly with a very small increase in stress S_v (i.e. from 0 to 25 ft. S_v increases from 405 psi to 415 psi. Intuitively it is thought that this is too rapid and that a (1/x). load shedding function places too much additional stress on the adjacent unfailed slice causing this rapid successive failure.

It will also be noted after S_v = 550 psi there is very little difference in the depths of the fracture zone, whatever the value of α. This is due to the fact that the lateral stress P_3 builds up increasingly rapidly after about 25 ft. making it more difficult for each successive slice to fail and minimizing the influence of the value of α on the depth of the fracture zone.

These points are illustrated in Figure H 3.

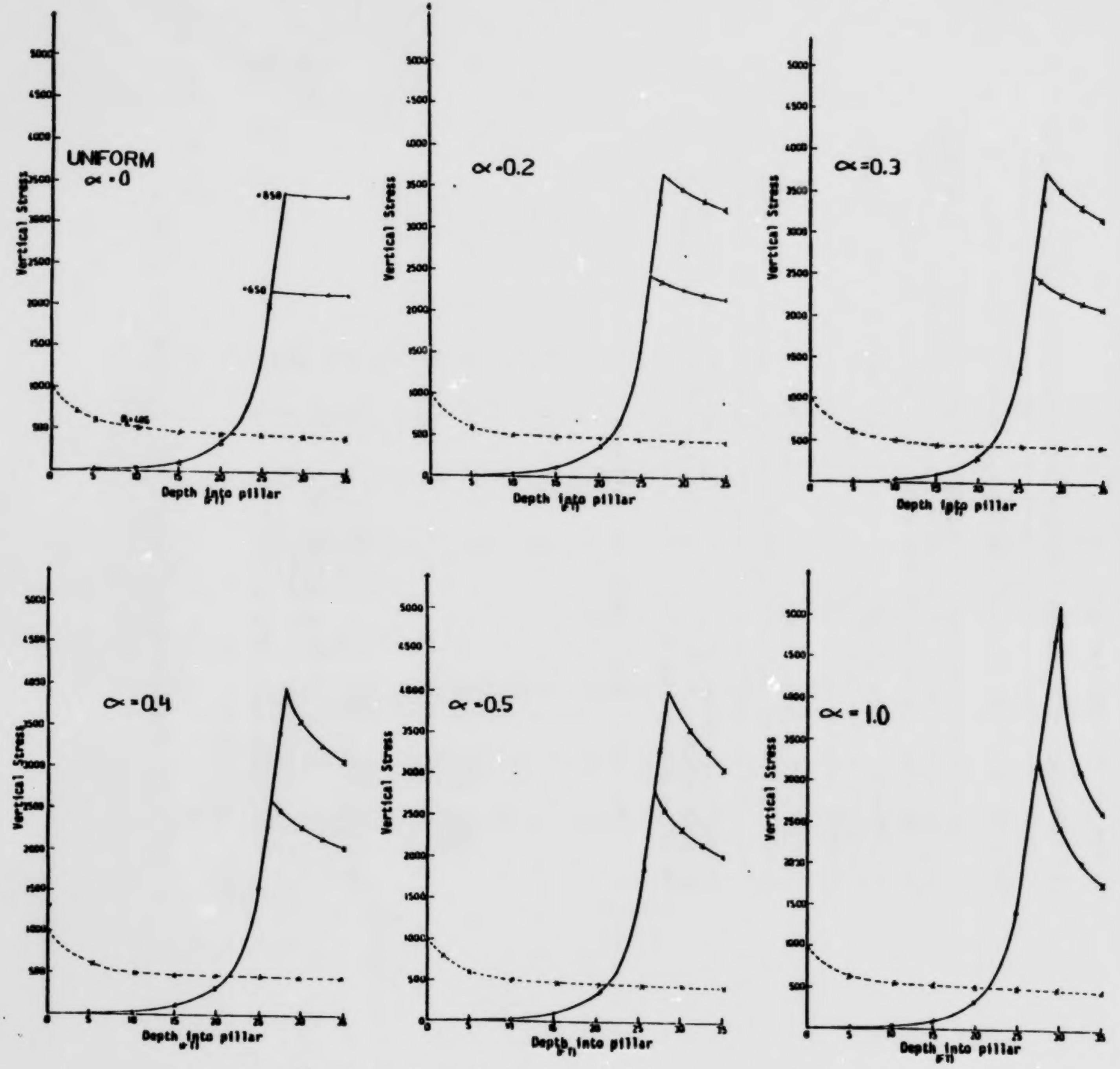

FIGURE H2: Effect of variation of load shedding function.

Table H2 : Influence of S_v on the fracture zone development for variation of α.

S_v	405	415	450	550	650	850	1050	1250	1450	1800	1942
$\bar{\sigma}_p$	503	515	558	683	807	1055	1303	1551	1799	2234	2410
α	Depth of fracture zone - ft.										
1	0	25.0	25.5	27.0	28.0	29.5	30.5	31.5	32.5	34.5	35.0
0.5	0	1.0	2.0	25.0	26.5	28.5	30.0	31.0	32.0	34.0	35.0
0.4	0	1.0	1.5	24.5	26.0	28.0	29.5	31.0	32.0	34.0	35.0
0.3	0	1.0	1.5	24.0	26.0	28.0	29.5	30.5	32.0	34.0	35.0
0.2	0	1.0	1.5	23.5	25.5	27.5	29.5	30.5	31.5	34.0	35.0
0.1	0	1.0	1.0	3.5	25.0	27.5	29.0	30.5	31.5	33.5	35.0
0	0	--	--	--	25.0	27.0	--	--	--	--	--

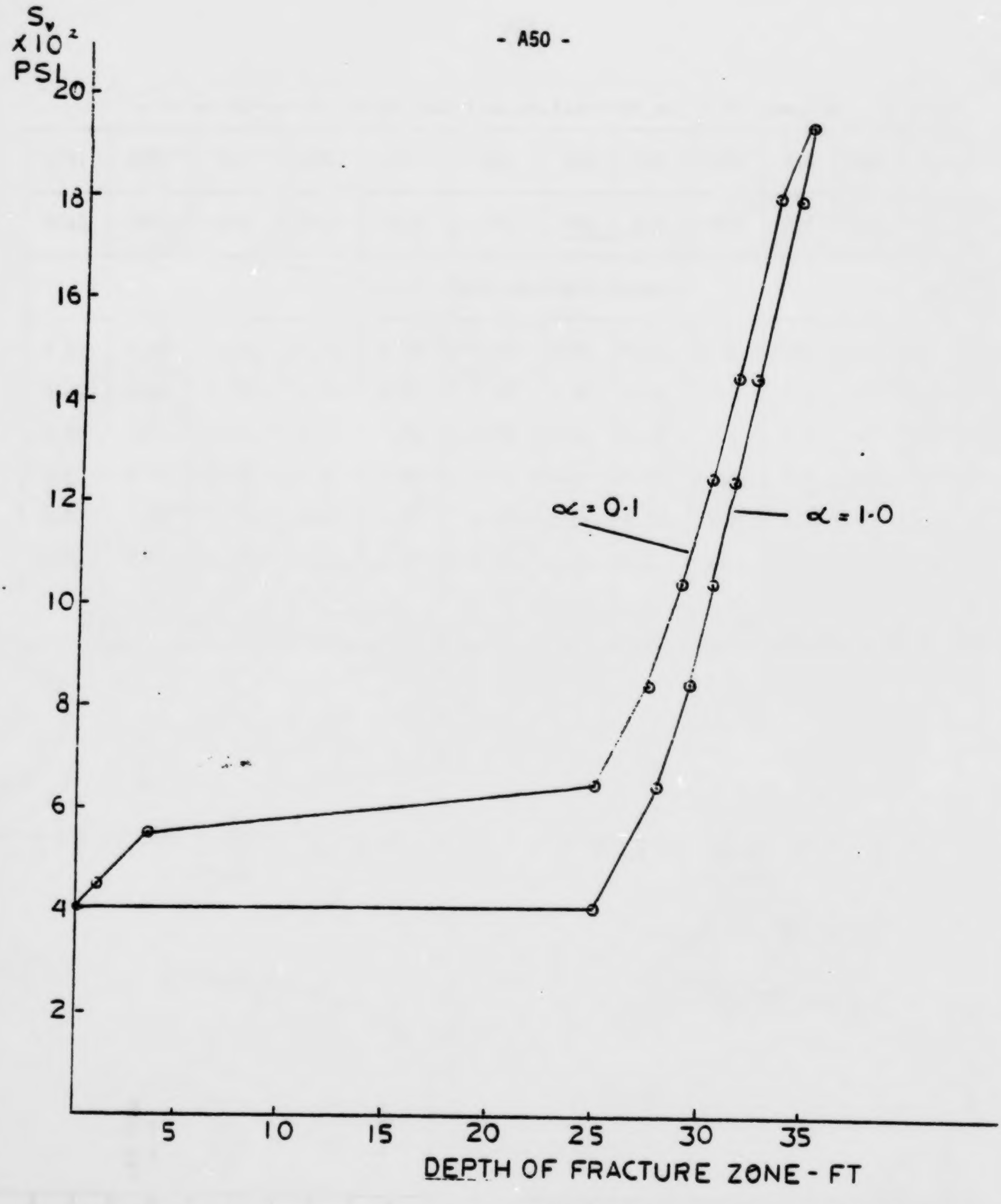

FIGURE H3: S_v versus depth of fracture zone for different load shedding functions

(II) Influence of change of S_v on the stress distribution in the central core with variation in α.

It is seen from Figure H2 that when $\alpha = 0$, the stress distribution becomes uniform exceptionally quickly even when there is a significant width of unfailed core remaining. It is thought that this occurs too quickly and thus that α is probably > 0.

However, when $\alpha = 1$ the slope of the stress distribution in the central core becomes increasingly steeper and steeper as the central core becomes smaller. This also does not intuitively seem correct.

Hence intuitively it is believed that $0 < \alpha < 1$.

It will therefore arbitrarily be assumed that $\alpha = 0.5$

This value $\alpha = 0.5$ will be used in the analysis in this paper pending its determination, or evidence that would indicated otherwise. The author has not been able to obtain information from the literature which might shed light on this value. Indeed, α may not necessarily be a constant but could well vary with the width of the pillar or with the width of the unfailed central core. Further study of this load shedding relationship is recommended as or when evidence becomes available. The computer program could be readily adapted to accomodate another value of α or even a variable α should that be desired and has, in fact, been written to allow α to be an input parameter of the users' choice.

Appendix I : Parabolic equation for a Mohr envelope

I.1 Mohr envelope

Let us assume a non-linear relationship between σ_1 and σ_3 at failure given by :-

$$\left\{\frac{\sigma_1 - \sigma_3}{2}\right\}^2 = A\left\{\frac{\sigma_1 + \sigma_3}{2}\right\} \qquad (I.1)$$

Let $r = \left\{\frac{\sigma_1 - \sigma_3}{2}\right\}$ and $s = \left\{\frac{\sigma_1 + \sigma_3}{2}\right\}$, then equation I.1 can be written as :-

$$r^2 = As \qquad (I.2)$$

Now the equation of a major principal stress circle in the Mohr diagram (see Figure I.1) is given by :-

$$(s - \sigma)^2 + \tau^2 = r^2 \qquad (I.3)$$

where τ and σ are the shear and normal stresses on the plane of failure respectively.

If r^2 is eliminated by using equation I.2 then equation I.3 may be written as :-

$$(s - \sigma)^2 + \tau^2 = As \qquad (I.4)$$

Partially differentiating this equation with respect to s gives :-

$$2\ (s - \sigma) = A \qquad (I.5)$$

Hence, by eliminating s between equations I.4 and I.5, the equation of the envelope to the family of principal stress circles is found to be :-

$$\frac{A^2}{4} + \tau^2 = A\left\{\frac{A}{2} + \sigma\right\}$$

$$\text{i.e.} \quad \tau^2 - A\sigma - \frac{A^2}{4} = 0 \qquad (I.6)$$

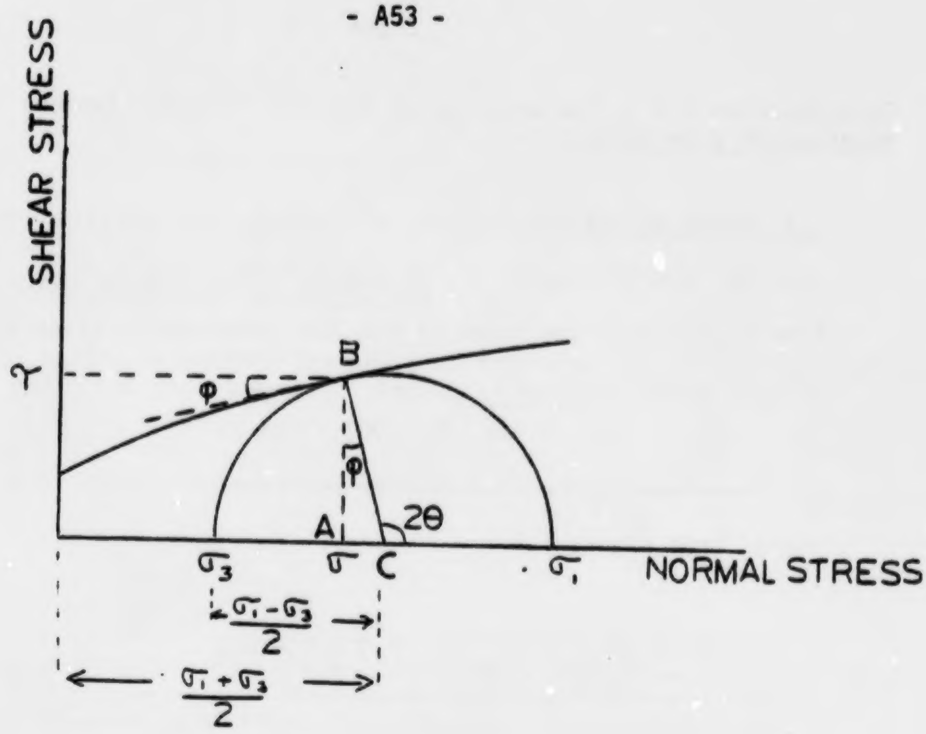
SHEAR STRESS
τ
B
φ
φ
A
2θ
σ3
σ
C
σ1
NORMAL STRESS
(σ1 - σ3)/2
(σ1 + σ3)/2

FIGURE I1: Parabolic Mohr envelope

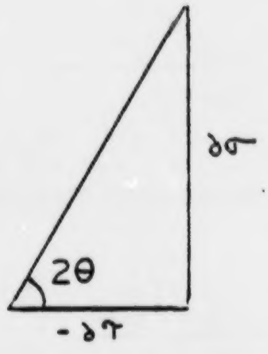

$$\text{COT. } 2\theta = \frac{-\partial\tau}{\partial\sigma} \quad \text{THUS} \quad \text{COS } 2\theta = \frac{-\partial\tau}{\sqrt{\partial\tau^2 + \partial\sigma^2}}$$

FIGURE I2: Relationship between $\frac{\partial\tau}{\partial\sigma}$ and θ

This equation I.6 is the equation of the Mohr failure envelope and is the equation of a parabola.

I.2 Angle of failure

Consider now the angle, θ , of the failure plane.

From Figure I.1, the slope of the Mohr envelope is given by :-

$$\frac{\partial T}{\partial \sigma} = \tan\phi = \tan(2\theta - 90) = \mathrm{Cot}\ 2\theta \qquad (I.7)$$

Hence, from Figure I.2 :-

$$\mathrm{Cos}\ 2\theta = \frac{-\partial T}{\left(\partial T^2 + \partial \sigma^2\right)^{\frac{1}{2}}} = \frac{-\frac{\partial T}{\partial \sigma}}{\left(1 + \left(\frac{\partial T}{\partial \sigma}\right)^2\right)^{\frac{1}{2}}} \qquad (I.8)$$

but, differentiating equation I.6 gives :-

$$\frac{\partial T}{\partial \sigma} = \frac{A}{2T} \qquad (I.9)$$

Hence, from equation I.8 and I.9 :-

$$\mathrm{Cos}^2\ 2\theta = \frac{\left(\frac{A}{2T}\right)^2}{1 + \left(\frac{A}{2T}\right)^2} = \frac{A^2}{4T^2 + A^2}$$

and, from equation I.2, I.5 and I.6 this equation can be written as :-

$$\mathrm{Cos}^2\ 2\theta = \frac{r^2}{4s^2} = \frac{\left[\sigma_1 - \sigma_3\right]^2}{4\left[\sigma_1 + \sigma_3\right]^2}$$

$$\text{i.e. } \cos 2\theta = \frac{-[\sigma_1 - \sigma_3]}{2[\sigma_1 + \sigma_3]} \qquad (I.10)$$

(Note: the negative root applies for positive values of τ).

I.3 Other relationships at failure

Hence, having determined the angle of fracture, the following relationships between τ and σ and the stresses σ_1 and σ_3 at failure can be derived :-

$$\sigma = \left\{\frac{\sigma_1 + \sigma_3}{2}\right\} + \left\{\frac{\sigma_1 - \sigma_3}{2}\right\} \cos 2\theta = \left\{\frac{\sigma_1 + \sigma_3}{2}\right\} - \left\{\frac{(\sigma_1 - \sigma_3)^2}{4\,(\sigma_1 + \sigma_3)}\right\} \qquad (I.11)$$

$$\tau = \left\{\frac{\sigma_1 - \sigma_3}{2}\right\} \sin 2\theta = \left\{\frac{\sigma_1 - \sigma_3}{2}\right\} \left\{\frac{\left[4\,(\sigma_1 + \sigma_3)^2 - (\sigma_1 - \sigma_3)^2\right]^{\frac{1}{2}}}{2\,(\sigma_1 + \sigma_3)}\right\} \qquad (I.12)$$

The following other useful relationships at failure can also be derived:-

$$\tau = \left\{A\sigma + \frac{A^2}{4}\right\}^{\frac{1}{2}} \qquad (I.13)$$

$$s = \left(\frac{A}{2} + \sigma\right) \qquad (I.14)$$

$$\tau = (As)^{\frac{1}{2}} \qquad (I.15)$$

and

$$\sigma_1 = s + r = \frac{A}{2} + \sigma + \left\{\frac{A^2}{2} + A\sigma\right\}^{\frac{1}{2}} \qquad (I.16)$$

$$\sigma_3 = s - r = \frac{A}{2} + \sigma - \left\{\frac{A^2}{2} + A\sigma\right\}^{\frac{1}{2}} \qquad (I.17)$$

In addition, from equation I.1, when $\sigma_3 = 0$, $\sigma_1 = \sigma_c$ the uniaxial compressive strength then :-

$$\underline{\sigma_c = 2A} \qquad (I.18)$$

I.4 Determination of A from triaxial data

Table I.1 gives triaxial strength data obtained for nine coals, with bedding planes parallel and perpendicular to the direction of the major principal stress, σ_1. This data is taken from the work of Hobbs (17).

I.4.1 Method 1 for determining A

From equation I. 1 we have:-

$$\left(\frac{\sigma_1 - \sigma_3}{2}\right)^2 = A\left(\frac{\sigma_1 + \sigma_3}{2}\right)$$

Let $Y = \left(\frac{\sigma_1 - \sigma_3}{2}\right)^2$ and $X = \left(\frac{\sigma_1 + \sigma_3}{2}\right)$

Then A can be determined from linear regression of Y or X by the method of least squares and is given by :-

$$A = \frac{\Sigma Yi}{\Sigma Xi}$$

and the correlation coefficient is given by $\left\{\frac{(\Sigma XiYi)^2}{\Sigma Xi^2\,\Sigma Yi^2}\right\}^{\frac{1}{2}}$

A has been determined by this method for the 18 sets of data for the nine coals studied by Hobbs. Table I.1 gives the values of A so determined and the correlation coefficient. Figures I.4 to I.21 show the Mohr circles for this data, and the envelopes given by the dotted lines on these figures are those obtained by using the values of A determined by this method.

It is seen that, despite the fact that the correlation coefficients are good, the fit to the Mohr circles is not ideal. This is particularly true for the lower confining stress circles. The cause of this is obvious; this method, by taking the square of Y, must give a bias in favour of the high values of Y. It would be better to solve for A using a method which did not have a built in bias. Method 2 gives such an approach.

TABLE I.1 : TRIAXIAL FRACTURE STRENGTH DATA FOR COALS (FROM HOBBS (17))

ORIENTATION OF WEAKNESS PLANES	CONFINING PRESSURE σ_3 P.S.I.	AXIAL FRACTURE STRENGTH - σ_1 P.S.I.								
		COAL 1	COAL 2	COAL 3	COAL 4	COAL 5	COAL 6	COAL 7	COAL 8	COAL 9
Bedding planes parallel, main cleat planes parallel.	0	2630	1020	320	1010	4390	3420	1960	2300	1510
	500	-	5080	3680	5810	7590	8780	7940	8480	5590
	1000	9650	6590	4480	7330	9770	10060	10190	10090	8250
	2000	13520	9460	6940	-	13940	-	-	11970	-
	3000	14280	12580	9980	14490	14380	15460	15890	14480	13360
	4000	19930	15110	13780	-	18920	-	-	16200	-
	5000	22540	16140	15330	18850	20130	19480	21010	18230	16570
Constant in $Y^2 = AX$	A	4628.9	2750.5	2126.9	3394.8	4158.1	3952.5	4257.2	3633.2	2938.5
Correlation Coefficient	r	0.987	0.993	0.978	0.991	0.993	0.997	0.993	0.999	0.996
Bedding planes perpendicular, main cleat planes parallel.	0	4580	1000	770	1920	7450	3460	2280	3160	3150
	500	-	5010	5990	6210	9320	7340	6730	7560	8780
	1000	11100	7350	6160	8520	14020	10460	9220	8350	11600
	2000	14200	9970	8160	-	14930	-	-	12060	-
	3000	18630	11620	11110	13690	16430	15710	15420	14350	17140
	4000	22920	14460	12670	-	17930	-	-	15300	-
	5000	29710*	16040	17000	18160	20030	19820	18910	17900	21230
Constant in $Y^2 = AX$	A	6391.7	2660.8	2457.6	3278.5	4629.0	3906.5	3700.6	3387.0	4581.2
Correlation Coefficient	r	0.973	0.996	0.979	0.994	0.996	0.996	0.994	0.997	0.996

*σ_3 = 4750 in this case.

COAL 1 - PENTEMAWR
COAL 2 - DEEP DUFFRYN
COAL 3 - OAKDALE
COAL 4 - CWMTILLERY
COAL 5 - BARNSLEY HARDS

COAL 6 - BARNSLEY BRIGHTS
COAL 7 - TEVERSAL
COAL 8 - MARKHAM
COAL 9 - LINBY

I.4.2. Method 2 for determining A

Consider Figure I.3; the distance BC = d is the deviation of the "best fit" Mohr envelope from any one Mohr circle. Clearly, for a series of Mohr circles, the "best fit" envelope will be given if we minimize the sums of these deviations squared. A method for solving for A by doing this is given below.

Assume that the Mohr envelope is given by :-

$$\tau^2 - A\sigma - \frac{A^2}{4} = 0 \qquad (I.6)$$

Referring to Figure I.3, to obtain the best fit of a curve of this form to a series of circles with centres s_1, s_2, s_3 etc. it is necessary to minimize the sums of the deviations squared, d_1^2, d_2^2, d_3^2 etc., where

$d = \ell - r$ where ℓ = distance OC and

$$s = \left(\frac{\sigma_1 + \sigma_3}{2}\right) \qquad \text{and} \qquad r = \left(\frac{\sigma_1 - \sigma_3}{2}\right)$$

Now by geometry from Figure I.3 we have :-

$$\ell^2 = \tau_F^2 + (s - \sigma_F)^2$$

and further, $(s - \sigma_F) = \tau_F \tan \phi$

Hence

$$\ell^2 = \tau_F^2 \, (1 + \tan^2 \phi) \qquad (I.19)$$

Thus, from equations I.6 and I.19 we have :-

$$\ell^2 = \left\{A\,\sigma_F + \frac{A^2}{4}\right\}\left\{1 + \tan^2 \phi\right\} \qquad (I.20)$$

Also, by geometry from Figure I.3, we have :-

$$s = \sigma_F + (d + r)\,\text{Sin}\phi$$

i.e.

$$\sigma_F = s - (d + r)\,\text{Sin}\phi \qquad (I.21)$$

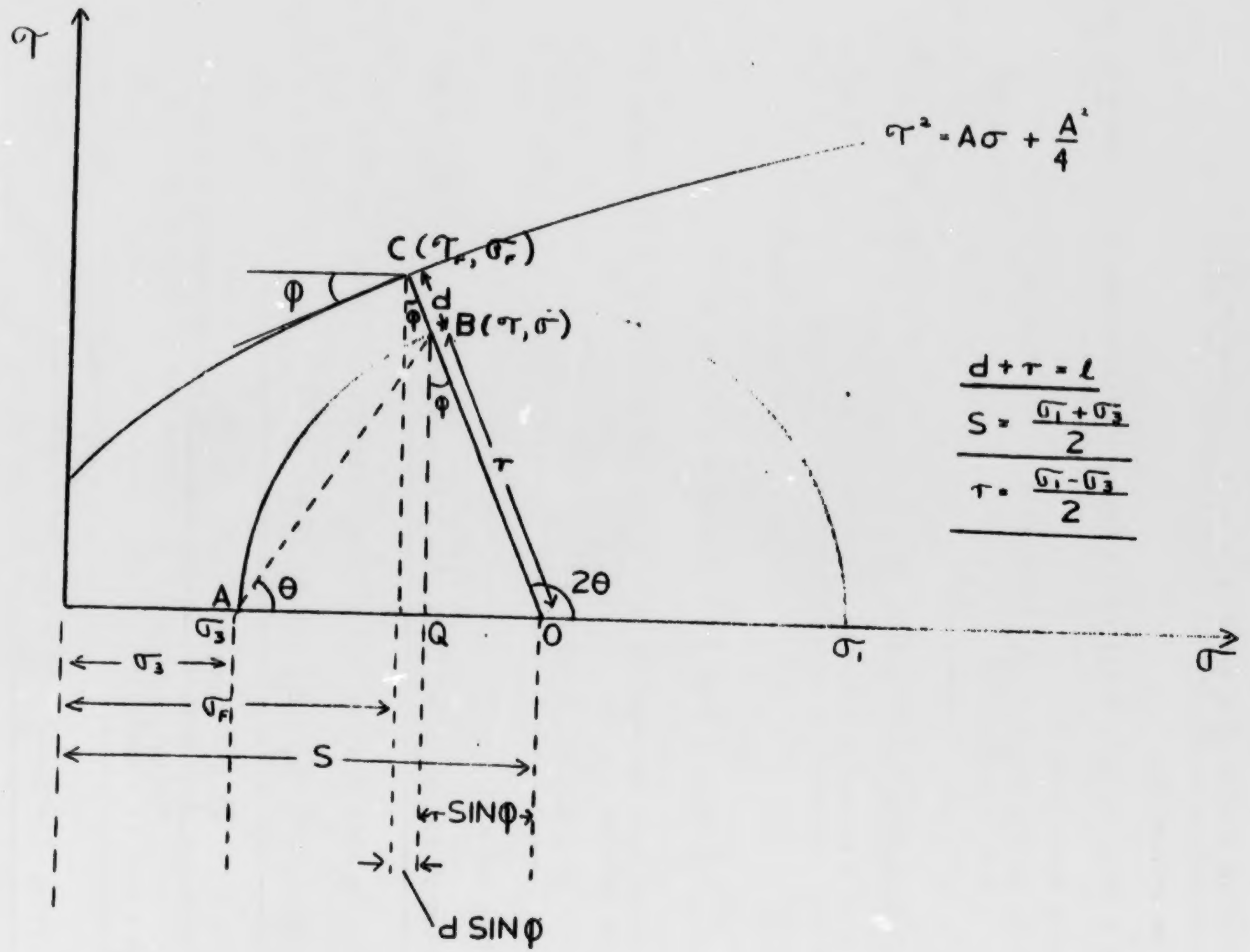
τ
$\tau^2 = A\sigma + \frac{A^2}{4}$
$C(\tau_F, \sigma_F)$
φ
d
$B(\tau, \sigma)$
φ
τ
A
θ
2θ
σ_3
Q
O
σ_1
σ
σ_3
σ_F
S
τ SINϕ
d SINϕ
$d + \tau = \ell$
$S = \frac{\sigma_1 + \sigma_3}{2}$
$\tau = \frac{\sigma_1 - \sigma_3}{2}$

FIGURE 13: Parabolic Mohr envelope

Therefore, from equation I.20 and I.21 :-

$$(d + r)^2 = \left(1 + \tan^2\phi\right)\left(A\left[s - (d + r)\,\mathrm{Sin}\phi\right] + \frac{A^2}{4}\right)$$

which can be written as:-

$$d^2 + d\,(2r + A\mathrm{Sin}\phi + A\tan^2\phi\,\mathrm{Sin}\phi) + r^2 + Ar\mathrm{Sin}\phi + Ar\tan^2\phi\cdot\mathrm{Sin}\phi + \left[1 + \tan^2\phi\right]\left[As + \frac{A^2}{4}\right] = 0$$

which solving for d gives :-

$$d = \frac{-E \pm \left(E^2 - 4F\right)^{\frac{1}{2}}}{2} \qquad \text{(I.22)}$$

where $E = 2r + A\mathrm{Sin}\phi + A\tan^2\phi\,\mathrm{Sin}\phi$ (I.23)

and $F = r^2 + Ar\mathrm{Sin}\phi\left[1 + \tan^2\phi\right] - \left[1 + \tan^2\phi\right]\left[As + \frac{A^2}{4}\right]$ (I.24)

and from I.22

$$d^2 = \frac{1}{4}\left(E^2 \pm 2E(E^2 - 4F)^{\frac{1}{2}} + E^2 - 4F\right)$$

and, noting that the negative root is the one applicable in this case, this equation becomes:-

$$d^2 = \frac{E^2}{2} - F - \frac{E}{2}\left(E^2 - 4F\right)^{\frac{1}{2}} \qquad \text{(I.25)}$$

Thus for n circles :-

$$(\text{the sum of the deviation})^2 = \Sigma\left[\frac{Ei^2}{2} - Fi - \frac{Ei}{2}\left(Ei^2 - 4Fi\right)^{\frac{1}{2}}\right] \qquad \text{(I.26)}$$

Differentiating this equation partially with respect to A gives :-

$$\frac{\partial(d^2)}{\partial A} = \Sigma\left\{Ei\,\frac{\partial Ei}{\partial A} - \frac{\partial Fi}{\partial A} - \frac{1}{2}\frac{\partial Ei}{\partial A}\left\{Ei^2 - 4Fi\right\}^{\frac{1}{2}} - \frac{Ei}{2}\left\{Ei^2 - 4Fi\right\}^{-\frac{1}{2}}\left[Ei\,\frac{\partial Ei}{\partial A} - 2\,\frac{\partial Fi}{\partial A}\right]\right. \qquad \text{(I.27)}$$

where $\frac{\partial Ei}{\partial A} = \mathrm{Sin}\phi\,(1 + \tan^2\phi)$ (I.28)

and $\frac{\partial Fi}{\partial A} = r\mathrm{Sin}\phi\left(1 + \tan^2\phi\right) - \left(1 + \tan^2\phi\right)\left(s + \frac{A}{2}\right)$ (I.29)

Thus, provided that ϕ is known, a computer program can be written to derive the value of A for which $\frac{\partial(d^2)}{\partial A}$ is zero; i.e. for which $\Sigma(d^2)$ is minimized. This can be done from an initial estimate of A.

Consider now the evaluation of ϕ.

The equation for a system of Mohr's circles can be written as:-

$$\left\{\sigma - \frac{(\sigma_1+\sigma_3)}{2}\right\}^2 + T^2 = \left\{\frac{\sigma_1-\sigma_3}{2}\right\}^2 \qquad (I.30)$$

if the partial derivative of σ_1 with respect to σ_3 is determined and solved for σ then:-

$$\sigma = \sigma_3 + \frac{(\sigma_1-\sigma_3)}{(\frac{\partial\sigma_1}{\partial\sigma_3} + 1)} \qquad (I.31)$$

and if equation I.31 is substituted into equation I.30 then :-

$$T = \frac{(\sigma_1-\sigma_3)}{(\frac{\partial\sigma_1}{\partial\sigma_3} + 1)} \sqrt{\frac{\partial\sigma_1}{\partial\sigma_3}} \qquad (I.32)$$

from these two equations the following ratio is obtained

$$\frac{T}{(\sigma_1-\sigma_3)} = \sqrt{\frac{\partial\sigma_1}{\partial\sigma_3}} \qquad (I.33)$$

and it is seen from the triangle BQA, Figure I.3, that this is the ratio of BQ to AQ which is equal to $\tan\theta$ where θ is the angle of failure

therefore $$\tan\theta = \sqrt{\frac{\partial\sigma_1}{\partial\sigma_3}} \qquad (I.34)$$

but also, by geometry:-

$$2\theta = \phi + 90^\circ$$

where ϕ is the slope of the tangent to the Mohr circle.

Hence

$$\frac{\partial T}{\partial \sigma} = \tan\phi = \frac{\left(\frac{\partial \sigma_1}{\partial \sigma_3} - 1\right)}{2\sqrt{\frac{\partial \sigma_1}{\partial \sigma_3}}} \tag{I.34}$$

but this slope is also of the Mohr envelope, $\frac{\partial T_F}{\partial \sigma_F}$

Hence

$$\tan\phi = \left\{\frac{\left(\frac{\partial \sigma_1}{\partial \sigma_3} - 1\right)}{2\sqrt{\frac{\partial \sigma_1}{\partial \sigma_3}}}\right\} \tag{I.35}$$

Hence ϕ can be evaluated from this equation.

The steps for solution are therefore as follows, given n data pairs (σ_1, σ_3)

1. Process the data to derive:-

   $\frac{\Delta\sigma_1}{\Delta\sigma_3}$, σ_1 and σ_3 for (n-1) data sets as illustrated in Table I.2

2. For each of the (n-1) data pairs, calculate ϕ from:-

$$\phi = \tan^{-1}\left\{\frac{\left(\frac{\Delta\sigma_1}{\Delta\sigma_3} - 1\right)}{2\sqrt{\frac{\Delta\sigma_1}{\Delta\sigma_3}}}\right\}$$

3. Evaluate Ei, Fi, $\frac{\partial Ei}{\partial A}$, $\frac{\partial Fi}{\partial A}$ from equation I.23, I.24, I.28, I.29 respectively, assuming an arbitary value of A.

Table I.2 : Processing of data for determination of A

INITIAL DATA		PROCESSED DATA - (n-1) data sets				
σ_1	σ_3	$\Delta\sigma_1$	$\Delta\sigma_3$	$\frac{\Delta\sigma_1}{\Delta\sigma_3}$	σ_1	σ_3
σ_{11}	σ_{31}					
		$(\sigma_{12} - \sigma_{11})$	$\sigma_{32} - \sigma_{31}$	$\frac{\sigma_{21} - \sigma_{11}}{\sigma_{32} - \sigma_{31}}$	$\frac{\sigma_{11} + \sigma_{12}}{2}$	$\frac{\sigma_{32} + \sigma_{31}}{2}$
σ_{12}	σ_{32}					
		$(\sigma_{13} - \sigma_{12})$	$\sigma_{33} - \sigma_{32}$	$\frac{\sigma_{13} - \sigma_{12}}{\sigma_{33} - \sigma_{32}}$	$\frac{\sigma_{12} + \sigma_{13}}{2}$	$\frac{\sigma_{33} + \sigma_{32}}{2}$
σ_{13}	σ_{33}					
		$\sigma_{1n} - \sigma_{1(n-1)}$	$\sigma_{3n} - \sigma_{3(n-1)}$	$\frac{\sigma_{1n} - \sigma_{1(n-1)}}{\sigma_{3n} - \sigma_{3(n-1)}}$	$\frac{\sigma_{1n} + \sigma_{1(n-1)}}{2}$	$\frac{\sigma_{3n} + \sigma_{3(n-1)}}{2}$
σ_{1n}	σ_{3n}					

4. Evaluate $\frac{\partial(d^2)}{\partial A}$ from equation I.27, repeat for different A values until $\frac{\partial(d^2)}{\partial A} = 0$.

A computer program has been written to carry out this operation. This program is given in Appendix J.

The results for Hobbs data are given in Table I.3 and the solid line envelopes shown on Figures I.4 to I.21 give the Mohr envelopes determined using this method. In all cases, the fit is apparently as good as or better than that obtained by the method 1. Table I.4 compares the values of A determined by both methods. On average there is an 8.7% difference between the two solutions for A but in some cases the difference is over 20%. Clearly the second method is preferable from the theoretical view point.

I.5 Conclusion

A parabolic Mohr envelope of the form assumed in this section gives an acceptable fit to the experimentally derived fracture data for a range of coals. It is preferable however to use Method 2 to derive the "Mohr" constant A.

TABLE I.3 : TRIAXIAL FRACTURE STRENGTH DATA FOR COALS (FROM HOBBS (17))

ORIENTATION OF WEAKNESS PLANES	CONFINING PRESSURE σ_3 P.S.I.	AXIAL FRACTURE STRENGTH - σ_1 P.S.I.								
		COAL 1	COAL 2	COAL 3	COAL 4	COAL 5	COAL 6	COAL 7	COAL 8	COAL 9
Bedding planes parallel, main cleat planes parallel.	0	2630	1020	320	1010	4390	3420	1960	2300	1510
	500	-	5080	3680	5810	7590	8780	7940	8480	5590
	1000	9650	6590	4480	7330	9770	10060	10190	10090	8250
	2000	13520	9460	6940	-	13940	-	-	11970	-
	3000	14280	12580	9980	14490	14380	15460	15890	14480	13360
	4000	19930	15110	13780	-	18920	-	-	16200	-
	5000	22540	16140	15330	18850	20130	19480	21010	18230	16570
	A	3859.8	2952.2	1853.2	3072.4	3357.1	3808.8	3900.6	3560.6	2791.9
Bedding planes perpendicular, main cleat planes parallel.	0	4580	1000	770	1920	7450	3460	2280	3160	3150
	500	-	5010	5990	6210	9320	7340	6730	7560	8780
	1000	11100	7350	6160	8520	14020	10460	9220	8350	11600
	2000	14200	9970	8160	-	14930	-	-	12060	-
	3000	18630	11620	11110	13690	16430	15710	15420	14350	17140
	4000	22920	14460	12670	-	17930	-	-	15300	-
	5000	29710*	16040	17000	18160	20030	19820	18910	17900	21230
	A	4913.5	2545.1	1769.4	3043.6	4387.3	3790.0	3494.2	3184.8	4352.8

*σ_3 = 4750 in this case.

COAL 1 - PENTEMAWR
COAL 2 - DEEP DUFFRYN
COAL 3 - OAKDALE
COAL 4 - CWMTILLERY
COAL 5 - BARNSLEY HARDS

COAL 6 - BARNSLEY BRIGHTS
COAL 7 - TEVERSAL
COAL 8 - MARKHAM
COAL 9 - LINBY

Table I. 4 : Comparison of A values by methods 1 and 2

Coal	Bedding planes parallel	Bedding planes perpendicular	A Method 1	A Method 2	% difference
Pentemawr	x		4629	3860	16.6
		x	6392	4914	23.1
Deep Duffryn	x		2750	2952	-7.3
		x	2660	2545	4.3
Oakdale	x		2127	1853	12.9
		x	2458	1769	28.0
Cwmtillery	x		3395	3072	9.5
		x	3279	3045	7.1
Barnsley Hards	x		4158	3357	19.3
		x	4629	4387	5.2
Barnsley Brights	x		3952	3809	3.6
		x	3907	3790	3.0
Teversal	x		4257	3901	8.4
		x	3701	3494	5.6
Markham	x		3633	3561	2.0
		x	3387	3185	6.0
Linby	x		2939	2792	5.0
		x	4581	4353	5.0

FIGURE 14:

MOHR DIAGRAM AND ENVELOPE FOR PENTREMAWR COAL BEDDING PLANES PARALLEL (COAL I)

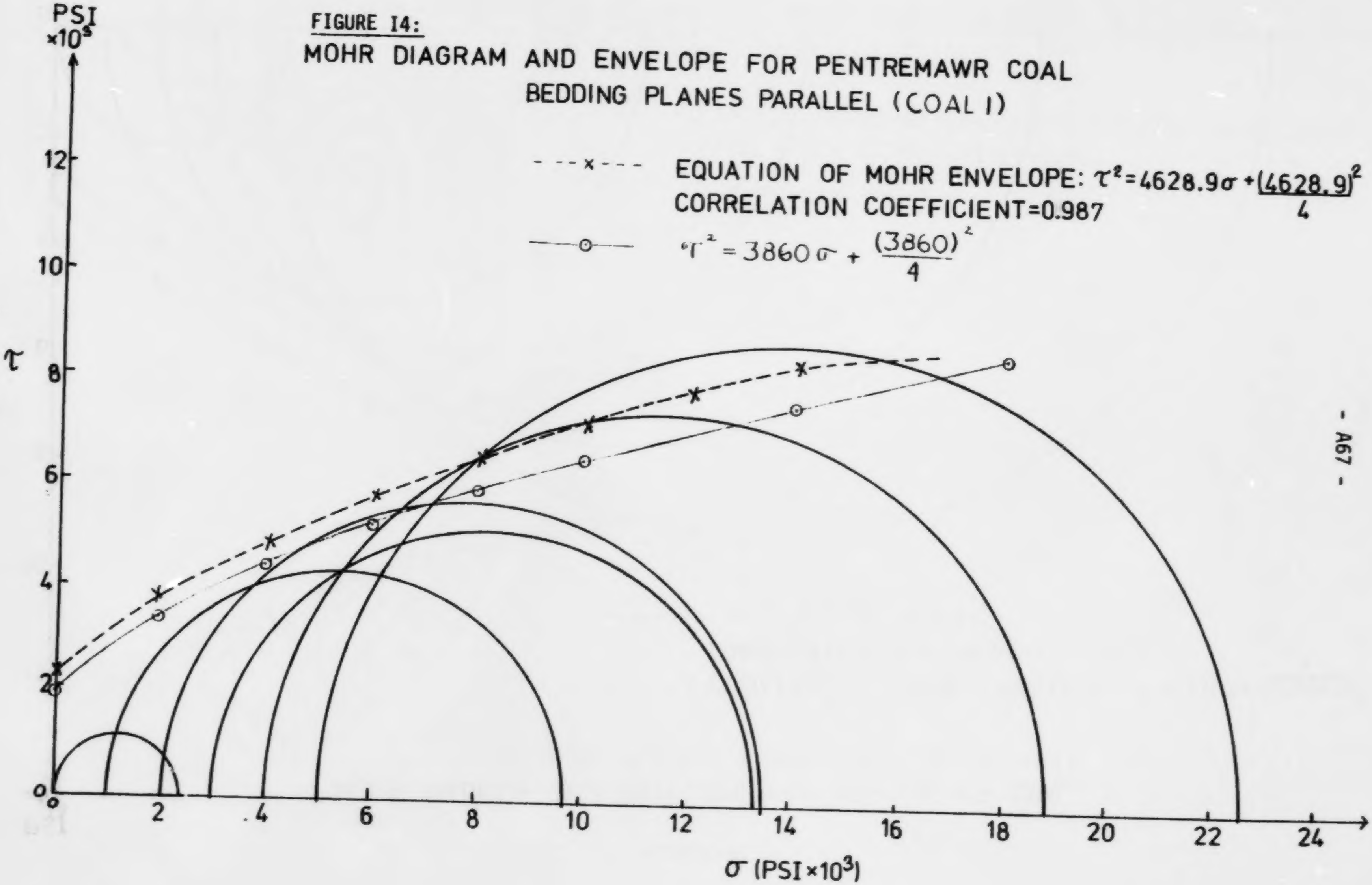

FIGURE 15:
MOHR DIAGRAM AND ENVELOPE FOR PENTEMAWR COAL BEDDING PLANES PERPENDICULAR (COAL I)

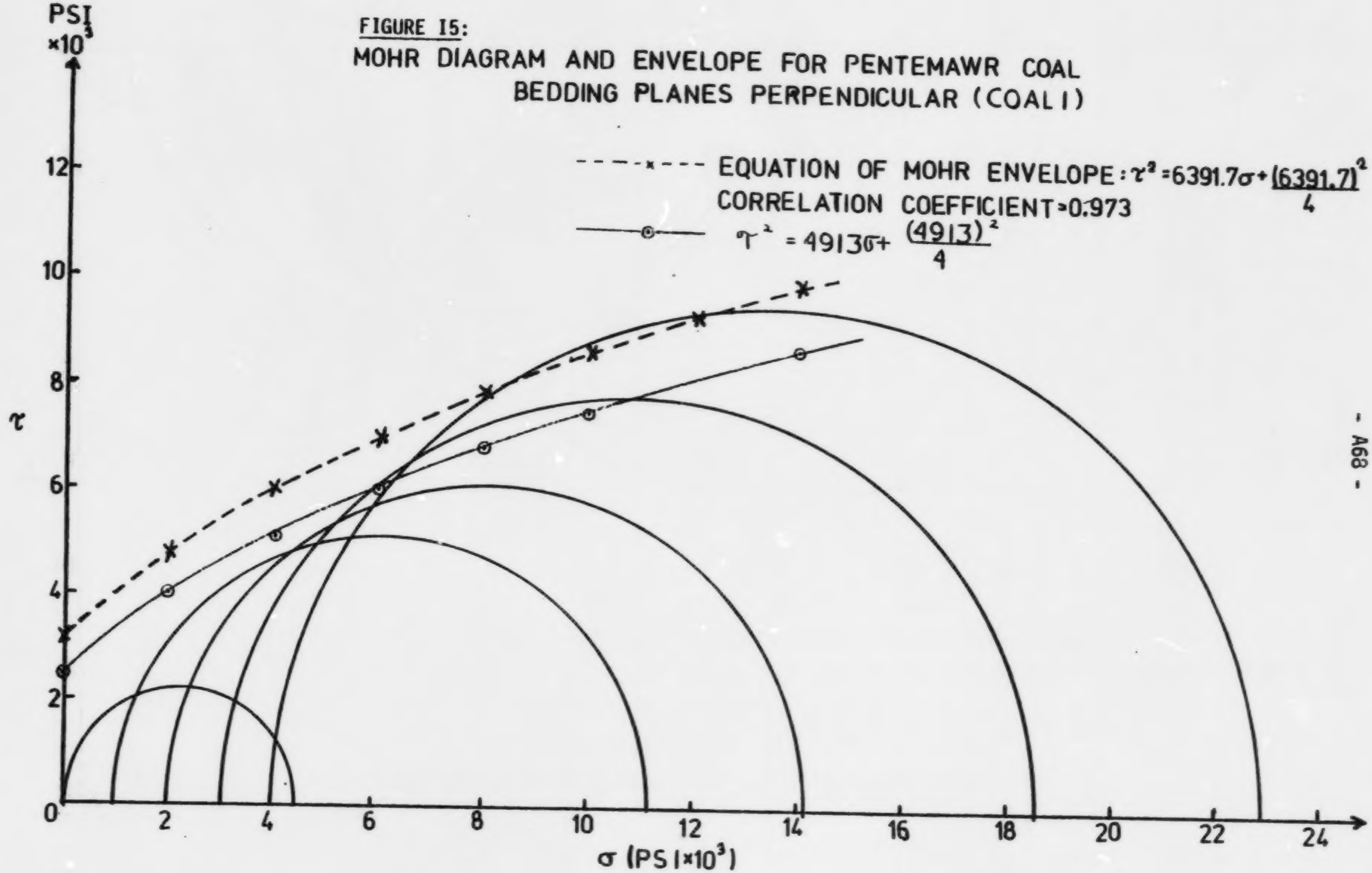

FIGURE I6:
MOHR DIAGRAM AND ENVELOPE FOR DEEP DUFFRYN COAL BEDDING PLANES PARALLEL (COAL 2)

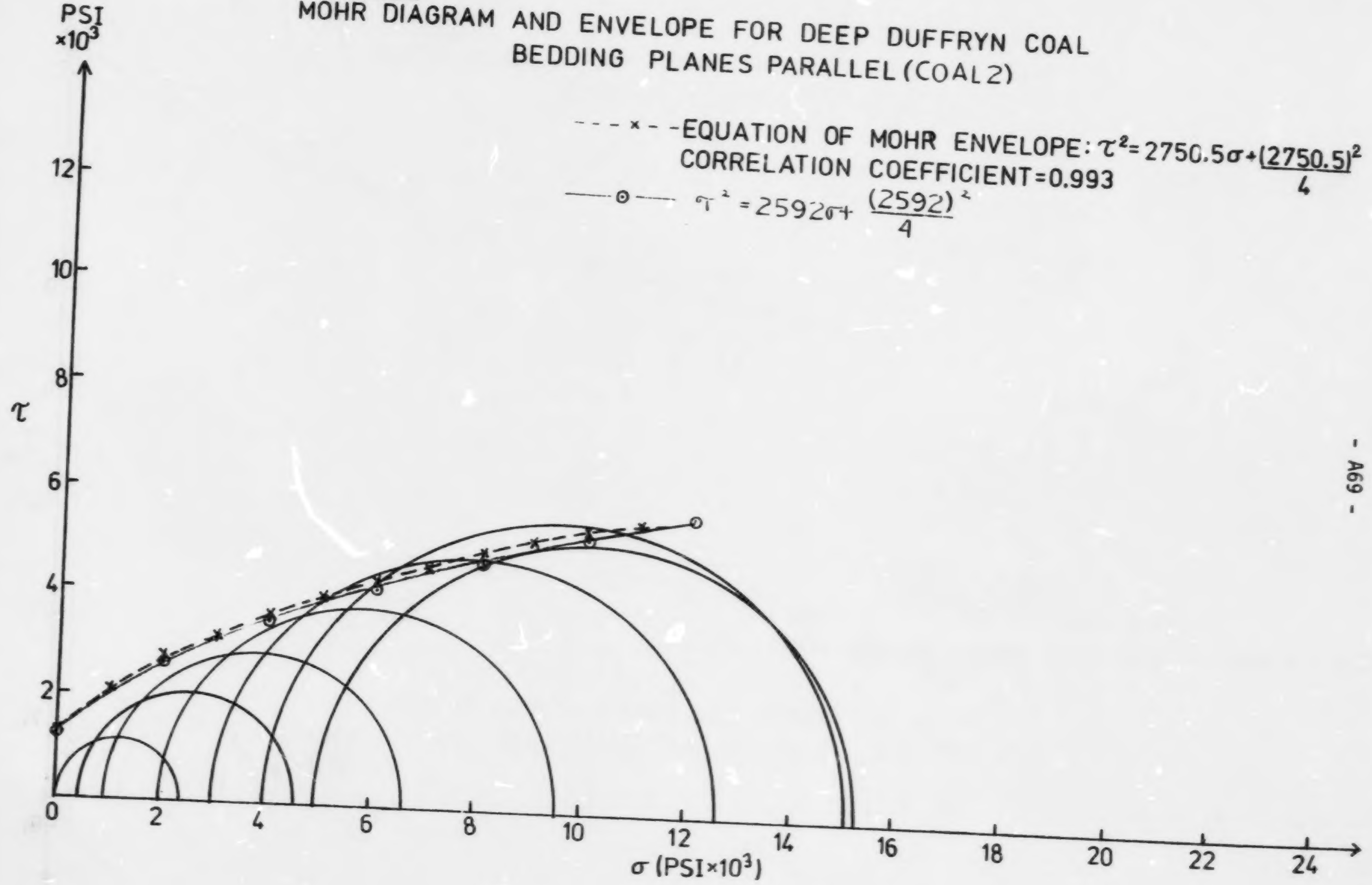

FIGURE 17:
MOHR DIAGRAM AND ENVELOPE FOR DEEP DUFFRYN COAL BEDDING PLANES PERPENDICULAR (COAL 2)

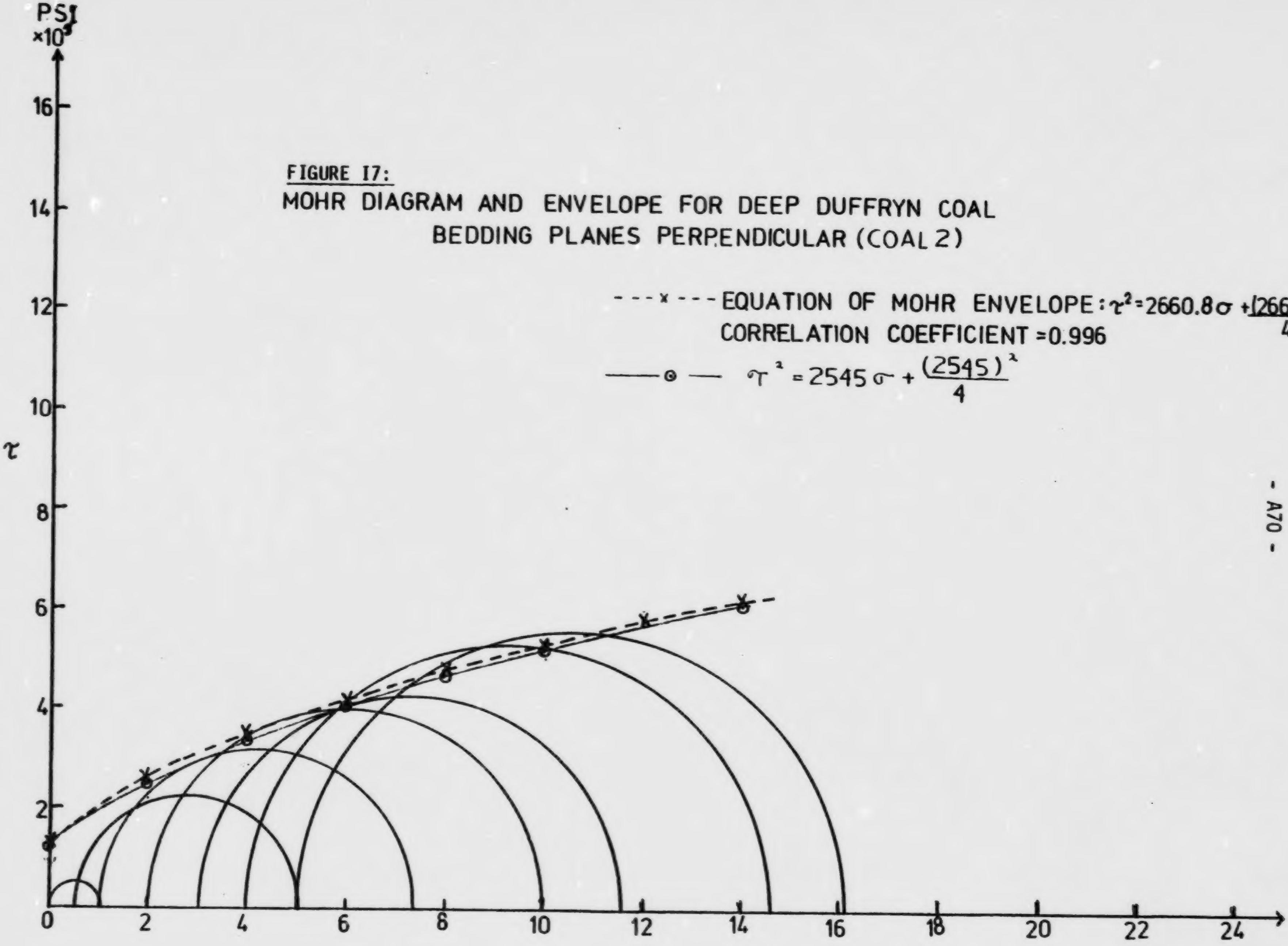

FIGURE 18:

MOHR DIAGRAM AND ENVELOPE FOR OAKDALE COAL BEDDING PLANES PARALLEL (COAL 3)

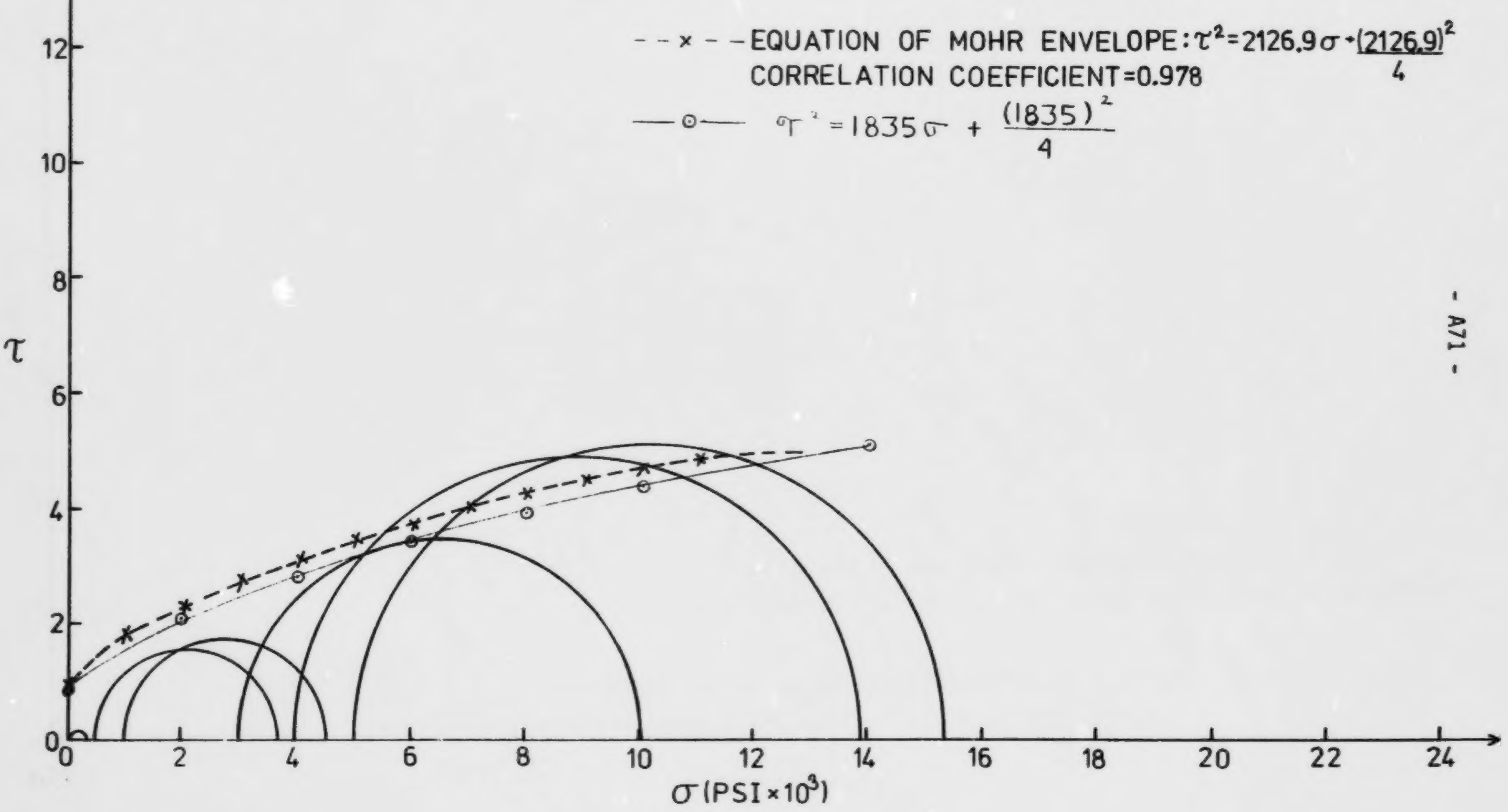

FIGURE 19:

MOHR DIAGRAM AND ENVELOPE FOR OAKDALE COAL
BEDDING PLANES PERPENDICULAR (COAL3)

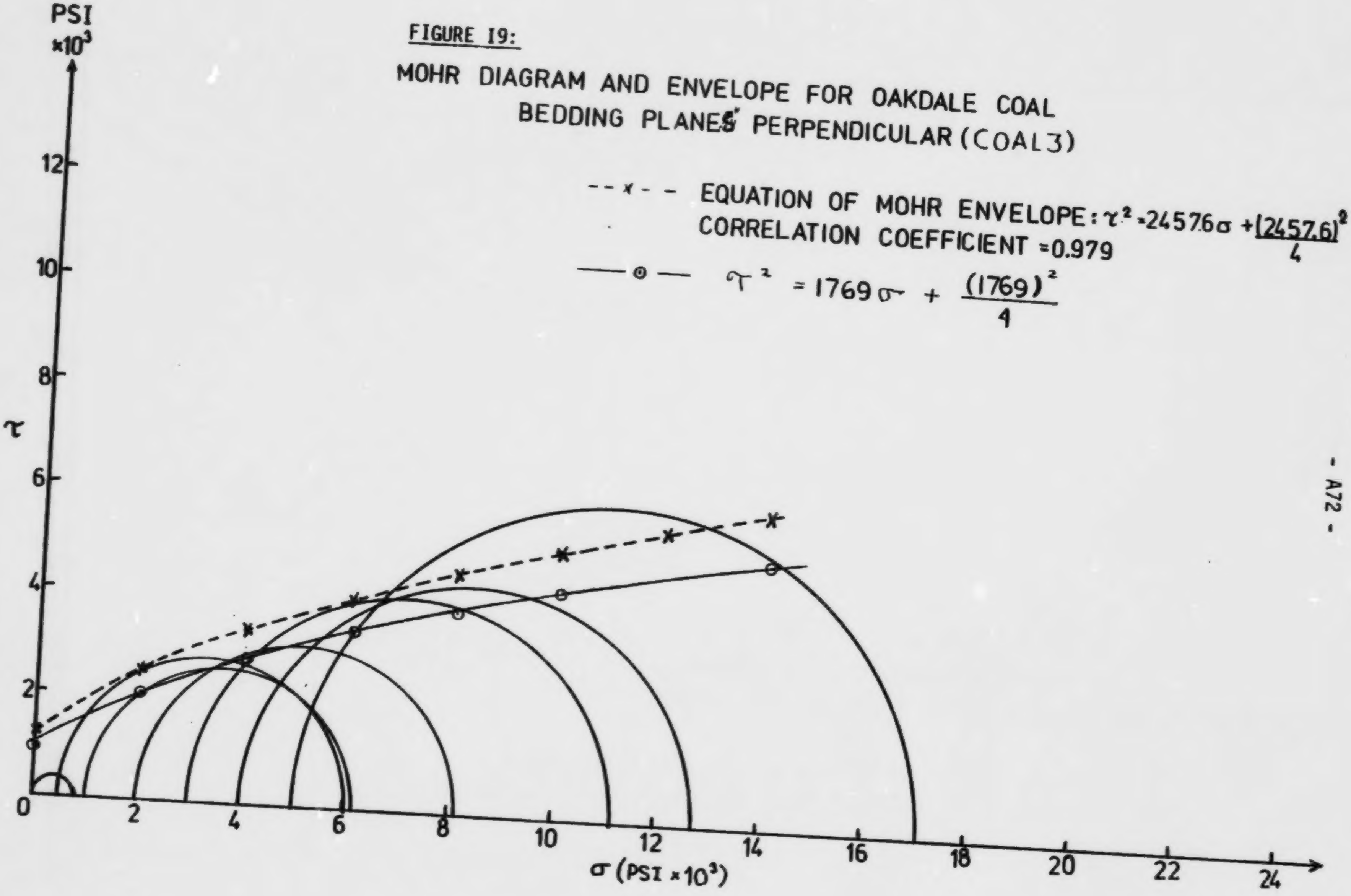

FIGURE I10:
MOHR DIAGRAM AND ENVELOPE FOR CWMTILLERY COAL BEDDING PLANES PARALLEL (COAL 4)

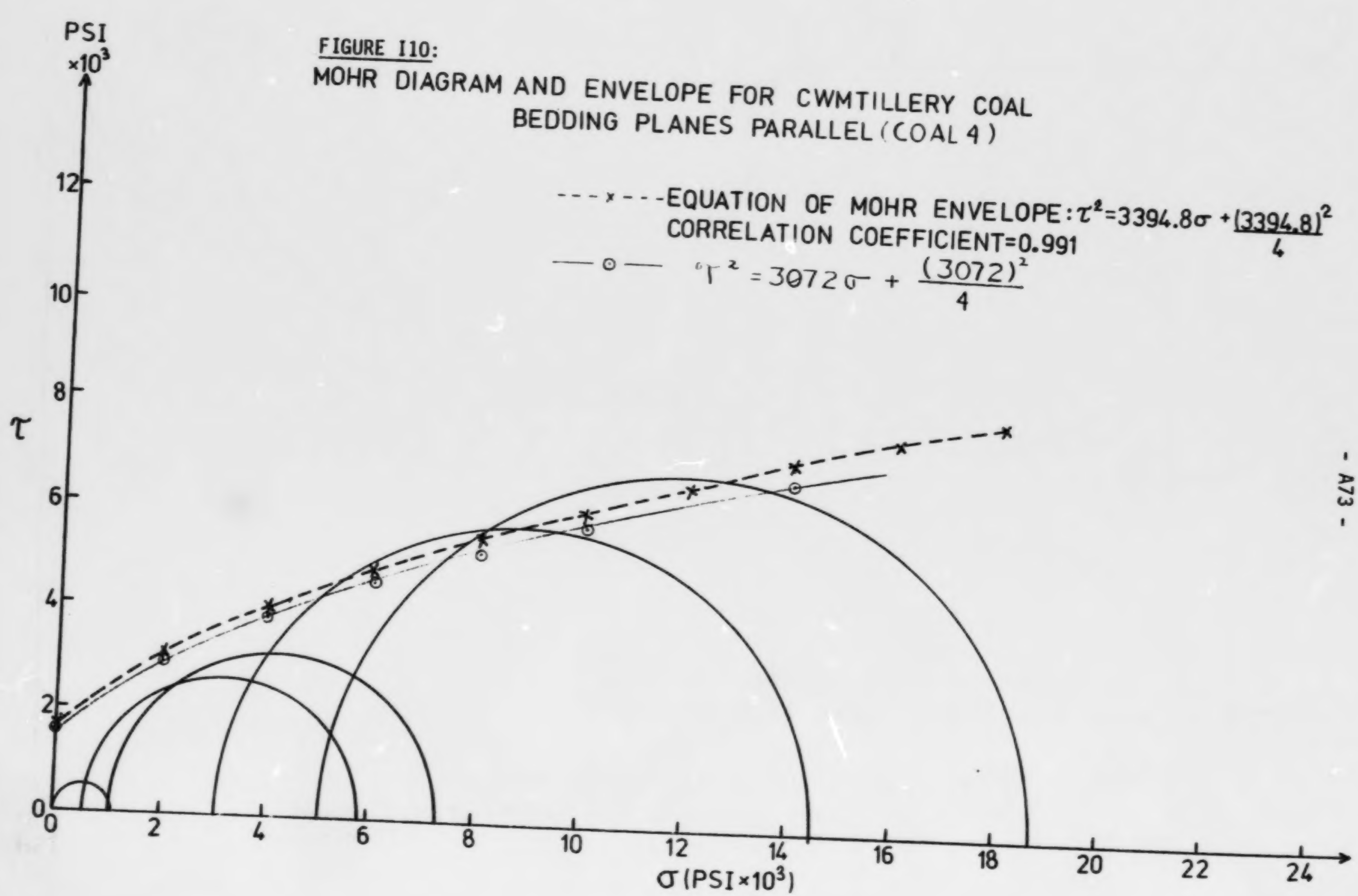

FIGURE I11:
MOHR DIAGRAM AND ENVELOPE FOR CWIMTILLERY COAL BEDDING PLANES PERPENDICULAR (COAL 4)

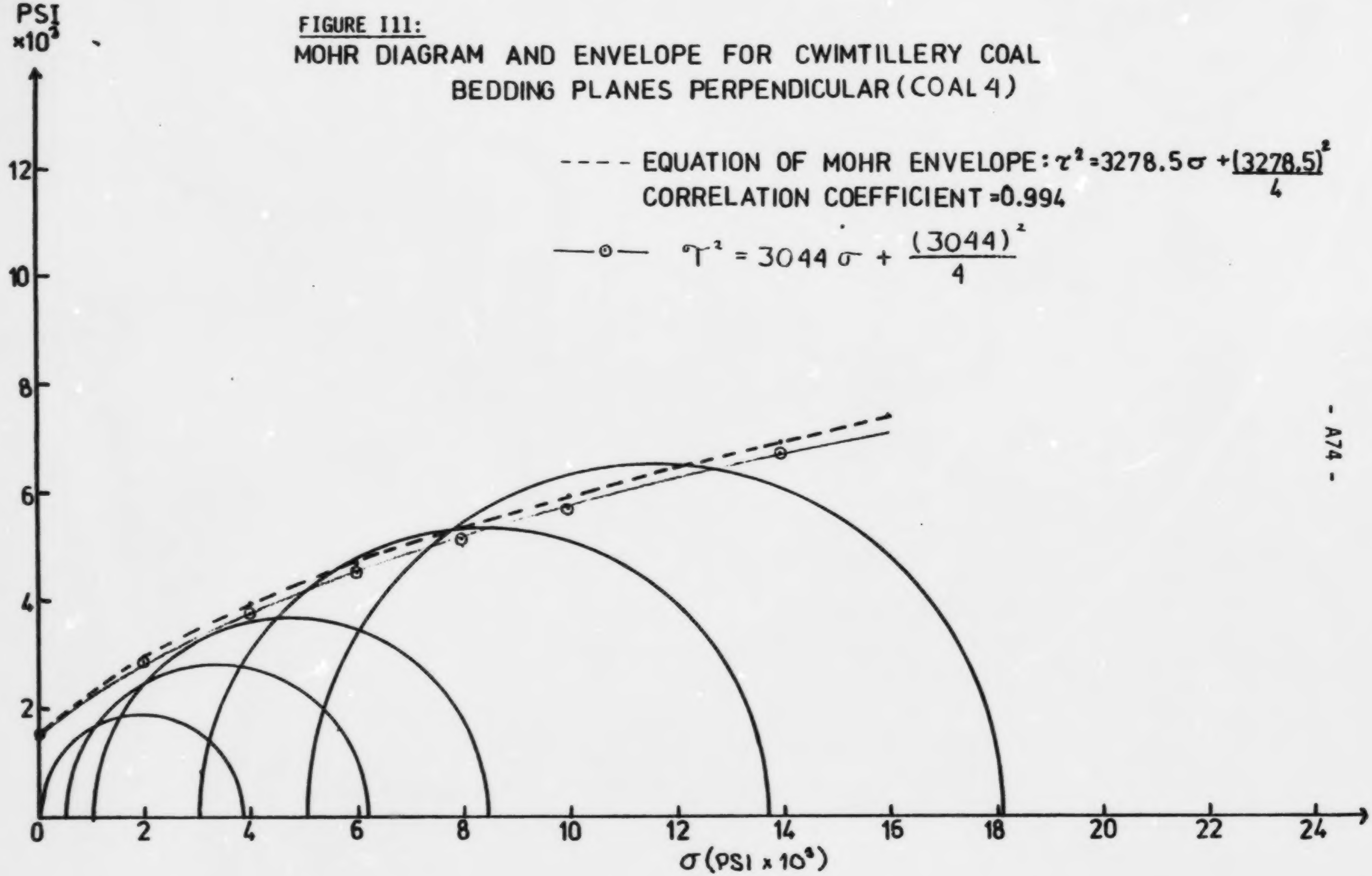

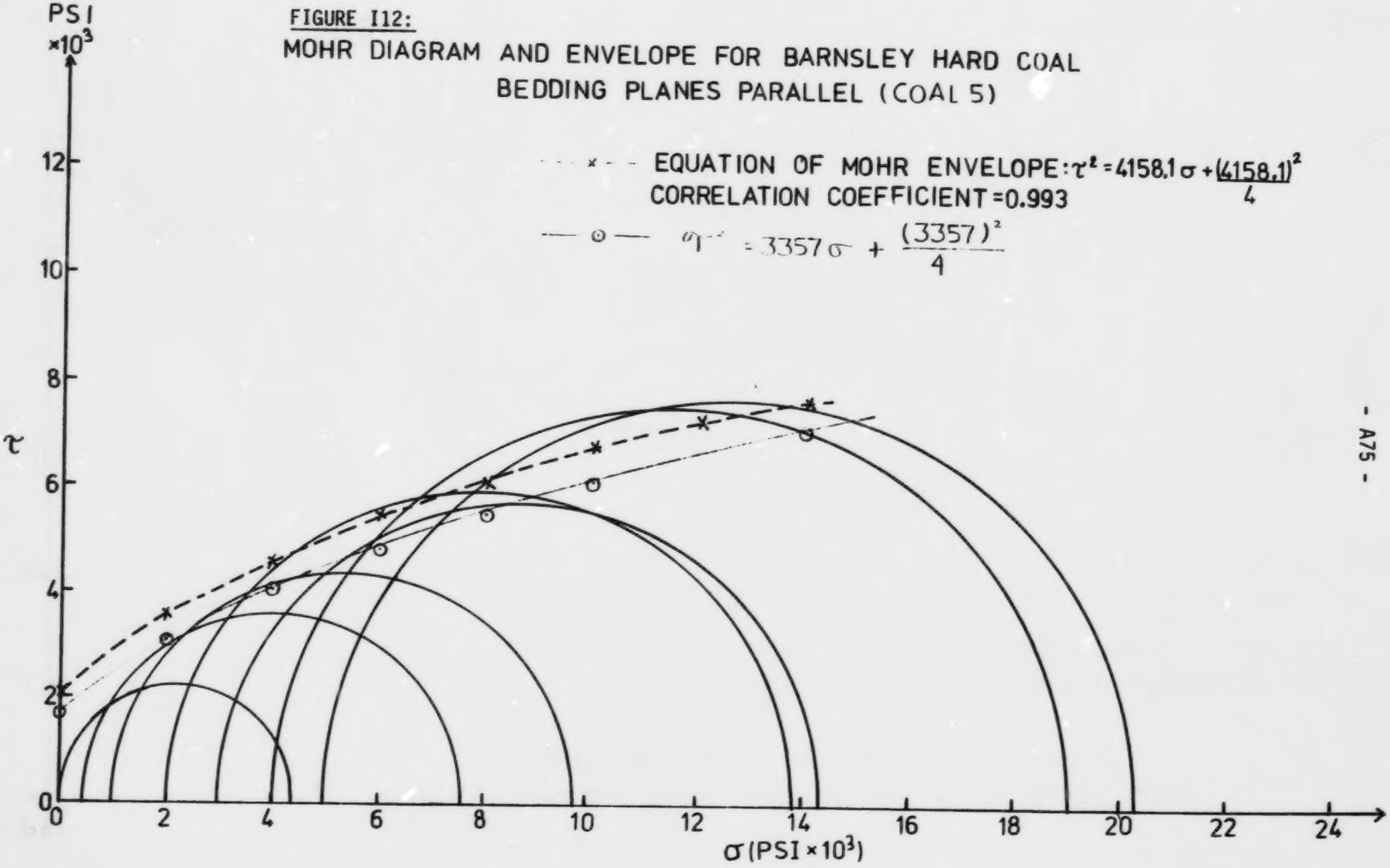

FIGURE I12:
MOHR DIAGRAM AND ENVELOPE FOR BARNSLEY HARD COAL
BEDDING PLANES PARALLEL (COAL 5)

FIGURE I13:
MOHR DIAGRAM AND ENVELOPE FOR BARNSLEY HARDS COAL BEDDING PLANES PERPENDICULAR (COAL 5)

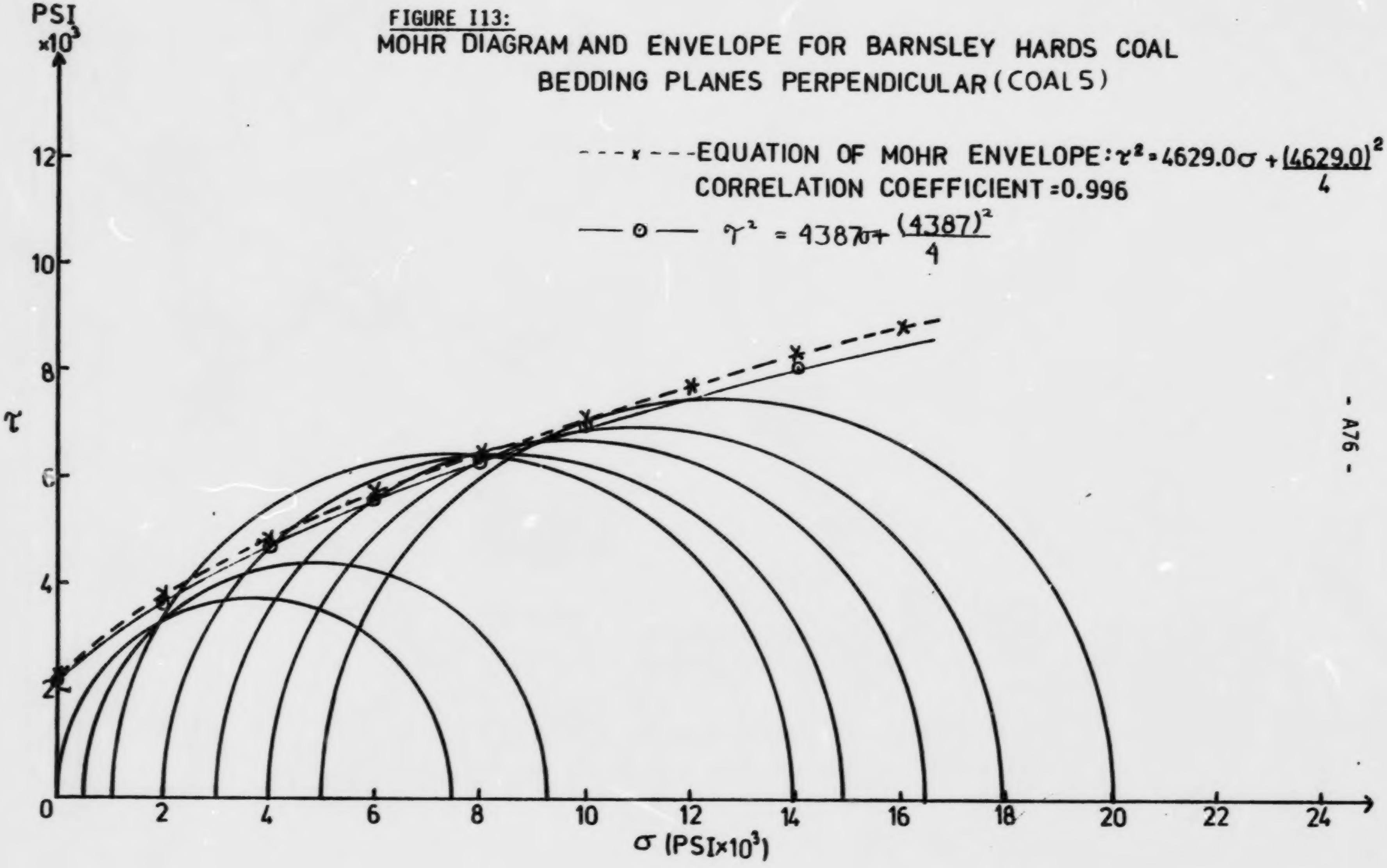

- - -×- - - EQUATION OF MOHR ENVELOPE: $\tau^2 = 4629.0\sigma + \frac{(4629.0)^2}{4}$
CORRELATION COEFFICIENT = 0.996

—⊙— $\tau^2 = 4387\sigma + \frac{(4387)^2}{4}$

FIGURE I14:
MOHR DIAGRAM AND ENVELOPE FOR BARNSLEY BRIGHTS COAL BEDDING PLANES PARALLEL (COAL 6)

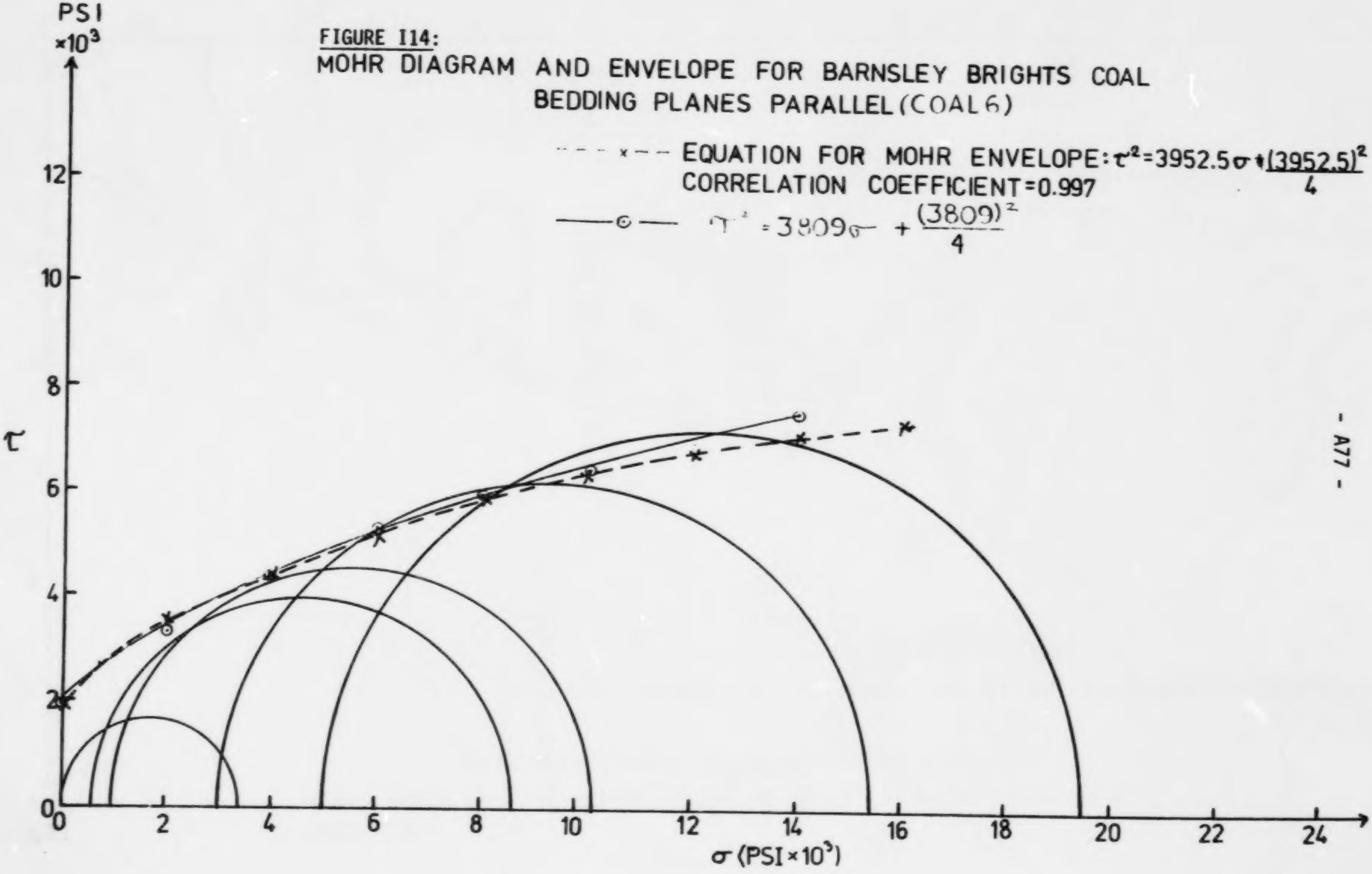

FIGURE I15:

MOHR DIAGRAM AND ENVELOPE FOR BARNSLEY BRIGHTS COAL BEDDING PLANES PERPENDICULAR (COAL6)

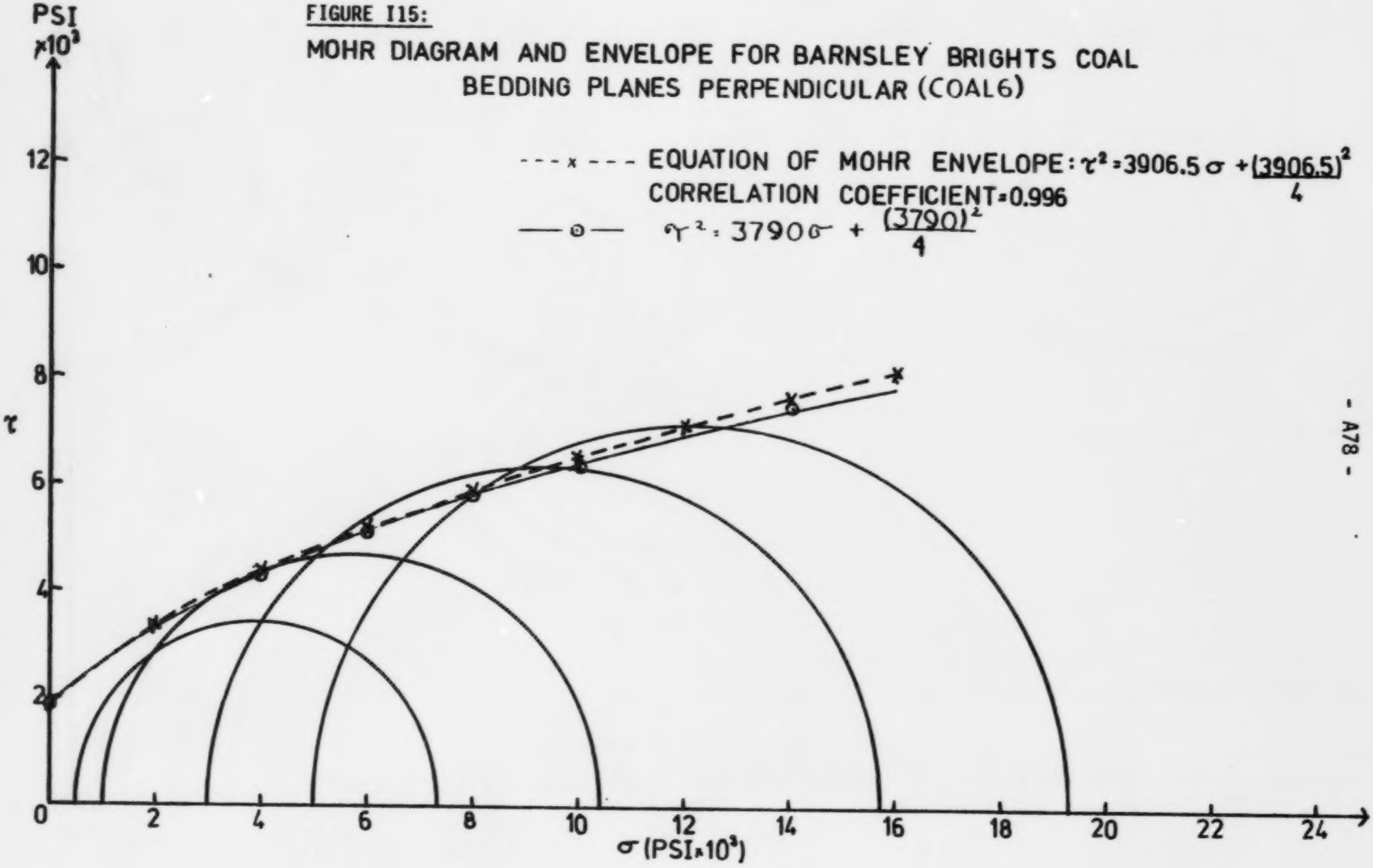

- - - x - - - EQUATION OF MOHR ENVELOPE: $\tau^2 = 3906.5\sigma + \frac{(3906.5)^2}{4}$

CORRELATION COEFFICIENT = 0.996

—⊙— $\tau^2 = 3790\sigma + \frac{(3790)^2}{4}$

FIGURE I16:

MOHR DIAGRAM AND ENVELOPE FOR TEVERSAL COAL BEDDING PLANES PARALLEL (COAL7)

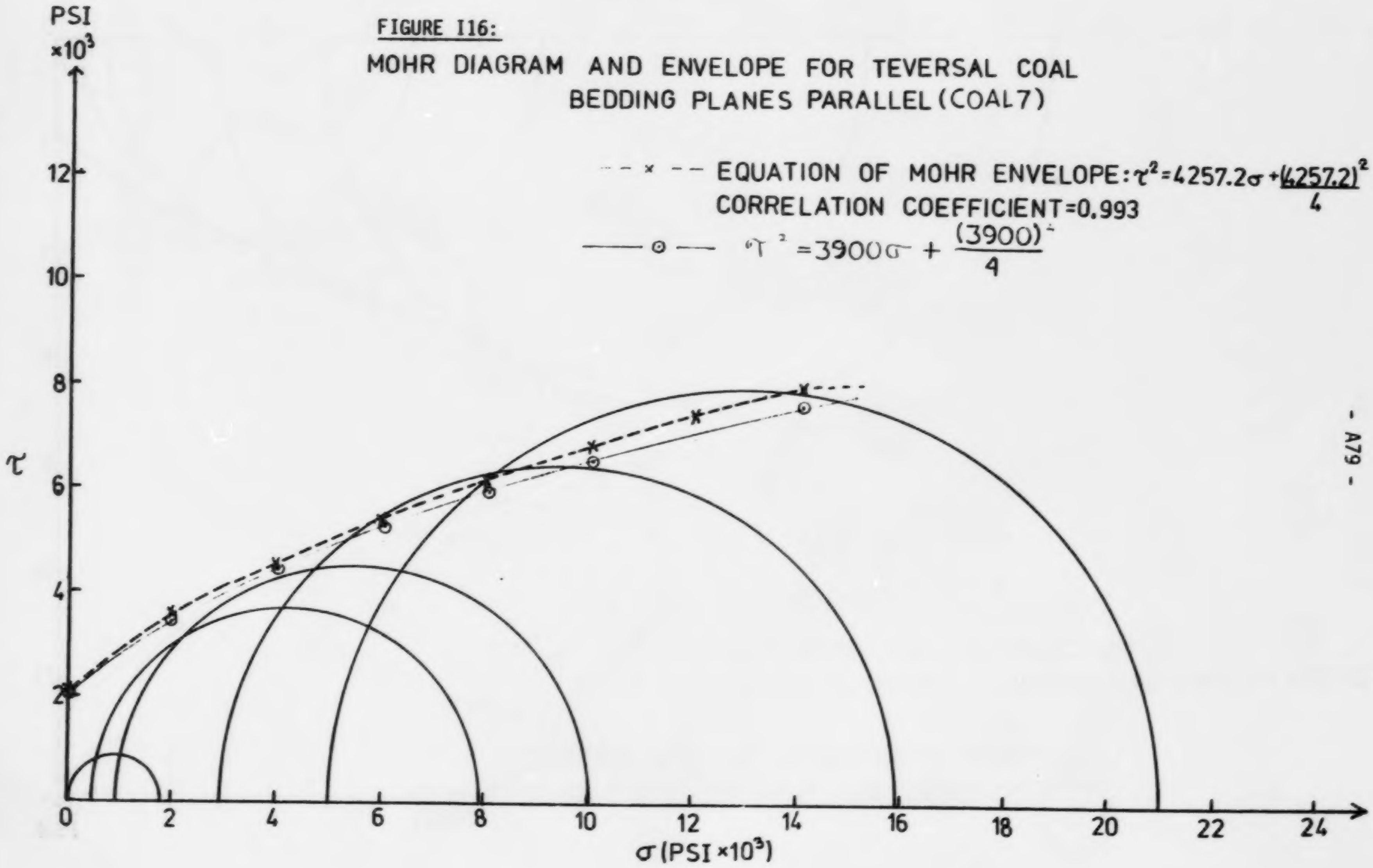

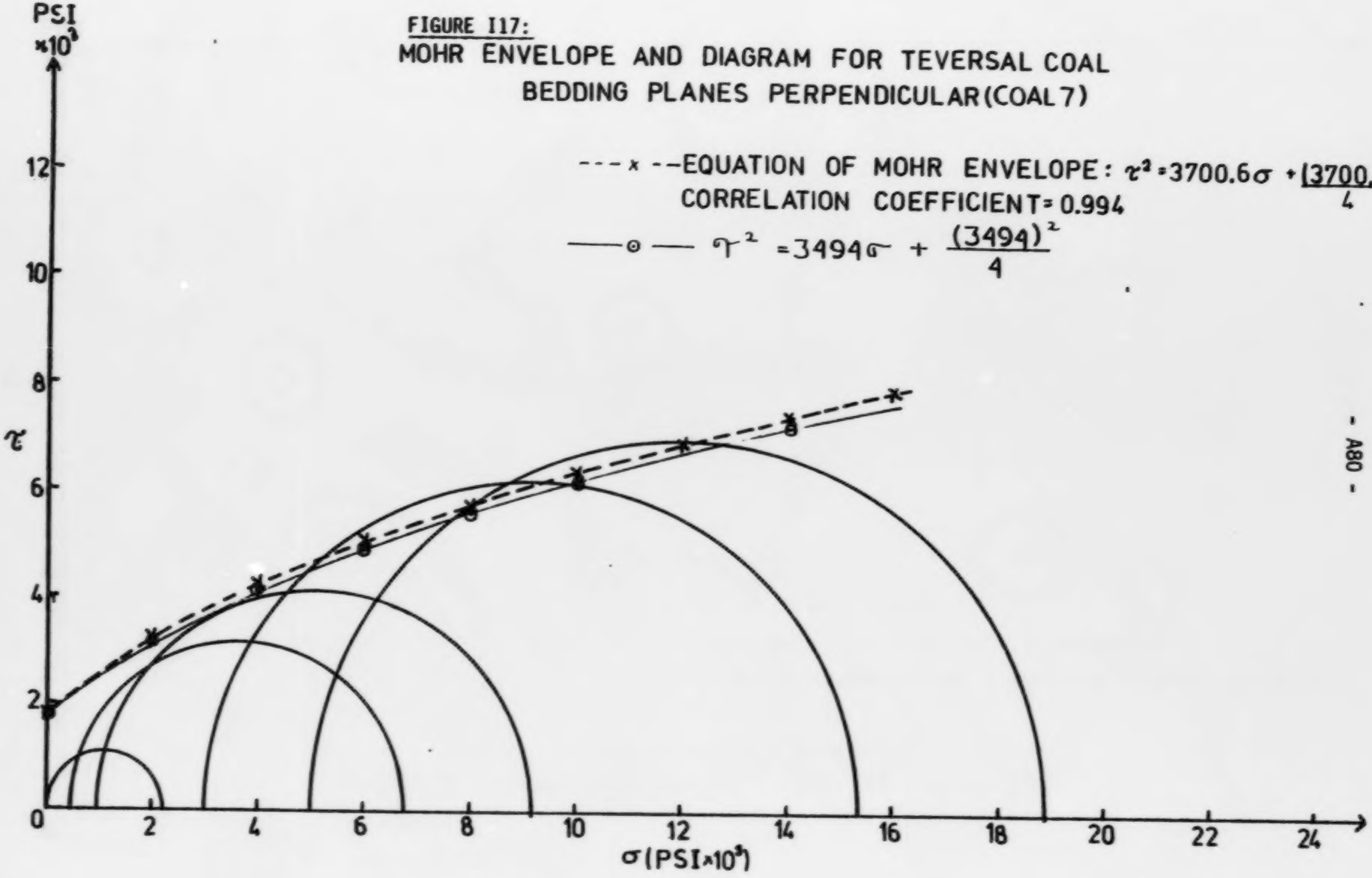
FIGURE I17:
MOHR ENVELOPE AND DIAGRAM FOR TEVERSAL COAL BEDDING PLANES PERPENDICULAR(COAL 7)

- - - x - -EQUATION OF MOHR ENVELOPE: $\tau^2 = 3700.6\sigma + \frac{(3700.6)^2}{4}$
CORRELATION COEFFICIENT= 0.994

——⊙—— $\tau^2 = 3494\sigma + \frac{(3494)^2}{4}$

FIGURE I18:

MOHR DIAGRAM AND ENVELOPE FOR MARKHAM COAL BEDDING PLANES PARALLEL (COAL 8)

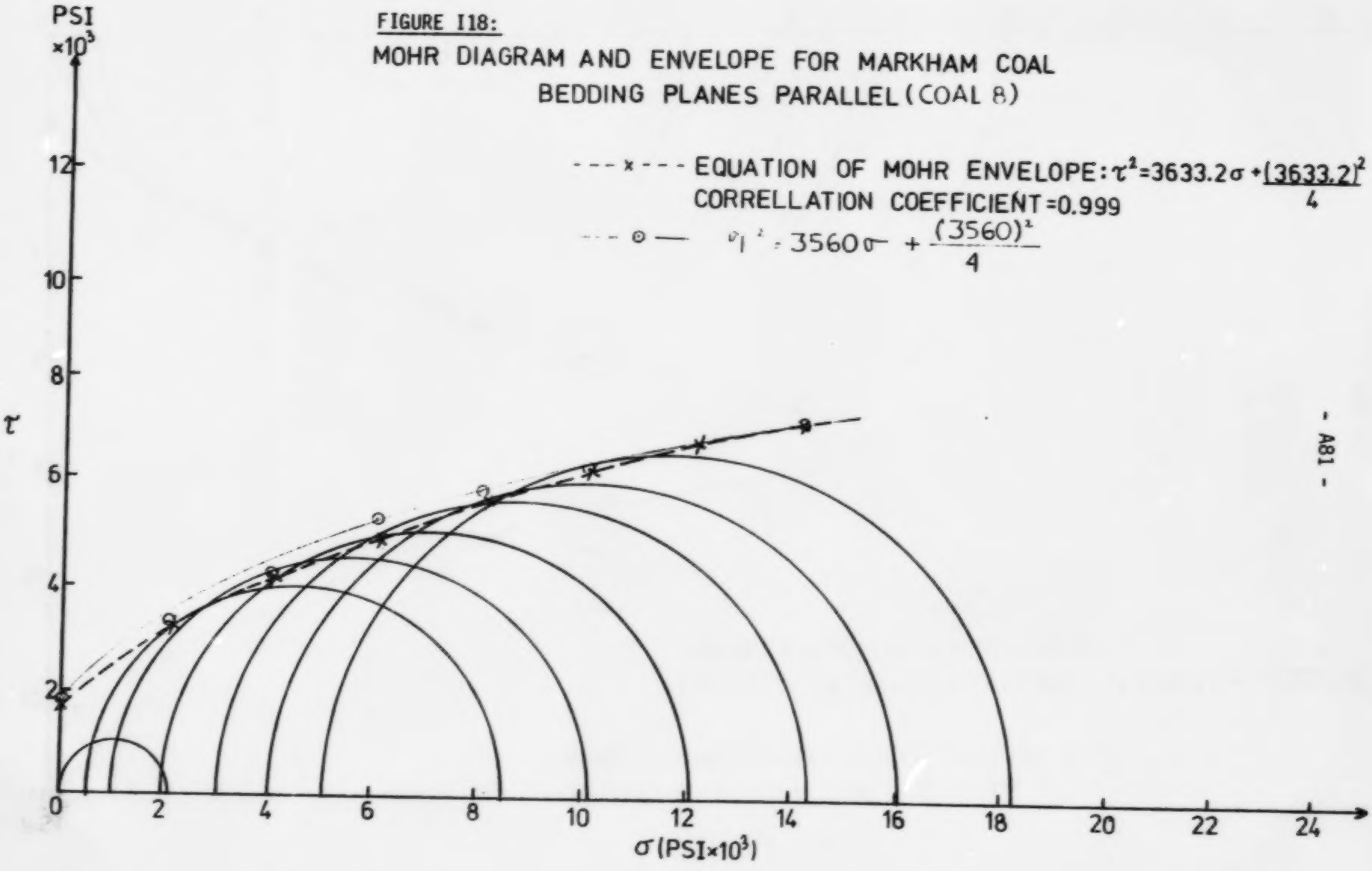

FIGURE I19:

MOHR DIAGRAM AND ENVELOPE FOR MARKHAM COAL BEDDING PLANES PERPENDICULAR (COAL 8)

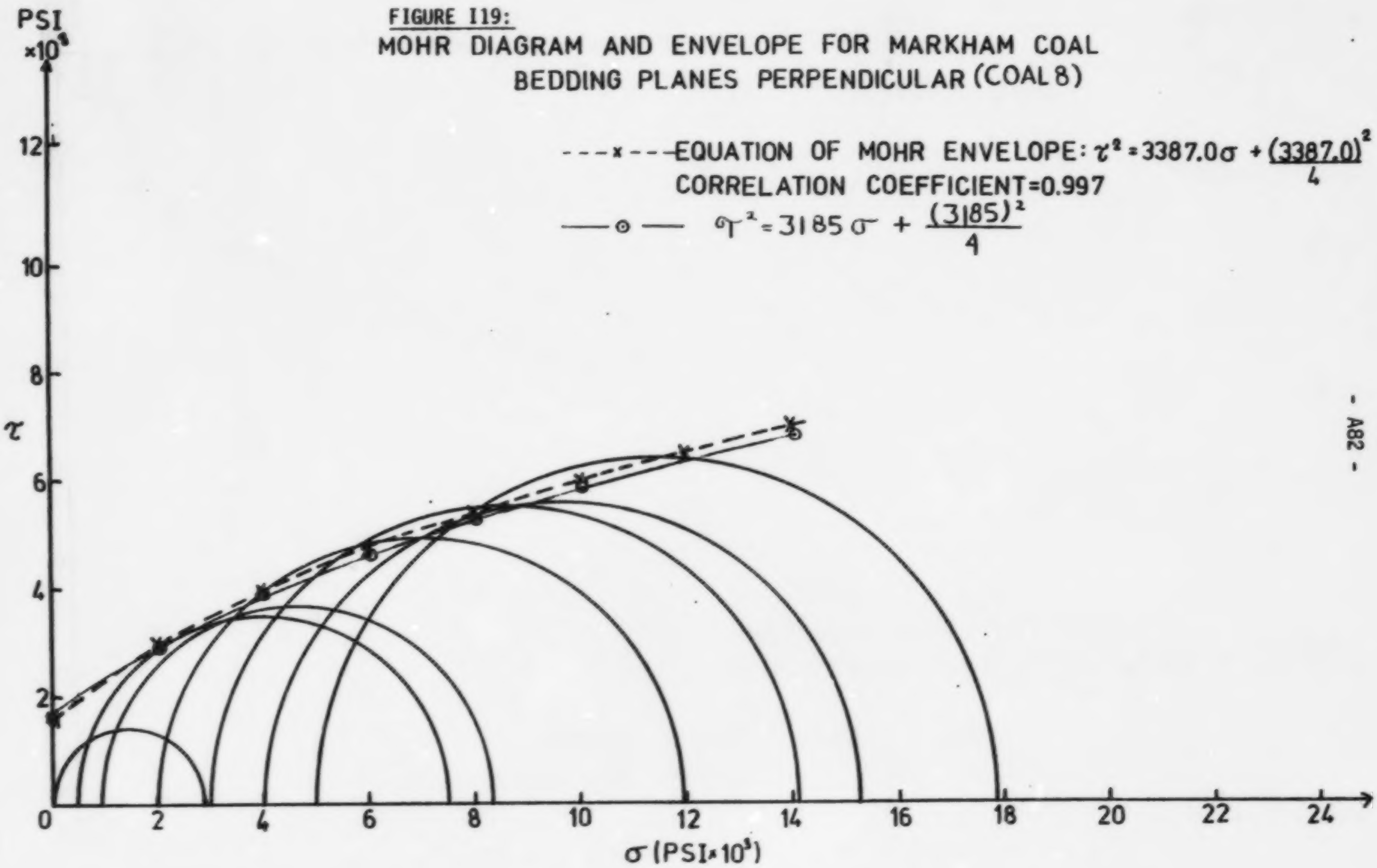

FIGURE I20:

MOHR DIAGRAM AND ENVELOPE FOR LINBY COAL
BEDDING PLANES PARALLEL (COAL9)

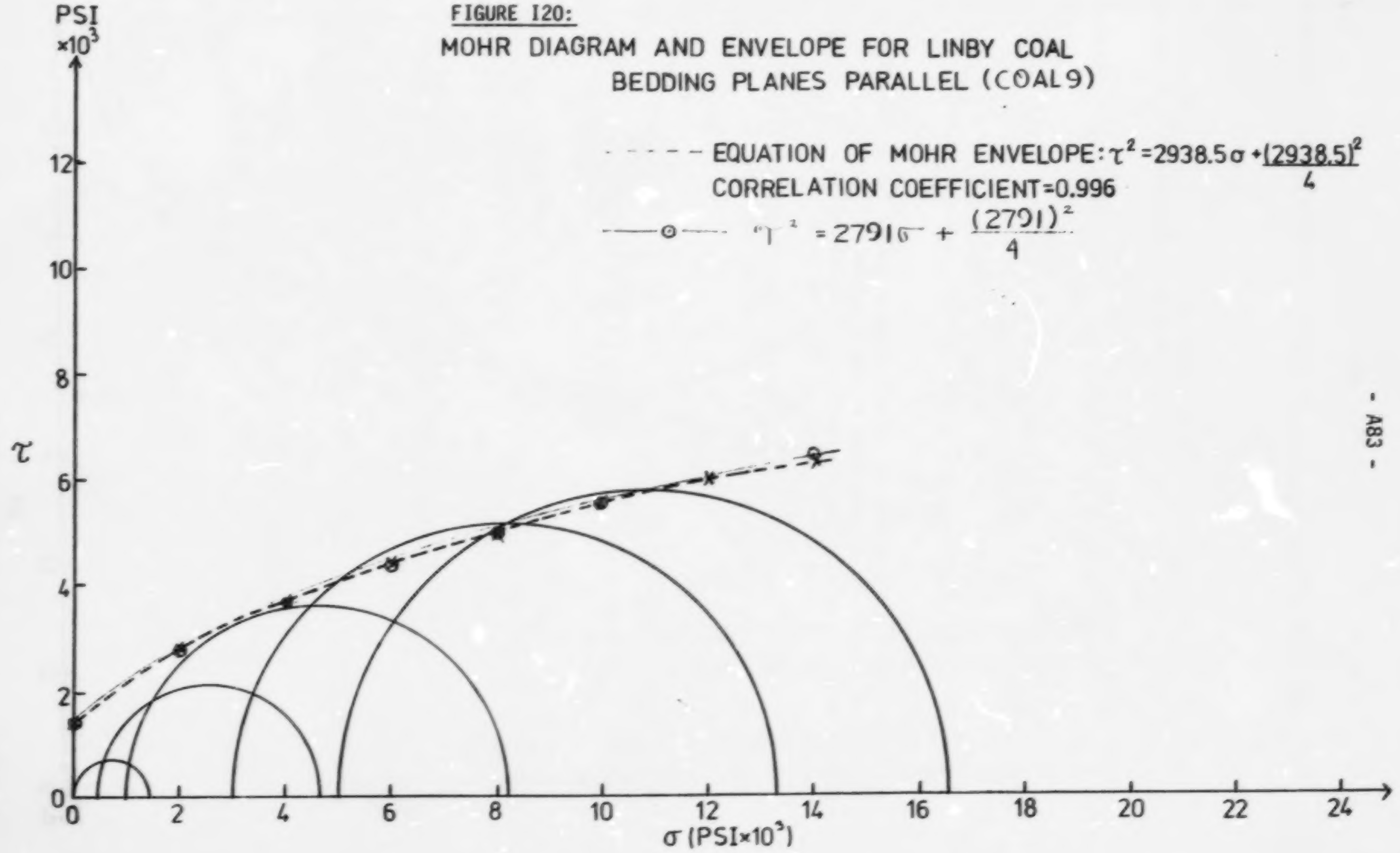

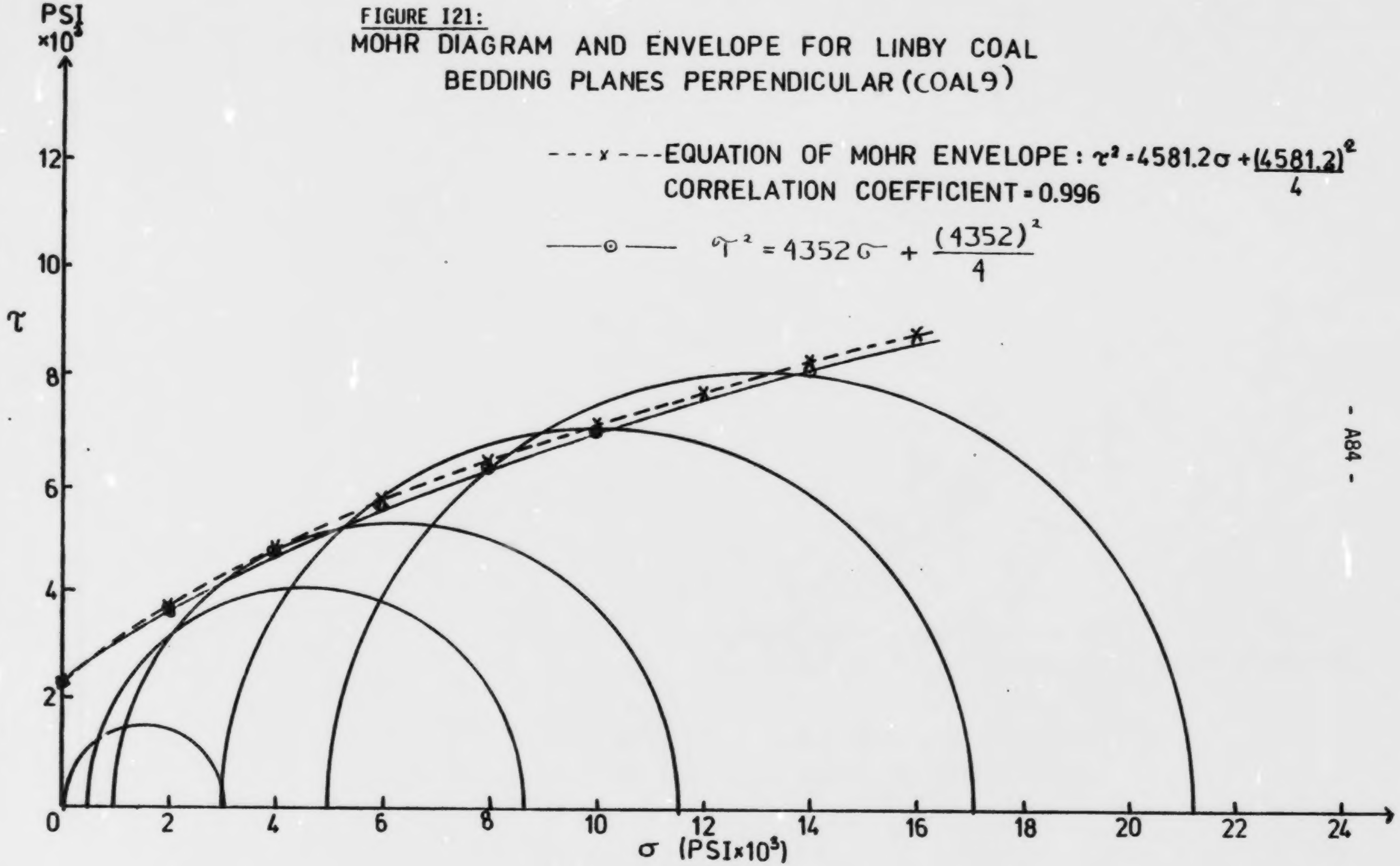

FIGURE I21:
MOHR DIAGRAM AND ENVELOPE FOR LINBY COAL BEDDING PLANES PERPENDICULAR (COAL9)

Appendix J: Mohr Program - "Best Fit" to a Curved Mohr Envelope

J.1 Mohr Program

Appendix I.4.2 gives the theory behind the determination of the parabolic Mohr envelope from triaxial test data.

This program is designed to give a value of "A" which minimized the deviation squared function. The function is of the form :-

$$\underline{d^2 = \Sigma\left[Ei^2 - Fi \pm \frac{Ei}{2}(Ei^2 - Fi)^{\frac{1}{2}}\right]}$$

where $Ei = 2r + A\ (\mathrm{Sin}\phi)\ (1 + \tan^2\phi)$

$Fi = r^2 + (r\mathrm{Sin}\phi - s)\ (1 + \tan^2\phi)A + (1 + \tan^2\phi)\ \frac{A^2}{4}$

The numerical analysis method which is chosen to determine the appropriate value of "A" is Newton's method (see Section on "Theory of Newton's Method"). This method however, requires a function equal to zero and the first derivative of this function.

It is stated in Appendix I.4.2 that the first derivative of the deviation squared function is equal to zero when the original function is minimized.

$$\frac{\partial(d^2)}{\partial A^2} = \left[Ei\ \frac{\partial E}{\partial A} - \frac{\partial F}{\partial A} \pm \frac{1}{2}\ \frac{\partial E}{\partial A}\ (Ei^2-4Fi)^{\frac{1}{2}} \pm \frac{Ei}{2}\ (Ei^2-4Fi)^{-\frac{1}{2}}\ \left(Ei\ \frac{\partial Ei}{\partial A} - 2\ \frac{\partial Fi}{\partial A}\right)\right]$$

where $\frac{\partial(d^2)}{\partial A} = 0$

$$\frac{\partial E}{\partial A} = \mathrm{Sin}\phi\ (1 + \tan^2\phi)$$

$$\frac{\partial F}{\partial A} = (r\mathrm{Sin}\phi - s)\ (1 + \tan^2\phi) - (1 + \tan^2\phi)\ \frac{A}{2}$$

In order to determine the derivative of this function the following steps are followed.

1. Break the equation into three major components

   a) $X = E\ \frac{\partial E}{\partial A} - \frac{\partial F}{\partial A}$

   b) $Y = \frac{1}{2}\frac{\partial E}{\partial A}(E^2 - 4F)^{\frac{1}{2}}$

   c) $Z = \frac{E}{2}\left[E^2 - 4F\right]^{-\frac{1}{2}}\left[E\ \frac{\partial E}{\partial A} - 2\ \frac{\partial F}{\partial A}\right]$

2. Create constants which will simplify the equations and insert into E and F equations

   a) $C_1 = 2r$

   b) $C_2 = \text{Sin}\phi\ (1 + \tan^2\phi)$

   c) $D_1 = r^2$

   d) $D_2 = (r\text{Sin}\phi - s)\ (1 + \tan^2\phi)$

   e) $D_3 = (1 + \tan^2\phi)4$

Hence

$$E = C_1 + C_2 A$$

$$\frac{\partial E}{\partial A} = C_2$$

$$F = D_1 + D_2 A - D_3 A^2$$

$$\frac{\partial F}{\partial A} = D_2 - 2D_3 A$$

3. Insert these values into the X, Y, Z equations and simplify :-

   a) $X = (C_1 + C_2 A)\ C_2 - D_2 + 2D_3 A$

   $$X = (C_1 C_2 - D_2) + (C_2 + 2D_3)A$$

   b) $Y = \frac{1}{2} C_2\ (C_1^2 + 2C_1C_2 A + C_2^2 A^2 - 4D_1 - 4D_2A + 4P_3A^2)^{\frac{1}{2}}$

   $$= \frac{1}{2} C_2 \left[(C_1^2 - 4D_1) + (2C_1C_2 - 4D_2)A + (C_2^2 + 4D_3)A^2\right]^{\frac{1}{2}}$$

where $K = (C_1^2 - 4D_1)$

$L = (2C_1C_2 - 4D_2)$

$M = (C_2^2 + 4D_3)$

$N = (1/2\ C_2)$

$$Y = N\left[K + LA + MA^2\right]^{\frac{1}{2}}$$

c) $Z = \frac{1}{2} (C_1+C_2\ A) \left[K+LA+MA^2\right]^{-\frac{1}{2}} \left[(C_1+C_2\ A)\ C_2-2(D_2-2D_3\ A)\right]$

$= \frac{1}{2} (C_1+ C_2\ A) \left[(C_1C_2-2D_2) + (C_2^{\ 2}+2D_3)A\right] \left[K+LA+MA^2\right]^{\frac{1}{2}}$

$= \frac{1}{2} \left[(C_1^{\ 2}C_1-2C_1D_2) + (2C_1C_2^{\ 2}+ 2C_1D_3-2C_2D_2)A + (C_2^{\ 3}+2C_2D_3\ A^2)\right.$

$\left.(K+LA+MA^2)\right]^{\frac{1}{2}}$

where : $H = C_1^{\ 2}C_2 - 2C_1D_2$

$I = 2C_1C_2^{\ 2} + 2C_1D_3 - 2C_2D_2$

$J = C_2^{\ 3} + 2C_2\ D_3$

$Z = \frac{1}{2} (H+IA+JA^2)\ (K+LA+MA^2)^{-\frac{1}{2}}$

4. Take the derivatives of x, y and z and simplify.

a) $\frac{dx}{dA} = C_2^{\ 2} + 2D_3$

where: $S = C_2^{\ 2} + 2D_3$

$\frac{dx}{dA} = S$

b) $\frac{dy}{dA} = 0.5\ (L + 2JA)\ (K + LA + MA^2\ )^{-\frac{1}{2}}$

c) $\frac{dz}{dA} = \frac{1}{2} (I + 2JA)\ (\ K + LA + MA^2\ )^{-\frac{1}{2}} - \frac{1}{4} (H + IA + JA^2)\ (L + 2MA)\ldots$

$\ldots*(K + LA + MA^2)^{-3/2}$

where: $O = HL$
$P = 2MH + IL$
$Q = 2MI + JL$
$R = 2MJ$

$$\frac{dz}{dA} = \frac{1}{2} (I + 2JA)\ (K + LA + MA^2)^{-\frac{1}{2}} - \frac{1}{4} (O + PA + QA^2 + RA^3)\ (K + LA + MA^2)^{-3/2}$$

The sum of $\frac{dx}{dA}$, $\frac{dy}{dA}$, and $\frac{dz}{dA}$ gives the value of the derivative needed.

It should be noted that this program is written in double precision due to the size of the numbers.

J.2 Program Flow

J.2.1 Main Program

Since this program uses an array type of set up it will be easiest to understand its flow by using table I.2 in Appendix I. The "*" shows the program equivalents and the "**" indicates the line numbers. (This table is reproduced again, below).

σ_1	σ_3	$\Delta\sigma_1$	$\Delta\sigma_3$	$\Delta\sigma_1/\Delta\sigma_3$	σ_1	σ_3
*R(1,J)	R(3,J)	DR(1,J)	DR(3,J)	DR1R3(J)	NR(1,J)	NR(3,J)
σ_{11}	σ_{31}	$\sigma_{12} - \sigma_{11}$	$\sigma_{32} - \sigma_{31}$	$\frac{\sigma_{12} - \sigma_{11}}{\sigma_{32} - \sigma_{31}}$	$\frac{\sigma_{11} + \sigma_{12}}{2}$	$\frac{\sigma_{32} + \sigma_{31}}{2}$
σ_{12}	σ_{32}	$\sigma_{13} - \sigma_{12}$	$\sigma_{33} - \sigma_{32}$	$\frac{\sigma_{13} - \sigma_{12}}{\sigma_{33} - \sigma_{32}}$	$\frac{\sigma_{12} + \sigma_{13}}{2}$	$\frac{\sigma_{33} + \sigma_{32}}{2}$
σ_{13}	σ_{33}	$\vdots$	$\vdots$	$\vdots$	$\vdots$	$\vdots$
$\vdots$	$\vdots$	$\sigma_{1N}-\sigma_{1N-1}$	$\sigma_{3N}-\sigma_{3N-1}$	$\frac{\sigma_{1N}-\sigma_{1N-1}}{\sigma_{3N}-\sigma_{3N-1}}$	$\frac{\sigma_{1N-1}+\sigma_{1N}}{2}$	$\frac{\sigma_{3N}+\sigma_{3N-1}}{2}$
σ_{1N}	σ_{3N}					
**	(15)	(25)	(26)	(27)	(29)	(30)

With the new values of σ_1 and σ_3 it is possible to calculate the values of "r", "s", and "$\emptyset$" using the following equations:-

$$r = (\sigma_1 - \sigma_3) / 2 \qquad (31)$$

$$s = (\sigma_1 + \sigma_3) / 2 \qquad (32)$$

$$\emptyset = \tan^{-1} \left\{ \frac{\frac{\Delta\sigma_1}{\Delta\sigma_3} - 1}{2 \frac{\Delta\sigma_1}{\Delta\sigma_3}} \right\} \qquad (33)$$

The values of $\emptyset$, r, s, and A are then passed to the Newton Subroutine. (45) Once the subroutine has determined an appropriate reply it returns with one of three answers.

1. The new value of "A" was found.
2. The new value of "A" was not found so try again.
3. The initial guess of "A" was too high.
   (52-67)

J.2.2 Newton Subroutine

This subroutine uses Newtons method to find an appropriate value of "A". It uses both external functions FC1 (111-152) and D01 (153-199) to calculate values for $\delta(d^2)/\delta A$ and $\delta^2(d^2)/\delta A^2$ respectively for varying values of A. The theory by which these values of "A" are chosen is covered in the Section " Theory of Newton's Method".

Once all values are read in and initiallized into the subroutine (72-82) the initial value of FC1 is determined (83). The value of "A" is then varied by the equation:-

$$A = \frac{A - FC1}{D01} \qquad (87\text{-}91)$$

The values of FC1 are recalculated and FC1 and $\frac{FC1}{D01}$ are checked against the specified tolerance. (94-95) If the tolerance is met the program returns to main, if not the program continues.

An error check has been inserted into this program.(142) When an initial guess of "A" is too large the equations will attempt to take the square root of a negative number. If this occurs the message "A" too large will reply. In this case chose a smaller value of "A".

J.3. FLOW CHART

J.3.1. MAIN PROGRAM

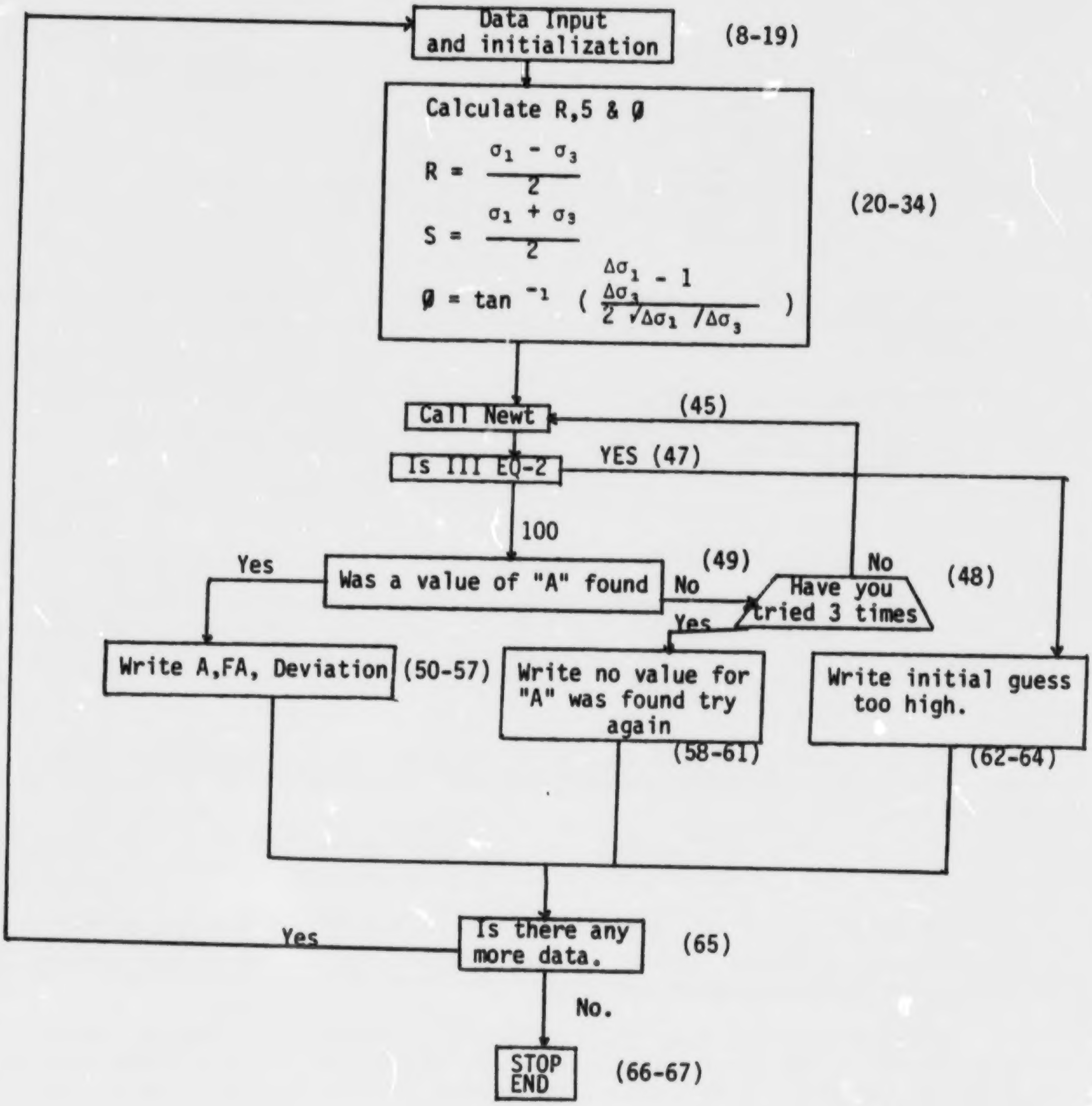
Data Input and initialization
(8-19)
Calculate R,5 & Ø
$R = \frac{\sigma_1 - \sigma_3}{2}$
$S = \frac{\sigma_1 + \sigma_3}{2}$
$Ø = \tan^{-1} \left(\frac{\frac{\Delta\sigma_1}{\Delta\sigma_3} - 1}{2 \sqrt{\Delta\sigma_1 / \Delta\sigma_3}} \right)$
(20-34)
Call Newt
(45)
Is III EQ-2
YES (47)
100
Was a value of "A" found
(49)
Yes
No
Have you tried 3 times
(48)
No
Yes
Write A,FA, Deviation
(50-57)
Write no value for "A" was found try again
(58-61)
Write initial guess too high.
(62-64)
Is there any more data.
(65)
Yes
No.
STOP END
(66-67)

J3.2 Newton (NEWT) and Functions (FC1 & D01)

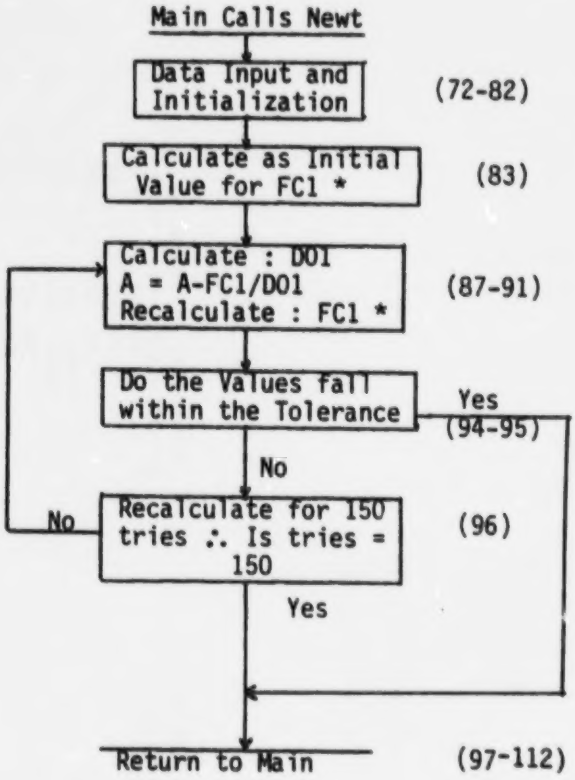
Main Calls Newt
Data Input and Initialization
(72-82)
Calculate as Initial Value for FC1 *
(83)
Calculate : D01
A = A-FC1/D01
Recalculate : FC1 *
(87-91)
Do the Values fall within the Tolerance
Yes
(94-95)
No
Recalculate for 150 tries ∴ Is tries = 150
No
(96)
Yes
Return to Main
(97-112)

* FCI does an automatic check to ensure that A is not too large for the functions.

J.3.3 Program Listing

```
MM        MM OOOOOOOOOOOO HH        HH RRRRRRRRRRR
MMM      MMM OOOOOOOOOOOO HH        HH RRRRRRRRRRRR
MMMM    MMMM OO        OO HH        HH RR        RR
MM MM  MM MM OO        OO HH        HH RR        RR
MM  MMMM  MM OO        OO HH        HH RR        RR
MM   MM   MM OO        OO HHHHHHHHHHHH RRRRRRRRRRRR
MM        MM OO        OO HHHHHHHHHHHH RRRRRRRRRRR
MM        MM OO        OO HH        HH RR    RR
MM        MM OO        OO HH        HH RR     RR
MM        MM OO        OO HH        HH RR      RR
MM        MM OOOOOOOOOOOO HH        HH RR       RR
MM        MM OOOOOOOOOOOO HH        HH RR        RR


 8888888888       11                            11       2222222222                  3333333333     00000000
888888888888     111                           111      222222222222                333333333333   0000000000
88        88    1111                          1111      22        22                33        33  00        00
88        88      11                            11                22                          33  00        00
 88      88       11                            11                22                          33  00        00
  88888888        11                            11               22                       3333    00        00
  88888888        11                            11              22                        3333    00        00
 88      88       11                            11            22                              33  00        00
88        88      11                            11          22                                33  00        00
88        88      11                            11        22                        33        33  00        00
888888888888  1111111111                    1111111111  222222222222                333333333333   0000000000
 8888888888   1111111111                    1111111111  222222222222                 3333333333     00000000
```

University of Alberta

```
C     ***********************************
C     *    MOHR ENVELOPE PROGRAM         *
C     *  WRITTEN BY STEPHEN E. THORNTON  *
C     *    FOR DR.K. BARRON FOR          *
C     *       TASK 81/15                 *
C     *                                  *
C     ***********************************
      LOGICAL*1 FREE(1)/'*'/
      DOUBLE PRECISION DR(3,100),DR1R3(100),NR(3,100),
     1 LS(100),LR(100),PHI(100),R(3,100),A,A1,DEV
      INTEGER I,K,M,J,III,JJ,NN,II,IJ
      EXTERNAL FC1,DO1
      IJ=1
  777 READ(5,FREE,END=778) N,A
      READ(5,FREE,END=778)(R(3,I),R(1,I),I=1,N)
      WRITE(6,666)IJ
  666 FORMAT(' ','                                          RUN ',I3)
      IJ=IJ+1
      M=N-1
C
C     CALCULATE THE VALUES OF R, S, AND PHIB.
C
      DO 100 J=1,M
      K=1+J
      DR(1,J)=R(1,K)-R(1,J)
      DR(3,J)=R(3,K)-R(3,J)
      DR1R3(J)=DR(1,J)/DR(3,J)
C
      NR(1,J)=(R(1,J)+R(1,K))/2.0
      NR(3,J)=(R(3,J)+R(3,K))/2.0
      LR(J)=(NR(1,J)-NR(3,J))/2.0
      LS(J)=(NR(1,J)+NR(3,J))/2.0
      PHI(J)=DATAN((DR1R3(J)-1.0)/(2.0*DSQRT(DR1R3(J))))
  100 CONTINUE
C
      A1=A
      II=0
  110 CONTINUE
      II=II+1
      III=0
C
C   THE NEWTON METHOD OF SOLUTION IS USED TO DETERMINE THE
C           MINIMUM VALUE OF D SQUARED
C
      CALL NEWT(FC1,DO1,A1,M,PHI,LR,LS,III,DEV)
C
      IF (III.EQ.-2) GO TO 109
      IF (II .EQ. 3) GO TO 111
      IF (III.EQ.-1) GO TO 110
C
C    THE RESULTS ARE PRINTED OUT.
C
      WRITE(6,101) A, A1, DEV
  101 FORMAT(' ','THE INITIAL VALUE OF A = ',F16.2,/,
     1          'THE FINAL VALUE OF A   = ',F16.2,/,
     1          'THE DEVIATION          = ',F16.2,/,/)
```

University of Alberta

```
            GO TO 112
  111       WRITE(6,102) A1
  102       FORMAT(' ','THE VALUE OF "A" WAS NOT FOUND. IF YOU WISH',/,
     1             'TO TRY AGAIN IT IS SUGGESTED THAT THE FOLLOWING',/,
     1                ' VALUE BE USED FOR "A": ',F8.2)
  109       WRITE(6,103) A
  103       FORMAT(' ','THE VALUE OF "A" CHOSEN AN INITIAL GUESS ',
     1             'WAS TOO LARGE. CHOSE ONE SMALLER THAN ',F6.2,'.',/)
  112       GO TO 777
  778       STOP
            END
```

University of Alberta

```
C
C     THIS SUBROUTINE USES NEWTONS METHOD TO DETERMINE THE
C                          VALUE OF "A"
C
      SUBROUTINE NEWT(FCN,FDER,A,NN,PHI,LR,LS,III,DEV)
      LOGICAL PRINT
      LOGICAL*1 FREE(1)/'*'/
      DOUBLE PRECISION A,PHI(100),LR(100),LS(100),FA,TRIAL,
     1   DEV,FC1,DD1,AERR,FERR,DER
      INTEGER III,NN,MAX
      PRINT=.TRUE.
      IF (III .NE. 0) PRINT=.FALSE.
      AERR=0.000005
      FERR=0.000001
      MAX=150
      FA=FCN(A,NN,PHI,LR,LS,III)
      IF (III.GT.-2) GO TO 65
      RETURN
C
 65   DO 20 J=1,MAX
      DER=FDER(A,NN,PHI,LR,LS,DEV)
      TRIAL=FA/DER
      A=A-TRIAL
      FA=FCN(A,NN,PHI,LR,LS,III)
      IF (III.GT.-2) GO TO 5
      RETURN
 5    IF (DABS(TRIAL).LE.AERR) GO TO 60
      IF (DABS(FA).LE.FERR)GO TO 70
 20   CONTINUE
C
C     THE VALUE OF A HAS NOT BEEN FOUND IN 150 ATTEMPTS.
C
      III=-1
      RETURN
C
C     THE TOLERANCE OF "A" WAS MET.
C
 60   III=1
      RETURN
C
C     THE TOLERANCE OF FA WAS MET.
C
 70   III=2
      RETURN
      END
```

University of Alberta

```
C
C
C  THE FOLLOWING FUNCTIONS WILL BE USED FOR THE NEWTON'S
C             METHOD OF SOLUTIONS.
C
C  THIS FUNCTION IS THE DERIVATIVE OF THE D SQUARED EQUATION
C
          DOUBLE PRECISION FUNCTION FC1(A,NN,PHI,LR,LS,III)
          DOUBLE PRECISION FC11,FC22,FC33,C1,C2,D1,D2,D3,H,I,
     1    J,L,K,M,N,O,P,Q,R,PHI(100),A,LS(100),LR(100),INT11,
     1    INT22,INT33,DD2,ERRCH
          INTEGER JJ,NN,IJK,III
          FC1=0
          FC11=0
          FC22=0
          FC33=0
          DO 1001 JJ=1,NN
          C1=2*LR(JJ)
          C2=DSIN(PHI(JJ))*(1+DTAN(PHI(JJ))**2)
          D1=LR(JJ)**2
          D2=(LR(JJ)*DSIN(PHI(JJ))-LS(JJ))*(1+DTAN(PHI(JJ))**2)
          D3=(1+DTAN(PHI(JJ))**2)/4
          H=((C1**2)*C2)-2*C1*D2
          I=2*C1*C2**2+4*C1*D3-2*C2*D2
          J=C2**3+4*C2*D3
          K=C1**2-4*D1
          L=2*C1*C2-4*D2
          M=C2**2+4*D3
          N=0.5*C2
          ERRCH=(K+L*A+M*A**2)
          IF (ERRCH.GT.0.0) GO TO 333
          III=-2
          GO TO 334
C
  333     FC11=C1*C2-D2+(C2**2+2*D3)*A
          FC22=N*DSQRT(K+L*A+M*A**2)
          FC33=0.5*(H+I*A+J*A**2)/DSQRT(K+L*A+M*A**2)
          FC1=FC11-FC22-FC33+FC1
C
 1001     CONTINUE
  334     RETURN
          END
```

University of Alberta

```
C
C
C  THIS FUNCTION IS THE SECOND DERIVATIVE OF THE D SQUARED EQUATION
C
C
      DOUBLE PRECISION FUNCTION D01(A,NN,PHI,LR,LS,DEV)
      DOUBLE PRECISION C1,C2,D1,D2,D3,H,I,J,L,K,
     1 M,N,O,P,Q,R,S,PHI(100),A,DEV,D011,D022,D033,D01,
     1 LR(100),LS(100),INT11,INT22,INT33
      INTEGER JJ,NN
      D01=0
      D011=0
      D022=0
      D033=0
      DEV=0
      DO 1000 JJ=1,NN
      C1=2*LR(JJ)
      C2=DSIN(PHI(JJ))*(1+DTAN(PHI(JJ))**2)
      D1=LR(JJ)**2
      D2=(LR(JJ)*DSIN(PHI(JJ))-LS(JJ))*(1+DTAN(PHI(JJ))**2)
      D3=(1+DTAN(PHI(JJ))**2)/4
      H=((C1**2)*C2)-2*C1*D2
      I=2*C1*C2**2+4*C1*D3-2*C2*D2
      J=C2**3+4*C2*D3
      K=C1**2-4*D1
      L=2*C1*C2-4*D2
      M=C2**2+4*D3
      N=0.5*C2
      O=H*L
      P=2*M*H+I*L
      Q=2*M*I+J*L
      R=2*M*J
      S=C2**2+2*D3
C
      D011=S
      D022=0.5*(N*(L+2*M*A)/((K+L*A+M*A**2)**0.5))
      D033=(0.5*(I+2*J*A)/((K+L*A+M*A**2)**0.5))-
     1 0.25*(O+P*A+Q*A**2+R*A**3)/((K+L*A+M*A**2)**1.5)
      D01=D011-D022-D033+D01
C
      INT11=(C1**2/2-D1)+(C1*C2-D2)*A+(C2**2/2+D3)*A**2
      INT22=0.5*(C1+C2*A)
      INT33=DSQRT((C1+C2*A)**2-4*(D1+D2*A-D3*A**2))
      DEV=INT11-INT22*INT33+DEV
 1000 CONTINUE
      RETURN
      END
```

University of Alberta

J.4 User's Manual

J.4.1 Mohr Circle Input List

Each line of the input file must have two numbers. The numbers can be separated by either spaces or commas. The first line contains:

a) the total number of pairs (N)
b) the initial guess for A

The rest of the lines are simply the pairs of data. They can be entered as:-

σ_{31},	σ_{11}	or	σ_{31}	σ_{11}
σ_{32},	σ_{12}		σ_{32}	σ_{12}
σ_{33},	σ_{13}		σ_{33}	σ_{13}
σ_{34},	σ_{14}		σ_{34}	σ_{14}
:			:	
σ_{3n},	σ_{1N}		σ_{3N}	σ_{N}

Example of total data input (from Appendix I)

Coal 2 - Parallel Bedding Planes

Line	1	7, 3000	or	7	3000
	2	0, 1020		0	1020
	3	500, 5080		500	5080
	4	1000, 6590		1000	6590
	5	2000, 9460		2000	9460
	6	3000, 12580		3000	12580
	7	4000, 15110		4000	15110
	8	5000, 16140		5000	16140

J.4.2 Program Use

* To set up the file, and run it complete the following steps:-

1. Create testfile (anyname can be used which is not already in use)
2. Input data (using the file description previously described)

Example

```
#Ed testfile

      : i
      ? 7, 3000
      ? 0, 1020
      ? 500, 5080
          :
          :
```

```
          ? 5000, 16140
**        ? (blank line)
          : MTS
          #
```

3. Compile the main program:

```
#$RUN *fortg scards=mohr   t=2
```

4. Run program

```
#$RUN -LOAD# 5=testfile  6=outputfile (-a)  t=2
```

5. a) Obtain data on terminal

```
#$COPY -a
```

   b) Obtain page printer output

```
#$CONTROL *print* format=FMTL1  PRINTON=ONESIDE   PAPER=X3
#$COPY -a *PRINT*
#$RELEASE *PRINT*
```

Notes:-

* These steps should be followed when using the MTS system at the University of Alberta. Other installations may use variations of these steps.

** If more than one set of data is being tested it can by adding additional information at this point. See sample input at end.

J.5 Variables and Constants

1. R (1,I) - the input array for the measured verticle stress (σ_{1N})
2. R (3,I) - the input array for the measured horizontal stress (σ_{3N})
3. DR (1,J) & DR (3,J) - the changes of the σ_{1N} and σ_{3N} are calculated ($\Delta\sigma_{1N}$, $\Delta\sigma_{3N}$)
4. DR1R3 - $\frac{\Delta\sigma_{1N}}{\Delta\sigma_{3N}}$
5. NR (1,I) & NR (3,I) - the average value of σ_{1N} and σ_{3N}
6. LR (J) - the value $\frac{\sigma_1 - \sigma_3}{2}$ (r)
7. LS (J) - the value $\frac{\sigma_1 + \sigma_3}{2}$ (s)
8. A - Mohr's constant
9. DEV - the value of d^2
10. AERR and FERR - tolerances for the Newton subroutine
11. MAX - maximum number of tries which will be used to obtain A
12. FA = FC1 the derivative of the d^2 formula
13. DER = D01 the second derivative of the d^2 formula
14. FC11, FC22, FC33, D011, D022, D033, INT11, INT22, INT33 - all are intermediate steps

BREAK DOWN OF CONSTANTS FOR FUNCTIONS

15. $C_1 = 2r$
16. $C_2 = \sin\phi\ (1+\tan^2\phi)$
17. $D_1 = r^2$
18. $D_2 = (r\mathrm{Sin}\phi - s)\ (1+\tan^2\phi)$
19. $D_3 = (1+\tan^2\phi)$

H - S are variations of these five constants

20. ERRCH - checks for negative values to prevent the square root of these numbers from being attempted.

J.6 Newton's Method

The algorithm for Newton's method specifies

1. $f(x) = 0$
2. $f'(x) \neq 0$
3. Initial guess must be close to the root desired

The form of the algorithm is:

$$x_{n+1} = x_n - \frac{f(x)_n}{f'(x)_n}$$

Derivation of Algorithm

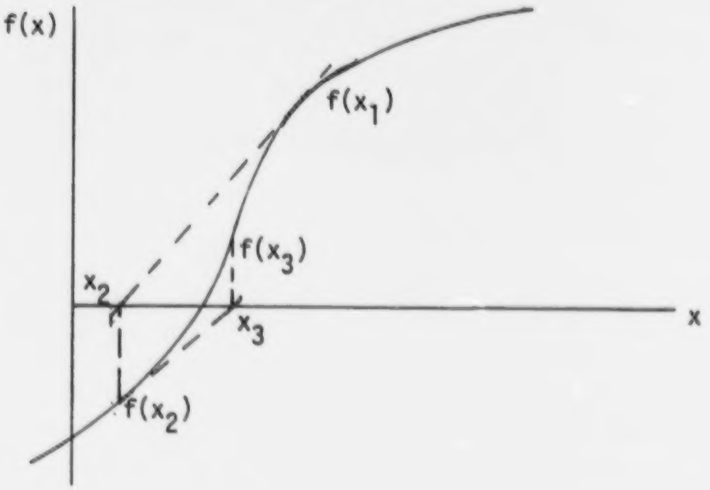

1. Make an initial guess for x_1 and calculate the function value.
2. Find a tangent to the point x_1 and take it to zero on y axis.
3. Find a new function value with new x value and repeat process.

Point 1 to Point 2

$$m = \frac{y_2 - y_1}{x_2 - x_1} \quad \text{but } y_2 = 0$$

$$= \frac{-y_1}{x_2 - x_1}$$, make $y_1 = f(x_1)$ and since the derivative is a tangeant

$$f'(x_1) = \frac{-f(x_1)}{x_2 - x_1}$$

$$x_2 = x_1 - \frac{f(x)}{f'(x)}$$

FORTRAN CODE:

```
FERR =  0.0001
                        Tolerances
AERR =  0.0005
MAX  =  150             # of iterations or A guesses made
A1   =  A GUESS         A value fairly close to answer
FA   =  F(AGUESS)       FIRST FUNCTION VALUE


DO  20 J=1 MAX
DER  = FDER (A)         -calculate derivative
A    = A - FA/Der       -find next A
FA   = F                -use new A to determine F

IF ( A2-A  .LE AERR) Return A Value - Is A tolerance met
IF ( FA  .LE. FERR) Return A Value  - Is FA tolerance met


20  CONTINUE                            -IF NOT TRY A NEW "A" VALUE
```

J.7 Examples

Table J.1 gives the input data for the 18 coal data sets given in Appendix I. Table J.2 gives the output results for these data sets.

Table J1: Example inputs for the Mohr program (18 data sets)

```
  1     6   500
  2     0  2630
  3  1000  9650
  4  2000 13520
  5  3000 14280
  6  4000 19930
  7  5000 22520
  8
  9
 10     6   500
 11     0  4580
 12  1000 11100
 13  2000 14200
 14  3000 18630
 15  4000 22920
 16  4750 29710
 17
 18     7   500
 19     0  1020
 20   500  5080
 21  1000  6590
 22  2000  9460
 23  3000 12580
 24  4000 15110
 25  5000 16140
 26
 27     7   500
 28     0  1000
 29   500  5010
 30  1000  7350
 31  2000  9970
 32  3000 11620
 33  4000 14460
 34  5000 16040
 35
 36     7   500
 37     0   320
 38   500  3680
 39  1000  4480
 40  2000  6940
 41  3000  9980
 42  4000 13780
 43  5000 15330
 44
 45     7   500
 46     0   770
 47   500  5990
 48  1000  6160
 49  2000  8160
 50  3000 11110
 51  4000 12670
 52  5000 17000
 53
 54     5   500
 55     0  1010
 56   500  5810
 57  1000  7330
 58  3000 14490
 59  5000 18850
 60
 61     5   500
 62     0  1920
 63   500  7210
 64  1000  8520
 65  3000 13690
 66  5000 18160
 67
 68     7   500
 69     0  4390
 70   500  7590
 71  1000  9770
 72  2000 13940
 73  3000 14380
 74  4000 18920
 75  5000 20130
 76
 77     7   500
 78     0  7450
 79   500  9320
 80  1000 14020
 81  2000 14930
 82  3000 16430
 83  4000 17930
 84  5000 20030
 85
 86     5   500
 87     0  3420
 88   500  8780
 89  1000 10060
 90  3000 15460
 91  5000 19480
 92
 93     5   500
 94     0  3460
 95   500  7340
 96  1000 10460
 98  3000 15710
100  5000 19820
101
102     5   500
103     0  1960
104   500  7940
105  1000 10190
107  3000 15890
109  5000 21010
110
111     5   500
112     0  2280
113   500  6730
114  1000  9220
116  3000 15420
118  5000 18910
119
120     7   500
121     0  2300
122   500  8480
123  1000 10090
124  2000 11970
125  3000 14480
126  4000 16200
127  5000 18230
128
129     7   500
130     0  3160
131   500  7560
132  1000  8350
133  2000 12060
134  3000 14350
135  4000 15300
136  5000 17900
137
138     5   500
139     0  1510
140   500  5590
141  1000  8250
143  3000 13360
145  5000 16570
146
147     5   500
148     0  3150
149   500  8780
150  1000 11600
152  3000 17140
154  5000 21230
```

Table J2: Example outputs from the Mohr program (18 data sets)

```
                                  RUN   1                                         RUN  11
THE INITIAL VALUE OF A =        500.00       THE INITIAL VALUE OF A =           500.00
THE FINAL VALUE OF A   =       3859.84       THE FINAL VALUE OF A   =          3808.78
THE DEVIATION          =    2557656.59       THE DEVIATION          =        653734.26

                                  RUN   2                                         RUN  12
THE INITIAL VALUE OF A =        500.00       THE INITIAL VALUE OF A =           500.00
THE FINAL VALUE OF A   =       4913.49       THE FINAL VALUE OF A   =          3789.98
THE DEVIATION          =    1462823.15       THE DEVIATION          =        991271.12

                                  RUN   3                                         RUN  13
THE INITIAL VALUE OF A =        500.00       THE INITIAL VALUE OF A =           500.00
THE FINAL VALUE OF A   =       2592.20       THE FINAL VALUE OF A   =          3900.64
THE DEVIATION          =     938621.32       THE DEVIATION          =       1272564.96

                                  RUN   4                                         RUN  14
THE INITIAL VALUE OF A =        500.00       THE INITIAL VALUE OF A =           500.00
THE FINAL VALUE OF A   =       2545.15       THE FINAL VALUE OF A   =          3494.16
THE DEVIATION          =     719881.81       THE DEVIATION          =       1085424.15

                                  RUN   5                                         RUN  15
THE INITIAL VALUE OF A =        500.00       THE INITIAL VALUE OF A =           500.00
THE FINAL VALUE OF A   =       1853.18       THE FINAL VALUE OF A   =          3560.58
THE DEVIATION          =    1589275.83       THE DEVIATION          =        631227.46

                                  RUN   6                                         RUN  16
THE INITIAL VALUE OF A =        500.00       THE INITIAL VALUE OF A =           500.00
THE FINAL VALUE OF A   =       1769.38       THE FINAL VALUE OF A   =          3184.79
THE DEVIATION          =    1704438.41       THE DEVIATION          =        500525.59

                                  RUN   7                                         RUN  17
THE INITIAL VALUE OF A =        500.00       THE INITIAL VALUE OF A =           500.00
THE FINAL VALUE OF A   =       3072.42       THE FINAL VALUE OF A   =          2791.84
THE DEVIATION          =    1349986.68       THE DEVIATION          =        715355.81

                                  RUN   8                                         RUN  18
THE INITIAL VALUE OF A =        500.00       THE INITIAL VALUE OF A =           500.00
THE FINAL VALUE OF A   =       3043.63       THE FINAL VALUE OF A   =          4352.84
THE DEVIATION          =     781406.04       THE DEVIATION          =       1305902.39

                                  RUN   9
THE INITIAL VALUE OF A =        500.00
THE FINAL VALUE OF A   =       3357.15
THE DEVIATION          =    2551227.60

                                  RUN  10
THE INITIAL VALUE OF A =        500.00
THE FINAL VALUE OF A   =       4387.26
THE DEVIATION          =     240725.44
```

Appendix K : Short Version of the Pillar Program

K.1 Program Flow

K.1.1 Main

This version of the pillar program is written to obtain a quick method of determining the mode of failure, strength and safety factor of a pillar. The program uses the tributary area theory to calculate the mean pillar stress concentration ($\overline{Y}$) and the extraction ratio (R), as described in Section 10 of the main text. Figure K1 shows the flow diagram.

Three types of pillar can be considered:-

a) Rib pillars (37 - 40)
b) Square pillars (41 - 45)
c) Rectangular pillars (46 - 49)

In all cases the rooms are considered to be rectangular.

The value of the maximum pillar stress concentration (Y_{mm}) is determined using the equation for rectangular rooms:-

$$Y_{mm} = (2.048 - 0.919k) + 0.572 \log_e \left(\frac{W}{H}\right) + 0.09 \left\{\left(\frac{W}{B} + 1\right)^2 - 1\right\} \qquad (50)$$

In the case where Y_{mm} is calculated to be less than $\overline{Y}$ the values are made equal. (51)

A check of the input data is now made to insure the following limitations are not exceeded:-

a) $\frac{1}{2} < \frac{W}{H} < 4$ (56)

b) $K > 1.5$ (61)

If either limitation is not met a warning will be printed describing which has been exceeded (57-60). All input data can be printed at this point if requested (62-91).

The values of the vertical stress (P_{1T}), the transition point (d_T), and the minimum pillar capacity can now be calculated (103-115). A comparison of the values of "d_T" and "b" will determine if the pillar will be in a fracture mode or a yield mode. When "d_T" is greater than "b" the pillar will fracture. (137)

If the pillar enters the fracture mode, the residual mean pillar capacity ($\bar{\sigma}_{PR}$) is calculated (142-144). The values of the critical pillar dimension to avoid catastrophic fracture (b_{cF}) and ultimate fracture (b_{cFu}) are derived by Newton's Method (145-148). (See Newton Subroutine)

Figure K1: Flow Diagram - Short Program

PILLAR STRENGTHS, SAFETY FACTORS FOR UNIFORM PILLAR LAYOUTS WITH RECTANGULAR ROOMS

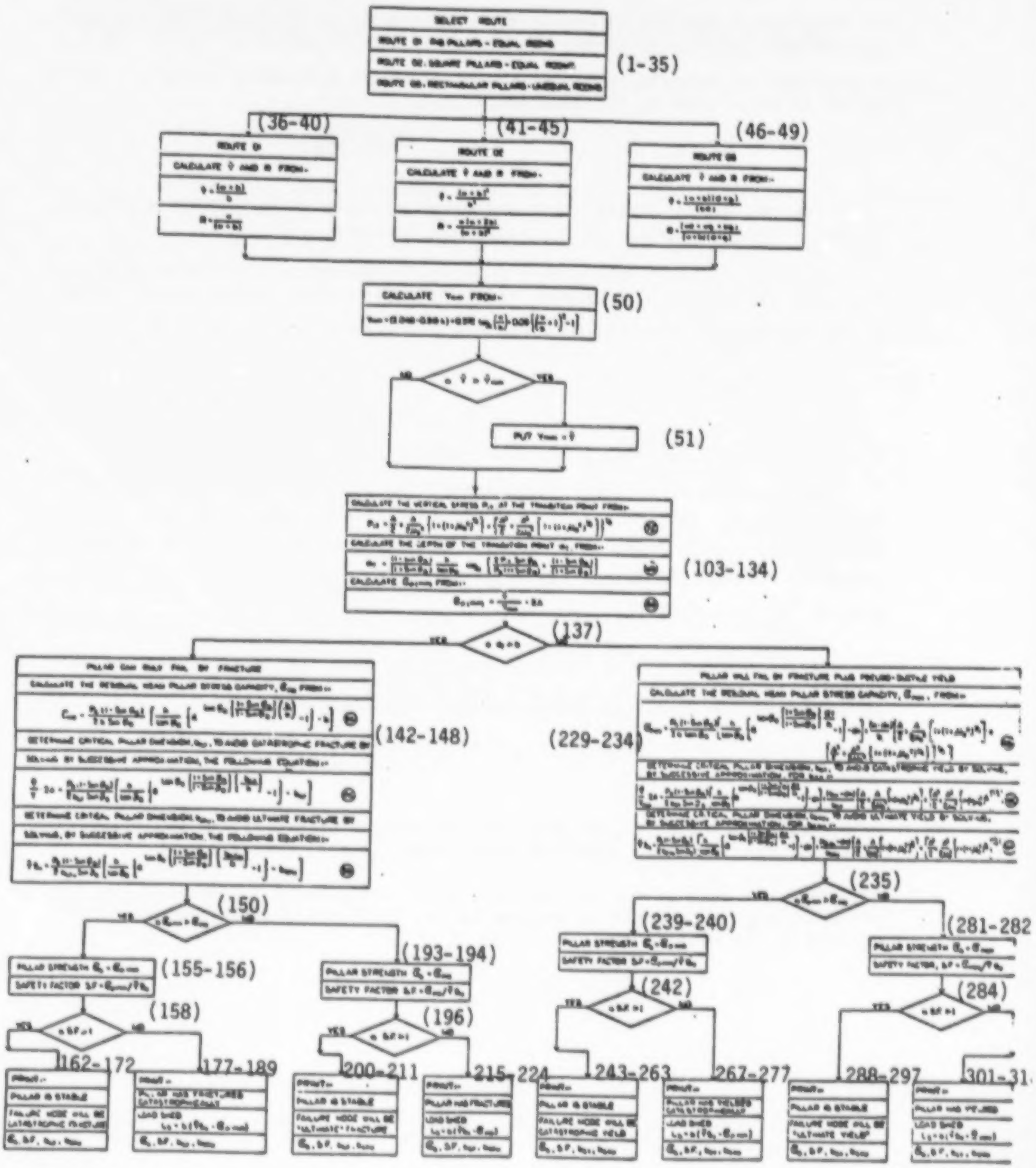
SELECT ROUTE
ROUTE 01: RIB PILLARS - EQUAL ROOMS
ROUTE 02: SQUARE PILLARS - EQUAL ROOMS
ROUTE 03: RECTANGULAR PILLARS - UNEQUAL ROOMS
(1-35)
(36-40)
ROUTE 01
CALCULATE AND R FROM:
(41-45)
ROUTE 02
CALCULATE AND R FROM:
(46-49)
ROUTE 03
CALCULATE AND R FROM:
CALCULATE FROM:
(50)
NO
YES
(51)
(103-134)
YES
(137)
PILLAR CAN ONLY FAIL BY FRACTURE
(142-148)
PILLAR WILL FAIL BY FRACTURE PLUS PSEUDO-DUCTILE YIELD
(229-234)
(150)
YES
NO
PILLAR STRENGTH
SAFETY FACTOR
(155-156)
(193-194)
(158)
(196)
(235)
(239-240)
(281-282
(242)
(284)
162-172
177-189
200-211
215-224
243-263
267-277
288-297
301-31
PRINT:
PILLAR IS STABLE

The value assigned to the pillar strength is the larger of the residual mean stress capacity (σ_{PR}) and the minimum pillar capacity ($\sigma_{p\ min}$). If the minimum pillar capacity is larger the strength is equated to it and the safety factor is calculated by the equation:-

$$SF = \bar{\sigma}_{p\ min} / (\bar{Y} \cdot S_v) \qquad (155\text{-}156)$$

A safety factor greater than one gives a stable pillar, while a safety factor of less than one gives catastrophic fracture. (158-190)

When the residual mean stress capacity is larger than the minimum pillar capacity, the strength is equated to σ_{PR} and the safety factor is calculated by the equation :-

$$SF = \sigma_{PR} / (\bar{Y} \cdot S_v) \qquad (193\text{-}194)$$

A safety factor greater than one again gives a stable pillar but a value of less than one indicates that the pillar has been fractured. (196-224)

The strength of a pillar which enters the yielding mode is calculated basically in the same way. The residual mean pillar capacity (σ_{pry}), and the critical pillar dimensions to avoid catastrophic yield (b_{cy}) and ultimate yield (b_{cyu}) are calculated. (229-233) A check is made at this point to determine if "b_{cyu}" is infinity. (234-235)

If the minimum pillar capacity is greater than the residual mean pillar capacity the next step is to equate the pillar's strength to the minimum pillar capacity and calculate the safety factor. The equation safety factor is :-

$$SF = \sigma_{p\ min} / (S_v \cdot \bar{Y}) \qquad (239\text{-}240)$$

A safety factor if more than one indicates a stable pillar while a safety factor of less than one indicates catastrophic yield. (242-277)

With the case of the residual stress capacity being larger than the minimum pillar capacity, strength is equated to the first and a safety factor is calculated by the equation:-

$$SF = \sigma_{pry} / (S_v \cdot \bar{Y})$$

Again a safety factor of more than one will indicate a stable pillar, but a value of less than one will indicate ultimate yield. (282-318)

In all cases of fracture or yield the value of the load shed is calculated.

K.1.2 Newton Subroutine

This subroutine uses Newton's method to determine the values of the critical pillar dimensions to avoid catastrophic fracture (b_{cF}) and ultimate fracture (b_{cFu}). It uses the external functions FC1 and D01 for determining "b_{CF}" and FC2 and D02 for determining "b_{cFu}".

Once all values are read in and initiallized into the subroutine (323-333) an initial value of FC1 (or FC2) is determined (334). The value of D01 (or D02) is then found and a new value for "b_{cF}" (or "b_{cFu}") is found using the equation :-

$$b_{cF} = b_{cF} - FC1 / D01 \qquad (336\text{-}339)$$

The value of FC1 (or FC2) is recalculated and the tolerance of FC1 (or FC2) and FC1 / D01 (or FC2 / D02) are checked. (341 - 342) If the tolerance are met the program returns to main. Otherwise a new value for "b_{cF}" (or "b_{cFu}") is calculated and tested. (344)

Two responses can occur from this subroutine.

1. a new value for b is found.
2. a value has not been found that meets either tolerance (347-362)

In the case of the second reply it is suggested to try another initial guess for b.

K.2 Program Listing

```
SHRTPILL
B1 1230
```

University of Alberta

```
C    ************************************
C    *   SHORT VERSION OF THE PILLAR    *
C    *        FAILURE PROGRAM           *
C    *   AS PART OF CMRC TASK 81/15     *
C    *     BY STEPHEN THORNTON FOR      *
C    *          DR. K. BARRON           *
C    ************************************
          LOGICAL*1 FREE(1)/'*'/
          INTEGER  ROUTE,I,PRINT,YES,NO,III,IIII,T
          REAL  W,B,H,R,STREN,PONE,SV,MUB,A,YMM,ALOG,
     1        D,SPSV,PHIB,PHIBD,BCY,BCYU,BCF,BCFU,
     1        XBC1,XBC2,XBC3,XBC4,C,TT,CANTA,CANTB,RPR,RPRY,
     1        PTHREE,SIN,PB,TAN,XBC1,XBC2,XBC3,XBC4,INTVAL,
     1        AA,BB,CC,DD,EE,FF,GG,FERR,BERR,K,Q,BBB,TEST
          IIII=1
          READ(5,FREE) T,INTVAL
  888     READ(5,FREE,END=999) ROUTE,W,D,Q,H
          READ(5,FREE,END=999) PRINT,SV,K,A,MUB,PHIBD,PB
          WRITE(6,889)IIII
  889     FORMAT('1','                                              RUN ',I3)
          IIII=IIII+1
           EXTERNAL FC1,DD1,FC2,DD2
           YES=1
           NO=0
           B=0.0
           DO 3 III=1,T
           B=B+INTVAL
C
C              THIS SECTION OF THE PROGRAM IS THE
C                    TRIBUTARY AREA THEORY FOR
C                      DETERMINATION OF YMM
C                             AND SPSV
C
           IF (ROUTE.EQ.3) GO TO 200
           IF (ROUTE.EQ.2) GO TO 157
           WRITE(6,78)
   78      FORMAT(' ','RIB PILLAR CALCULATION-EQUAL ROOMS',/)
           SPSV=(W+B)/B
           R=W/(W+B)
           GO TO 300
  157      WRITE(6,77)
   77      FORMAT(' ','SQUARE PILLAR CALCULATION-EQUAL ROOMS',/)
           SPSV=(W+B)**2/B**2
           R=(W+B*2)*W/(W+B)**2
           GO TO 300
  200      WRIIE(6,79)
   79      FORMAT(' ','RECTANGULAR PILLAR CALCULATION-UNEQUAL ROOMS',/)
           SPSV=(W+B)*(D+Q)/(B*D)
           R=(W*D+W*Q+B*Q)/((W+B)*(D+Q))
  300      YMM=(2.048-.919*K)+.572*ALOG(W/H)+0.09*((W/B+1)**2-1)
           IF (SPSV.GT.YMM)YMM=SPSV
C
C
C    PRINT OUT ALL INPUT DATA IF REQUESTED
C
           IF(W/H .LT. 0.25 .OR. W/H .GT. 4) WRITE(6,1010)
```

University of Alberta

```
 1010   FORMAT(' ','WARNING:VALUE OF W/H IS NOT WITHIN RECOMENDED',
     1    ' RANGE OF 0.25 GT W/H LT 4')
 1005  FORMAT(' ','WARNING:VALUES OF K EXCEED RECOMMENDED VALUE OF',
     1    ' K .LT. 1.5')
        IF(K .GE. 1.5) WRITE(6,1005)
        IF (PRINT.EQ.NO)GO TO 737
        IF (ROUTE .LT.3)GO TO 739
        WRITE(6,738)W,B,D,Q
  738   FORMAT(' ','SEMI-PILLAR WIDTH ADJACENT TO MINIMUM PILLAR ',
     1           /,'DIMENSION = ',F6.2,
     1           /,'SEMI-PILLAR WIDTH = ',F6.2,
     1           /,'SEMI-PILLAR DEPTH = ',F6.2,
     1           /,'SEMI-PILLAR WIDTH ADJACENT TO MAXIMUM PILLAR ',
     1           /,'DIMENSION = ',F6.2)
  739   WRITE(6,741)W,B
  741   FORMAT(' ','SEMI-ROOM WIDTH   = ',F6.2,
     1           /,'SEMI-PILLAR WIDTH = ',F6.2)
  740   WRITE(6,742)K,H,A,MUB,PHIBD,SV,PB
  742   FORMAT(' ','VIRGIN STRESS RATIO = ',F7.2,
     1           /,'SEMI-PILLAR HEIGHT  = ',F7.2,
     1           /,'MOHR ENVELOPE CONSTANT = ',F9.2,
     1   /,'COEFFICIENT OF SLIDING FRICTION FOR COAL = ',F7.4,
     1   /,'ANGLE OF INTERNAL FRICTION FOR BROKEN COAL = ',F7.2,
     1   /,'APPLIED VIRGIN VERTICAL STRESS = ',F9.2,
     1  /,'UNIAXIAL COMPRESSIVE STRENGTH OF BROKEN COAL = ',F9.2,/)
  737   CONTINUE
C
C       THE RESULTS OF THE TRIBUTARY AREA THEORY ARE AS FOLLOWS:
C
         WRITE(6,777)
  777    FORMAT(' ','THE RESULTS ARE:',/)
        WRITE(6,743)SPSV,YMM,R
  743   FORMAT(' ','MEAN PILLAR STRESS CONCENTRATION = ',F6.2,
     1           /,'MAXIMUM PILLAR STRESS CONCENTRATION = ',F6.2,
     1           /,'EXTRACTION RATIO = ',F7.4)
C
C
C
C
C     STRENGTH SUBROUTINE WAS ORIGINALLY DEVELOPED FOR THE
C       MAIN PILLAR PROGRAM, AND IS USED HERE TO GIVE A
C        QUICK IDEA OF CRITICAL PILLAR DIMENSIONS.
C
C    BLOCK 1 - CALCULATE THE VERTICL STRESS, DEPTH OF TRANSITION
C                    POINT AND MINIMUM PILLAR CAPACITY.
C
        PHIB=PHIBD*3.14159/180
        C=SIN(PHIB)
        D=TAN(PHIB)
        ANTA=A/2+A/2/(MUB**2)*(1+SQRT(1+MUB**2))
        ANTB=A*SQRT(0.5+0.5/MUB**2*(1+SQRT(1+MUB**2)))
        PONE=ANTA+ANTB
        XBC1=(1-C)/(1+C)
        XBC2=H/D
        XBC3=((1-C)/(1+C))
        XBC4=2*PONE*C/(PB*(1+C))
```

University of Alberta

```
            XBC=XBC1*XBC2*ALOG(XBC3+XBC4)
            RBX=XBC
            STREO=2*A*SPSV/YMM
C
C     THESE ARE OTHER NECESSARY VARIABLES WHICH WILL NEEDED IN
C               THE NEWTON SUBROUTINE.
C
                   AA=PB*(1-C)/2/C
                   BB=H/D
                   CC=D/H*((1+C)/(1-C))
                   DD=2*A*SPSV/YMM
                   EE=SPSV*SV
                   FF=ANTA+ANTB
                   GG=XBC
                   TT=(BB*(EXP(CC*GG)))-BB-GG-FF*GG/AA
                   BBB=B
                   IF (B.GT.15) GO TO 9997
                   BBB=6*B
 9997              BCY=2*BBB
                   BCYU=2*BBB
                   BCF=2*BBB
                   BCFU=2*BBB
C
C
            IF(XBC.LE.B)GO TO 100
C
C    BLOCK 2 - CALCULATE THE RESIDUAL MEAN STRESS CAPACITY AND
C              CRITICAL PILLAR DIMENSIONS FOR FRACTURED PILLARS.
C
            BANTA=PB*(1-C)/(2*B*C)
            BANTB=D*((1+C)/(1-C))*B/H
            RPR=BANTA*((H/D)*(EXP(BANTB)-1)-B)
            I = 0
            CALL NEWT(FC1,D01,BCF,AA,BB,CC,DD,EE,I)
            I = 0
            CALL NEWT(FC2,D02,BCFU,AA,BB,CC,DD,EE,I)
C
             IF(STREO.LE.RPR) GO TO 80
C
C
C    BLOCK 3 - CALCULATE PILLAR STRENGTH AND SAFETY FACTORS.
C
            STREN=STREO
            SF=STREO/(SPSV*SV)
C
          IF (SF.LE.1) GO TO 70
C
C    BLOCK 4 - PRINT OUT RESULTS - STABLE (CATASTROPHIC FAILURE)
C
            WRITE(6,6000)
 6000        FORMAT(' ','PILLAR IS STABLE.')
            WRITE(6,6001)
 6001        FORMAT(' ','FAILURE MODE IS CATASTROPHIC FAILURE.')
            WRITE(6,6002) STREN, SF
 6002        FORMAT(' ','THE PILLAR STRENGTH = ', F9.2,
     1              /,'THE SAFETY FACTOR   = ',F5.2)
```

University of Alberta

```
              WRITE(6,7001)BCF,BCFU
      7001    FORMAT(' ','THE CRITICAL PILLAR DIMENSION TO AVOID: ',
     1          /,'         A) CATASTROPHIC FRACTURE IS ',F6.2,
     1          /,'         B) ULTIMATE FRACTURE IS ',F6.2)
              GO TO 10
C
C     BLOCK 5 - PRINT OUT RESULTS - FRACTURED CATASTROPHICALLY.
C
        70    WRITE(6,6003)
      6003     FORMAT(' ','PILLAR HAS FRACTURED CATASTROPHICALLY.')
                 SHEDDO=B*(SPSV*SV-STREN)
              WRITE(6,6004) SHEDDO
      6004     FORMAT(' ','THE SHED LOAD = ',F9.2)
              WRITE(6,6005) STREN,SF
      6005     FORMAT(/,'THE PILLAR STRENGTH = ', F9.2,
     1                /,'THE SAFETY FACTOR    = ',F9.2)
              WRITE(6,7002)BCF,BCFU
      7002    FORMAT(' ','THE CRITICAL PILLAR DIMENSION TO AVOID: ',
     1          /,'         A) CATASTROPHIC FRACTURE IS ',F6.2,
     1          /,'         B) ULTIMATE FRACTURE IS ',F6.2)
              GO TO 10
C
C     BLOCK 6 - CALCULATE PILLAR STRENGTH AND SAFETY FACTOR.
C
        80    STREN=RPR
              SF=RPR/(SPSV*SV)
C
              IF (SF.LE.1)GO TO 60
C
C     BLOCK 7 - PRINT OUT RESULTS - STABLE (ULTIMATE FRACTURE).
C
              WRITE(6,6006)
      6006     FORMAT(' ','PILLAR IS STABLE.')
              WRITE(6,6007)
      6007     FORMAT(' ','FRACTURE MODE WILL BE ULTIMATE FRACTURE.')
              WRITE(6,6008) STREN, SF
      6008     FORMAT(' ','THE PILLAR STRENGTH = ', F9.2,
     1                /,'THE SAFETY FACTOR    = ',F5.2)
              WRITE(6,7003)BCF,BCFU
      7003    FORMAT(' ','THE CRITICAL PILLAR DIMENSION TO AVOID: ',
     1          /,'         A) CATASTROPHIC FRACTURE IS ',F6.2,
     1          /,'         B) ULTIMATE FRACTURE IS ',F6.2)
              GO TO 10
C
C     BLOCK 8 - PRINT OUT RESULTS - FRACTURED.
C
        60    WRITE(6,6009)
      6009     FORMAT(' ','PILLAR HAS FRACTURED.')
                SHEDDO=B*(SPSV*SV-STREN)
              WRITE(6,6010) SHEDDO
      6010     FORMAT(' ','THE SHED LOAD       = ',F9.2)
              WRITE(6,6011) STREN, SF
      6011     FORMAT(' ','THE PILLAR STRENGTH = ', F9.2,
     1                /,'THE SAFETY FACTOR    = ',F5.2)
              WRITE(6,7003)BCF,BCFU
              GO TO 10
```

University of Alberta

```
C
C    BLOCK 9 - CALCULATE RESIDUAL MEAN STRESS CAPACITY AND
C              CRITICAL PILLAR DIMENSIONS FOR YIELDING.
C
  100      CANTA=PB*(1-C)/(2*B*C)
           CANTB=D*((1+C)/(1-C))*XBC/H
           RPRY=CANTA*((H/D)*(EXP(CANTB)-1)-XBC)+(1-XBC/B)*PONE
           BCY=(TT*AA)/(DD-FF)
           BCYU=(TT*AA)/(EE-FF)
           TEST=EE/(TT*AA/BCYU+FF)
           IF (STREO.LE.RPRY) GO TO 50
C
C    BLOCK 10 - CALCULATE PILLAR STRENGTH AND SAFETY FACTOR.
C
         STREN=STREO
         SF=STREO/(SPSV*SV)
C
         IF (SF.LE.1) GO TO 40
C
C    BLOCK 11 - PRINT OUT RESULTS - STABLE (CATASTROPHIC YIELD).
C
          WRITE(6,6012)
 6012      FORMAT(' ','THE PILLAR IS STABLE.')
          WRITE(6,6013)
 6013      FORMAT(' ','FAILURE MODE WILL BE CATASTROPHIC YIELD.')
          WRITE(6,6014) STREN,SF
 6014      FORMAT(' ','THE PILLAR STRENGTH = ', F9.2,
     1             /,'THE SAFETY FACTOR   = ',F9.2)
          IF (TEST.GE. 1.0) GO TO 6100
          WRITE(6,7004)BCY,BCYU
 7004     FORMAT(' ','THE CRITICAL PILLAR DIMENSION TO AVOID: ',
     1          /,'          A) CATASTROPHIC YIELD IS ',F6.2,
     1          /,'          B) ULTIMATE YIELD IS ',F6.2)
          GO TO 10
 6100     WRITE(6,7100) BCY
 7100     FORMAT(' ','THE CRITICAL PILLAR DIMENSION TO AVOID: ',
     1          /,'          A) CATASTROPHIC YIELD IS ',F6.2,
     1          /,'          B) ULTIMATE YIELD IS INFINITY.')
          GO TO 10
C
C    BLOCK 12 - PRINT OUT RESULTS - CATASTROPHIC YIELD.
C
   40       WRITE(6,6015)
 6015      FORMAT(' ','THE PILLAR HAS YIELDED CATASTROPHICALLY.')
             SHEDDO=B*(SPSV*SV-STREN)
          WRITE(6,6016) SHEDDO
 6016      FORMAT(' ','THE SHED LOAD        =',F9.2)
          WRITE(6,6017)STREN,SF
 6017      FORMAT(' ','THE PILLAR STRENGTH = ', F9.2,
     1             /,'THE SAFETY FACTOR   = ',F9.2)
          IF (TEST.GE. 1.0) GO TO 6100
          WRITE(6,7004)BCY,BCYU
          GO TO 10
C
C    BLOCK 13 - CALCULATE PILLAR STRENGTH AND SAFETY FACTOR.
C
```

University of Alberta

```
   50      STREN=RPRY
           SF=RPRY/(SPSV*SV)
C
           IF (SF.LE.1)GO TO 30
C
C        BLOCK 14 - PRINT OUT RESULTS - STABLE (ULTIMATE YIELD).
C
           WRITE(6,6018)
 6018       FORMAT(' ','THE PILLAR IS STABLE.')
           WRITE(6,6019)
 6019       FORMAT(' ','THE FAILURE MODE WILL BE ULTIMATE YIELD.')
           WRITE(6,6020) STREN,SF
 6020       FORMAT(' ','THE PILLAR STRENGTH = ', F9.2,
     1             /,'THE SAFETY FACTOR    = ',F9.2)
           IF (TEST.GE. 1.0) GO TO 6100
           WRITE(6,7004)BCY,BCYU
           GO TO 10
C
C        BLOCK 15 - PRINT OUT RESULTS - YIELDED.
C
   30      WRITE(6,6021)
 6021       FORMAT(' ','THE PILLAR HAS YIELDED.')
                SHEDDO=B*(SPSV*SV-STREN)
           WRITE(6,6022) SHEDDO
 6022       FORMAT(' ','THE LOAD SHED         = ',F9.2)
           WRITE(6,6023) STREN, SF
 6023       FORMAT(' ','THE PILLAR STRENGTH = ', F9.2,
     1             /,'THE SAFETY FACTOR    = ',F9.2)
           IF (TEST.GE. 1.0) GO TO 6100
           WRITE(6,7004)BCY,BCYU
   10      WRITE(6,88)XBC
   88      FORMAT(' ','DEPTH OF TRANSITION POINT = ',F6.2,/,/)
           WRITE(7,455)B,STREN
  455       FORMAT(' ',F10.2,/,F10.2,/,/)
    3      CONTINUE
           GO TO 888
  999      STOP
           END
```

University of Alberta

University of Alberta

```
C
C
C   SUBROUTINE TO DETERMINE THE ROUTES OF THE QUESTIONABLE
C                          FORMULAE
C
      SUBROUTINE NEWT(FCN,FDER,B,AA,BB,CC,DD,EE,I)
      LOGICAL PRINT
      LOGICAL*1 FREE(1)/'*'/
      PRINT=.TRUE.
      REAL B,AA,BB,CC,DD,EE,BERR,FERR,TRIAL,DER
      INTEGER I,J,MAX
      IF (I .NE. O) PRINT=.FALSE.
      BERR=.05
      FERR=O.1
      MAX=75
      FB=FCN(B,AA,BB,CC,DD,EE)
C
      DO 20 J=1,MAX
      DER=FDER(B,AA,BB,CC,DD,EE)
      TRIAL=FB/DER
      B=B-TRIAL
      FB=FCN(B,AA,BB,CC,DD,EE)
 5    IF (ABS(TRIAL).LE.BERR) GO TO 60
      IF (ABS(FB).LE.FERR)GO TO 70
20    CONTINUE
C
C   WHEN LOOP IS NORMALLY COMPETED, .MAX IS EXCEEDED.
C
      I=-1
      WRITE (6,200) MAX,B,FB
200   FORMAT (' ',' TOLERANCE NOT MET. AFTER ', I4,
     1  '  ITERATIONS',/,' B= ',F12.5, ' AND F(B) = ', F12.5)
      RETURN
C
C   THIS SECTION RETURNS AFTER MEETING BERR.
C
60    I=1
      RETURN
C
C   THIS SECTION RETURNS AFTER MEETING F(B) TOLERANCE.
C
70    I=2
      RETURN
      END
```

```
C
C      THE FUNCTIONS NEEDED FOR THE ABOVE PROGRAM ARE:
C
C   THIS FUNCTION DETERMINES THE VALUE FOR CATASTROPHIC FAILURE
C
         FUNCTION FC1(B,AA,BB,CC,DD,EE)
         FC1=AA*BB/B*(EXP(CC*B)-1)-AA-DD
         RETURN
         END
```

FUNC FC1

University of Alberta

```
C
C     THIS IS THE DERIVATIVE OF THE BCF FUNCTION
C
      FUNCTION DO1(B,AA,BB,CC,DD,EE)
      DO1=(AA*BB/B**2)*(CC*B*EXP(CC*B)-EXP(CC*B)+1)
      RETURN
      END
```

University of Alberta

```
C
C     THIS FUNCTION DETERMINES THE VALUE OF ULTIMATE FAILURE
C
      FUNCTION FC2(B,AA,BB,CC,DD,EE)
      FC2=AA*BB/B*(EXP(CC*B)-1)-AA-EE
      RETURN
      END
```

University of Alberta

```
C
C     THIS IS THE DERIVATIVE FOR THE BCFU FUNCTION
C
         FUNCTION DO2(B,AA,BB,CC,DD,EE)
         DO2=(AA*BB/B**2)*(CC*B*EXP(CC*B)-EXP(CC*B)+1)
         RETURN
         END
```

University of Alberta

K.3 User's Manual

K.3.1 Input List - insert as listed*, separated by commas (sample at end)

First Line

1. T - total number of pillar widths to be considered.
2. Intval - the difference between pillar widths.

Second Line

1. Route:
   a) Rib pillars - equal rooms (1)
   b) Square pillars - equal rooms (2)
   c) Rectangular pillars - unequal rooms (3)
2. W - semi-room width (adjacent to minimum pillar dimension)
3. D - semi-pillar depth
4. Q - semi-room width (adjacent to maximum pillar dimension)
5. H - semi-pillar height

Third Line

1. Print
   a) Yes (1 or 'Yes') - print input data
   b) No (0 or 'No') - do not print input data
2. S_v - virgin vertical stress (psi)
3. K - S_{H/S_v}
4. A - Mohr's constant
5. MUB - coefficient of sliding friction for broken coal
6. PHIBD - angle of internal friction for broken coal
7. PB - uniaxial compressive strength of broken coal

* - the first line may appear only once in the data file but the second and third for as many specifications as needed. See sample input.

K.3.2 Program Use

* To run program :

1. Create test file (anyname can be used which is not already in use)
2. Input data (using the file description previously given)

```
Example : #Ed testfile
          : 1
          ? 7, 5
          ? 1, 10, 0, 0, 5
          ? 'YES', 1000, .33, 500, .577, 30, 0.1
       ** ? (blank line)
          : MTS
          #
```

3. Compile the main program:

```
#$ RUN *fortg  SCARDS=SHRTPILL      T=2
```

4. Run program

```
#$RUN -LOAD# 5=testfile   6=outputfile (-a)  7=plotfile (-aa)
t=2
```

5. a) Obtain output on terminal

```
#$COPY -a
```

b) Obtain page printer output

```
#$CONTROL *Print* format=fmt11 Printon=oneside  Paper=X3

#$COPY -a *print*

#$RELEASE *PRINT*
```

Notes:-

* - These steps should be followed when using the MTS system at the University of Alberta. Other installations may vary these steps.

** - It should be noted that if more than one set of test data is being used, enter them at this point. See end for example.

K.4 Variables and Constants

1. T = total number of pillar widths
2. INTVAL = the difference between pillar widths
3. ROUTE = the type of pillar being analysed
4. W = semi-room width (adjacent to minimum pillar dimension)
5. D = semi-pillar depth
6. Q = semi-room width (adjacent to maximum pillar dimension)
7. H = semi-pillar height
8. PRINT = either yes or no to print out input data
9. SV = virgin vertical stress
10. K = SH/SV
11. A = Mohr's constant
12. MUB = μ_B coefficient of sliding friction for broken coal
13. PHIBD = ϕ_B = angle of internal friction for broken coal
14. PB = uniaxial compressive strength of broken coal
15. B = semi-pillar width
16. SPSU = mean pillar stress concentration
17. R = extraction ratio
18. YMM = maximum pillar stress concentration, before failure
19. PHIB = radian value of PHIBD
20. C, D, ANTA, ANTB, XBC1, XBC2, XBC3, XBC4, AA, BB, CC, DD, EE, FF, BANTA, BANTB, CANTA, CANTB = are all intermediate calculations
21. PONE (P_1) = the verticle stress acting on the element of broken coal
22. RBX = XBC = the depth of the fracture zone
23. STREO = the strength of a pillar which has fractured catastrophically
24. BCY = the "B" value for catastrophic yield
25. BCYU = the "B" value for ultimate yield
26. BCF = the "B" value for catastrophic fracture
27. BCFY = the "B" value for ultimate fracture
28. STREN = the calculated strength of the pillar
29. SF = the safety factor
30. RPR = the calculated residual mean pillar stress capacity
31. BERR AND FERR = tolerances for B subroutine
32. MAX = the maximum number of tries for the B subroutine to obtain "B"
33. FB = FC1 or FC2 = the functions for determining BCF or BCFU respectively
34. DER = DO1 or DO2 = the derivatives for determining BCF or BCFU respectively

K.5 Newton's Method

The algorithm for Newton's method specifies

1. $f(x) = 0$
2. $f'(x) \neq 0$
3. Initial guess must be close to the root desired

The form of the algorithm is:

$$x_2 = x_1 - \frac{f(x)}{f'(x)}$$

Derivation of Algorithm

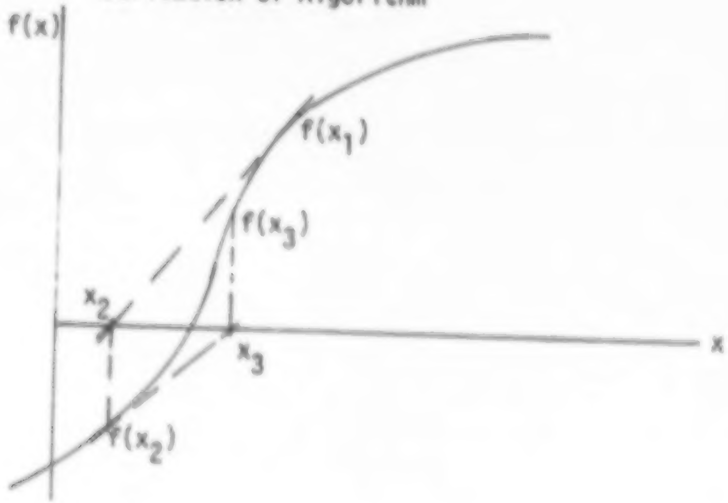

1. Make an initial guess for x_1 and calculate the function value.
2. Find a tangant to the point x_1 and take it to $y=0$ for x_2.
3. Find the value for $f(x_2)$ and take a tangeant and repeat total process.

Point 1 to Point 2

$$m = \frac{y_2 - y_1}{x_2 - x_1} \quad \text{but } y_2 = 0$$

$$= \frac{-y_1}{x_2 - x_1}$$, make $y_1 = f(x)$ and the derivative of the function is defined as the tangeant. ($m = f'(x)$)

$$f'(x_1) = \frac{-f(x_1)}{x_2 - x_1}$$

$$x_2 = x_1 - \frac{f(x)}{f'(x)}$$

FORTRAN CODE

```
FERR = 0.1
BERR = .05              TOLERANCES
MAX = 75                Total maximum number of B guesses
$B_1$ = BGUESS          "B" Value fairly close to answer
FB = F (BGuess)

DO  20  J=1, MAX
DER = FDER (B)                                  - CALCULATE DERIVATIVE
B = B - FB/DER                                  - CALCULATE NEW B
FB = F(B)                                       - CALCULATE NEW FB

IF ( $|B_2 - B_1|$  .LE. BERR) RETURN B VALUE - IS B TOLERANCE MET

IF ( |FB| .LE. FERR) RETURN B VALUE - IS FB TOLERANCE MET
```

K.6 Equations

Table K.1 gives 9 example sets of input data for this short program.

Table K.2 gives the example outputs for the first two sets of the above input data.

Table K1: Example inputs for the short program (13 data sets)

```
7,5
1,10,0,0,5
'YES',1000,.33,500,.577,30,0.1
1,10,0,0,5
'YES',1000,.33,500,.577,30,1.0
1,10,0,0,5
'YES',1000,.33,500,.577,30,10.0
1,10,0,0,5
'YES',1000,.33,500,.577,27,1.0
1,10,0,0,5
'YES',1000,.33,500,.577,33,1.0
1,10,0,0,15
'YES',1000,.33,500,.51,30,1.0
1,10,0,0,5
'YES',1000,.33,500,.65,30,1.0
1,10,0,0,5
'YES',1000,.33,250,.577,30,1.0
1,10,0,0,5
'YES',1000,.33,1000,.577,30,1.0
1,5,0,0,5
'YES',1000,.33,500,.577,30,1.0
1,5,0,0,5
'YES',1000,.33,500,.577,30,1.0
1,10,0,0,2.5
'YES',1000,.33,500,.577,30,1.0
1,10,0,0,10
'YES',1000,.33,500,.577,30,1.0
```

Table K2: Example outputs from the short program (2 data sets)

```
                                                      RUN    1
RIB PILLAR CALCULATION-EQUAL ROOMS

SEMI-ROOM WIDTH     =   10.00
SEMI-PILLAR WIDTH =     5.00
VIRGIN STRESS RATIO =     0.33
SEMI-PILLAR HEIGHT   =     5.00
MOHR ENVELOPE CONSTANT =      500.00
COEFFICIENT OF SLIDING FRICTION FOR COAL =  0.5770
ANGLE OF INTERNAL FRICTION FOR BROKEN COAL =    30.00
APPLIED VIRGIN VERTICAL STRESS =     1000.00
UNIAXIAL COMPRESSIVE STRENGTH OF BROKEN COAL =        0.10

THE RESULTS ARE:

MEAN PILLAR STRESS CONCENTRATION =    3.00
MAXIMUM PILLAR STRESS CONCENTRATION =    3.00
EXTRACTION RATIO =  0.6667
PILLAR HAS FRACTURED CATASTROPHICALLY.
THE SHED LOAD =  10000.00

THE PILLAR STRENGTH =    1000.00
THE SAFETY FACTOR    =        0.33
THE CRITICAL PILLAR DIMENSION TO AVOID:
        A) CATASTROPHIC FRACTURE IS  32.40
        B) ULTIMATE FRACTURE IS  35.86
DEPTH OF TRANSITION POINT =  28.42

RIB PILLAR CALCULATION-EQUAL ROOMS

SEMI-ROOM WIDTH     =   10.00
SEMI-PILLAR WIDTH =   10.00
VIRGIN STRESS RATIO =     0.33
SEMI-PILLAR HEIGHT   =     5.00
MOHR ENVELOPE CONSTANT =      500.00
COEFFICIENT OF SLIDING FRICTION FOR COAL =  0.5770
ANGLE OF INTERNAL FRICTION FOR BROKEN COAL =    30.00
APPLIED VIRGIN VERTICAL STRESS =     1000.00
UNIAXIAL COMPRESSIVE STRENGTH OF BROKEN COAL =        0.10

THE RESULTS ARE:

MEAN PILLAR STRESS CONCENTRATION =    2.00
MAXIMUM PILLAR STRESS CONCENTRATION =    2.41
EXTRACTION RATIO =  0.5000
PILLAR HAS FRACTURED CATASTROPHICALLY.
THE SHED LOAD =  11705.40

THE PILLAR STRENGTH =     829.46
THE SAFETY FACTOR    =        0.41
THE CRITICAL PILLAR DIMENSION TO AVOID:
        A) CATASTROPHIC FRACTURE IS  31.81
        B) ULTIMATE FRACTURE IS  34.59
DEPTH OF TRANSITION POINT =  28.42
```